

CONFIRMATORY
SOIL-STRUCTURE INTERACTION ANALYSES
FOR GESSAR II

Prepared for:

General Electric Company
Nuclear Engineering Division
San Jose, California 95125

Prepared by:

Impell Corporation
350 Lennon Lane
Walnut Creek, California 94598

Impell Report No. 04-0030-0077

July 1983

IMPELL CORPORATION
REPORT APPROVAL COVER SHEET

Client: General Electric Company

Project: GESSAR II SSI Analyses Job Number: 0030-069

Report Title: Confirmatory Soil-Structure Interaction Analyses for GESSAR II

Report Number: 04-0030-0077 Rev. 0

The work described in this Report was performed in accordance with the Impell Corporation Quality Assurance Program. The signatures below verify the accuracy of this Report and its compliance with applicable quality assurance requirements.

Prepared By: Miguel A. Manrique Date: July 28, 1983
~~M.A. Manrique, Lead Sr. Engineer~~

Prepared By: D. Pandya Date: July 28, 1983
 D.C. Pandya, Sr. Engineer

Reviewed By: R.L. Grubb Date: July 28, 1983
 R.L. Grubb, Section Manager

Approved By: J.P. Morray Date: July 28, 1983
 J.P. Morray, Division Manager

REVISION RECORD

| Rev. No. | Prepared | Reviewed | Approved | Approval Date | Revision |
|----------|----------|----------|----------|---------------|----------|
| | | | | | |

TABLE OF CONTENTS

| | <u>Page</u> |
|-----------------------------------------------|-------------|
| 1.0 INTRODUCTION | 1 |
| 2.0 SCOPE OF WORK | 3 |
| 2.1 Site Parameters | 3 |
| 2.2 Structural Models | 4 |
| 2.3 Control Motions | 5 |
| 3.0 ANALYSIS METHOD | 7 |
| 3.1 CLASSI Substructuring Approach | 8 |
| 3.2 Determination of Foundation Input Motions | 8 |
| 3.3 Determination of Foundation Impedances | 10 |
| 3.4 Analysis of Coupled Soil-Structure System | 11 |
| 4.0 ANALYSIS RESULTS | 12 |
| 5.0 CONCLUSIONS | 14 |
| REFERENCES | 15 |
| TABLES | |
| FIGURES | |

LIST OF TABLES

| <u>Table</u> | <u>Title</u> |
|--------------|--------------------------------------------------------------------------|
| 2.1 | Cases Considered for CLASSI Analyses |
| 2.2 | Summary of Soil Properties for CLASSI Analyses |
| 2.3 | Material Damping Values for Reactor Building Components |
| 2.4 | Reactor Building Horizontal Model - Frequency Analysis Results |
| 2.5 | Reactor Building Vertical Model - Frequency Analysis Results |
| 4.1 | Locations in Horizontal Model for Evaluation of In-Structure Response |
| 4.2 | Locations in Vertical Model for Evaluation of In-Structure Response |
| 4.3 | Maximum Acceleration Responses for Horizontal Analysis Cases 1 to 7 |
| 4.4 | Comparison of Envelopes of Maximum Accelerations for Horizontal Analyses |
| 4.5 | Maximum Acceleration Responses for Vertical Analysis |

LIST OF FIGURES

| <u>Figure</u> | <u>Title</u> |
|---------------|----------------------------------------------------------------------|
| 2.1 | Variation of Shear Modulus and Damping Ratio with Shear Strain |
| 2.2 | Reactor Building Model for Horizontal Analyses |
| 2.3 | Detailed Portion of Horizontal Model Corresponding to RPV Section |
| 2.4 | Reactor Building Model for Vertical Analysis |
| 2.5 | Input Acceleration Time History - Direction H1 |
| 2.6 | Input Acceleration Time History - Direction H2 |
| 2.7 | Input Acceleration Time History - Direction V |
| 2.8 | Response Spectrum of Input Motion - Direction H1 |
| 2.9 | Response Spectrum of Input Motion - Direction H2 |
| 2.10 | Response Spectrum of Input Motion - Direction V |
| 4.1 | Comparison of Spectra Envelopes for Horizontal SSI Analyses, Node 1 |
| 4.2 | Comparison of Spectra Envelopes for Horizontal SSI Analyses, Node 18 |
| 4.3 | Comparison of Spectra Envelopes for Horizontal SSI Analyses, Node 22 |
| 4.4 | Comparison of Spectra Envelopes for Horizontal SSI Analyses, Node 42 |
| 4.5 | Comparison of Spectra Envelopes for Horizontal SSI Analyses, Node 46 |
| 4.6 | Comparison of Spectra Envelopes for Horizontal SSI Analyses, Node 71 |
| 4.7 | Comparison of Spectra Envelopes for Vertical SSI Analysis, Node 1 |
| 4.8 | Comparison of Spectra Envelopes for Vertical SSI Analysis, Node 22 |
| 4.9 | Comparison of Spectra Envelopes for Vertical SSI Analysis, Node 42 |
| 4.10 | Comparison of Spectra Envelopes for Vertical SSI Analysis, Node 41 |
| 4.11 | Comparison of Spectra Envelopes for Vertical SSI Analysis, Node 60 |
| 4.12 | Comparison of Spectra Envelopes for Vertical SSI Analysis, Node 64 |
| 4.13 | Comparison of Spectra Envelopes for Vertical SSI Analysis, Node 71 |
| 4.14 | Comparison of Spectra Envelopes for Vertical SSI Analysis, Node 72 |
| 4.15 | Comparison of Spectra Envelopes for Vertical SSI Analysis, Node 74 |
| 4.16 | Comparison of Spectra Envelopes for Vertical SSI Analysis, Node 80 |

1.0 INTRODUCTION

This report, prepared by Impell Corporation for General Electric Company, describes a series of soil-structure interaction (SSI) analyses performed for the GESSAR II Standard Plant. The objective of this work was to provide an independent assessment of SSI effects as stipulated by the NRC Standard Review Plan, Section 3.7.2. Previous SSI analyses for the GESSAR II design were performed using a general finite element approach (Reference 1). The results from those analyses form the existing seismic design basis for the standard plant. The present study was conducted using a substructure approach based upon continuum mechanics. The two approaches are fundamentally different in both theory and application, and thus satisfy the requirements outlined in the Standard Review Plan for a confirmatory analysis.

A corollary objective of this study was to evaluate the influence of the free-field control elevation on the predicted response of the structures. In the work described in Reference 1, the free-field control motion was defined at the ground surface and then deconvoluted to the bottom boundary of the finite element model. For the present study, the free-field motion is applied directly at the foundation level of the embedded Reactor Building. The results of this study may thus be used to determine the influence of the deconvolution process as applied in the previous work.

The scope of work involved a series of eight analyses which covered a very broad range of site conditions and thus form an adequate basis for a confirmatory analysis. Section 2.0 of this report describes the cases considered and provides the details of the site parameters, structure models, and control motions. Each analysis was designed to be as consistent as possible with the earlier finite element work (Reference 1). Such differences as do exist are the result of inherent limitations of the different analytical methods. Section 3.0 discusses the substructure approach used in this study and describes the steps taken to ensure a basic compatibility with the finite element analyses.

The results of the confirmatory analyses are presented in Section 4.0, and are directly compared with the existing seismic design bases for GESSAR II. Both maximum in-structure accelerations and acceleration response spectra are compared. The peak acceleration values obtained from the substructure approach are uniformly lower than the design values obtained from the previous finite element analyses. The response spectra from the present work are also generally well within the existing design envelopes, particularly for the frequency range of primary interest. Such exceedances as do occur are confined to the lower frequencies (below approximately 3 Hz) and are of secondary importance.

The conclusions of this study are presented in Section 5.0. The results demonstrate that, for the frequency range of interest, the existing envelopes are conservative, and the finite element approach as applied to the GESSAR II Standard Plant is adequate.

2.0 SCOPE OF WORK

The scope of work for this study involved a series of eight SSI analyses of the reactor building structure, using the continuum mechanics approach as implemented in the CLASSI series of computer programs. This section describes the site parameters considered for each analysis case, the structural models, and the control motions used for all the SSI analyses.

2.1 Site Parameters

The previous SSI analyses for GESSAR II were performed for a total of twelve analysis cases which covered a broad range of site conditions. For this study, the scope of work is limited to a total of eight analysis cases. Because this is a confirmatory study, this number of cases is considered sufficient, inasmuch as they cover the same broad range of site conditions used for the previous SSI analyses (Reference 1). For this reason, it is not expected that any additional cases would significantly alter the results observed in this study.

The eight analysis cases that were considered are shown in Table 2.1. Seven of these cases are for analysis in the horizontal direction and one for analysis in the vertical direction. The soil properties (at low strain levels) corresponding to each analysis case are identical to those used in the previous SSI evaluations.

For horizontal excitations, the two main soil parameters influencing soil-structure interaction are the soil shear stiffness (or shear wave velocity) and damping of the soil material. For vertical excitations, the constrained modulus (or P-wave velocity) is the most significant parameter. Consequently, these constitute the main parameters considered in this study.

The nonlinear behavior of soil was taken into account by factoring the properties at low strain by appropriate coefficients obtained by considering the range of strain levels expected at each site. Both the shear modulus and the damping were modified to arrive at strain-compatible soil properties in accordance with Figure 2.1. Other soil properties, such as unit weight and Poisson's ratio were kept constant for all analysis cases. Table 2.2 summarizes the soil properties used in this study for all the cases. The range of shear wave velocities for the horizontal analysis cases varies from 648 ft/sec. to 3422 ft/sec. Thus, soil properties varying from "soft" to "very stiff" were covered. This is essentially the same range considered for the previous SSI analyses (Reference 1).

A single analysis was performed in the vertical direction, corresponding to a site with "average" soil properties. This is considered sufficient for a confirmatory study, since the results of this analysis case are similar to those obtained by the finite element method; and the controlling analysis is the fixed base case.

2.2 Structural Models

Two separate mathematical models of the reactor building were developed, one for the horizontal analyses and one for the vertical analysis. These models were constructed based on the models used by GE for the previous SSI evaluations (Reference 1).

Horizontal Model: The model used for all the analyses in the horizontal direction is shown in Figure 2.2. The detailed portion of the model corresponding to the Reactor Pressure Vessel (RPV) section is shown in Figure 2.3. The reactor building model contains the following different areas:

- Shield Building
- Containment
- Drywell
- Shield Wall
- RPV Pedestal
- RPV and Internals

Each area of the model consists of a series of interconnected vertical beam elements having the appropriate shear and bending properties. Masses resulting from structural and hydrodynamic effects were added and lumped at the nodal points. A lumped-mass formulation was used in the solution of the equations of motion; for this reason, the off-diagonal hydrodynamic mass coupling terms were not incorporated in the model. This is the only significant difference between the model used in this study and the model used by GE to perform the SSI analysis using the finite element method. These off-diagonal mass terms represent only about 1.3 percent of the total mass of the reactor building and internals. Consequently, neglecting these terms should have no significant effect on global SSI response of the reactor building. However, because these off-diagonal masses couple the RPV and its internals, the local response obtained for these areas of the model are not expected to be identical to those of the model used by GE for the previous SSI analyses. For this reason, comparison of structural responses is limited to those areas in which the effects of the coupling masses are not present (Reactor Shield Building, Containment, Drywell). Trends observed for these areas can reasonably be extended to other areas as well.

An eigenvalue analysis was performed on the model in order to determine its dynamic characteristics. The Impell proprietary program EDSGAP was used for this purpose. A total of 20 frequencies and mode shapes were extracted. Material damping for each material type was specified as shown in Table 2.3. The composite modal damping technique was used to determine the appropriate damping for each mode.

Table 2.4 summarizes the results of the eigenvalue analysis. The first 20 frequencies of the model and corresponding modal dampings and mass participation factors are tabulated. A very good match is obtained between these results and those obtained by GE and reported in Reference 2 for modes corresponding to the Shield Building, Containment, and Drywell. As expected, modes corresponding to the Shield Wall, RPV, and Internals show some differences which are directly attributed to the absence of the off-diagonal mass terms.

Vertical Model: The model used for analysis in the vertical direction is shown in Figure 2.4. As with the horizontal case, the model consists of a series of interconnected vertical beam elements with the appropriate axial properties. The translational vertical masses are concentrated at the nodal points. An eigenvalue analysis was performed on this model using the Impell program EDSGAP. Frequency analysis results for the vertical model are shown in Table 2.3. These results are identical to those reported by GE in Reference 2.

2.3 Control Motions

Three statistically independent, synthetic earthquake acceleration time histories were used for the SSI analyses performed in this study. They are identified as H1, H2, and V. H1 and H2 correspond to the two horizontal directions and V corresponds to the vertical direction. They were developed based on the specified NRC Regulatory Guide 1.60 design response spectra. The development of these earthquake acceleration time histories is discussed in Reference 1.

Plots of each component of the acceleration time histories are shown in Figures 2.5 to 2.7 for H1, H2, and V respectively. The horizontal motion H1 and vertical motion V have a duration of 22 seconds. The horizontal motion H2 has a duration of 20 seconds. All motions are discretized at time steps of 0.01 seconds and were scaled to have a peak acceleration value of 0.15g.

The response spectrum at 2 percent damping, generated from each of the time histories, is shown in Figures 2.8 to 2.10 for motions H1, H2, and V respectively. These response spectra provide a reasonable fit to the Regulatory Guide 1.60 response spectrum.

For the SSI analyses in the horizontal directions, the control motions H1 and H2 were assumed to consist of vertically propagating shear waves. For the SSI analysis in the vertical direction, the motion was assumed to consist of vertically propagating compressional waves. Both of the above assumptions are consistent with previous analyses for GESSAR II using finite element techniques.

In the previous finite element study, which forms the existing seismic design basis for GESSAR II, the control motion was applied in the free-field at the ground surface and then deconvoluted to the bottom boundary of the finite element model. For this confirmatory study, the control motion is applied in the free-field at the foundation level of the structure. This is consistent with the current version of NRC Standard Review Plan Section 3.7.2 (Reference 3). Therefore, the results of this confirmatory study can be used to verify the adequacy of the GE approach, which consists of a surface definition of motion, combined with extensive parametric variations of site conditions.

3.0 ANALYSIS METHOD

The soil structure interaction analyses described in this report were performed using an adaptation of the CLASSI series of computer codes. These codes employ a general substructure approach to the SSI problem, and are based upon a linear viscoelastic formulation of a three-dimensional continuum. In the CLASSI approach, the soil foundation system is modeled by a series of frequency-dependent impedance functions. The influence of a seismic wave field on this system is defined in terms of the driving force vector or foundation input motion. The driving force vector and system impedances can be combined with the dynamic properties of the structure to evaluate the SSI behavior and determine the complete response of the structure.

While the theory underlying CLASSI is reasonably well developed, there are certain limitations of practical application of the code. Industry versions of CLASSI can treat a broad range of problems involving surface-founded structures. Research versions of the code can also evaluate selected cases involving embedded structures; e.g., single isolated foundations with regular geometry (hemispherical, cylindrical etc.). At present, however, CLASSI has not been developed to the point where it is capable of treating the general problem of multiple embedded structures. The basic limitation, therefore, is the inability to simultaneously consider both embedment and structure-to-structure interaction.

Of these two effects, embedment is probably the more significant. With the possible exception of well tuned adjacent structures, the primary influence of structure-to-structure interaction is on rigid body response. In terms of peak accelerations and in-structure response spectra, it can reasonably be considered a second-order effect and one which would tend to reduce overall response levels. Embedment, however, is known to affect both the site impedance functions and the driving force vectors. In the case of deeply embedded structures such as those of GESSAR II, both of these effects are significant.

For the present study, therefore, the choice was made to incorporate the influence of embedment rather than structure-to-structure interaction. Such an approach is believed to be more consistent with the previous finite element study than would be an analysis based upon surface-founded structures. For these confirmatory analyses, then, the industry version of CLASSI has been used, but applicable research results have been employed to make the appropriate adjustments to incorporate the effects of embedment in both the impedances and the driving force vectors.

Details of this approach to CLASSI are in the following sections.

3.1 CLASSI Substructuring Approach

The CLASSI substructure approach divides the SSI problem into the following three steps:

- a. Determination of the foundation input motions.
- b. Determination of the frequency-dependent impedance functions.
- c. Analysis of the coupled soil-structure system, using results from steps a and b and the dynamic properties of the structure.

In the first step -- determination of the foundation input motion -- the CLASSI program applies the design earthquake motion at the foundation level of the reactor building in the free field. This free-field motion is then used in conjunction with the complex, frequency-dependent scattering matrix in order to determine the foundation input motion. Details on the development of the foundation input motion based on scattering matrices obtained for embedded rigid foundations are described in Section 3.2.

In the second step, the foundation impedances corresponding to rigid foundations, embedded in a uniform viscoelastic media, are developed. The procedure used for the development of the frequency-dependent impedances is described in Section 3.3.

The third step -- analysis of the coupled soil-structure system -- is carried out by CLASSI in the frequency domain. Time history of responses are obtained by inverse Fourier transform techniques.

3.2 Determination of Foundation Input Motions

In the context of the CLASSI approach, the foundation input motion corresponds to the response of the rigid, massless foundation to the seismic environment described by the free-field in the absence of the superstructure. The response of the rigid massless foundation to the seismic excitation can be described by the six-component vector:

$$\{U_0^*\} = (\Delta_x^*, \Delta_y^*, \Delta_z^*, \theta_x^*, \theta_y^*, \theta_z^*)^T$$

in which $\Delta_x^*, \Delta_y^*, \Delta_z^*$ represent the translational components of the response, while $\theta_x^*, \theta_y^*, \theta_z^*$ represent the rotational components of the response.

The foundation input motion $\{U_0^*\}$ is related to the free-field ground motion by means of the complex-valued, frequency-dependent scattering matrix $[S(\omega)]$:

$$\{U_0^*\} = [S(\omega)] \{f(\omega)\}$$

where the vector $\{f(\omega)\}$ is the complex Fourier transform of the free-field ground motion. At a given frequency, ω , each complex number in $\{f(\omega)\}$ corresponds to the amplitude and phase of a wave component of the free-field motion. Each column of the scattering matrix $[S(\omega)]$ represents the response of a massless rigid foundation to a given incident wave of unit amplitude. The matrix product $[S(\omega)] \{f(\omega)\}$ is therefore the response of the rigid massless foundation to a particular free-field motion. Thus, in general, the foundation input motion depends on the geometry of the foundation, the characteristics of the soil (material properties and configuration), and the type of wave field assumed for the free-field motion.

For a surface-founded rigid foundation subjected to vertically propagating shear or compressional waves, the response of the foundation includes only translational components with amplitudes equal to those of the free-field motion on the ground surface. However, if the foundation is embedded, a horizontal component of the control motion consisting of vertically propagating shear waves produces both a horizontal translation and a rocking motion of the massless foundation. This is primarily due to the scattering of waves from the soil-foundation interface and the kinematic constraints imposed on the soil by the rigid foundation. Thus, for embedded foundations, the combined effect of translation and rocking must be considered in order to obtain accurate structural responses.

In this study, the effects due to embedment of a rigid cylindrical foundation on the foundation input motions have been explicitly accounted for by modifying the scattering matrix obtained by CLASSI for the surface foundation case. Both the translation and rocking components of the foundation input motion were modified throughout the frequency range considered for each analysis case. The basis of these modifications was results reported in References 4 and 5, which considered the effects of embedment depth on the foundation input motion for cylindrical foundations subjected to vertically incident shear waves. Both the real and imaginary terms of the scattering matrices corresponding to horizontal translational and rocking response were developed.

As shown in these references, one resulting effect of embedment on the foundation input motion is that the resulting translational component is modified with respect to the free-field motion. This is in contrast with the case of surface foundations subjected to vertically incident shear waves, in which the translational response of the foundation has the same amplitude as the free-field motion. The other resulting effect of embedment on the foundation input motion is the

presence of a rocking component, which is absent in the case of surface foundations. Thus, for this study, the combined effect of both translational and rocking motion of the massless foundation were considered.

For the vertical analysis case, no modification to the scattering matrices obtained for the surface foundation has been made. This is conservative, since embedment leads to a reduction in the vertical motion (as shown in Reference 5), and a corresponding reduction in vertical structural response would be expected.

3.3 Determination of Foundation Impedances

The foundation impedances are complex-valued, frequency-dependent functions which relate the dynamic forces that the foundation exerts on the soil to the resulting soil displacements, i.e.:

$$\{F_S(\omega)\} = [K(\omega)] \{U_S\}$$

where $\{F_S(\omega)\}$ represents the generalized forces, $[K(\omega)]$ is the complex impedance matrix, and $\{U_S\}$ represents the generalized displacements. The real part of the complex impedance matrix represents the stiffness of the soil and the imaginary part represents the energy dissipation of the soil, including both radiation and material damping.

For a rigid foundation, the impedances are uniquely defined by a 6 x 6 matrix relating a resulting set of forces and moments to the six rigid-body degrees of freedom. Results reported in the literature (References 6,7,8,9) indicate that the impedances for embedded foundations are generally higher than those of surface foundations. The real part (stiffness terms) is increased because of the additional soil resistance provided by the side walls. The imaginary part (damping terms) -- which tend to be more affected than the real part -- also increase because of additional radiation of energy into the soil adjacent to the side walls of the embedded foundation. This mechanism of energy dissipation is not present in surface foundations.

The difference in impedance values between surface and embedded foundations can be significant depending on the degree of embedment. In this study, correction to the impedances obtained by CLASSI for the surface foundation were deemed necessary in order to obtain accurate structural responses. These corrections were based on detailed results reported in Reference 7. By interpolation of the impedances given in this reference for various embedment depths, to the appropriate embedment depth corresponding to the GESSAR II reactor building, frequency-dependent impedances which account for embedment of the foundation were determined.

Both the horizontal translation and the rocking impedances were obtained. The translation/rocking coupling impedances were not modified to account for embedment. This was determined to be conservative, based on sensitivity analysis specifically performed to evaluate the influence of the coupling impedances in structural response. For the vertical analysis case, no modification to the vertical impedances obtained for the surface foundation was made. This is conservative since it is well known that embedment tends to reduce the amplitude of structural response.

3.4 Analysis of Coupled Soil-Structure System

The final step in the CLASSI substructure approach is to perform the actual soil-structure interaction analysis. The impedances and scattering matrices calculated in the previous steps are used to solve the equations of the coupled soil-structure system. For this step, the dynamic characteristics of the structure (previously calculated and described in Section 2.2) are used to reduce the effects of the superstructure to six dynamic inertial parameters (modal participation factors) for each mode and a 6 x 6 rigid-body mass matrix of the structure about a reference point on the foundation (top of foundation basemat) where the SSI response is determined. Once the motion of the foundation has been obtained, the time history response at any level of the structure is computed using Fourier transform techniques. The method described above permits modeling of the structure to any desired degree of complexity in order to obtain accurate in-structure responses.

4.0 ANALYSIS RESULTS

This section summarizes the results of the confirmatory SSI analyses performed for GESSAR II using the continuum mechanics approach. Also, the results of this study were compared with those generated by GE using the finite element approach. This latter set forms the existing seismic design basis for the GESSAR II standard plant.

Peak accelerations and in-structure response spectra at the top of the basemat and at various locations of the reactor building were generated from the CLASSI analyses. The locations in the horizontal and vertical reactor building models at which the responses were generated are described in Tables 4.1 and 4.2, respectively. Other design parameters such as shear forces and bending moments are directly related to peak acceleration response. Thus, they were not specifically generated. Trends observed for the peak accelerations can be extended to shear forces and bending moments as well.

Peak accelerations at the various locations in the reactor building, corresponding to each horizontal analysis case are presented in Table 4.3. A comparison of the envelopes obtained from the CLASSI and the finite element analyses is shown in Table 4.4. This comparison shows that similar responses are obtained at the top of the basemat level; however, the continuum mechanics approach yields consistently lower in-structural peak accelerations. The decrease with respect to the finite element results is of the order of 13% at the top of the containment area (node 22) to 39% at the top of the drywell (node 42). As the amplitude of the response tends to increase with increasing soil stiffness, the continuum approach values are generally controlled by analysis Case 5 which corresponds to the very stiff soil configuration case.

Peak acceleration values obtained for the vertical analysis case are shown in Table 4.5. Also shown in this table are, for comparison purposes, the values corresponding to the existing seismic design basis for the vertical direction earthquake. It is observed that the continuum mechanics approach results -- for the case considered -- are well below those which form the existing seismic design basis. Additional reduction of responses would have been obtained had the impedances and scattering matrices been modified to incorporate effects of embedment. As explained in Sections 3.2 and 3.3 of this report, the impedances and scattering matrices corresponding to a surface founded structure were conservatively used for the analysis in the vertical direction.

For each analysis case, an acceleration response spectrum corresponding to 2% damping value was developed at all the building locations specified in Tables 4.1 and 4.2. The spectrum was developed for a total of 150 frequency points evenly distributed on a logarithmic scale of 0.5 to 33 Hz.

Enveloped response spectra covering the results of all the horizontal analyses cases were developed at each specified location. These envelopes were then compared with those similarly developed by GE and based on the finite element approach. Response spectra plots showing these comparisons are shown in Figures 4.1 through 4.16.

Comparison of enveloped response spectra shows that the envelopes based on the finite element approach, which form the GESSAR II seismic design basis, generally envelop the response spectra obtained from the continuum approach. This is especially valid for the frequency range of interest for seismic design of GESSAR II (3-33 Hz). In some isolated instances, minor exceedances are observed in the low frequency range but these are of no significance in seismic design.

For the vertical analysis case, the response spectra obtained using the continuum approach are very similar to the design envelopes up to approximately 3 Hz and well below in the frequency range of 3 - 33 Hz. This is because the fixed-base analysis case controls the design envelopes over this frequency range.

5.0 CONCLUSIONS

This report describes the results of a confirmatory set of soil-structure interaction analyses for the GESSAR II Standard Plant. These analyses were performed using a substructure approach based upon continuum mechanics. This approach is fundamentally different in both theory and application to the finite element method used for the existing seismic design basis. Thus, the substructure approach satisfies the SRP requirements for a confirmatory analysis.

The results demonstrate the conservatism of the seismic design basis envelopes in the frequency range of primary interest for design of GESSAR II. Any exceedances of the design envelopes are confined to the lower frequency range (below 3 Hz) and are of secondary importance. Thus, this study provides an independent assessment of the SSI effects as stipulated by Section 3.7.2 of the SRP to verify the conservatism of the existing seismic design basis.

In addition, the results of this study demonstrate that the design basis methodology, which consists of a surface definition of motion, combined with extensive parametric variations of site conditions, yields a conservative design basis.

In conclusion, the conservatism of the GE SSI approach to generate seismic design envelopes for the GESSAR II reactor building has been demonstrated. As a generic approach, the GE methodology will yield conservative results for any Nuclear Island structure because:

- a. As a result of extensive soil variational cases, attenuation effects due to any particular set of soil conditions are eliminated. In addition amplification effects occurring for each specific case are retained.
- b. The structure is subjected to the full energy content of the design spectrum through a fixed-base analysis using the R. G. 1.60 control motion as input.

REFERENCES

1. Seismic Soil-Structure Interaction Analysis of the Nuclear Island, Appendix 3A, General Electric Report.
2. Letter from General Electric Company to Impell Corporation Describing Input for SSI Analysis for GESSAR II, Dated March 21, 1983.
3. Standard Review Plan, Section 3.7.2, "Seismic System Analysis," NUREG-0800, Office of Nuclear Reactor Regulation, U.S. Nuclear Regulatory Commission.
4. Day, S. M., "Finite Element Analysis of Seismic Scattering Problems," Ph.D. Thesis, University of California at San Diego, 1977.
5. Day, S. M., "Seismic Response of Embedded Foundations," Presented at the ASCE Convention and Exposition, Chicago, October 1978.
6. Soil-Structure Interaction: The Status of Current Methods and Research, Seismic Safety Margins Research Program (SSMRP), Prepared for the U.S. NRC by Lawrence Livermore National Laboratory, January 1981.
7. Apsel, R. J., "Dynamic Green's Functions for Layered Media and Applications to Boundary-Value Problems," Ph.D. Thesis, University of California at San Diego, 1979.
8. Uncertainty in Soil-Structure Interaction Analysis Arising From Differences in Analytical Techniques, NUREG/CR-2077, Prepared for the U.S. NRC, Lawrence Livermore National Laboratory, July 1982.
9. Phase I Final Report, Soil Structure Interaction (Project III), Seismic Safety Margins Research Program (SSMRP), Prepared for the U.S. NRC, Lawrence Livermore National Laboratory, June 1982.

Table 2.1

Cases Considered for CLASSI Analyses

| <u>Case No.</u> | <u>Description</u> |
|-----------------|-------------------------------------------------------------------|
| 1 | Lower bound soil properties. Horizontal Motion H2. |
| 2 | Average soil properties. Horizontal Motion H2. |
| 3 | Upper bound soil properties. Horizontal Motion H2. |
| 4 | VP3 profile soil properties. Horizontal Motion H2. |
| 5 | Uniform rock profile with $V_S = 3422$ fps. Horizontal Motion H2. |
| 6 | Upper bound soil properties. Horizontal Motion H1. |
| 7 | VP5 profile soil properties. Horizontal Motion H2. |
| 8 | Average soil properties. Vertical Motion V. |

Table 2.2

Summary of Soil Properties for CLASSI Analyses

| Case No. | Shear Modulus $\times 10^6$ (psf) | Shear Wave Velocity (ft/sec) | Unit Weight (pcf) | Poisson's Ratio | Material Damping (%) | Constrained Modulus $\times 10^6$ (psf) | P-Wave Velocity (ft/sec) |
|----------|-----------------------------------------|---------------------------------|----------------------|-----------------|----------------------|-----------------------------------------------|-----------------------------|
| 1 | 1.63 | 648 | 125 | 0.35 | 8.0 | N/A | N/A |
| 2 | 2.70 | 834 | 125 | 0.35 | 6.6 | N/A | N/A |
| 3 | 6.00 | 1,243 | 125 | 0.35 | 5.0 | N/A | N/A |
| 4 | 11.50 | 1,721 | 125 | 0.35 | 5.0 | N/A | N/A |
| 5 | 45.50 | 3,422 | 125 | 0.35 | 2.0 | N/A | N/A |
| 6 | 6.00 | 1,243 | 125 | 0.35 | 5.0 | N/A | N/A |
| 7 | 27.20 | 2,647 | 125 | 0.35 | 5.0 | N/A | N/A |
| 8 | 2.70 | 834 | 125 | 0.35 | 6.6 | 11.7 | 1,736 |

Note:

N/A - not applicable

Table 2.3
Material Damping Values
for Reactor Building Components

| <u>Component</u> | <u>Critical Damping</u> |
|------------------|-------------------------|
| Shield Building | 0.04 |
| Containment | 0.02 |
| Drywell | 0.04 |
| Shield Wall | 0.04 |
| Pedestal | 0.04 |
| RPV | 0.02 |
| Fuel Assembly | 0.06 |
| CRD Guide Tubes | 0.01 |
| CRD Housing | 0.01 |
| Other Internals | 0.02 |

Table 2.4

Reactor Building Horizontal Model
- Frequency Analysis Results

| <u>Frequency Number</u> | <u>Modal Frequency (Hz)</u> | <u>Modal Damping Factor</u> | <u>Mass Participation Factor</u> |
|-------------------------|-----------------------------|-----------------------------|----------------------------------|
| 1 | 5.18 | 0.0399 | -945.7 |
| 2 | 5.32 | 0.0310 | -900.0 |
| 3 | 5.52 | 0.0368 | -721.4 |
| 4 | 8.05 | 0.0209 | 262.0 |
| 5 | 9.01 | 0.0277 | 140.2 |
| 6 | 10.86 | 0.0324 | -134.6 |
| 7 | 12.41 | 0.0525 | - 23.1 |
| 8 | 16.70 | 0.0399 | -482.3 |
| 9 | 19.33 | 0.0247 | 151.8 |
| 10 | 21.78 | 0.0400 | -417.7 |
| 11 | 21.92 | 0.0137 | - 45.1 |
| 12 | 22.81 | 0.0169 | - 49.4 |
| 13 | 25.62 | 0.0194 | - 91.3 |
| 14 | 26.24 | 0.0231 | -244.0 |
| 15 | 30.40 | 0.0377 | -296.1 |
| 16 | 30.73 | 0.0534 | - 46.5 |
| 17 | 32.89 | 0.0136 | - 31.3 |
| 18 | 35.28 | 0.0353 | 92.8 |
| 19 | 36.14 | 0.0400 | 229.3 |
| 20 | 40.06 | 0.0387 | -374.5 |

Table 2.5

Reactor Building Vertical Model
- Frequency Analysis Results

| <u>Frequency Number</u> | <u>Modal Frequency (Hz)</u> | <u>Modal Damping Factor</u> | <u>Mass Participation Factor</u> |
|-----------------------------|-------------------------------------|-------------------------------------|------------------------------------------|
| 1 | 14.45 | 0.0399 | -988.5 |
| 2 | 16.09 | 0.0400 | -1076.7 |
| 3 | 20.71 | 0.0208 | -332.5 |
| 4 | 23.66 | 0.0387 | -229.1 |
| 5 | 26.33 | 0.0388 | 202.3 |
| 6 | 32.53 | 0.0422 | 303.3 |
| 7 | 39.98 | 0.0490 | 31.5 |

Table 4.1

Locations in Horizontal Model For Evaluation of In-Structure Response

| <u>Node No.</u> | <u>Location</u> |
|-----------------|---------------------------|
| 1 | Top of Shield Building |
| 18 | Middle of Shield Building |
| 22 | Top of Containment |
| 42 | Top of Drywell |
| 46 | Middle of Drywell |
| 71 | Top of Basemat |

Table 4.2

Locations in Vertical Model for Evaluation of In-Structure Response

| <u>Node No.</u> | <u>Location</u> |
|-----------------|------------------------|
| 1 | Top of Shield Building |
| 22 | Top of Containment |
| 42 | Top of Drywell |
| 46 | Middle of Drywell |
| 60 | Middle of Shield Wall |
| 64 | Top of Pedestal |
| 71 | Top of Basemat |
| 72 | RPV Internals |
| 74 | Bottom of RPV |
| 80 | Middle of RPV |

Table 4.3

Maximum Acceleration Responses
for Horizontal Analysis Cases 1 to 7

| <u>Node Numbers</u> | <u>Maximum Accelerations (ft/sec²)</u> | | | | | | |
|-------------------------|---------------------------------------------------|---------------|---------------|---------------|---------------|---------------|---------------|
| | <u>Case 1</u> | <u>Case 2</u> | <u>Case 3</u> | <u>Case 4</u> | <u>Case 5</u> | <u>Case 6</u> | <u>Case 7</u> |
| 1 | 6.13 | 6.83 | 10.22 | 12.76 | 23.05 | 12.99 | 15.26 |
| 18 | 3.69 | 4.04 | 4.84 | 5.76 | 7.21 | 5.15 | 6.63 |
| 22 | 5.50 | 6.66 | 8.44 | 11.90 | 16.51 | 10.13 | 16.08 |
| 42 | 4.43 | 5.69 | 7.57 | 9.25 | 14.80 | 7.98 | 12.34 |
| 46 | 3.24 | 4.10 | 5.05 | 5.76 | 9.06 | 5.20 | 7.99 |
| 71 | 3.13 | 3.35 | 3.69 | 4.13 | 4.95 | 4.15 | 4.71 |

Table 4.4

Comparison of Envelopes of Maximum
Accelerations for Horizontal Analyses

| Node Numbers | Envelope of Maximum Accelerations (ft/sec ²) | |
|-----------------|----------------------------------------------------------|-------------------------|
| | Continuum Mechanics Approach | Finite Element Approach |
| 1 | 23.05 | 32.5 |
| 18 | 7.21 | 10.0 |
| 22 | 16.51 | 19.1 |
| 42 | 14.80 | 24.3 |
| 46 | 9.06 | 14.6 |
| 71 | 4.95 | 4.8 |

Table 4.5

Maximum Acceleration Responses
for Vertical Analysis

| <u>Node Number</u> | <u>Maximum Accelerations (ft/sec²)</u> | |
|--------------------|----------------------------------------------------------|----------------------------------------|
| | <u>Continuum Mechanics Approach (Case 8)</u> | <u>GE Seismic Design Envelopes</u> |
| 1 | 4.86 | 12.0 |
| 22 | 4.83 | 9.7 |
| 42 | 5.05 | 10.2 |
| 46 | 4.95 | 8.0 |
| 60 | 4.73 | 5.6 |
| 64 | 4.69 | 5.2 |
| 71 | 4.66 | 4.8 |
| 72 | 4.80 | 9.7 |
| 74 | 4.73 | 5.8 |
| 80 | 4.70 | 5.3 |

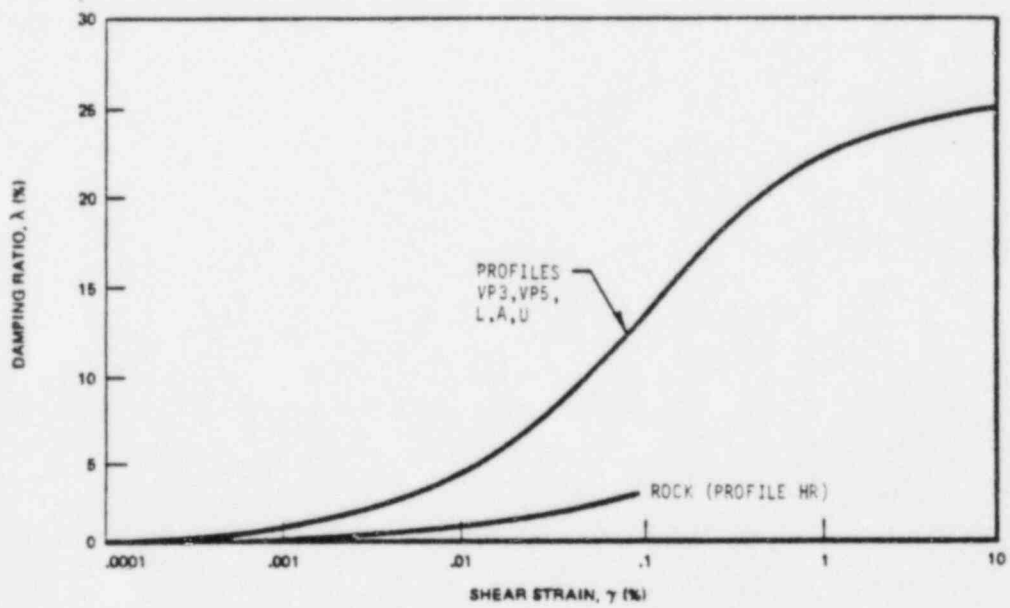
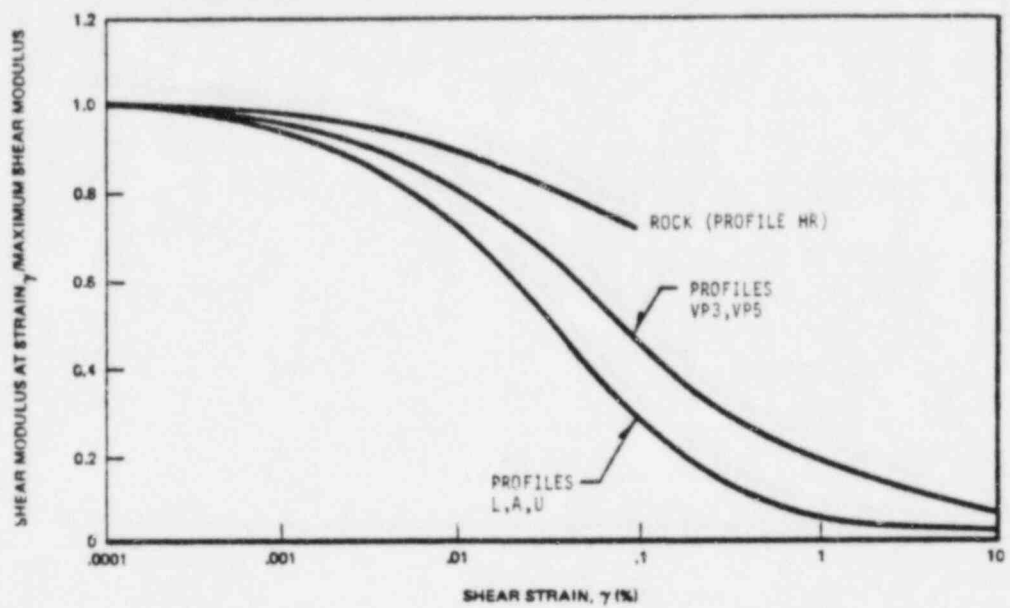


Figure 2.1 Variation of Shear Modulus and Damping Ratio with Shear Strain

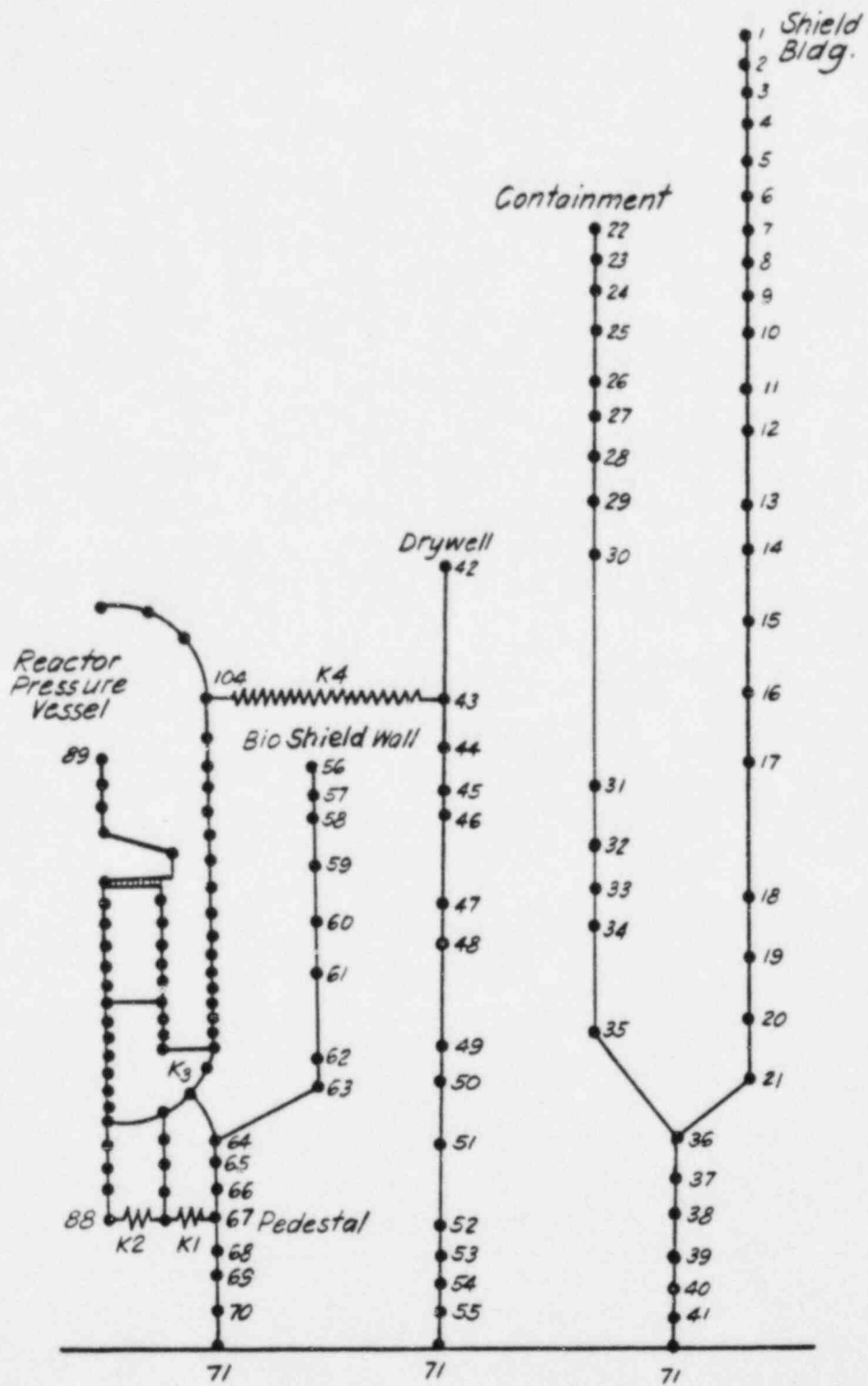


Figure 2.2 Reactor Building Model for Horizontal Analyses

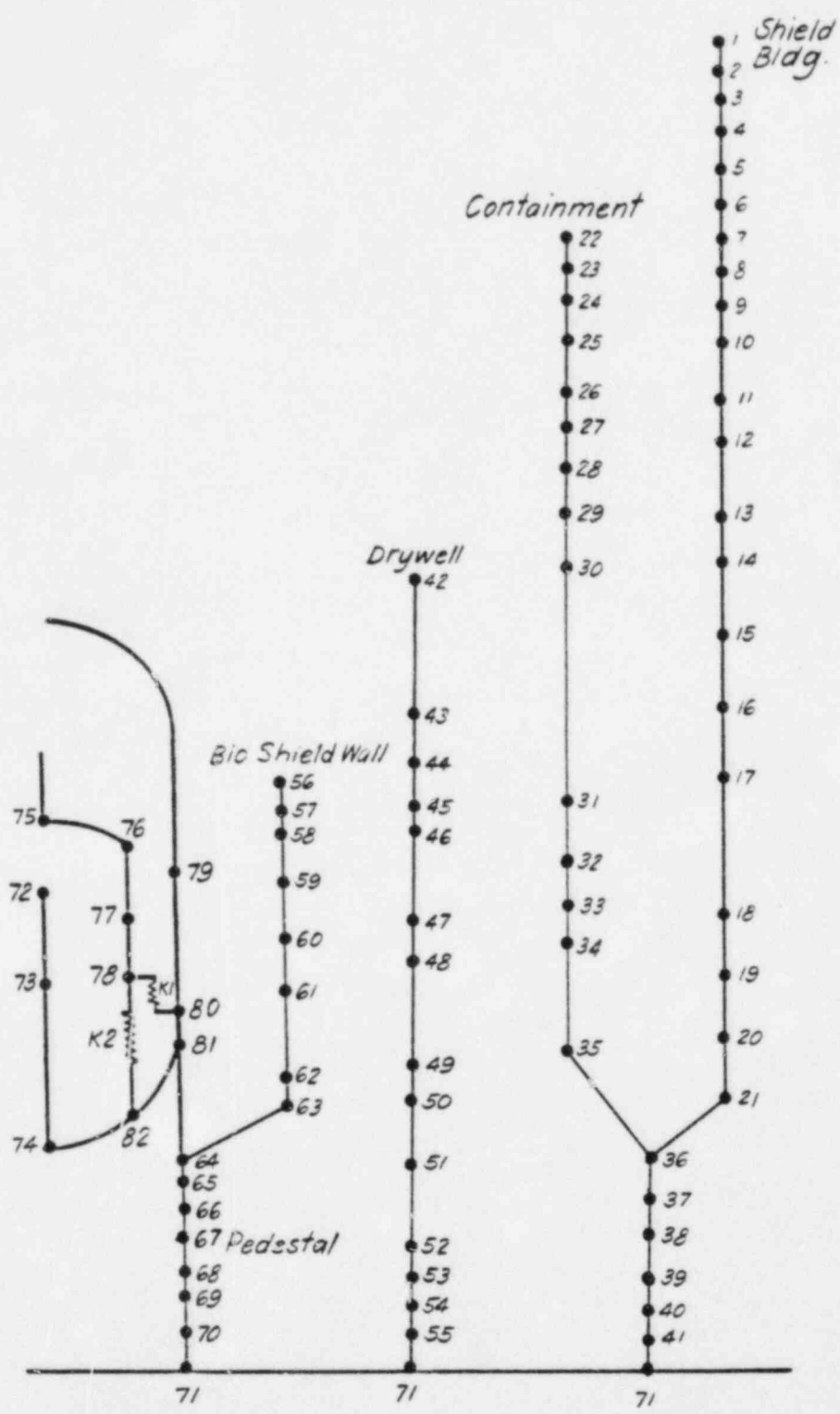
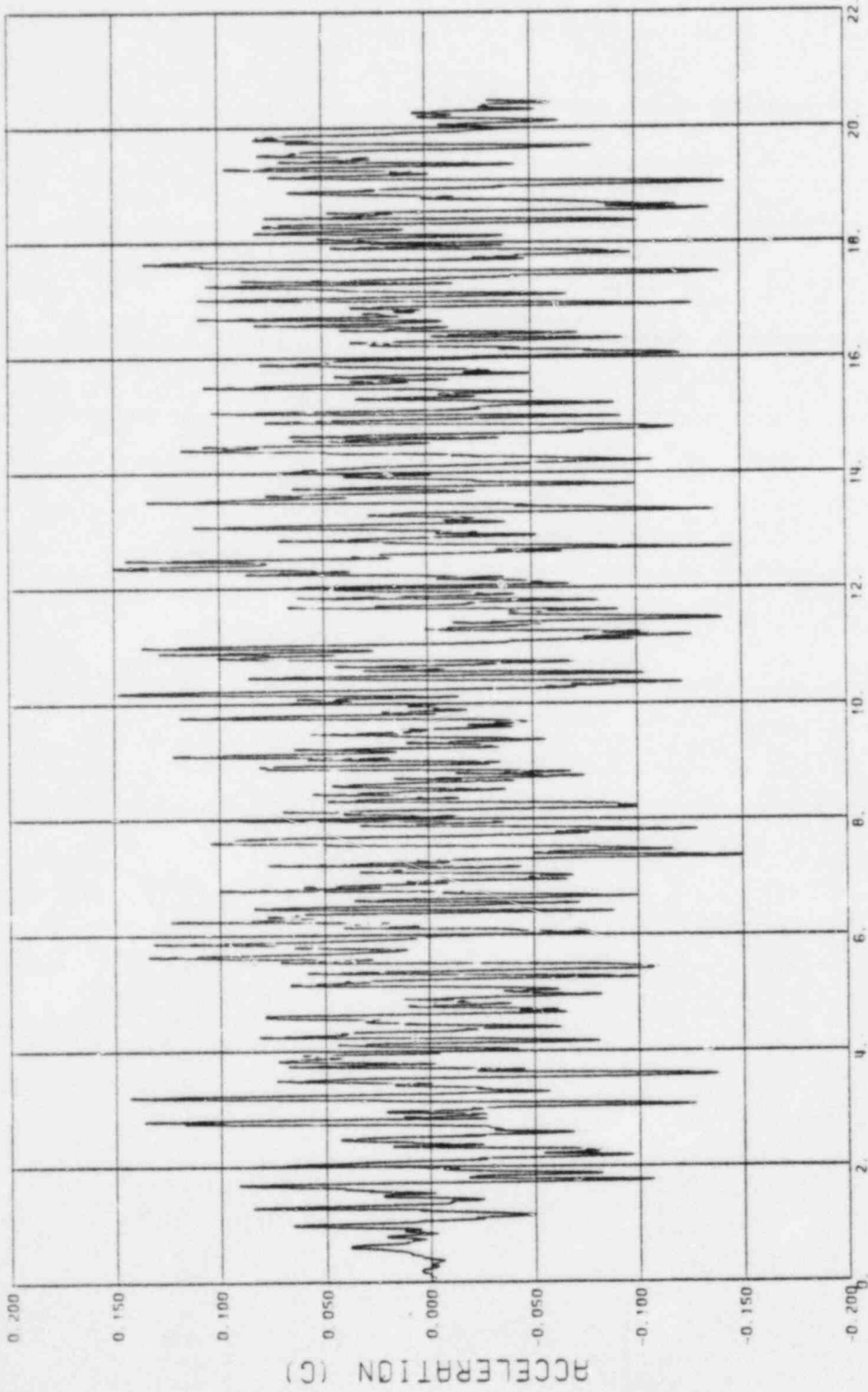
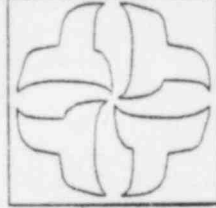


Figure 2.4 Reactor Building Model for Vertical Analysis



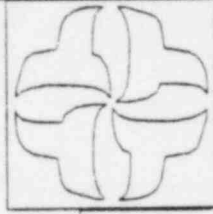
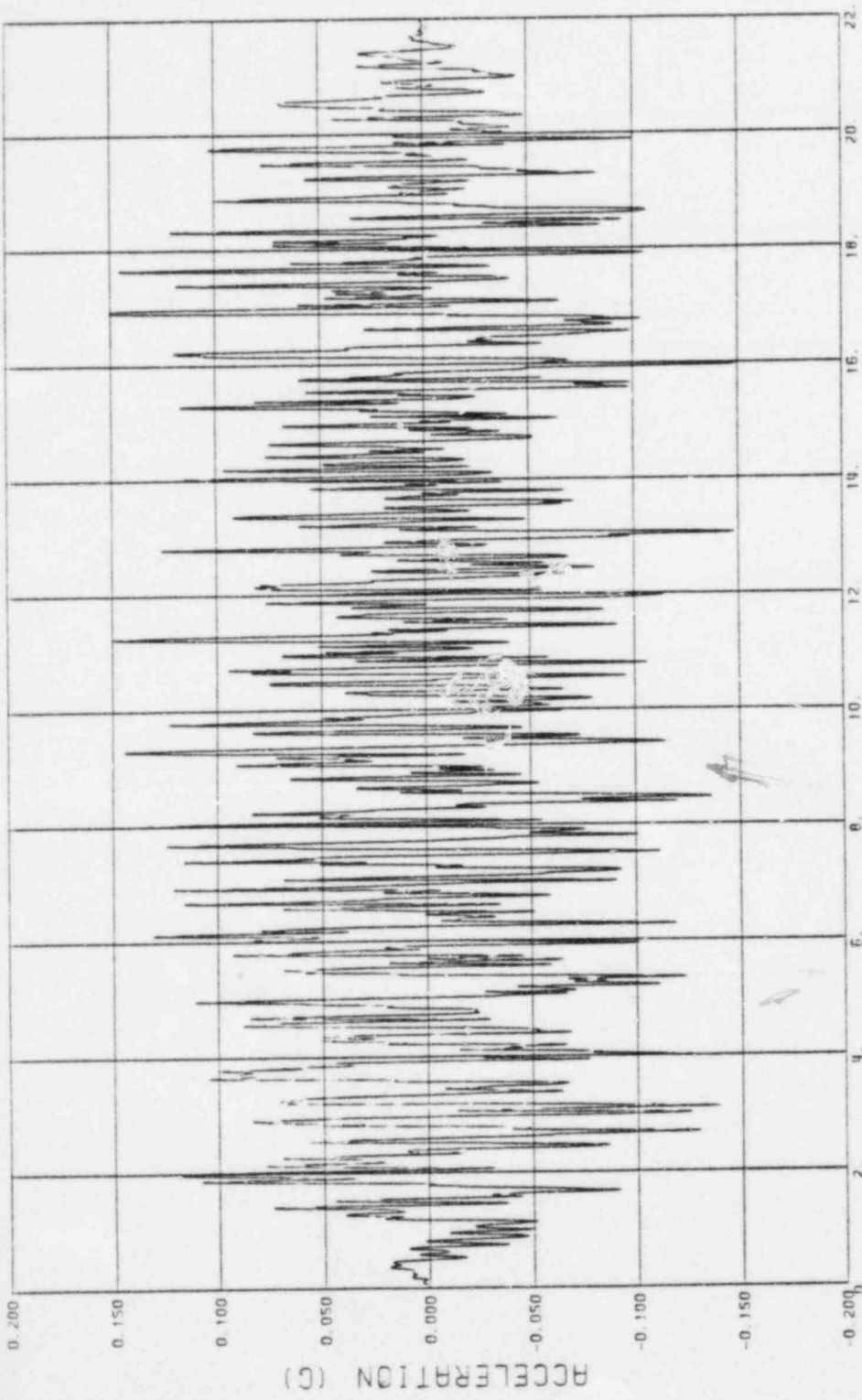
TIME (SEC.)

ACCELERATION TIME HISTORY
 INPUT MOTION - DIRECTION HI
 TIME STEP = 0.01



CESSAR II PLANT
 SOIL - STRUCTURE INTERACTION

Figure 2.5 Input Acceleration Time History - Direction HI



GESSAR II PLANT
 SOIL - STRUCTURE INTERACTION

Figure 2.6 Input Acceleration Time History - Direction H2

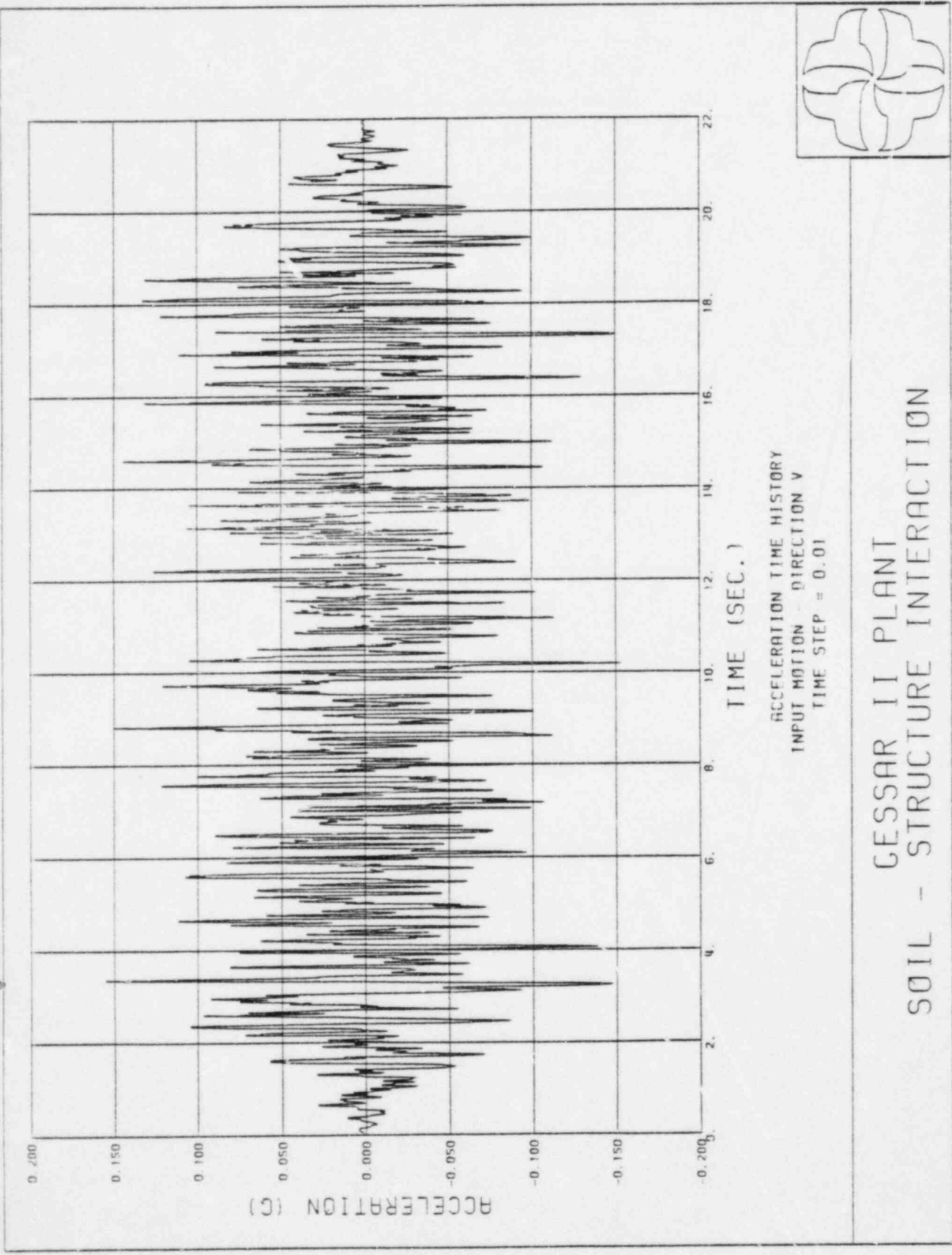
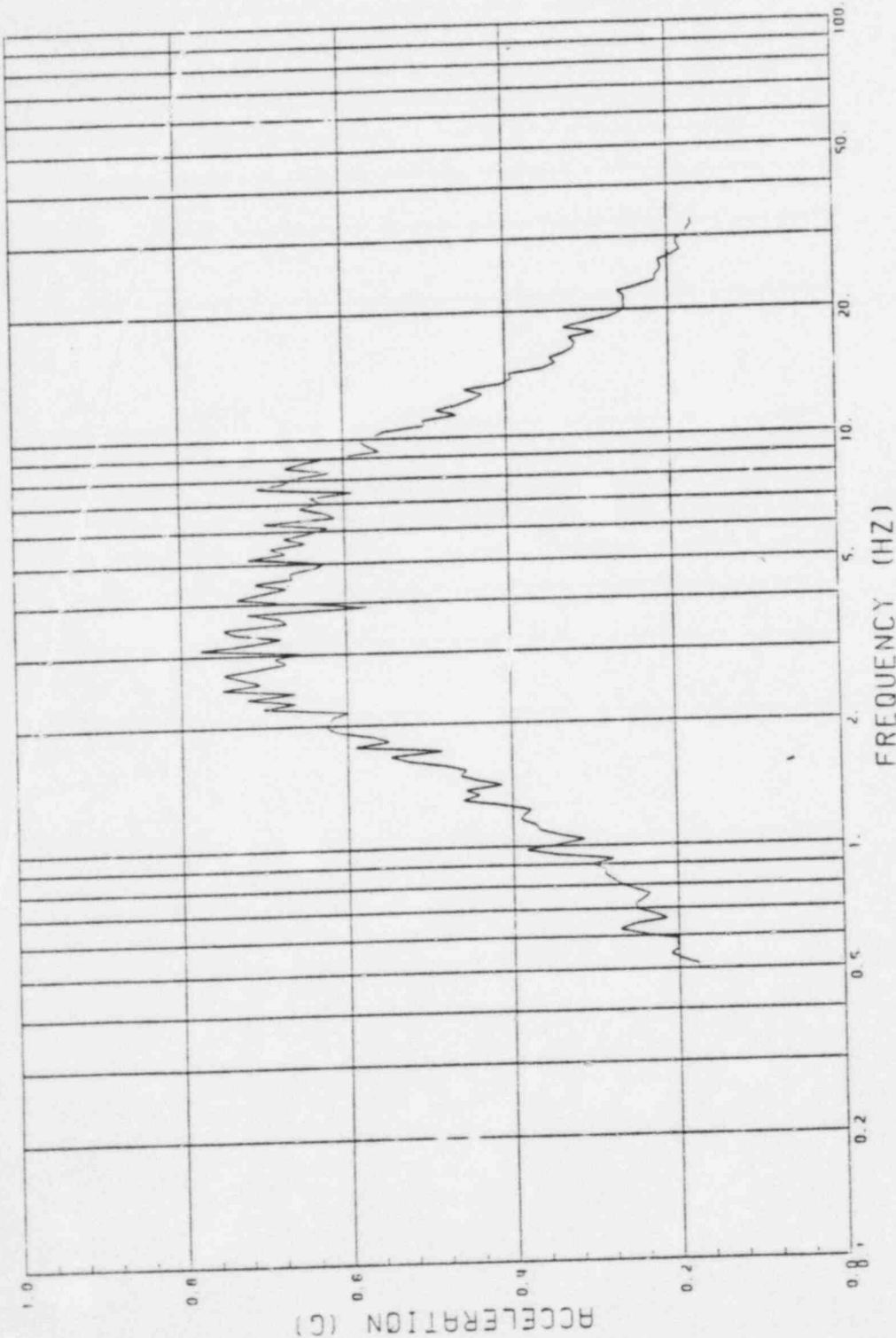
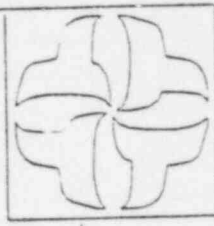


Figure 2.7 Input Acceleration Time History - Direction V



GE CLASSI ANALYSES
 ACCLN RESPONSE SPECTRUM
 INPUT MOTION-DIRECTION H1



CESSAR II PLANT
 SOIL - STRUCTURE INTERACTION

Figure 2.8 Response Spectrum of Input Motion - Direction H1

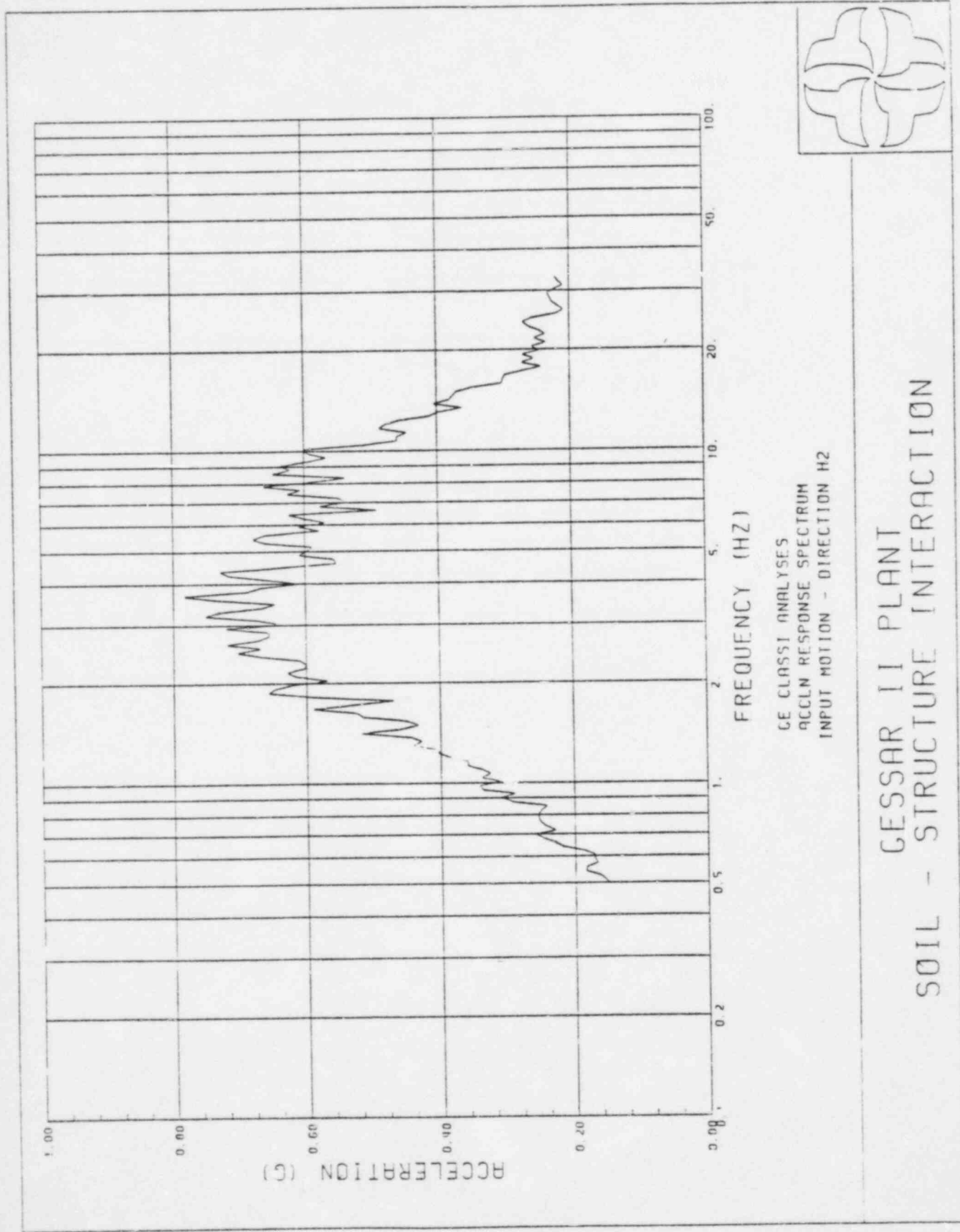
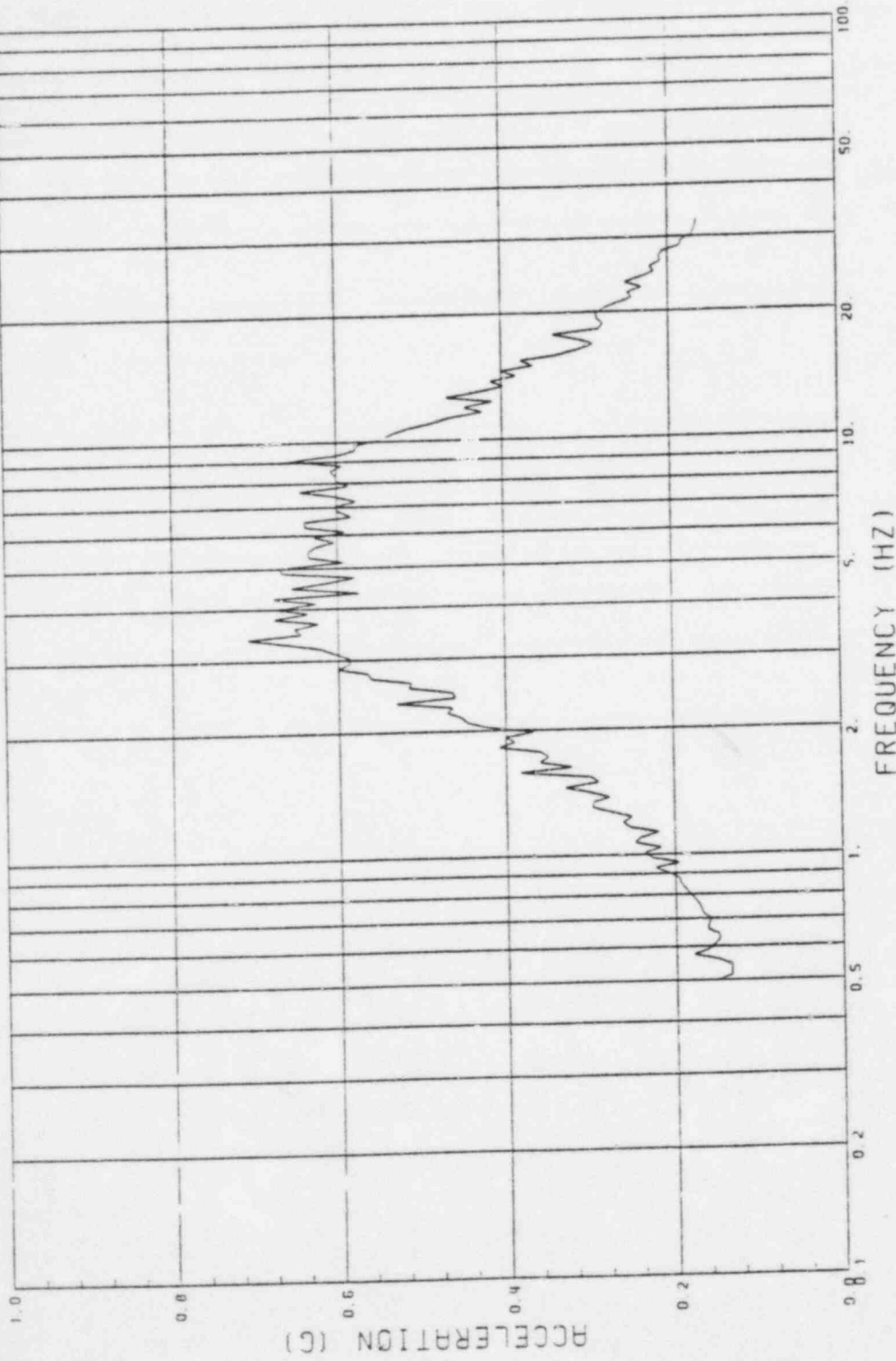
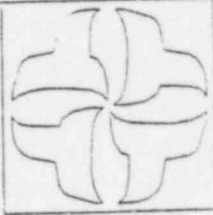


Figure 2.9 Response Spectrum of Input Motion - Direction H2



CE CLASSI ANALYSES
 ACCLN RESPONSE SPECTRUM
 INPUT MOTION - VERTICAL



CESSAR II PLANT
 SOIL - STRUCTURE INTERACTION

Figure 2.10 Response Spectrum of Input Motion - Direction V

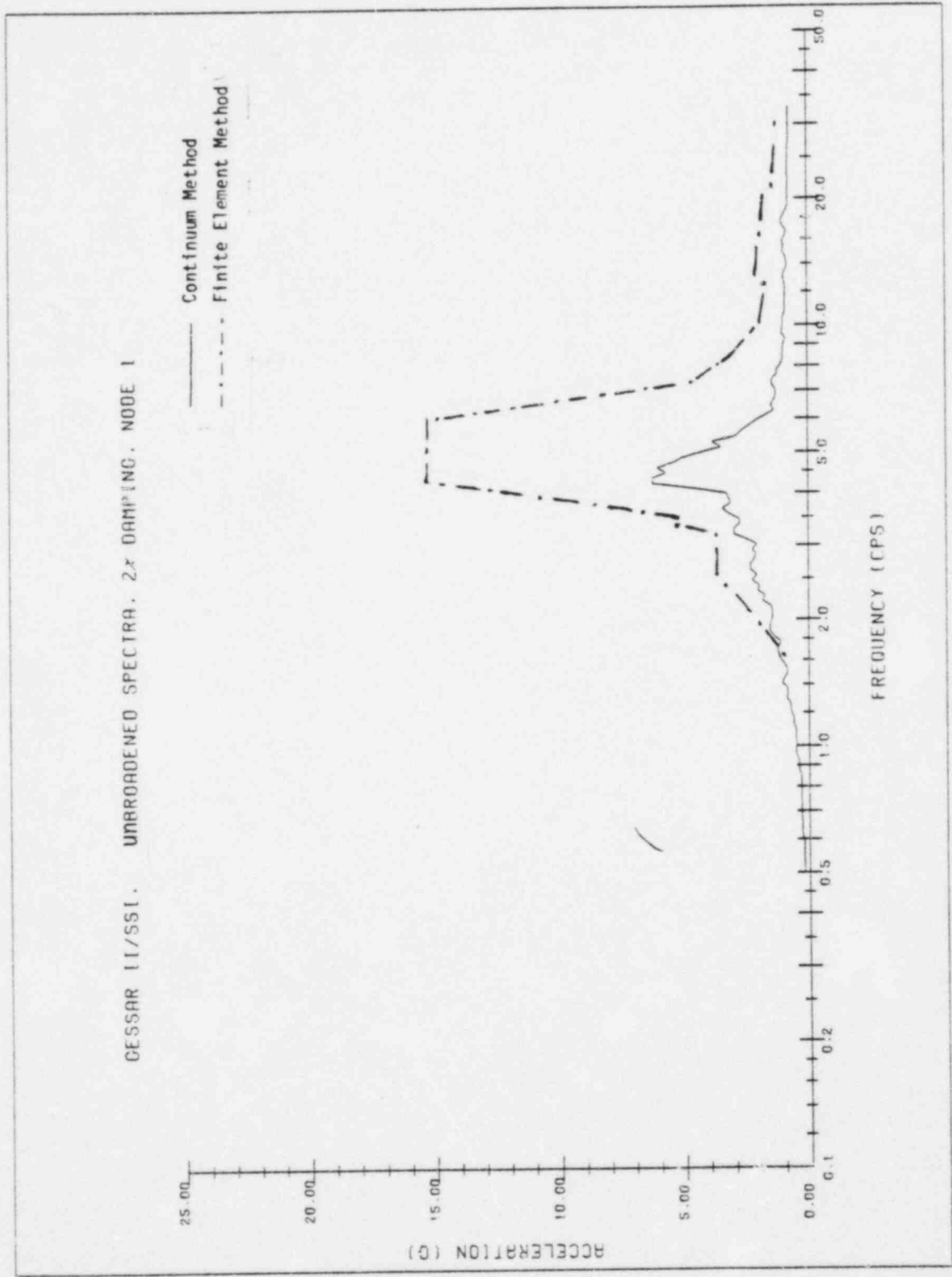


FIGURE 4.1 Comparison of Spectra Envelopes for Horizontal SSI Analyses, Node 1

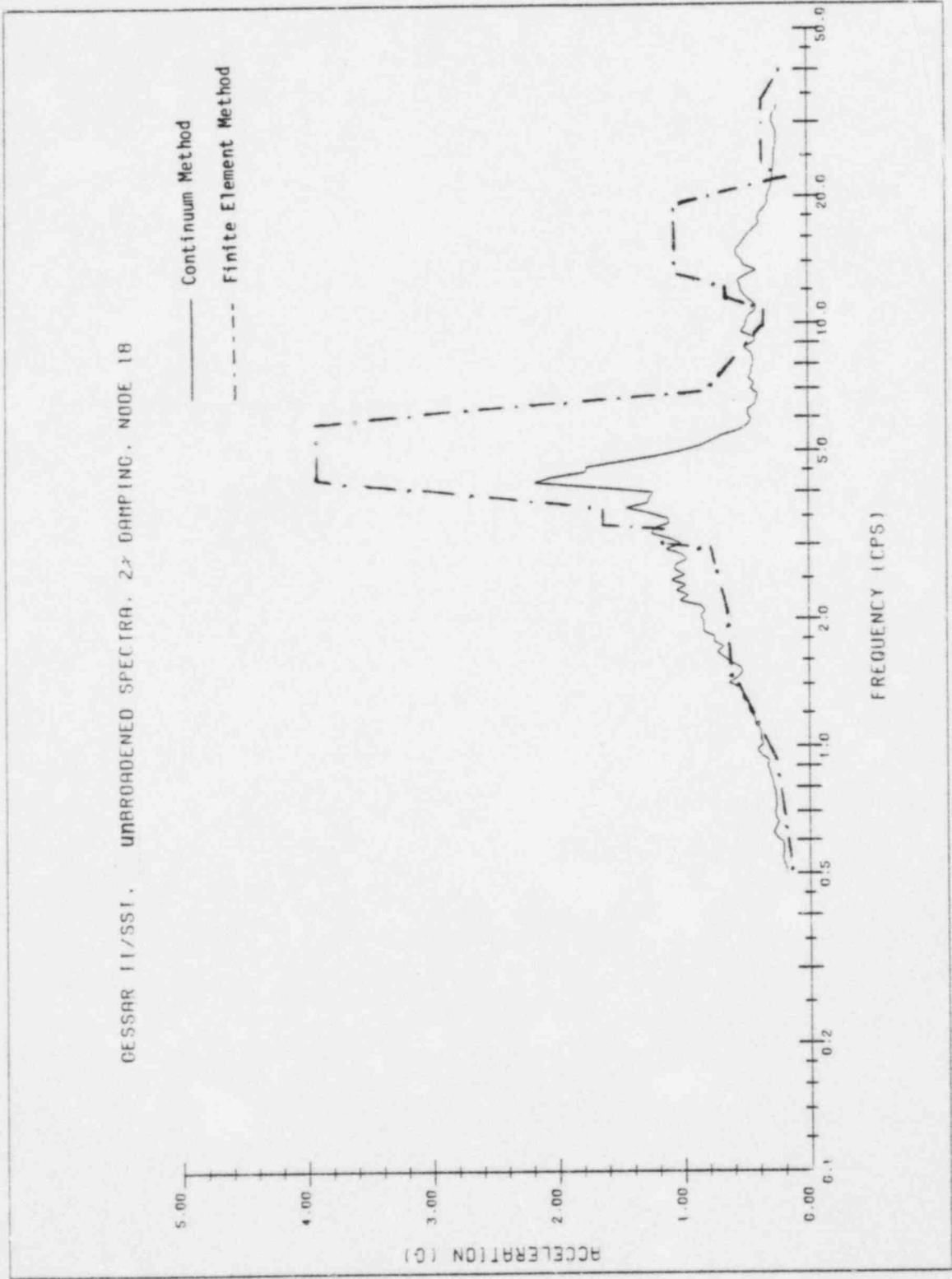


FIGURE 4.2 Comparison of Spectra Envelopes for Horizontal SSI Analyses, Node 18

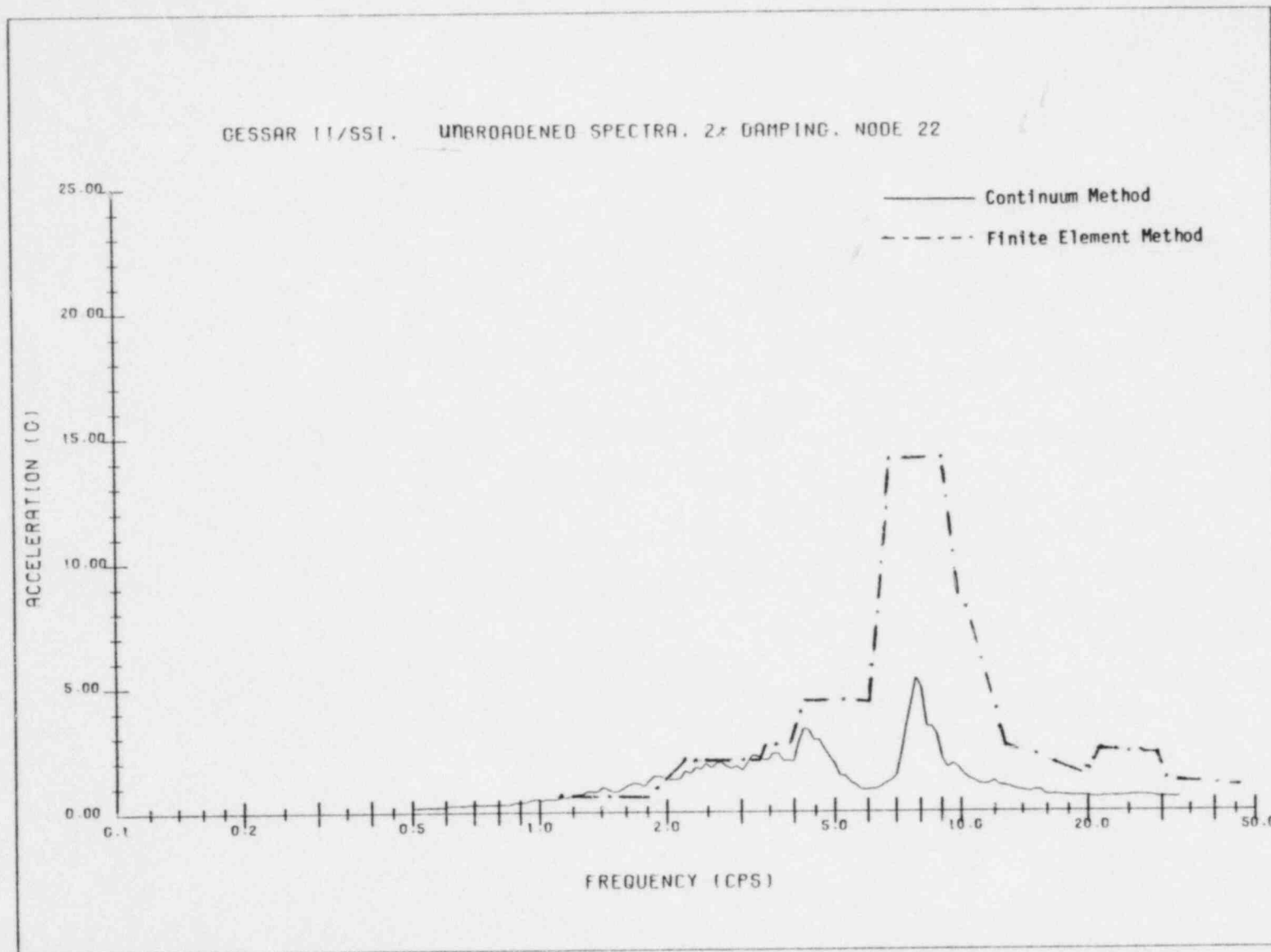


FIGURE 4.3 Comparison of Spectra Envelopes for Horizontal SSI Analyses, Node 22

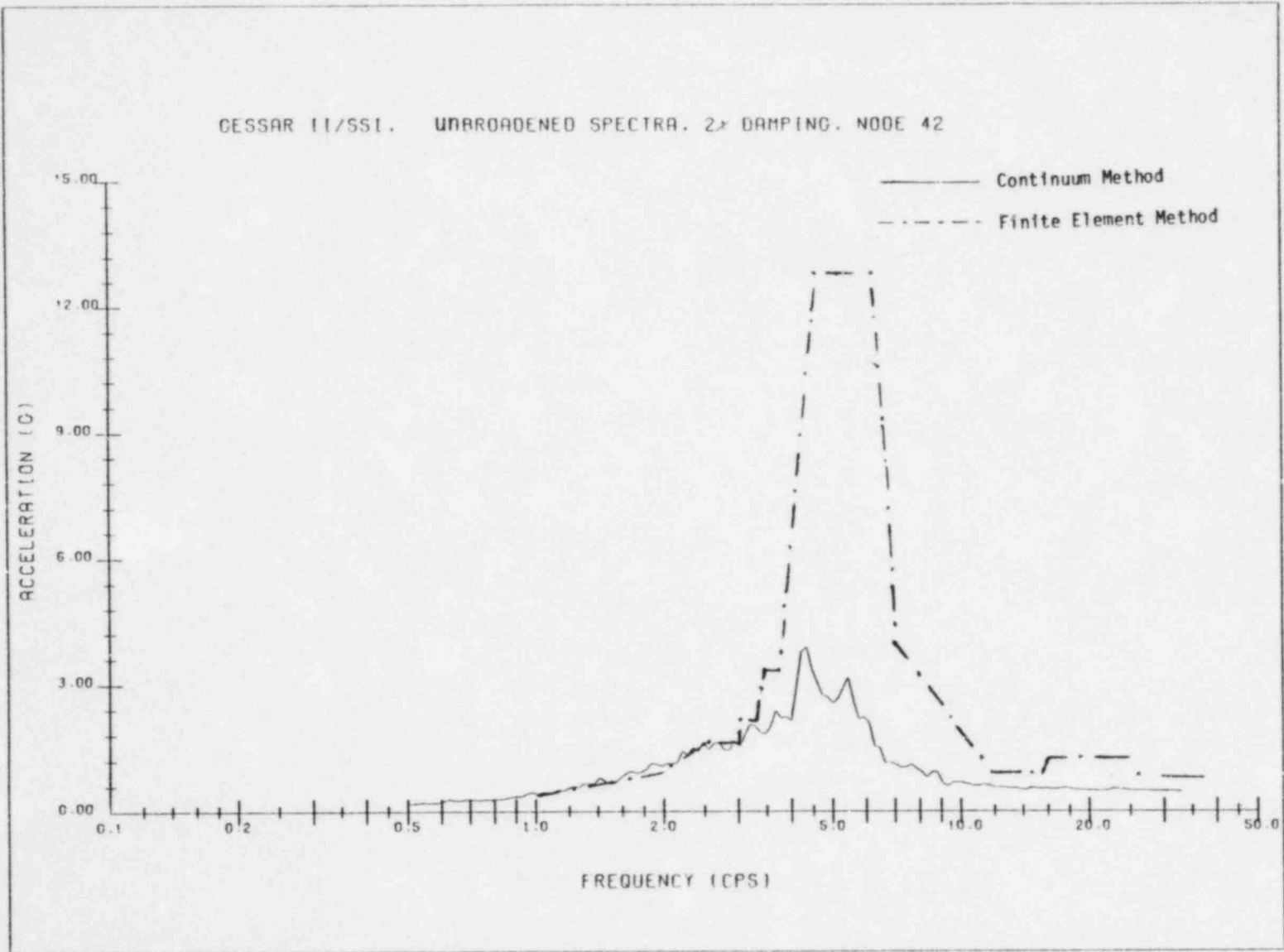


FIGURE 4.4 Comparison of Spectra Envelopes for Horizontal SSI Analyses, Node 42

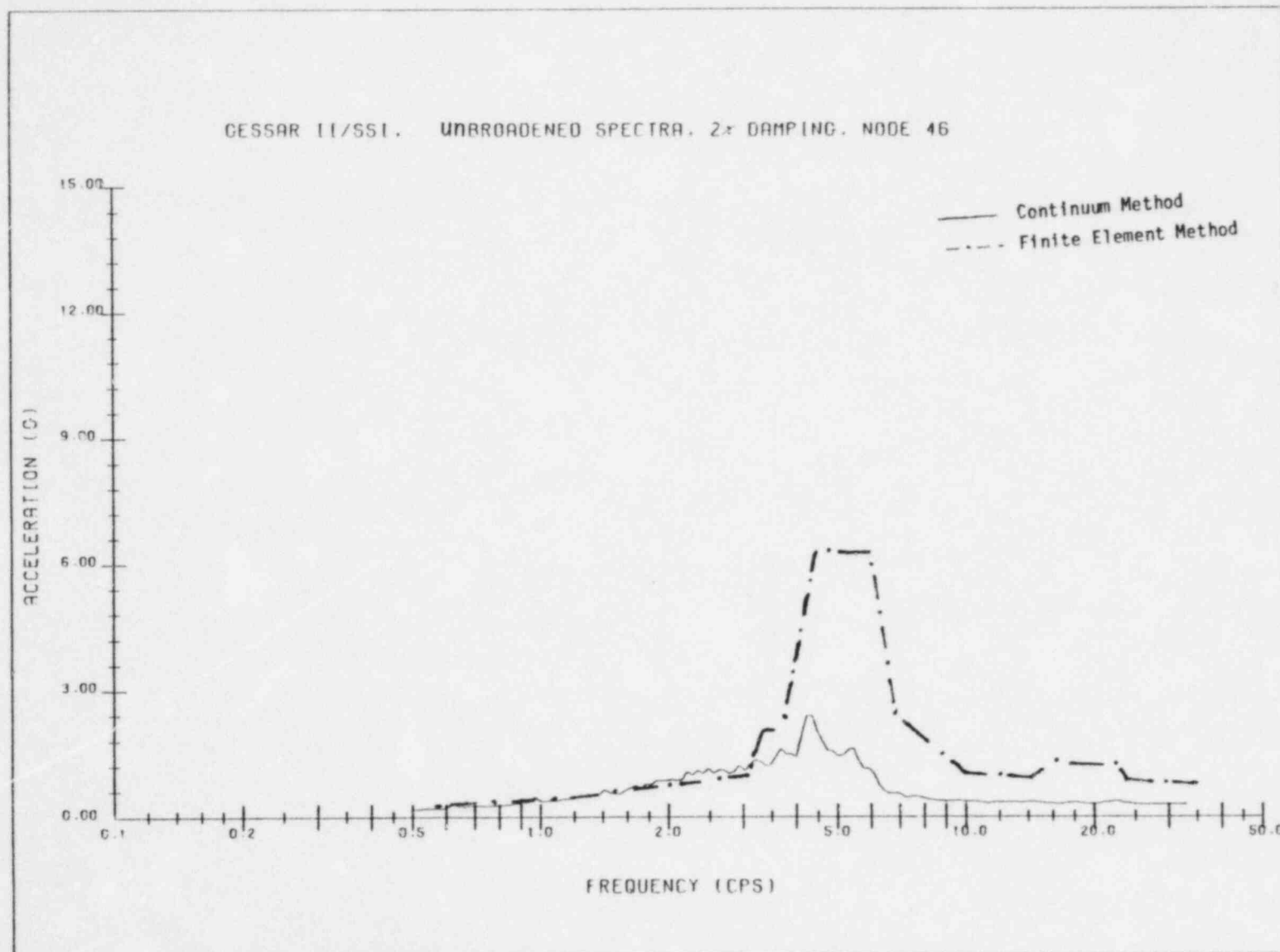


FIGURE 4.5 Comparison of Spectra Envelopes for Horizontal SSI Analyses, Node 46

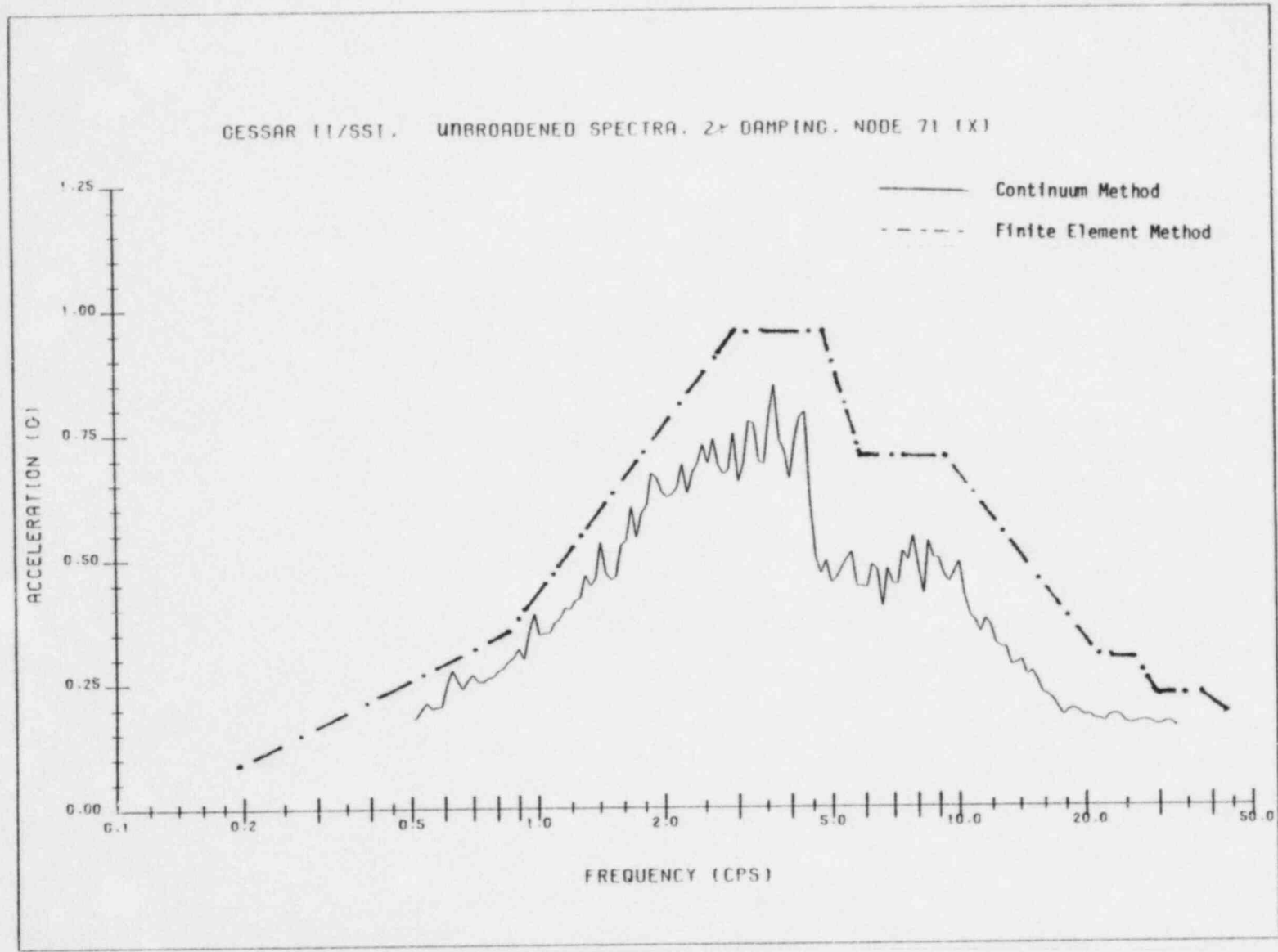


FIGURE 4.6 Comparison of Spectra Envelopes for Horizontal SSI Analyses, Node 71

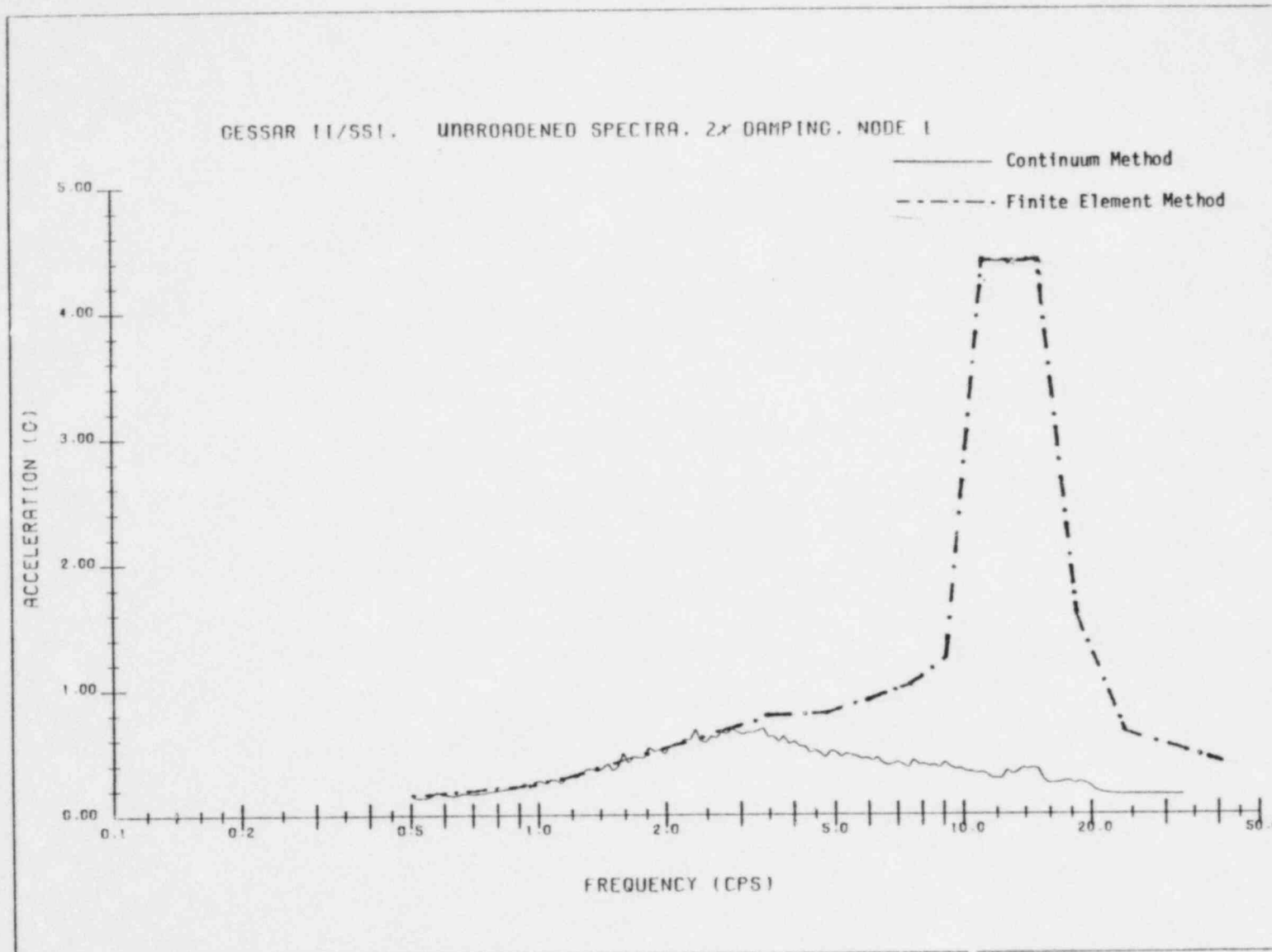


FIGURE 4.7 Comparison of Spectra Envelopes for Vertical SSI Analysis, Node 1

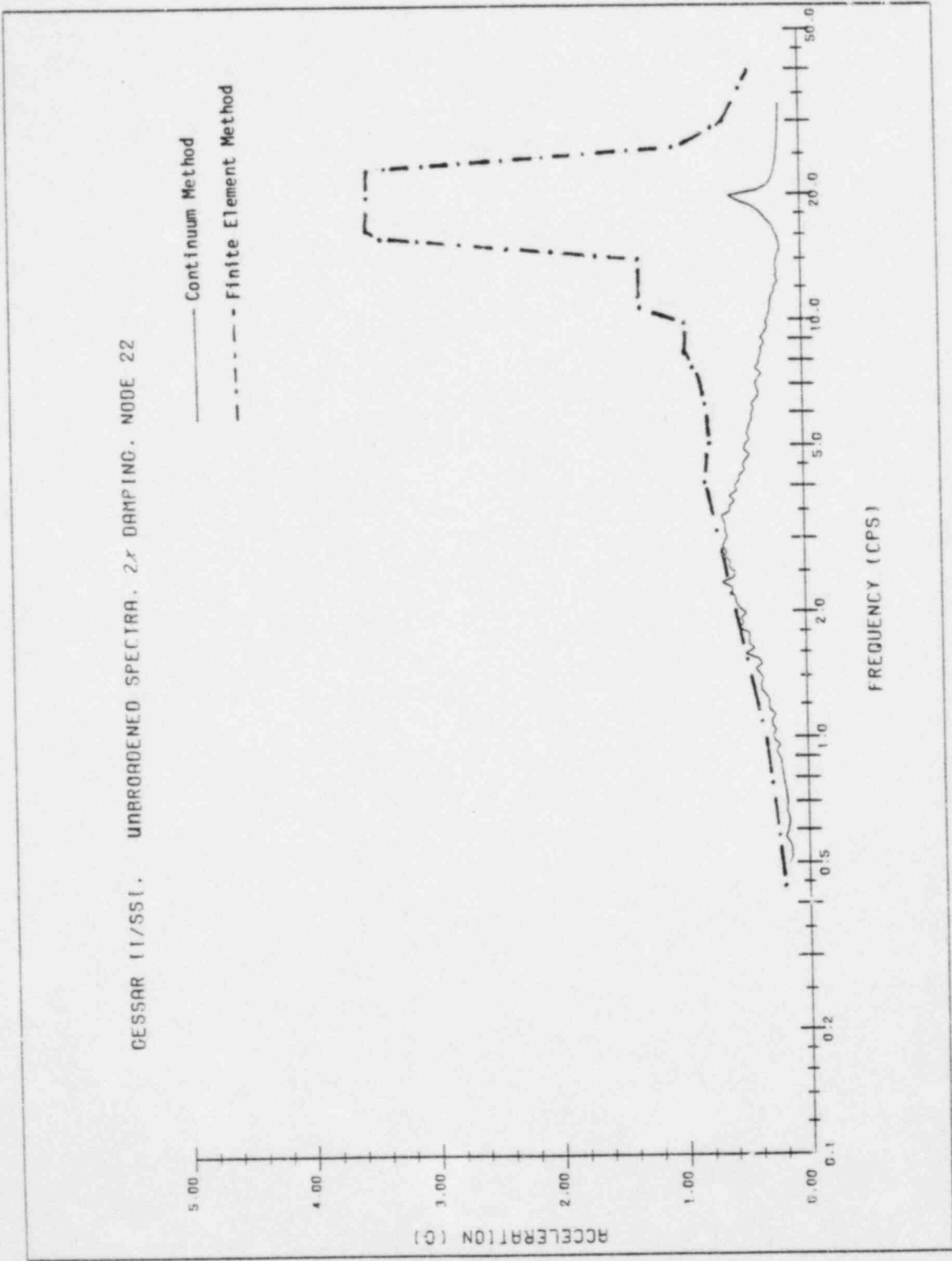


FIGURE 4.8 Comparison of Spectra Envelopes for Vertical SSI Analysis, Node 22

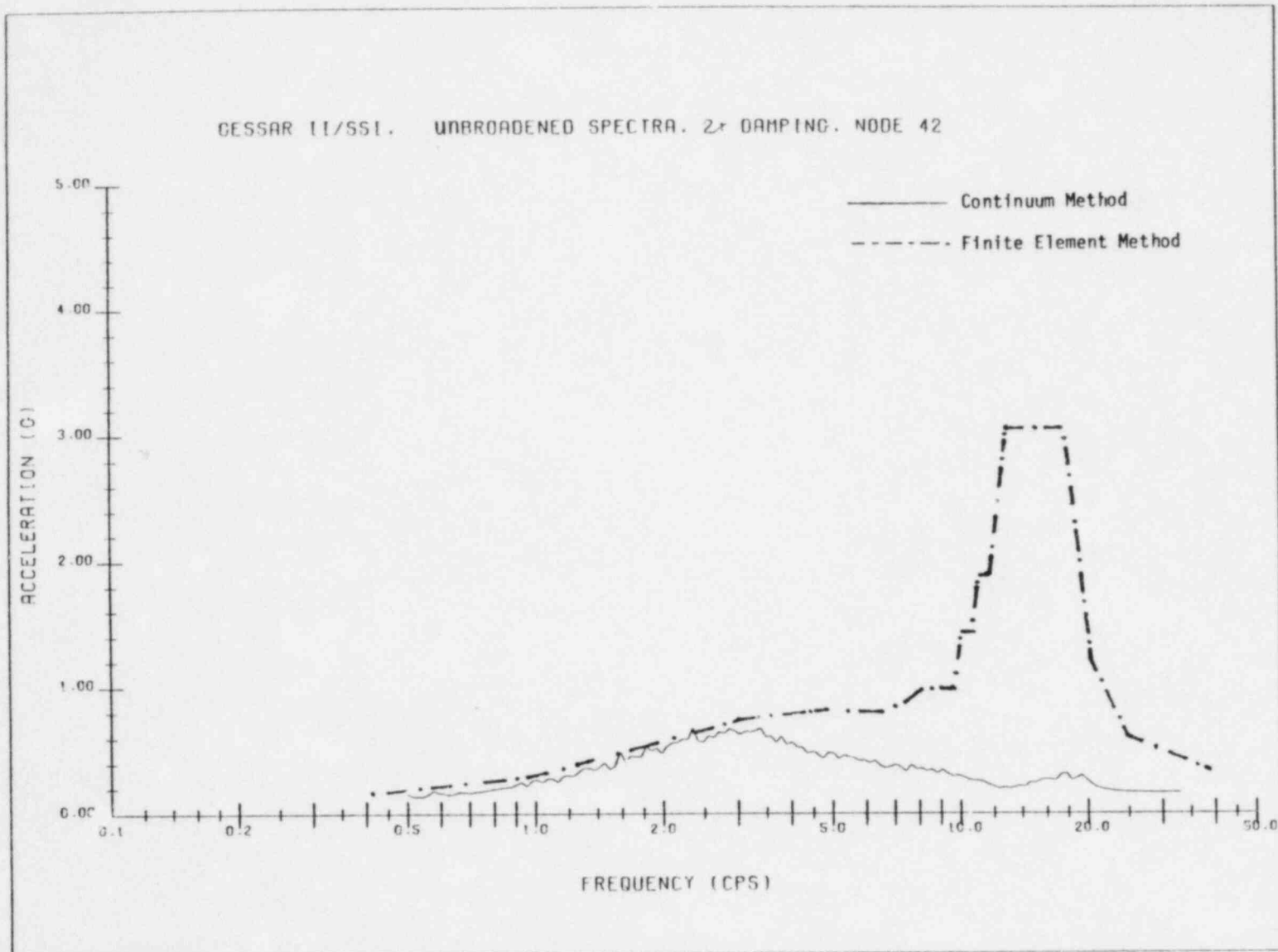


FIGURE 4.9 Comparison of Spectra Envelopes for Vertical SSI Analysis, Node 42

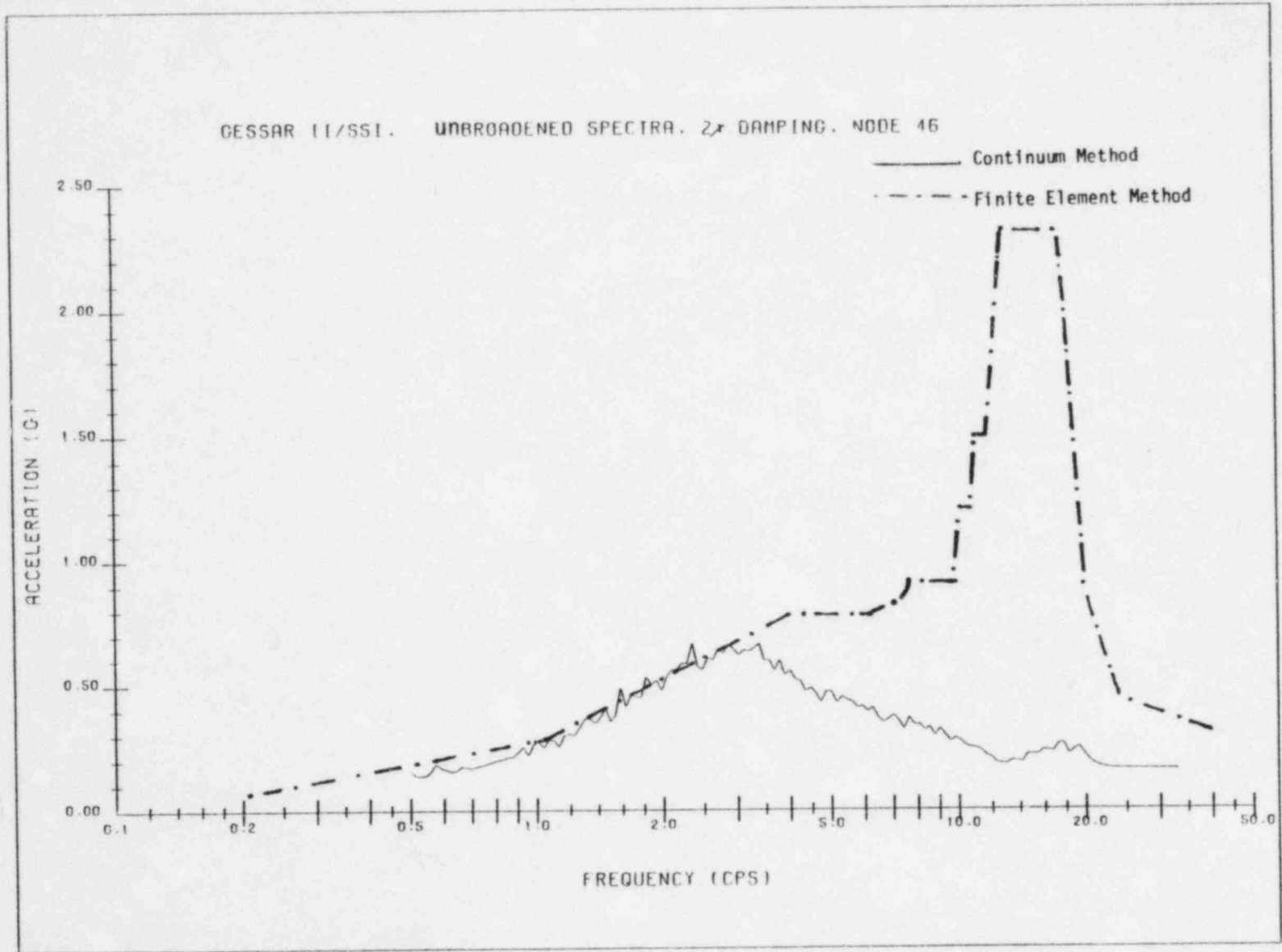


FIGURE 4.10 Comparison of Spectra Envelopes for Vertical SSI Analysis, Node 46

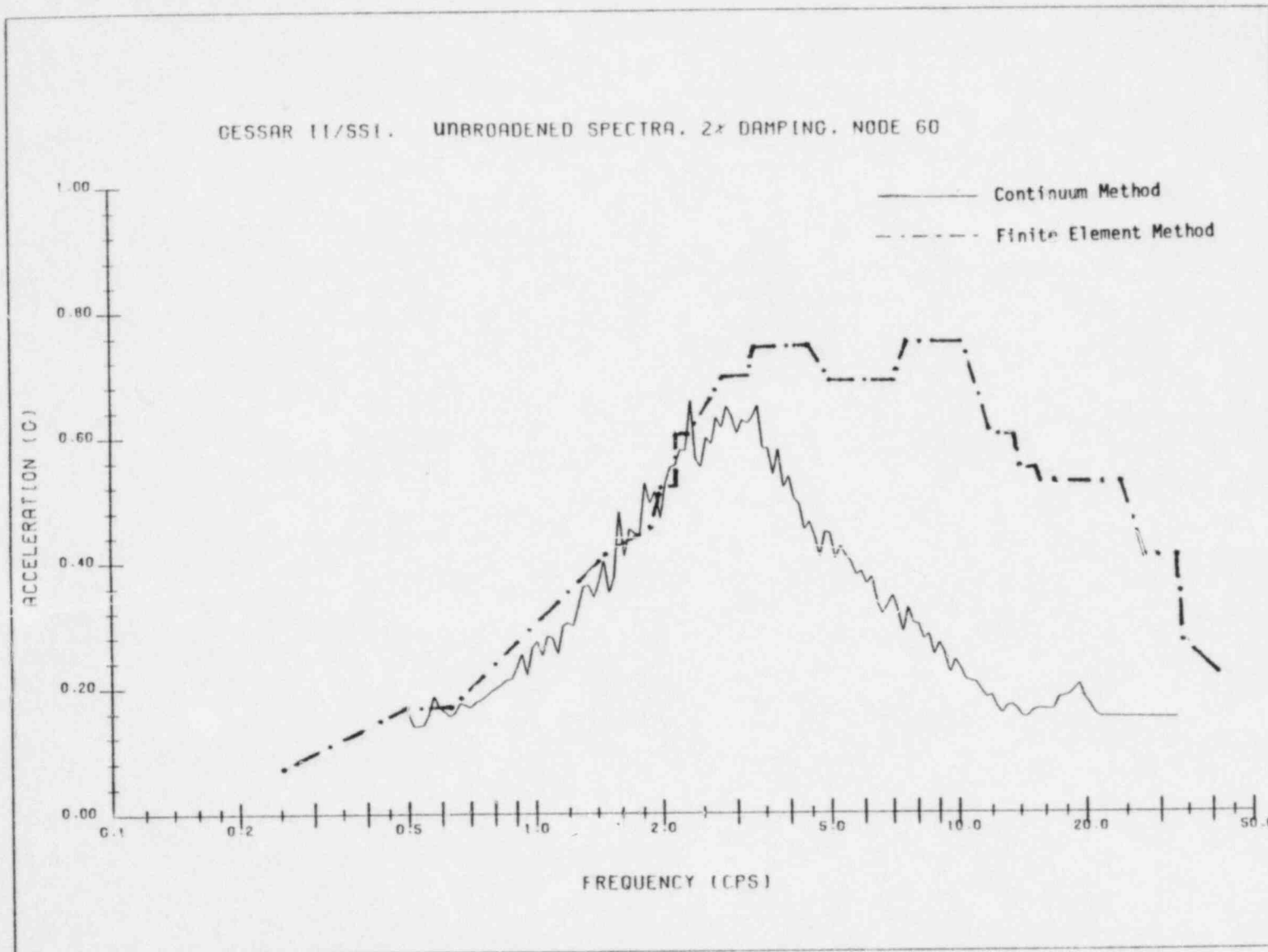


FIGURE 4.11 Comparison of Spectra Envelopes for Vertical SSI Analysis, Node 60

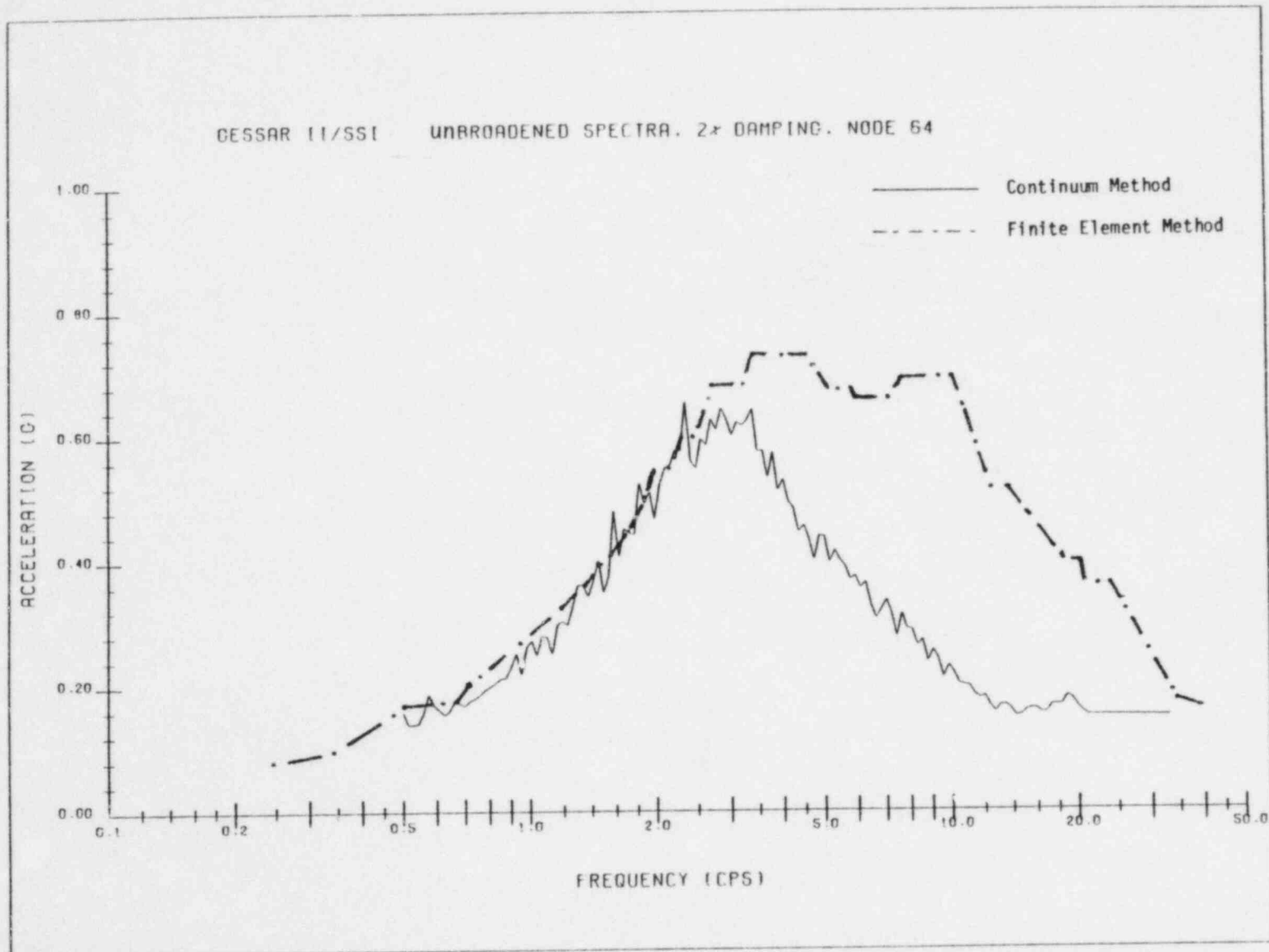


FIGURE 4.12 Comparison of Spectra Envelopes for Vertical SSI Analysis, Node 64

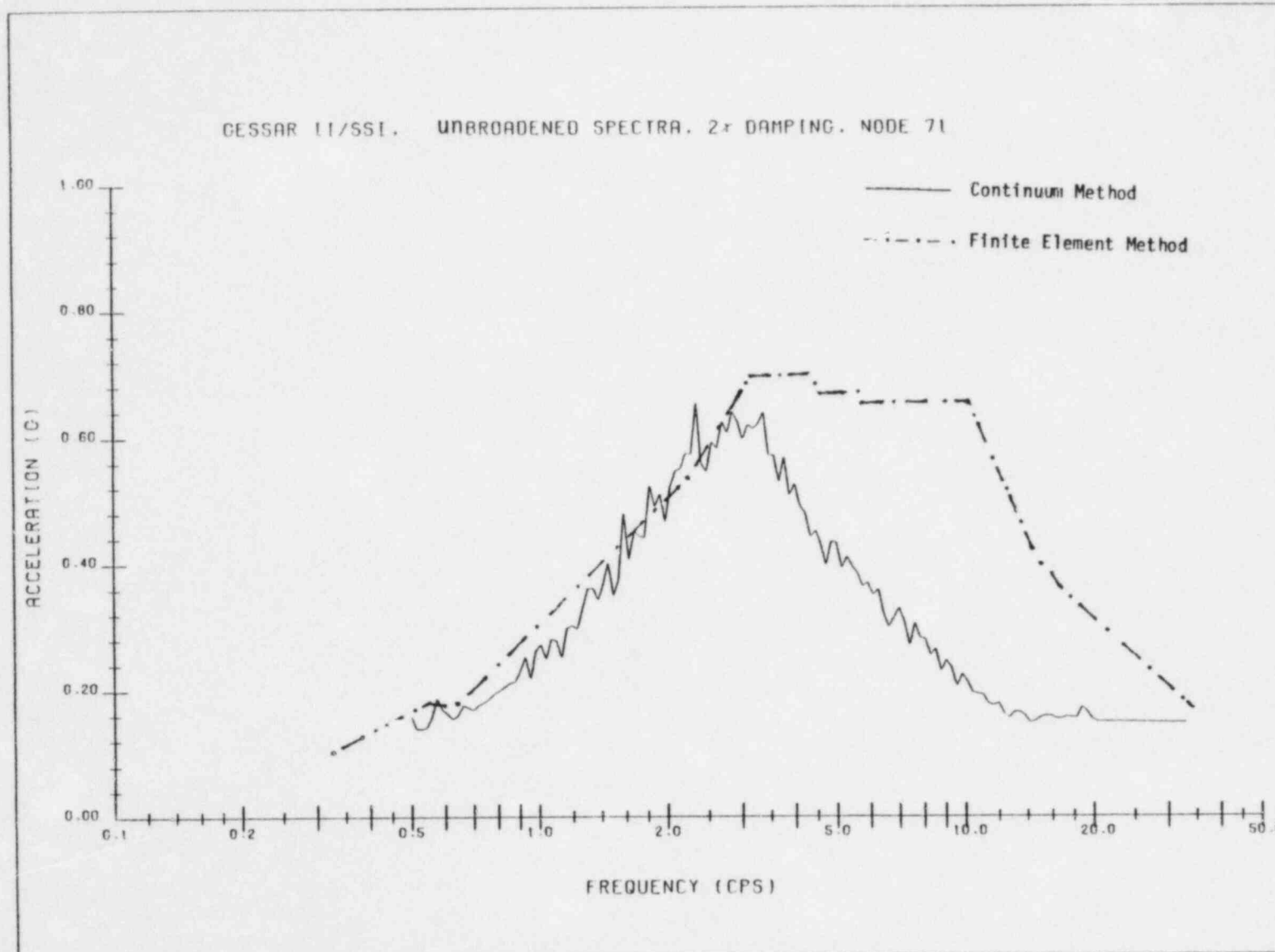


FIGURE 4.13 Comparison of Spectra Envelopes for Vertical SSI Analysis, Node 71

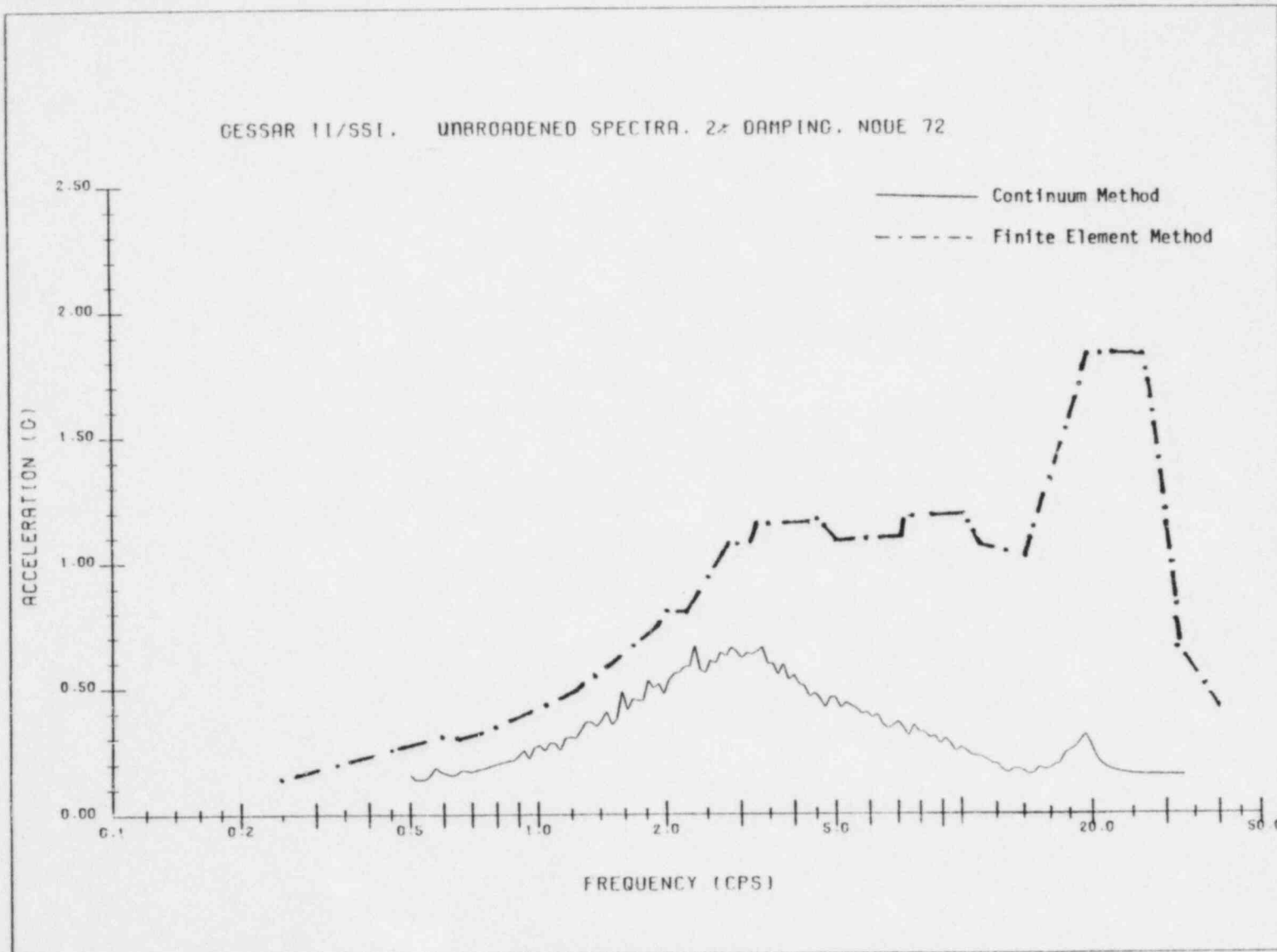


FIGURE 4.14 Comparison of Spectra Envelopes for Vertical SSI Analysis, Node 72

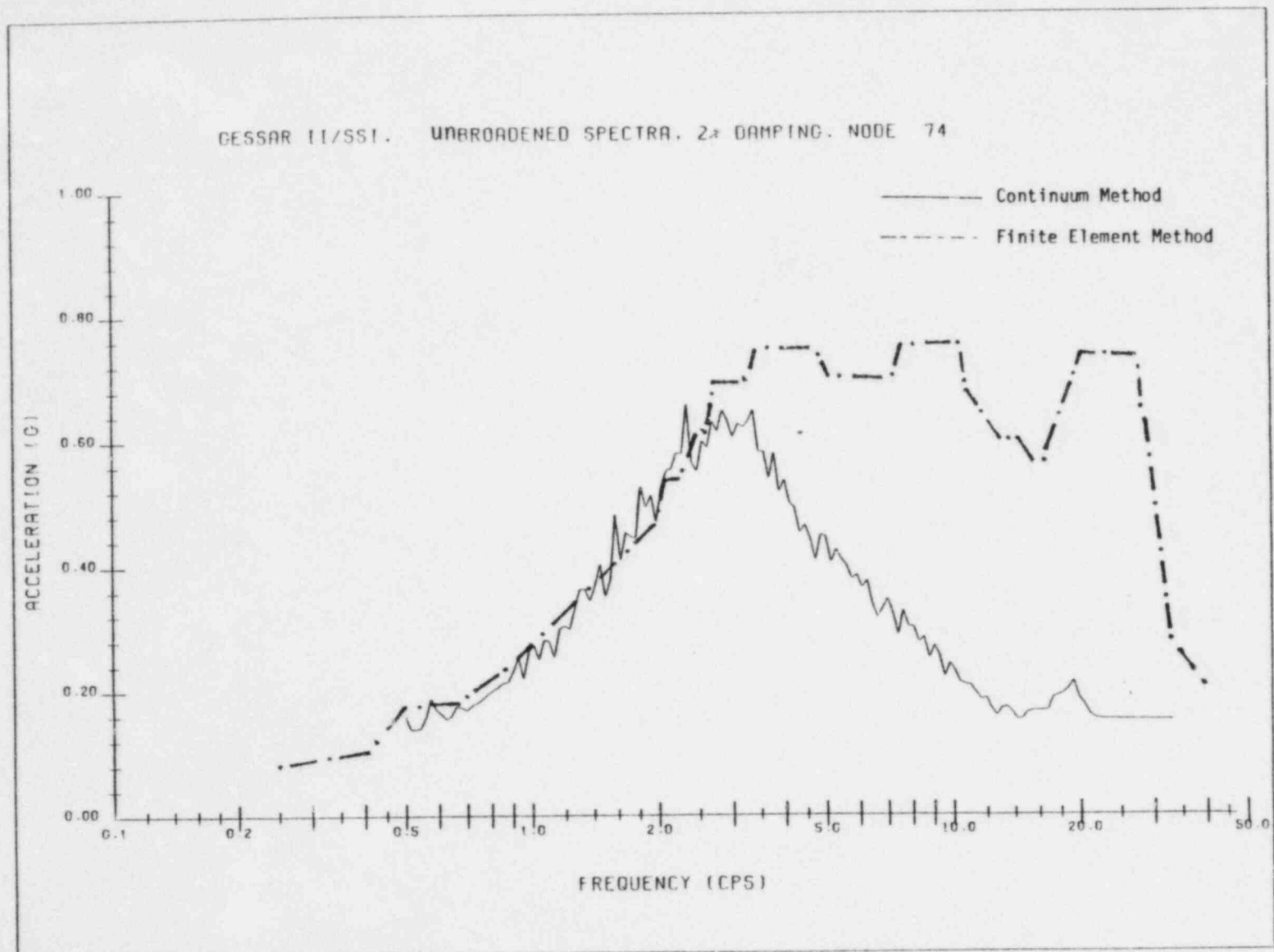


FIGURE 4.15 Comparison of Spectra Envelopes for Vertical SSI Analysis, Node 74

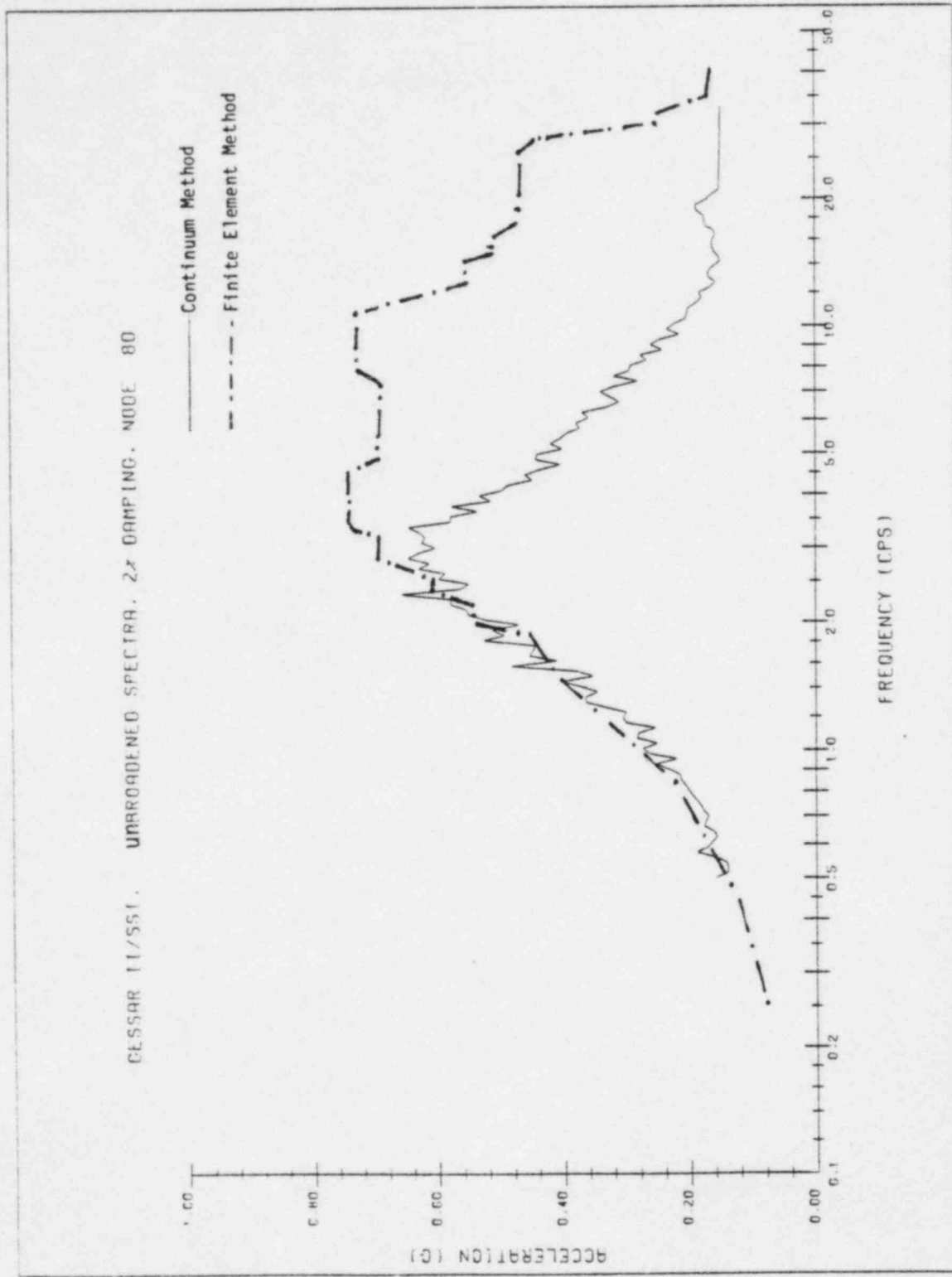


FIGURE 4.16 Comparison of Spectra Envelopes for Vertical SSI Analysis, Node 80

CONFIRMATORY
SOIL-STRUCTURE INTERACTION ANALYSES
FOR GESSAR II
(APPENDIX A)

Prepared for:

General Electric Company
Nuclear Engineering Division
San Jose, California 95125

Prepared by:

Impell Corporation
350 Lennon Lane
Walnut Creek, California 94598

Impell Report No. 04-0030-0077

July 1983

TABLE OF CONTENTS

DESCRIPTION OF CONTENTS

APPENDIX A: Acceleration Response Spectra for the
GESSAR II Horizontal and Vertical Analyses

DESCRIPTION OF CONTENTS

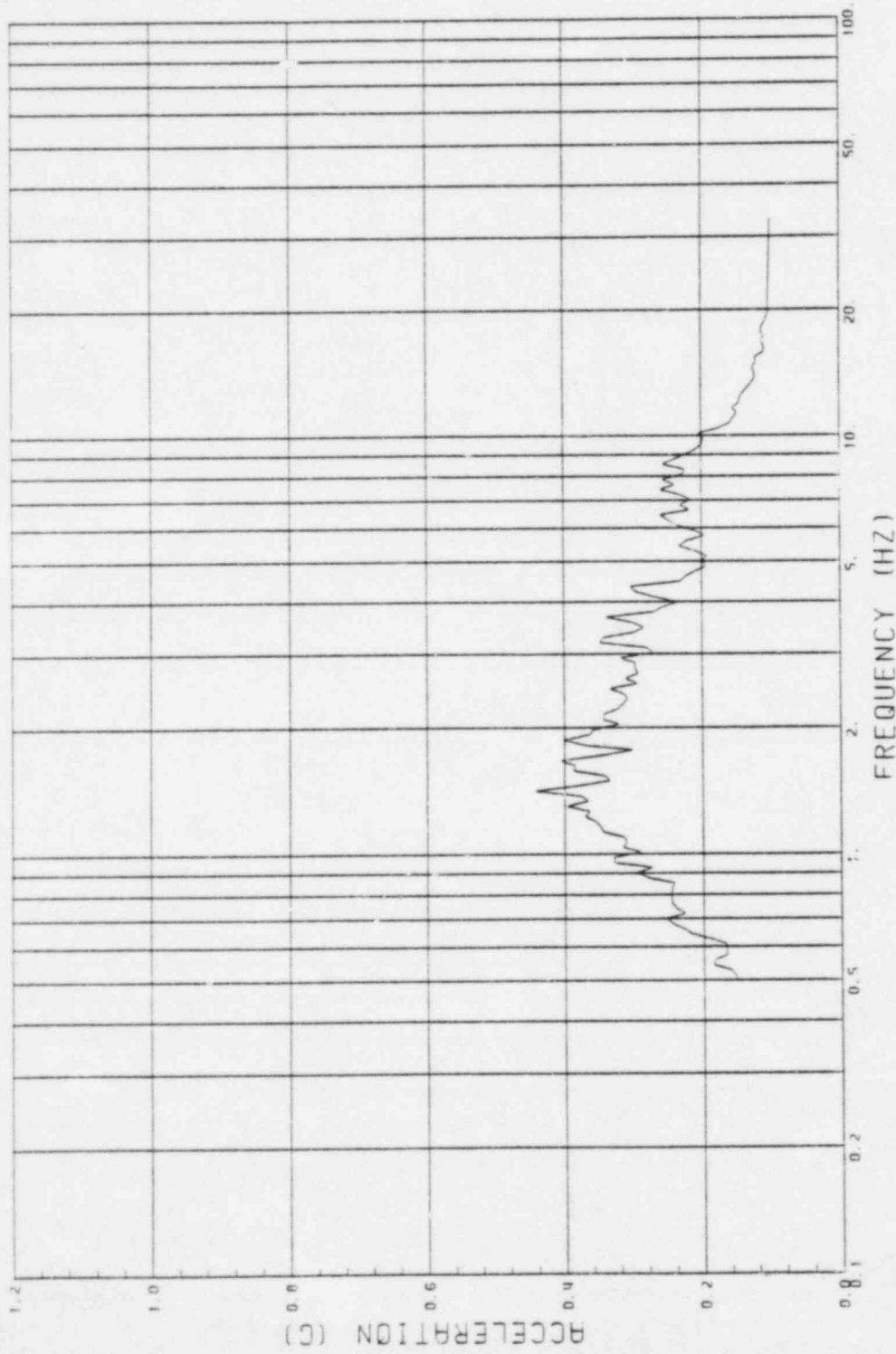
This appendix to Impell Report No. 04-0030-0077, prepared for General Electric Company, contains partial results corresponding to the series of confirmatory soil-structure interaction (SSI) analyses performed for the GESSAR II Standard Plant using the CLASSI series of computer codes.

The results presented consist of plots of acceleration response spectra, at 2 percent damping value, for a total of 10 locations throughout the GESSAR II Reactor Building structure. In addition, the rocking acceleration spectrum at the basemat level is included.

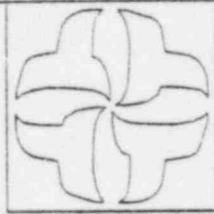
Figures A.1 through A.77 correspond to acceleration response spectra for the horizontal analyses. Figures A.78 through A.87 correspond to response spectra for the vertical analysis case.

APPENDIX A

ACCELERATION RESPONSE SPECTRA FOR THE
GESSAR II HORIZONTAL AND VERTICAL ANALYSES

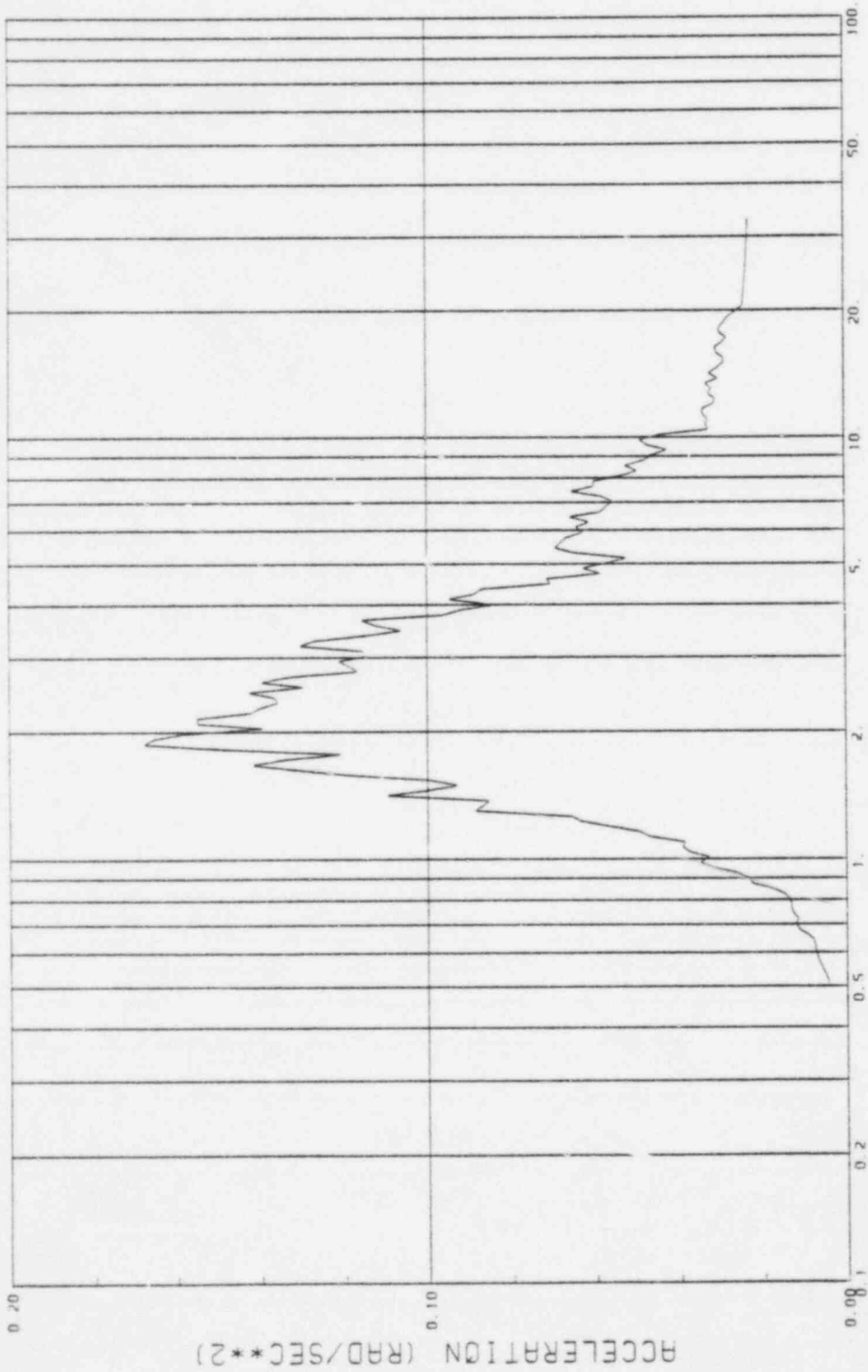


GE CLASSI ANALYSES
CASE 1, GE-75-L-H2
BASEMAT, NODE NO. 71 (TRANSLATION)

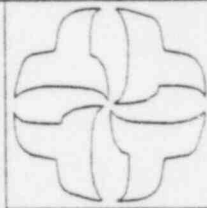


CESSAR II PLANT
SOIL - STRUCTURE INTERACTION

Figure A.1



GE CLASSI ANALYSES
CASE 1, GE-75-L-H2
BASEMAT, NODE NO. 71 (ROTATION)



CESSAR II PLANT
SOIL - STRUCTURE INTERACTION

Figure A.2

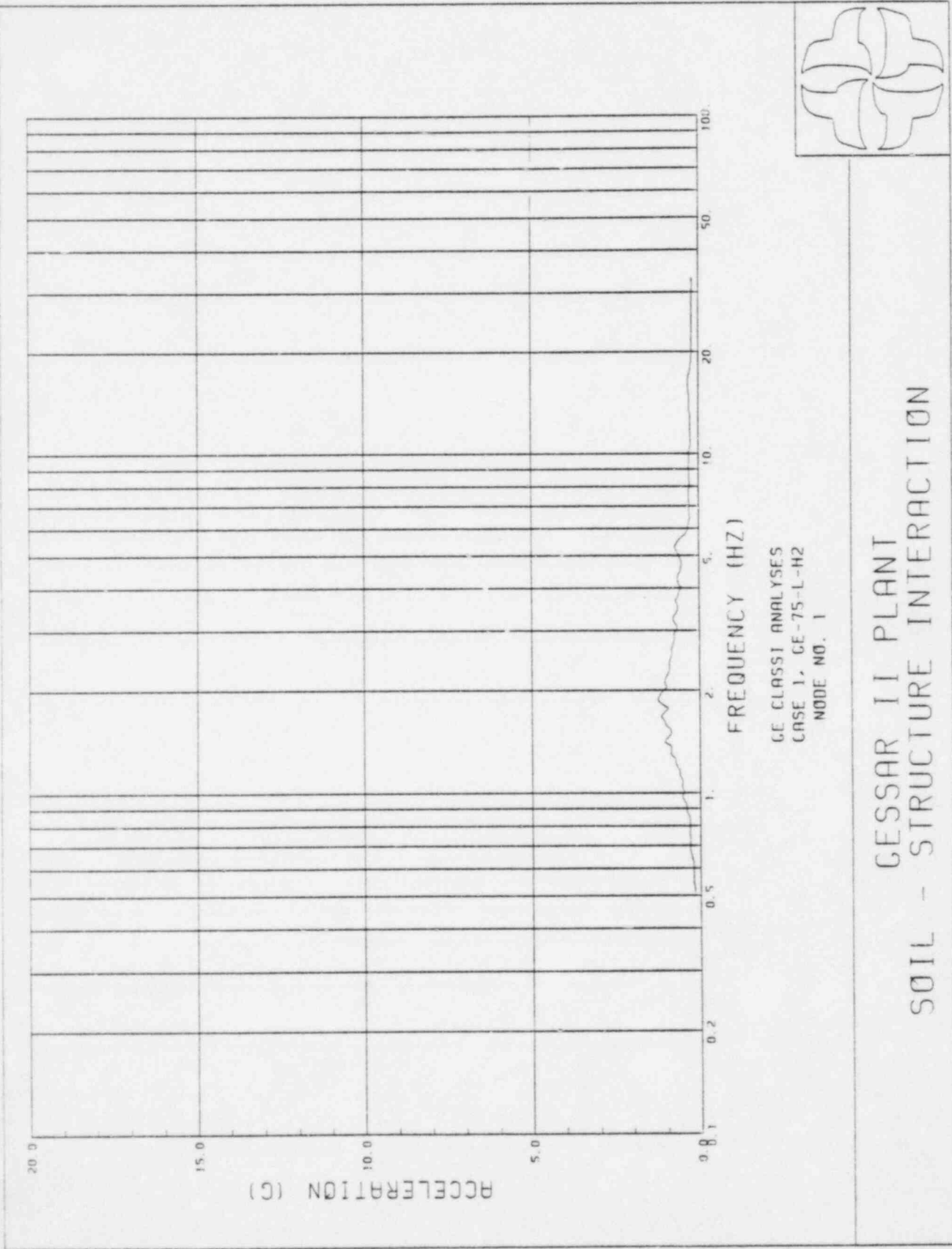
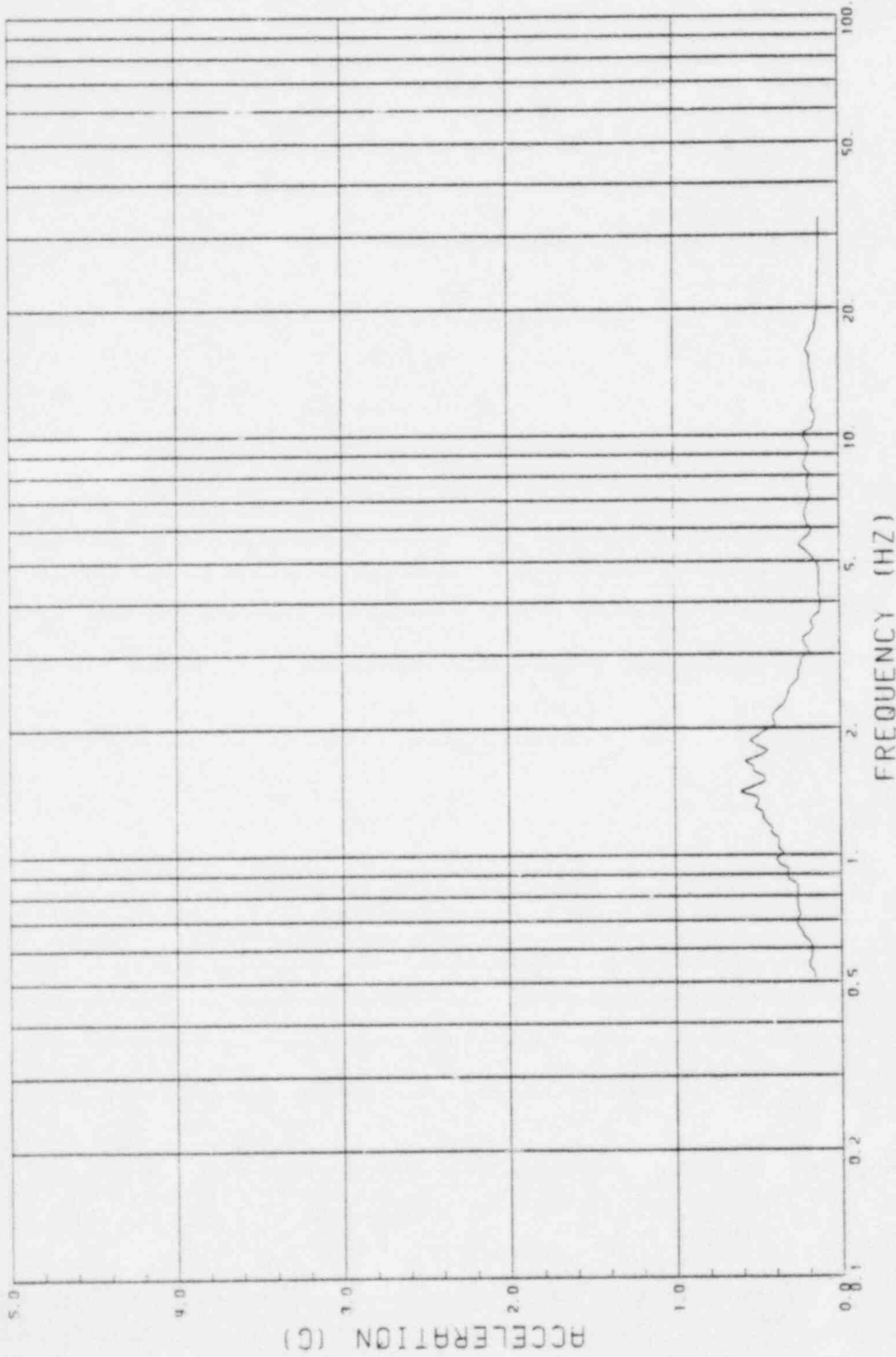
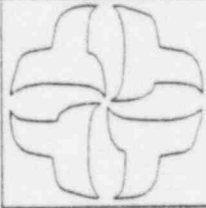


Figure A.3



GE CLASSI ANALYSES
CASE 1, GE-75-L-H2
NODE NO. 18

CESSAR II PLANT
SOIL - STRUCTURE INTERACTION

Figure A.4

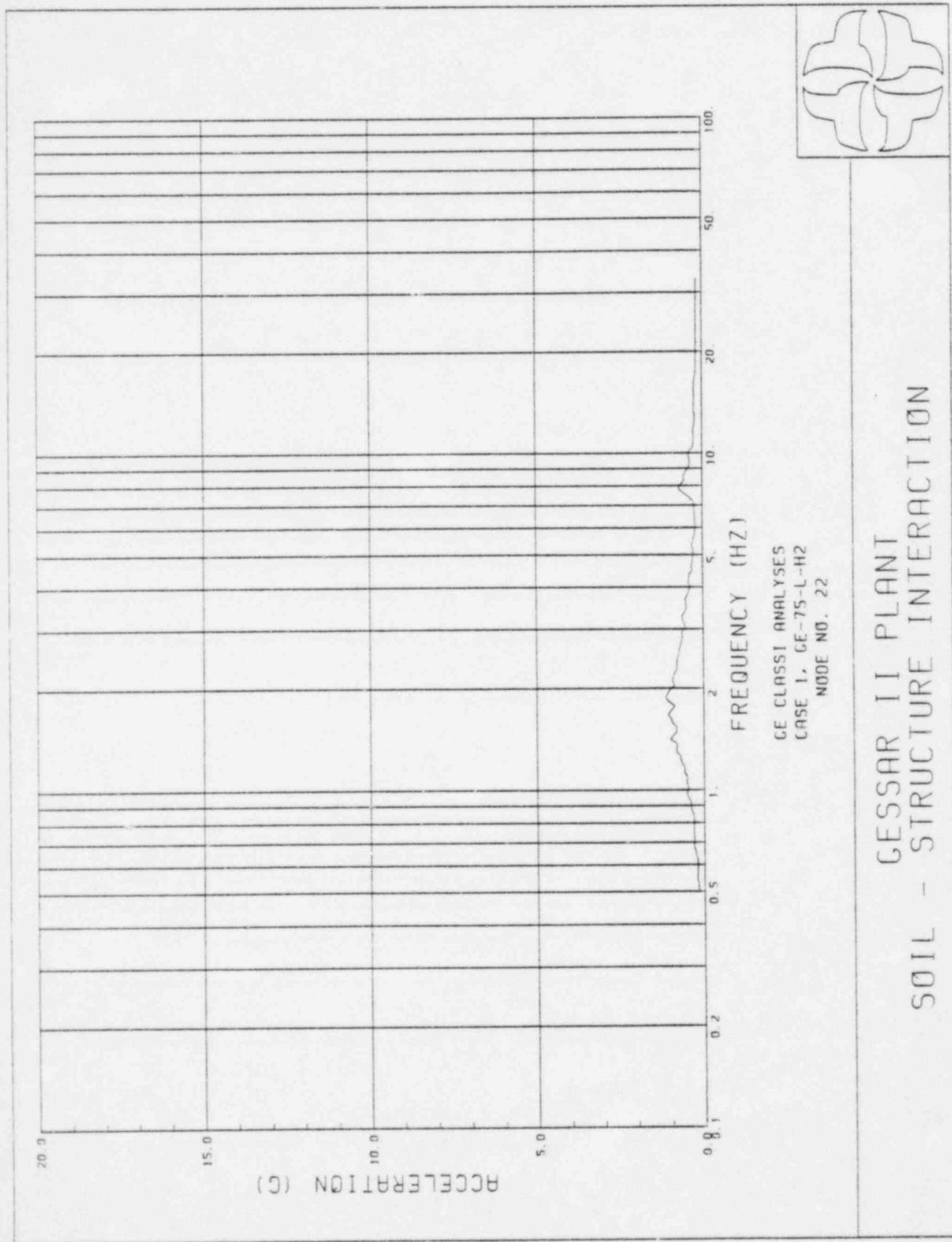
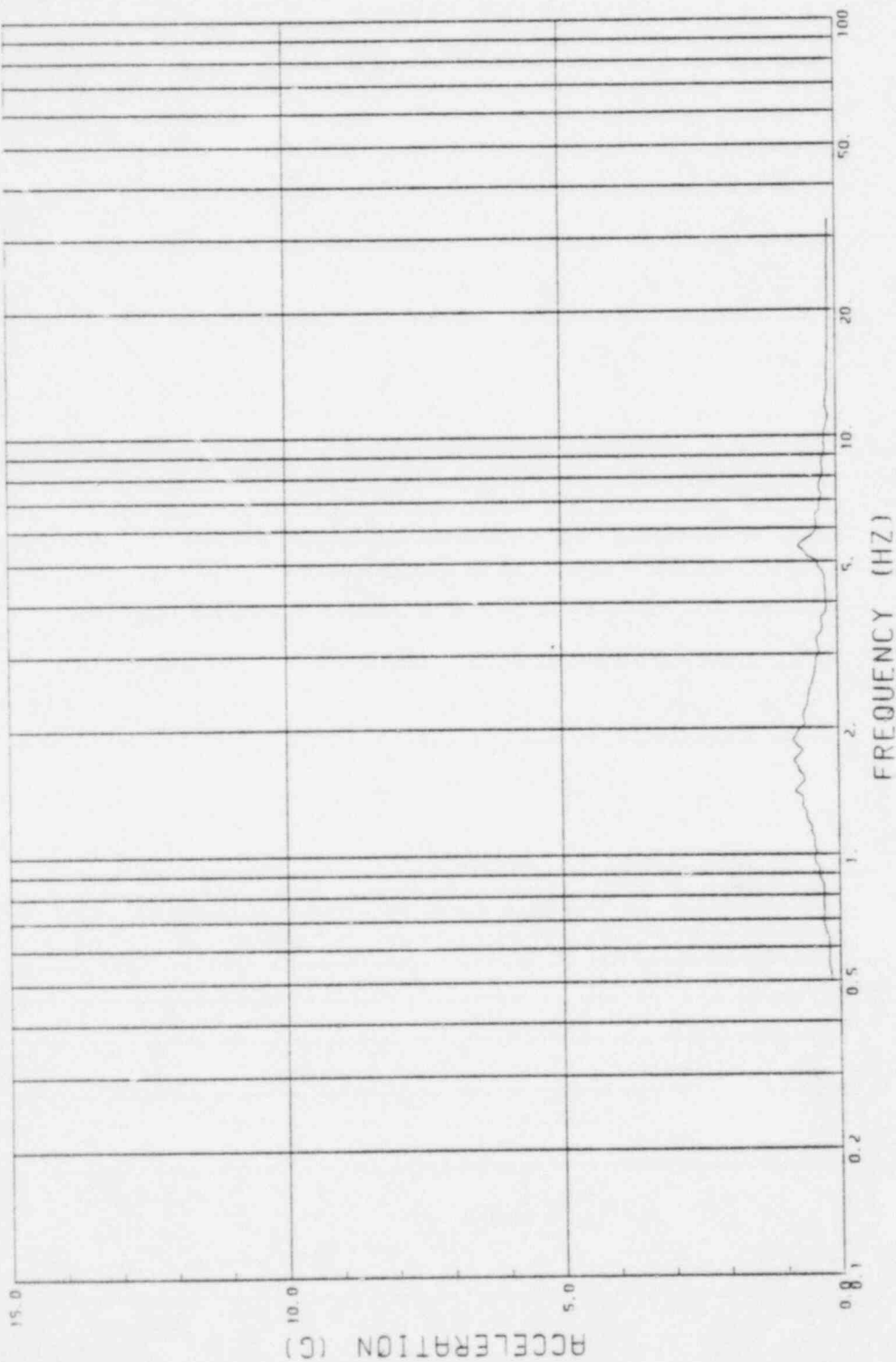
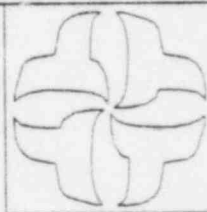


Figure A.5

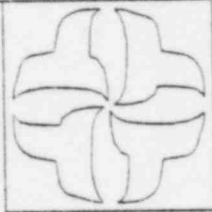


GE CLASSI ANALYSES
CASE 1, GE-75-L-H2
NODE NO. 42



CESSAR II PLANT
SOIL - STRUCTURE INTERACTION

Figure A.6



CESSAR II PLANT
SOIL - STRUCTURE INTERACTION

GE CLASS1 ANALYSES
CASE 1, GE-75-L-H2
NODE NO. 46

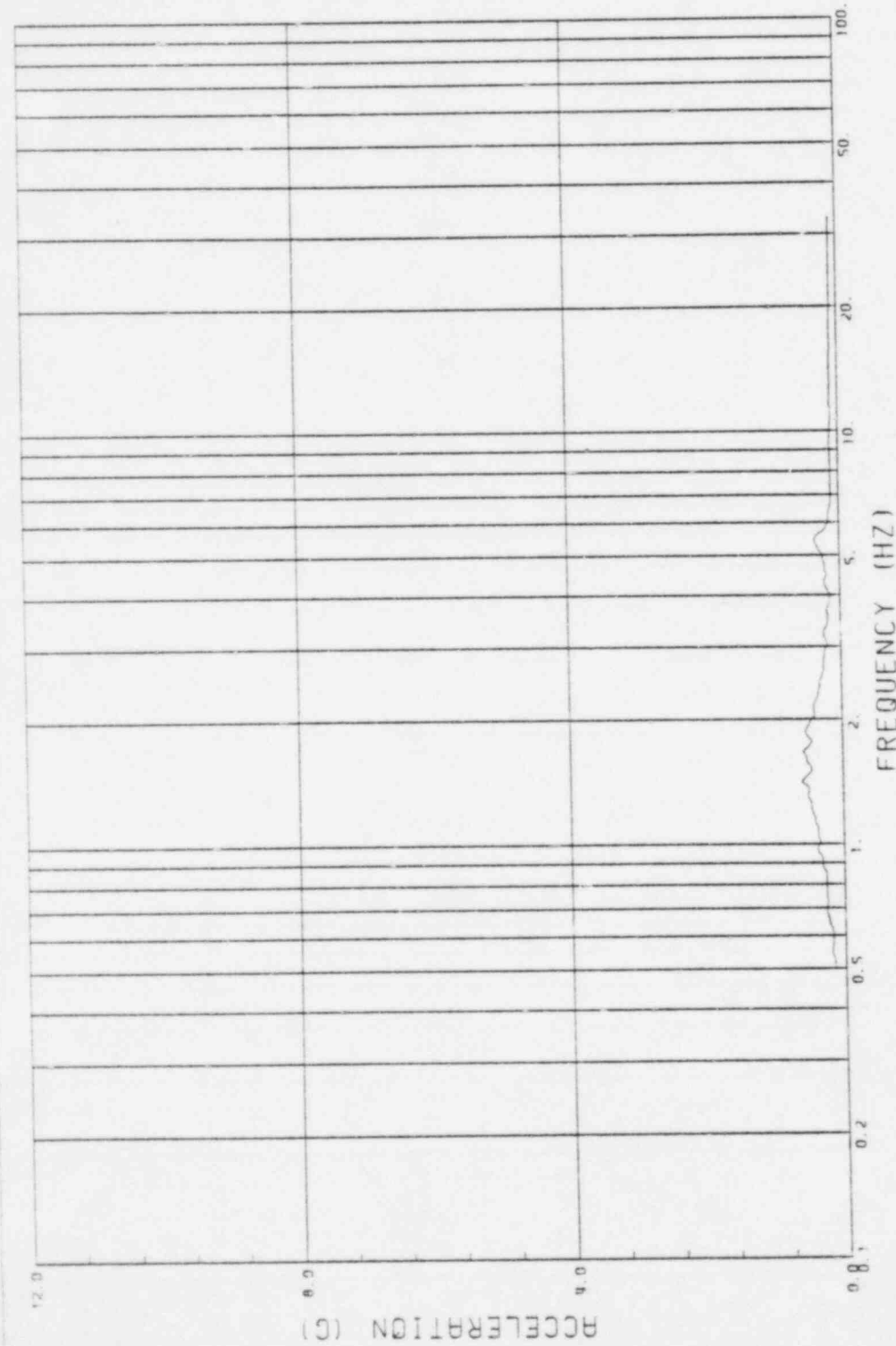


Figure A.7

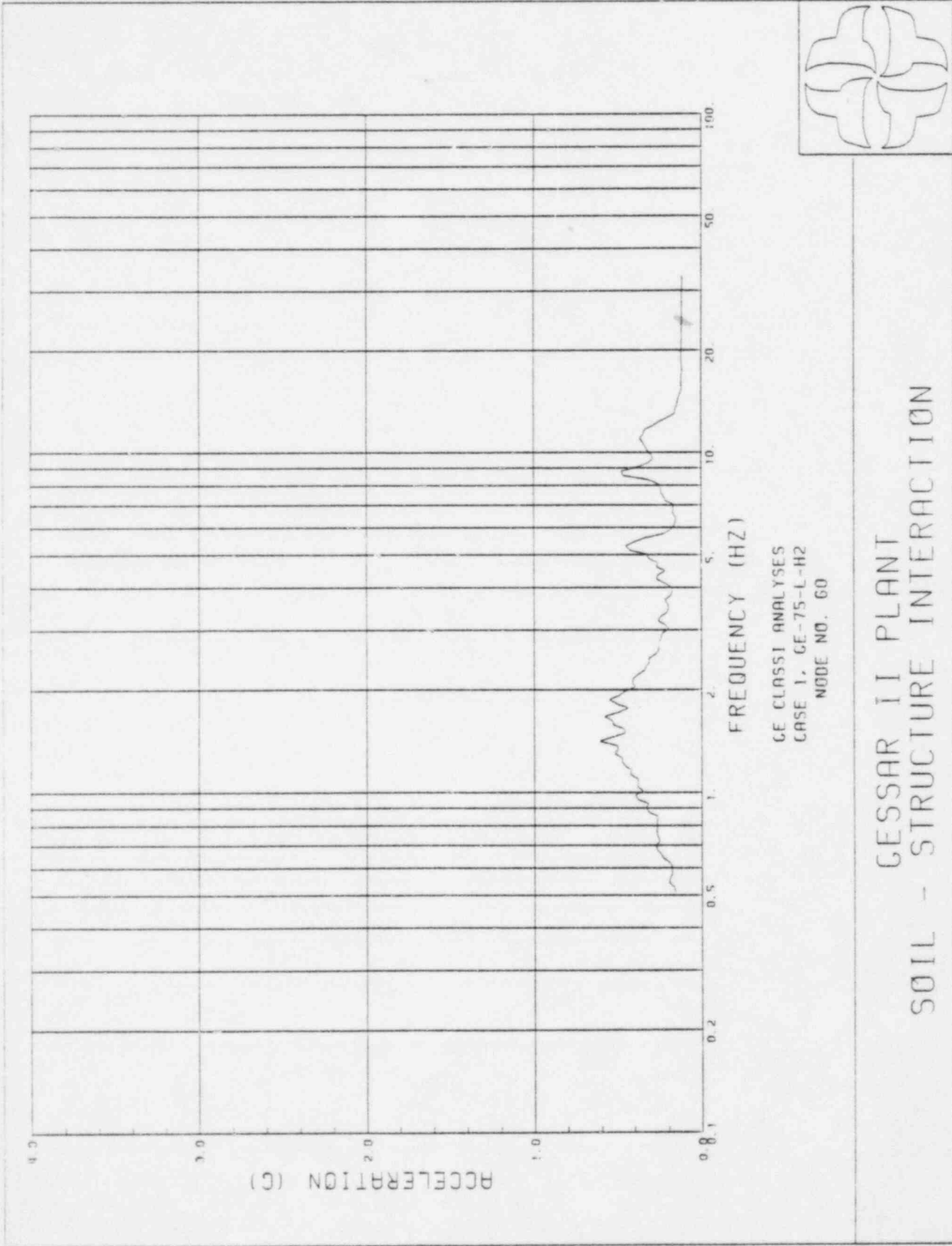


Figure A.8

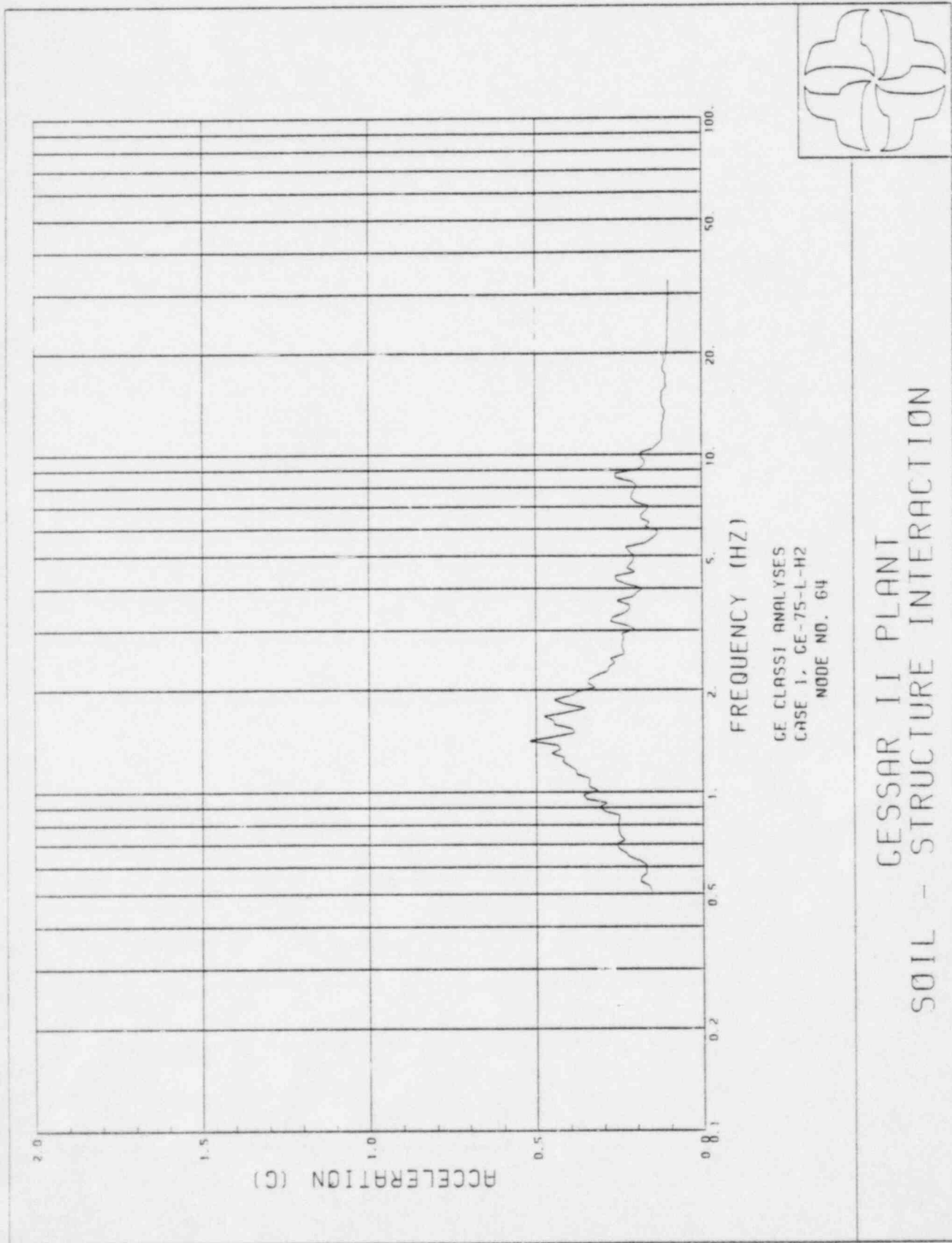
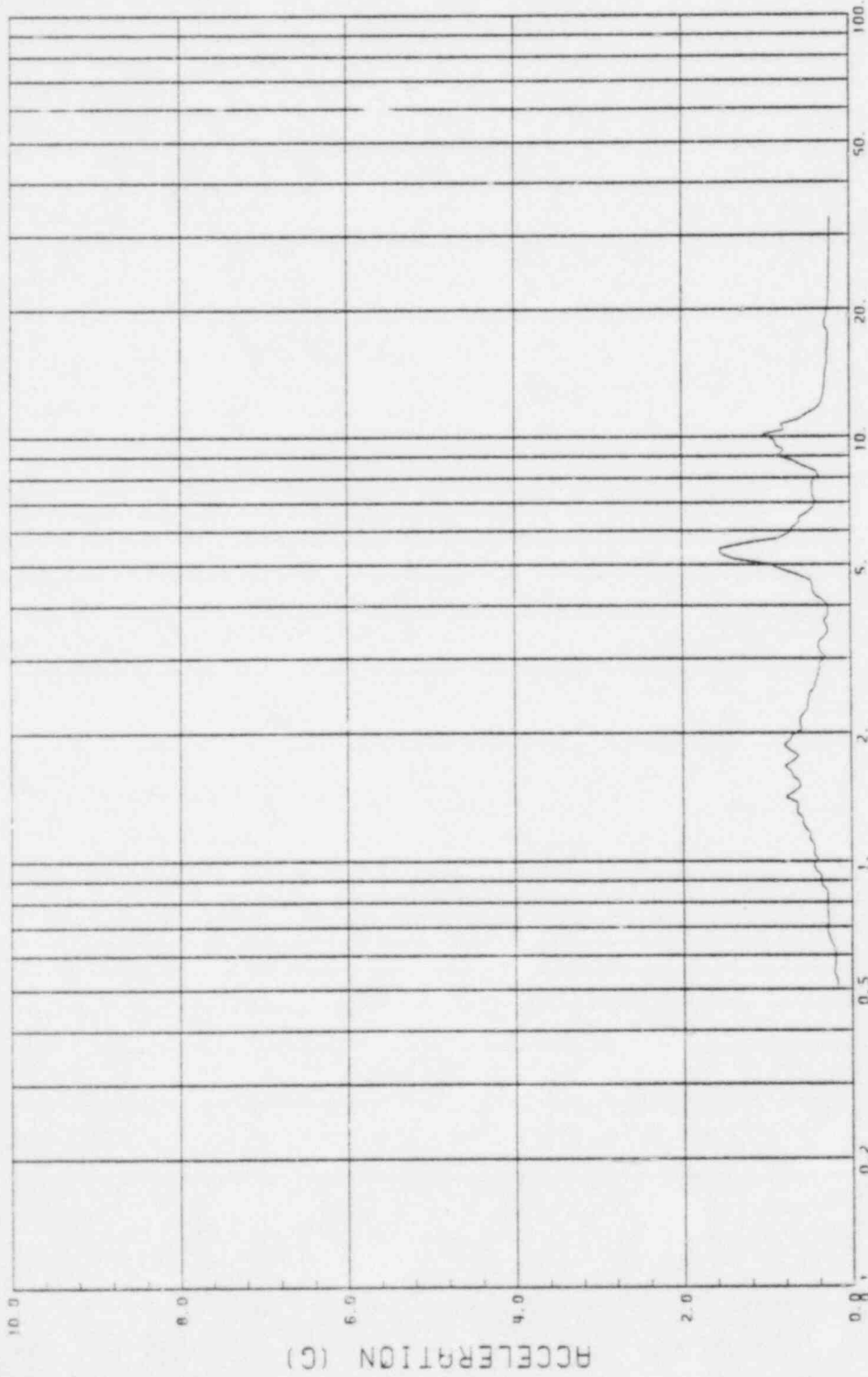
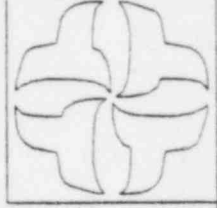


Figure A.9



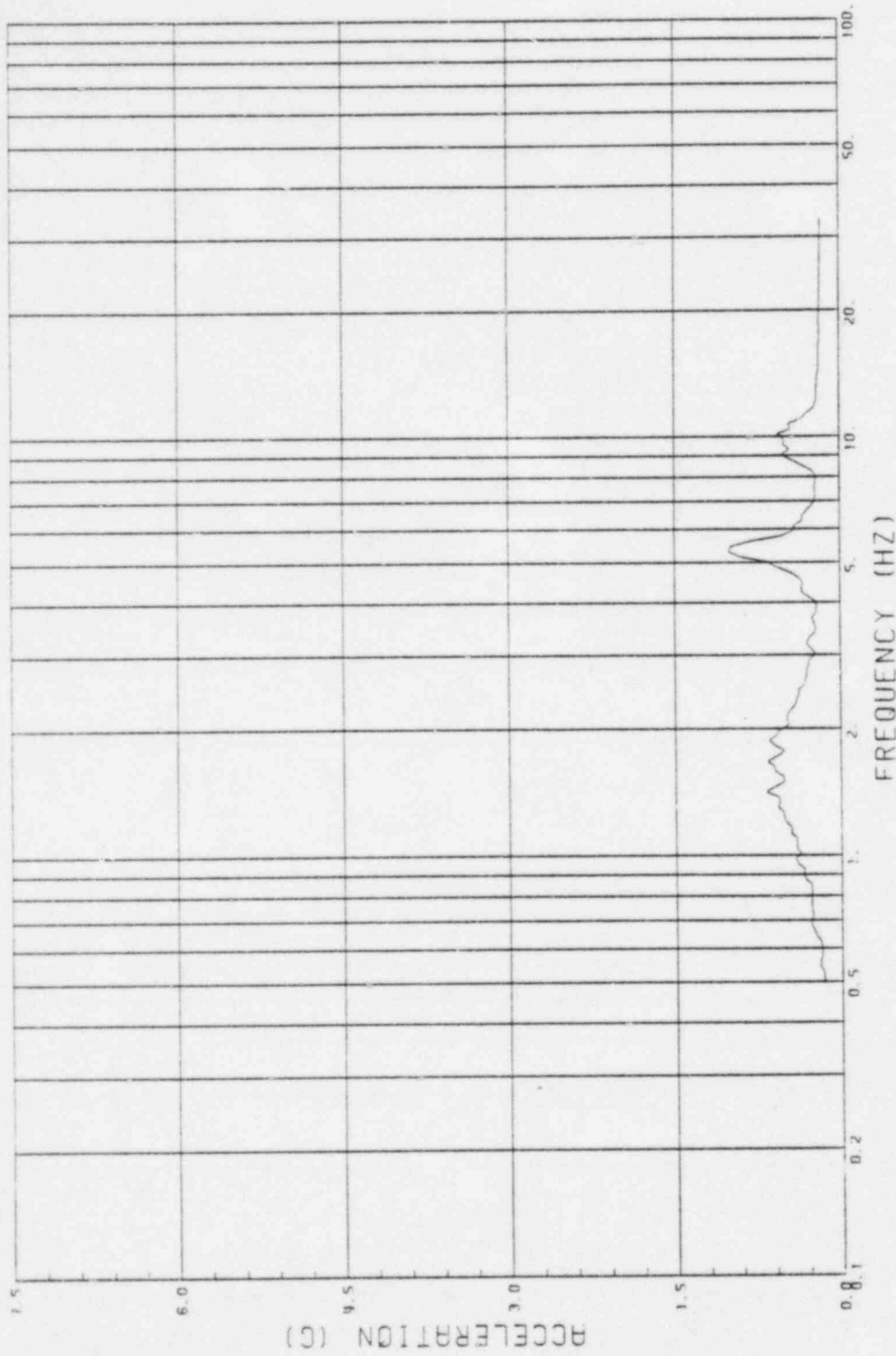
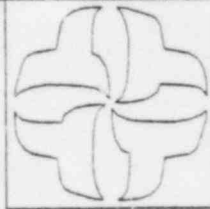
FREQUENCY (HZ)

GE CLASSI ANALYSES
CASE 1, GE-75-L-H2
MODE NO. 101



CESSAR II PLANT
SOIL - STRUCTURE INTERACTION

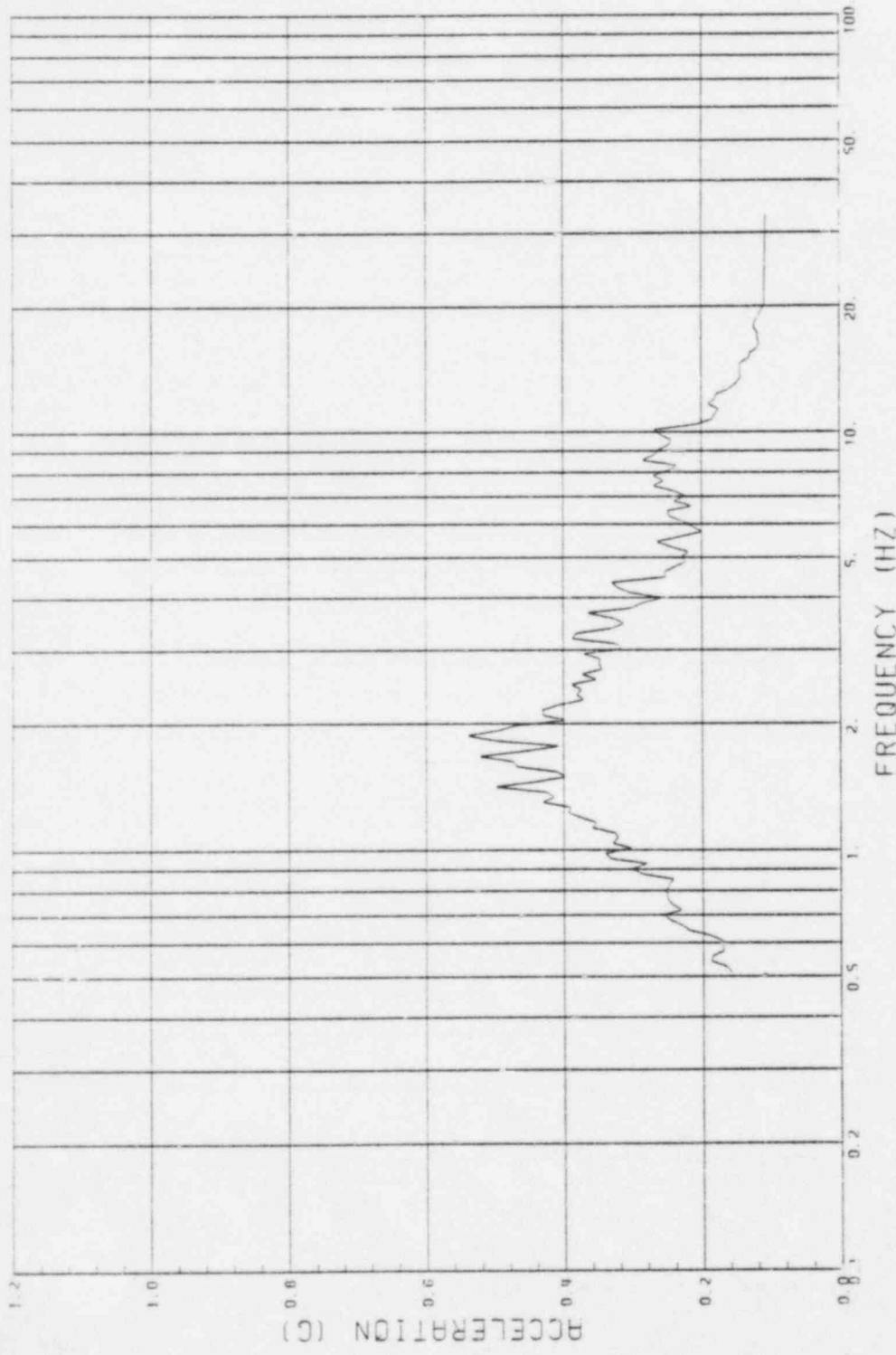
Figure A.10



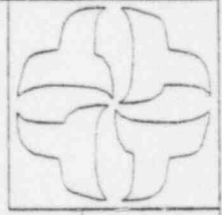
GE CLASSI ANALYSES
CASE 1, GE-75-L-H2
NODE NO. 109

CESSAR II PLANT
SOIL - STRUCTURE INTERACTION

Figure A.11

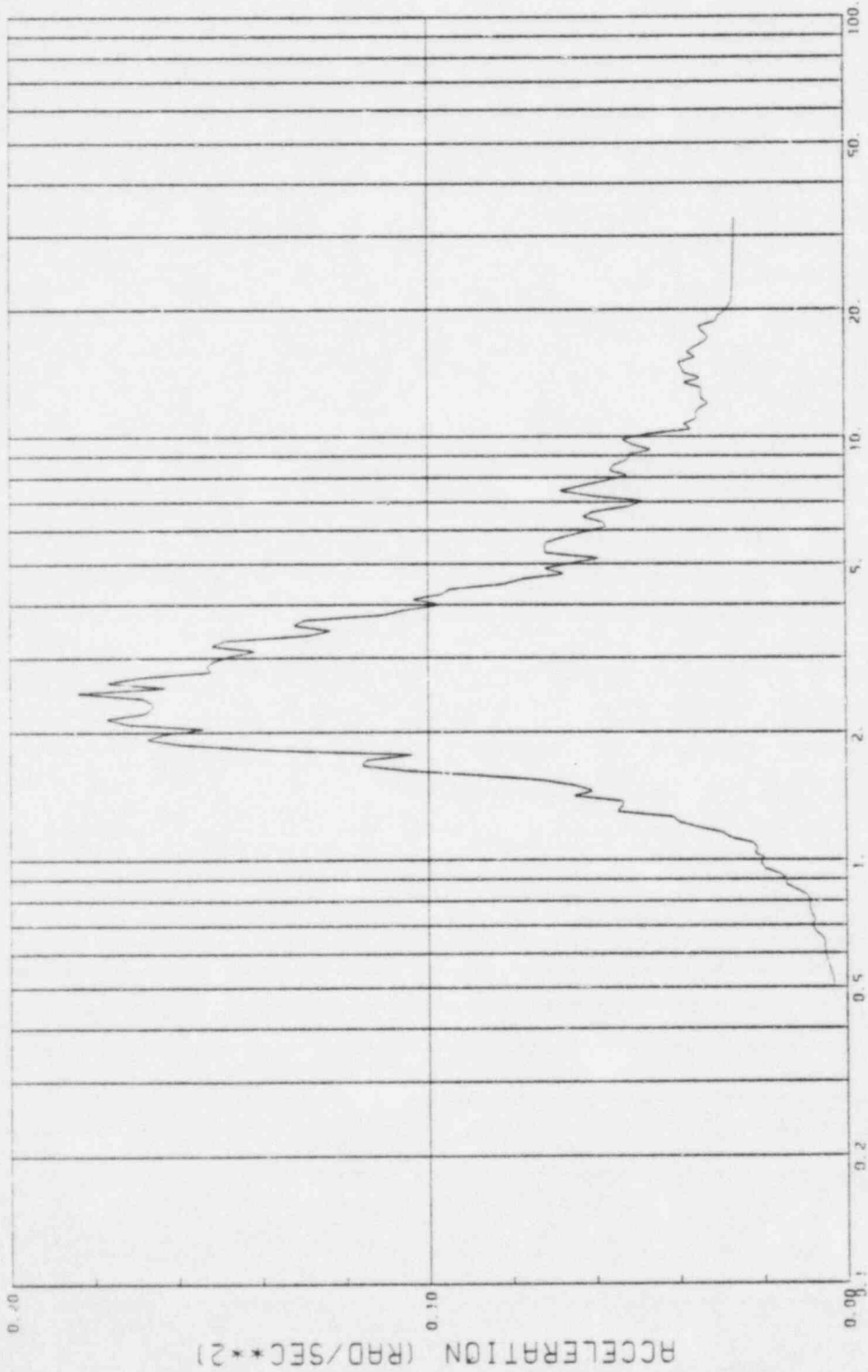


GE CLASSI ANALYSES
CASE 2, GE-75-A-H2
BASEMAT, NODE NO. 71 (TRANSLATION)



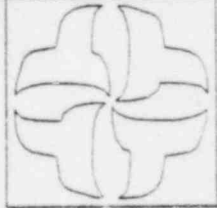
GESSAR II PLANT
SOIL - STRUCTURE INTERACTION

Figure A.12



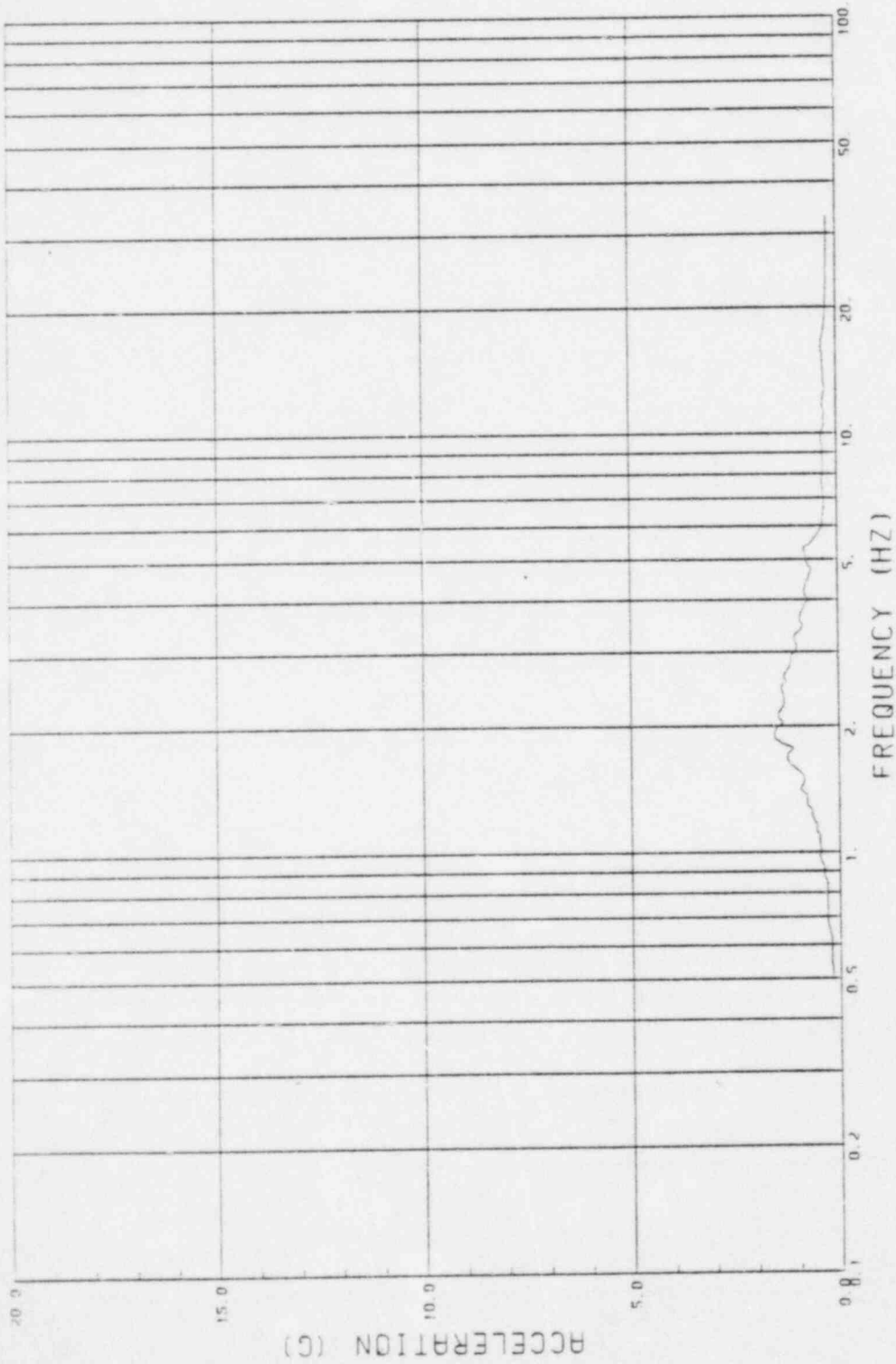
FREQUENCY (HZ)

GE CLASSI ANALYSES
CASE 2, GE-75-A-H2
BASEMAT, NODE NO. 71 (ROTATION)

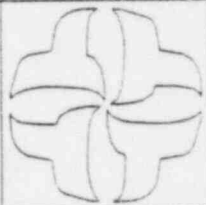


CESSAR II PLANT
SOIL - STRUCTURE INTERACTION

Figure A.13

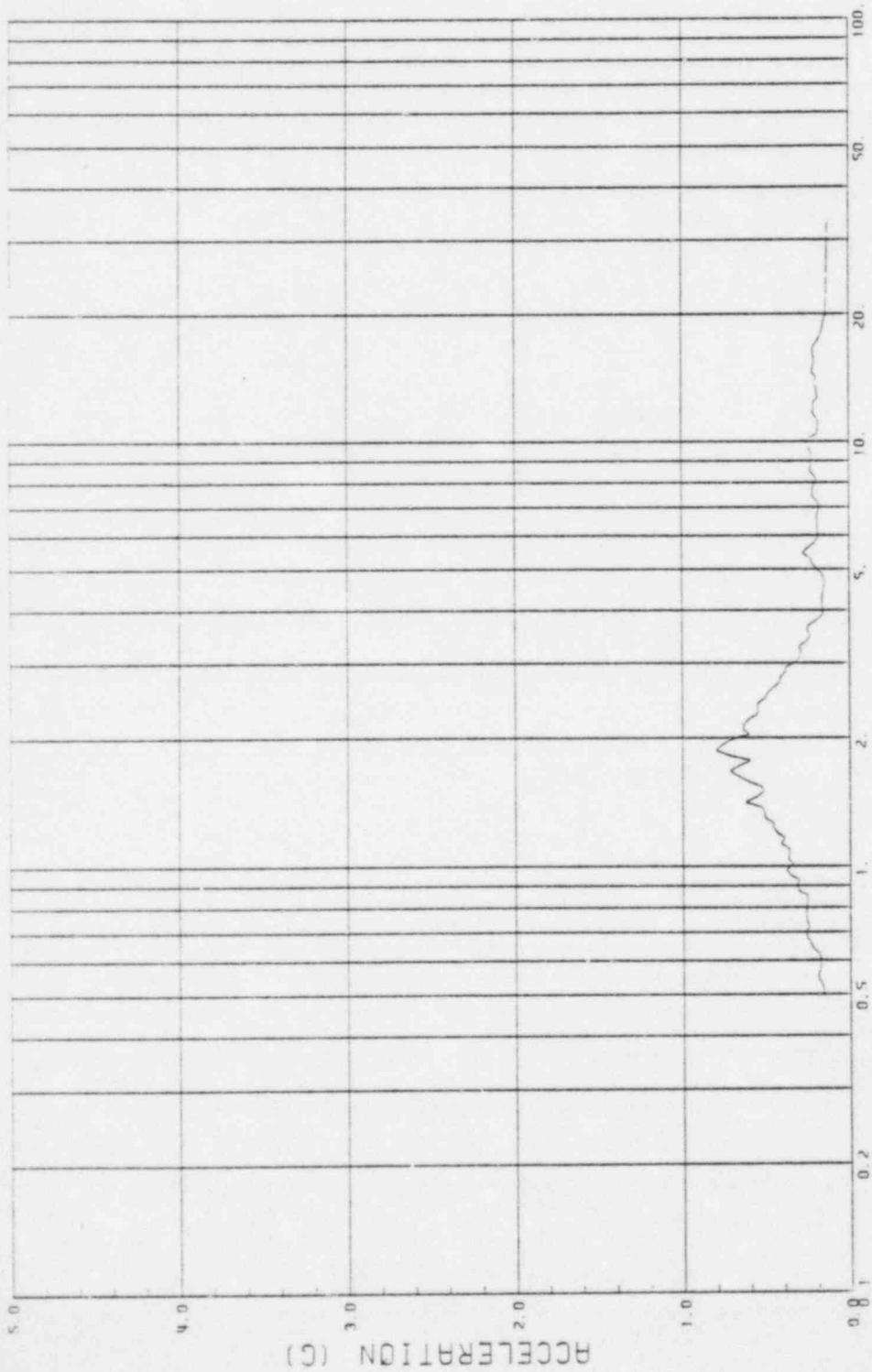


GE CLASSI ANALYSES
CASE 2, GE-75-A-H2
NODE NO. 1



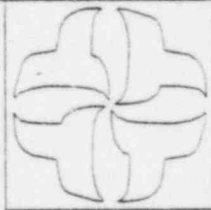
CESSAR II PLANT
SOIL - STRUCTURE INTERACTION

Figure A.14



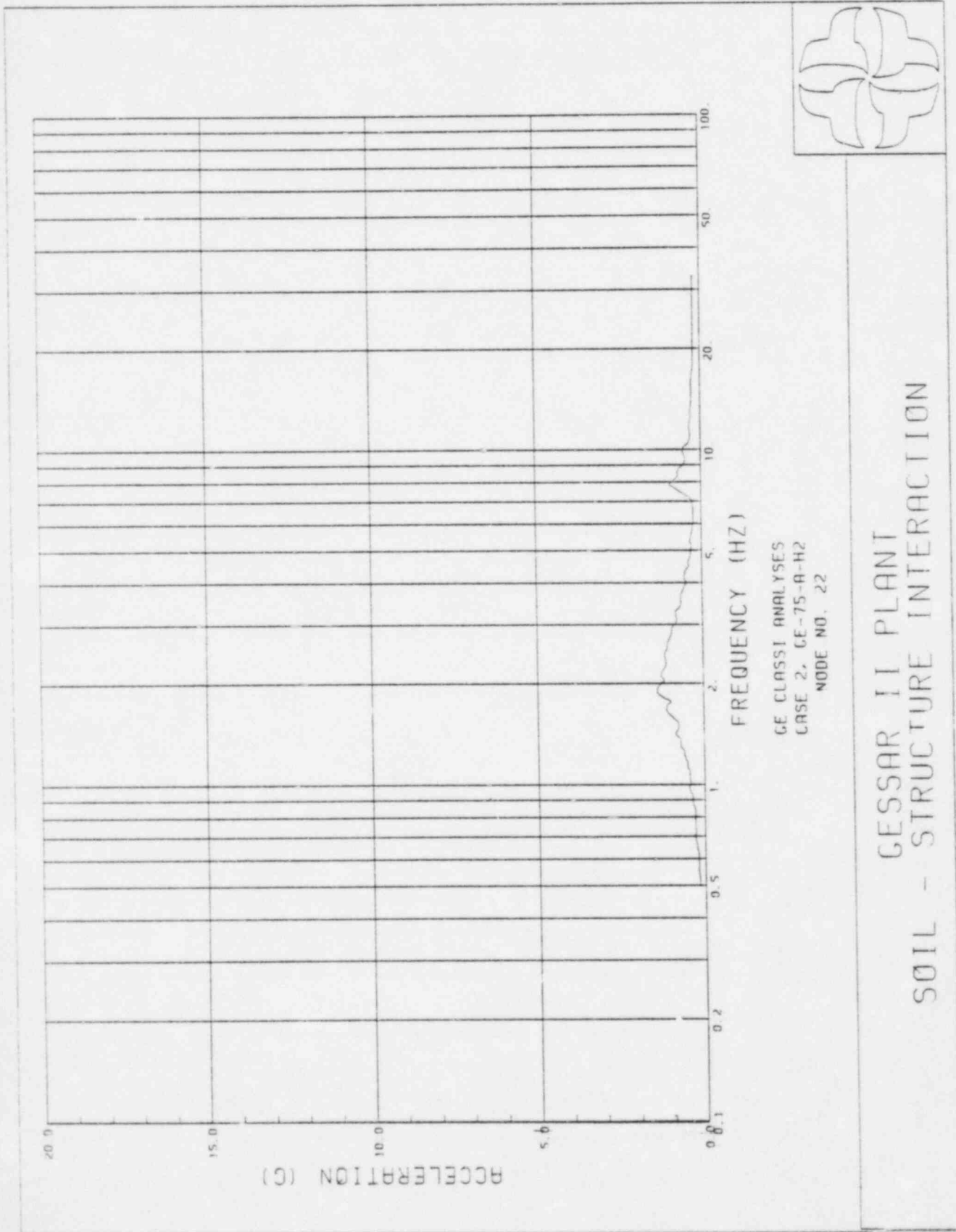
FREQUENCY (HZ)

GE CLASS1 ANALYSES
CASE 2, GE-75-A-H2
NODE NO. 18



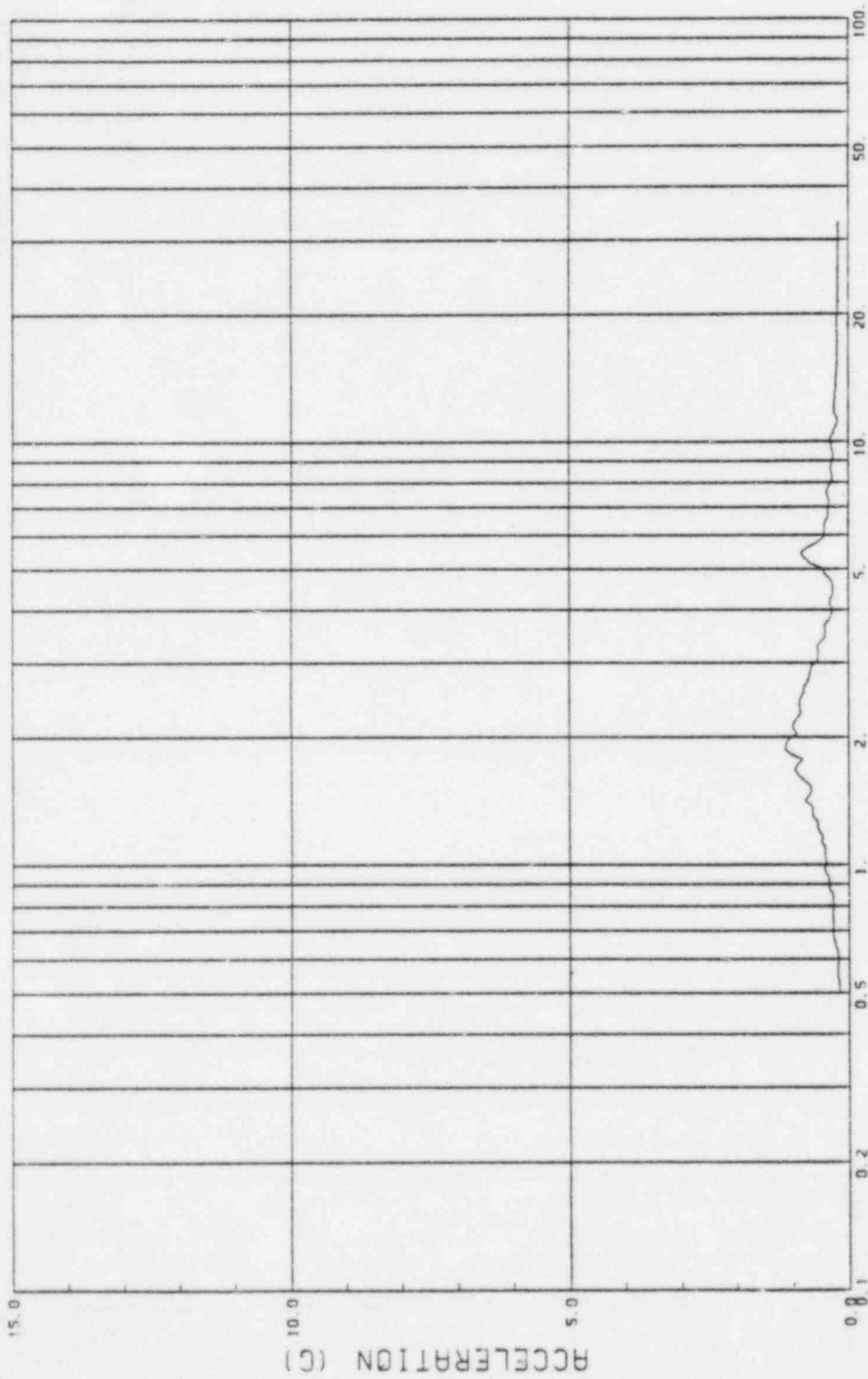
CESSAR II PLANT
SOIL - STRUCTURE INTERACTION

Figure A.15



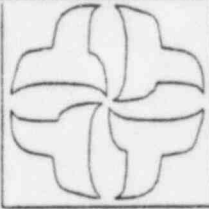
CESSAR II PLANT
SOIL - STRUCTURE INTERACTION

Figure A.16



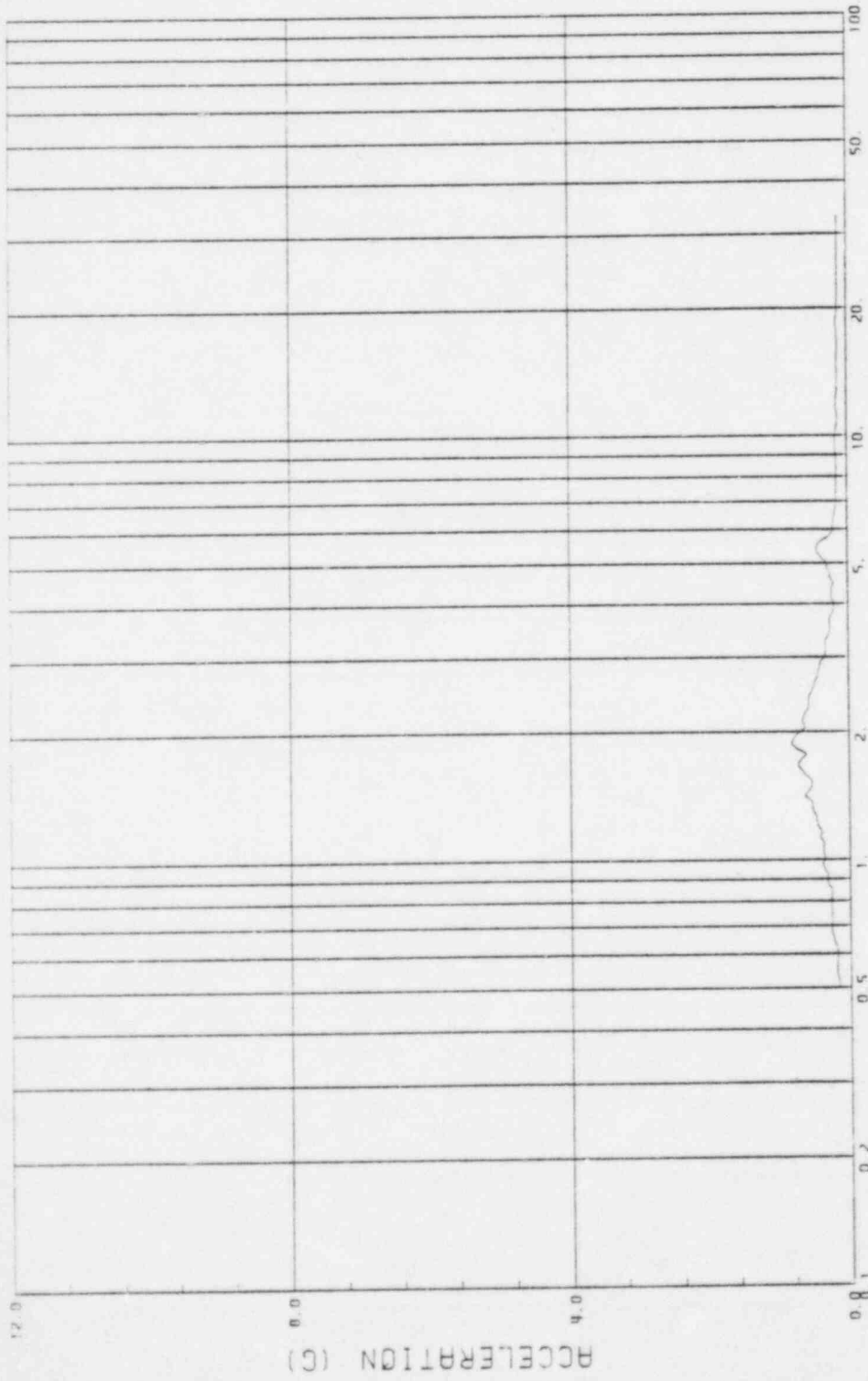
FREQUENCY (HZ)

GE CLASS1 ANALYSES
CASE 2, GE-75-A-H2
NODE NO. 42



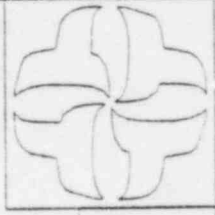
CESSAR II PLANT
SOIL - STRUCTURE INTERACTION

Figure A.17



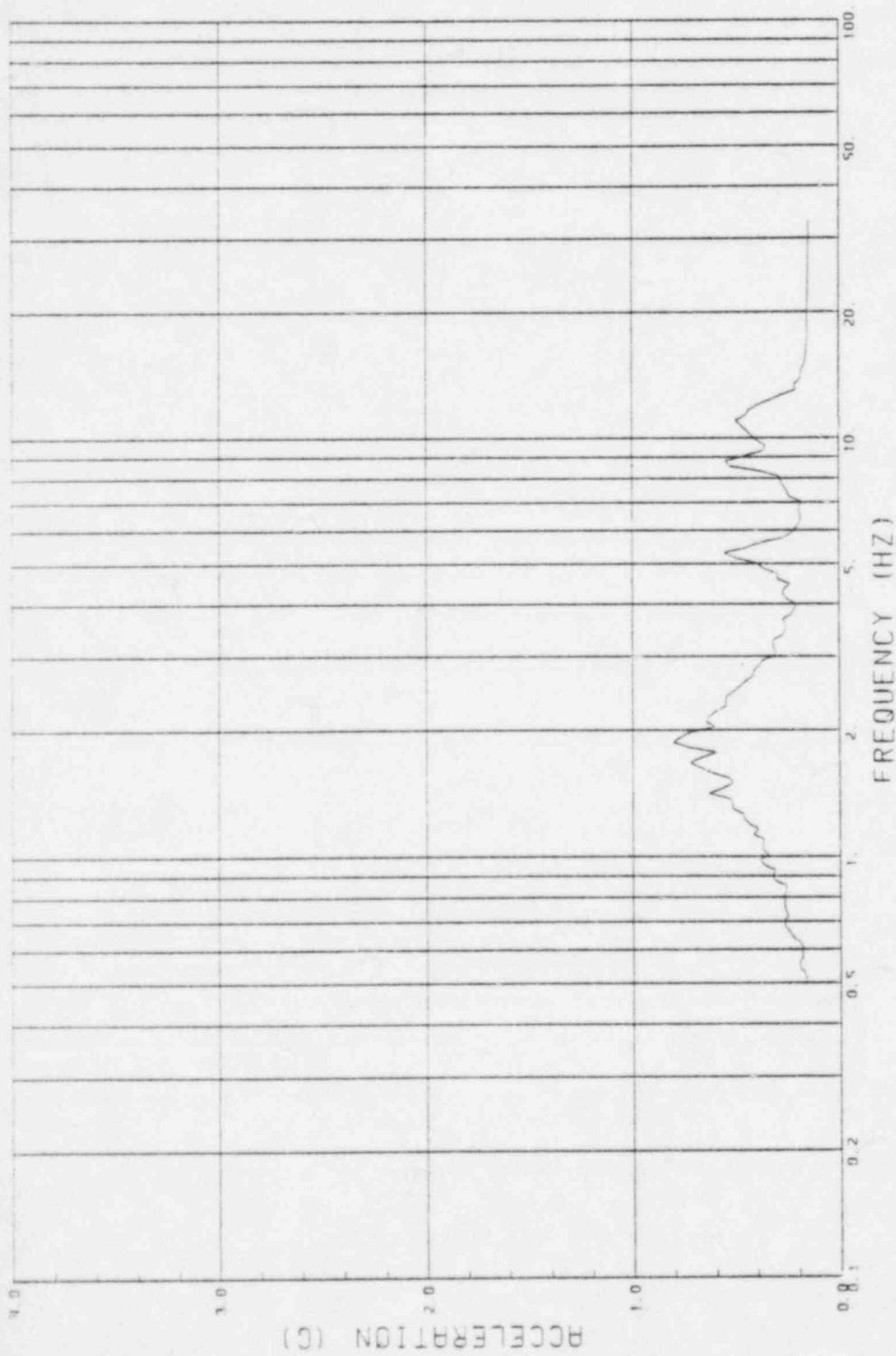
FREQUENCY (HZ)

GE CLASS1 ANALYSES
CASE 2, GE-75-A-H2
NODE NO. 46



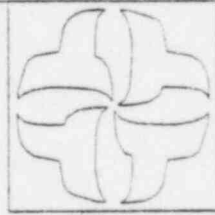
GESSAR II PLANT
SOIL - STRUCTURE INTERACTION

Figure A.18



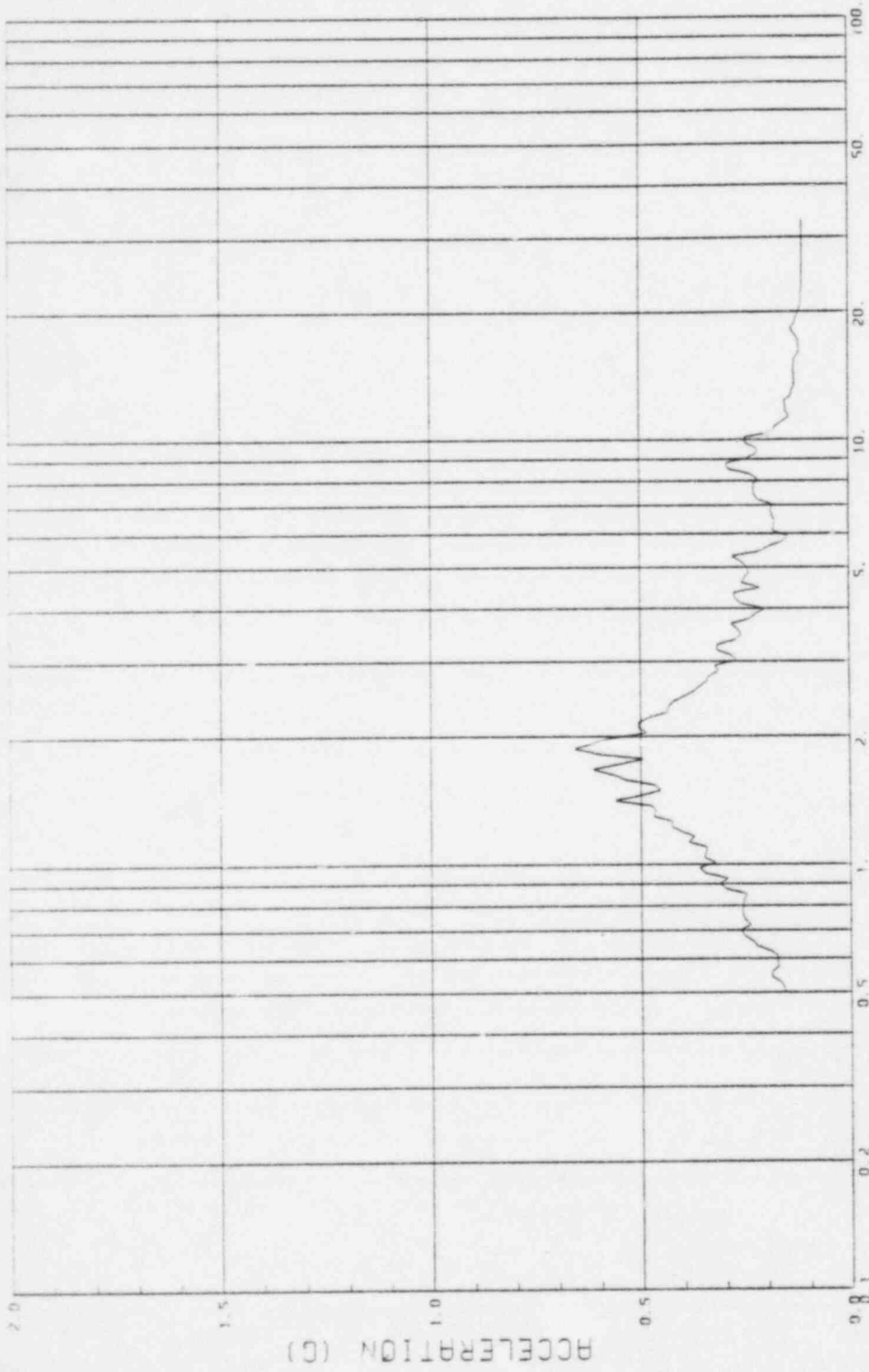
FREQUENCY (HZ)

GE CLASSI ANALYSES
CASE 2, GE-75-A-H2
NODE NO. 60



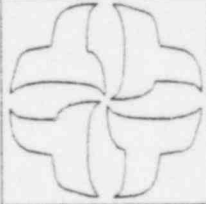
CESSAR II PLANT
SOIL - STRUCTURE INTERACTION

Figure A.19



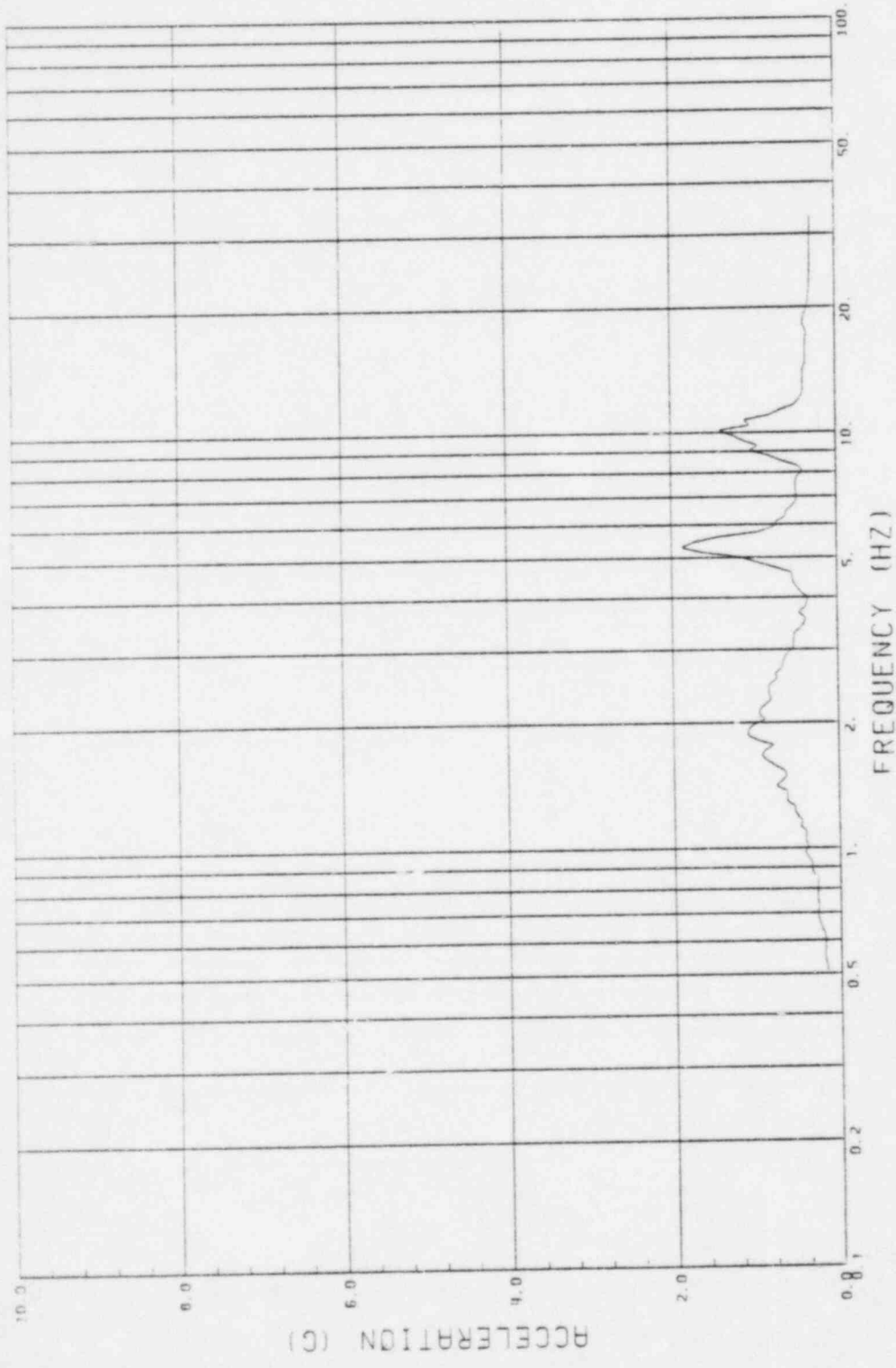
FREQUENCY (HZ)

GE CLASS1 ANALYSES
CASE 2, GE-75-A-H2
NODE NO. 64

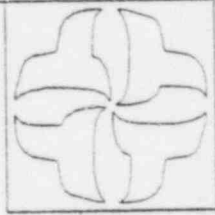


CESSAR II PLANT
SOIL - STRUCTURE INTERACTION

Figure A.20

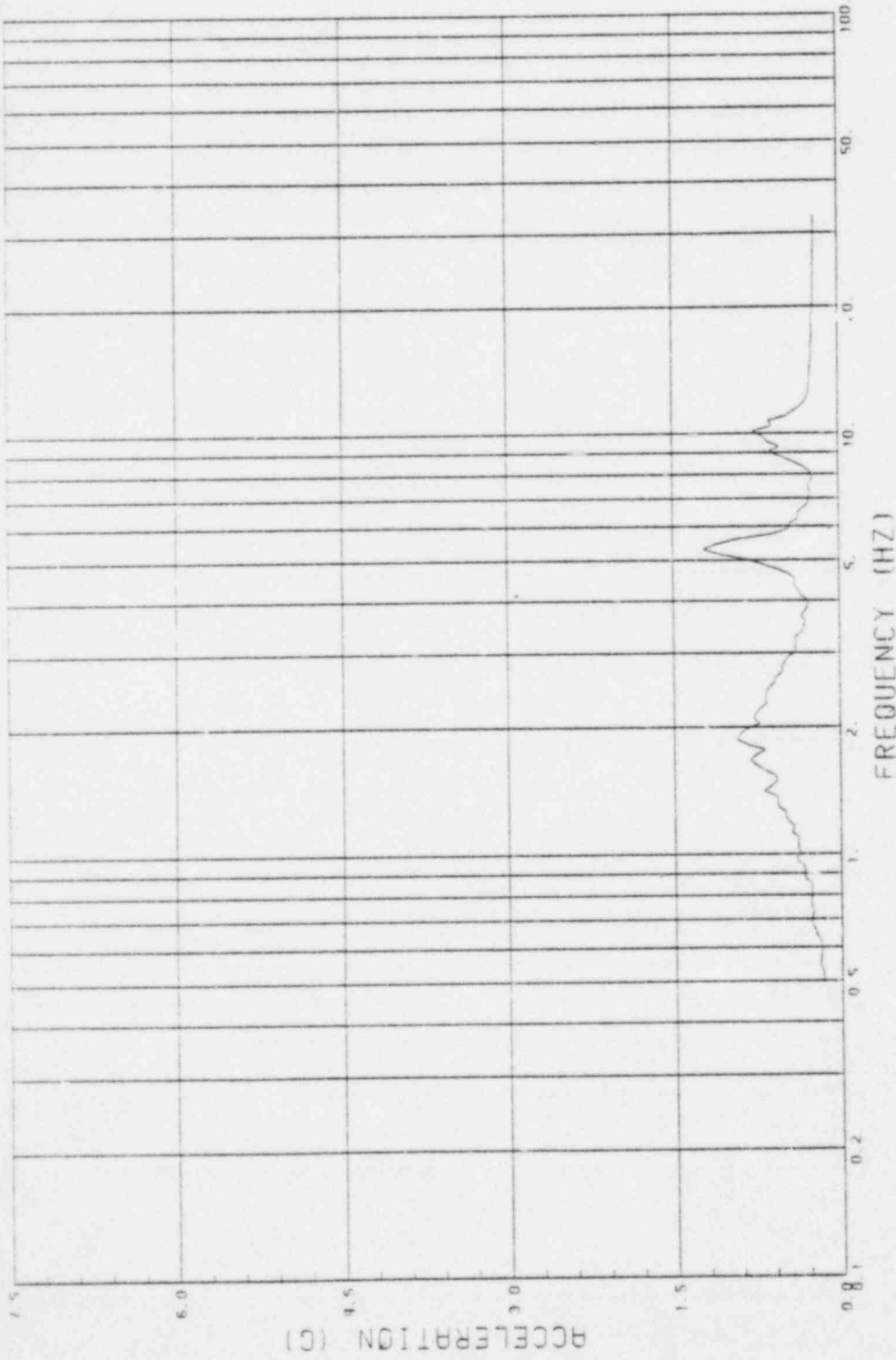


GE CLASS1 ANALYSES
CASE 2, GE-75-A-H2
NODE NO. 101

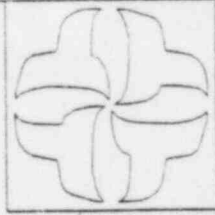


CESSAR 11 PLANT
SOIL - STRUCTURE INTERACTION

Figure A.21

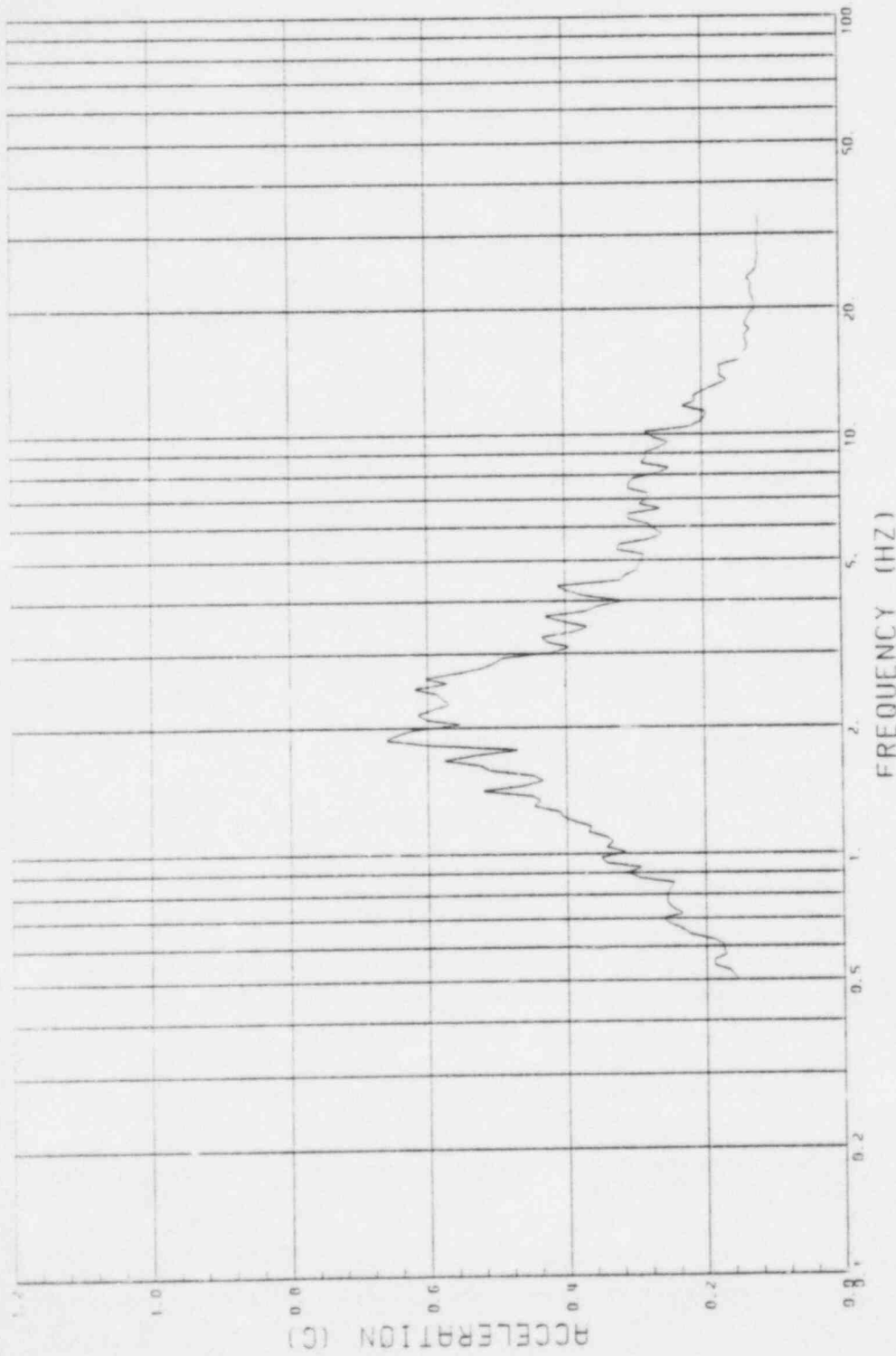


GE CLASS1 ANALYSES
CASE 2, GE-75-A-H2
MODE NO. 109

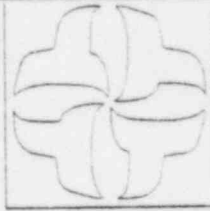


CESSAR II PLANT
SOIL - STRUCTURE INTERACTION

Figure A.22

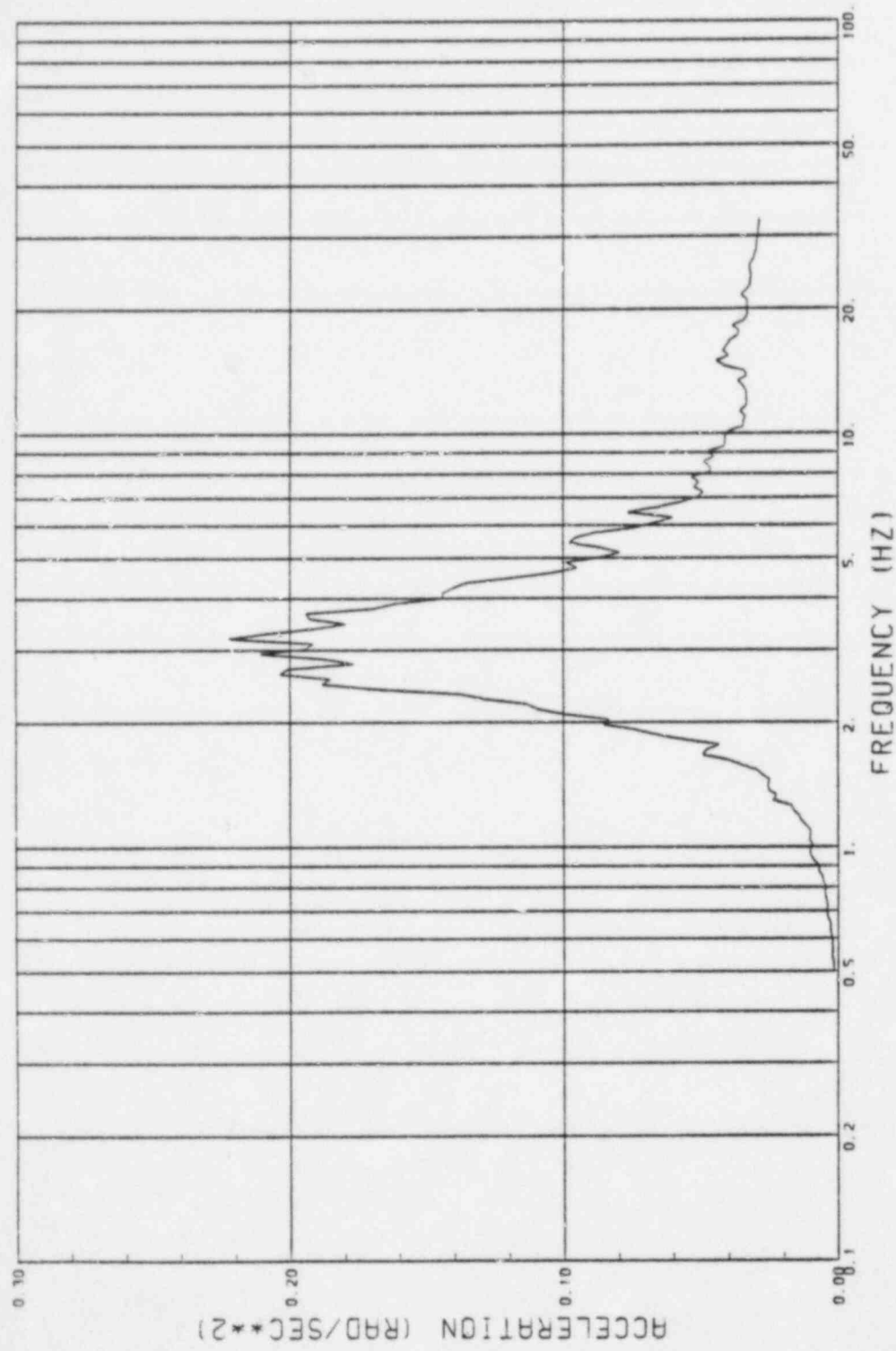
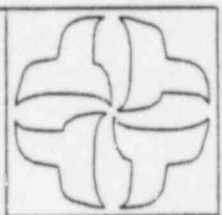


GE CLASSI ANALYSES
CASE 3, GE-75-U-H2
BASEMAT, NODE NO. 71 (TRANSLATION)



CESSAR II PLANT
SOIL - STRUCTURE INTERACTION

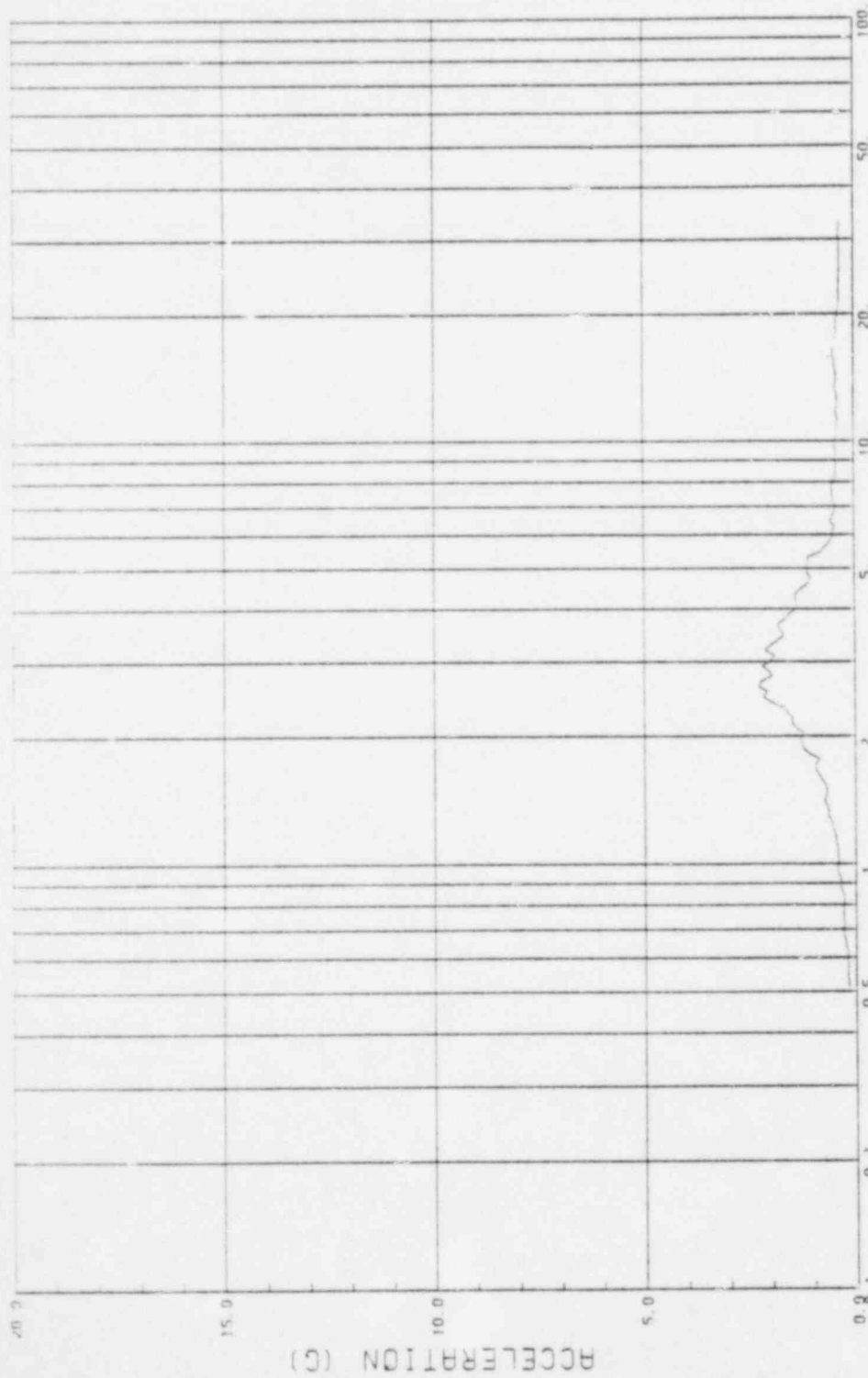
Figure A.23



GE CLASSI ANALYSES
CASE 3, GE-75-U-H2
BASEMAT, NODE NO. 71 (ROTATION)

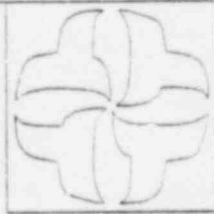
CESSAR II PLANT
SOIL - STRUCTURE INTERACTION

Figure A.24



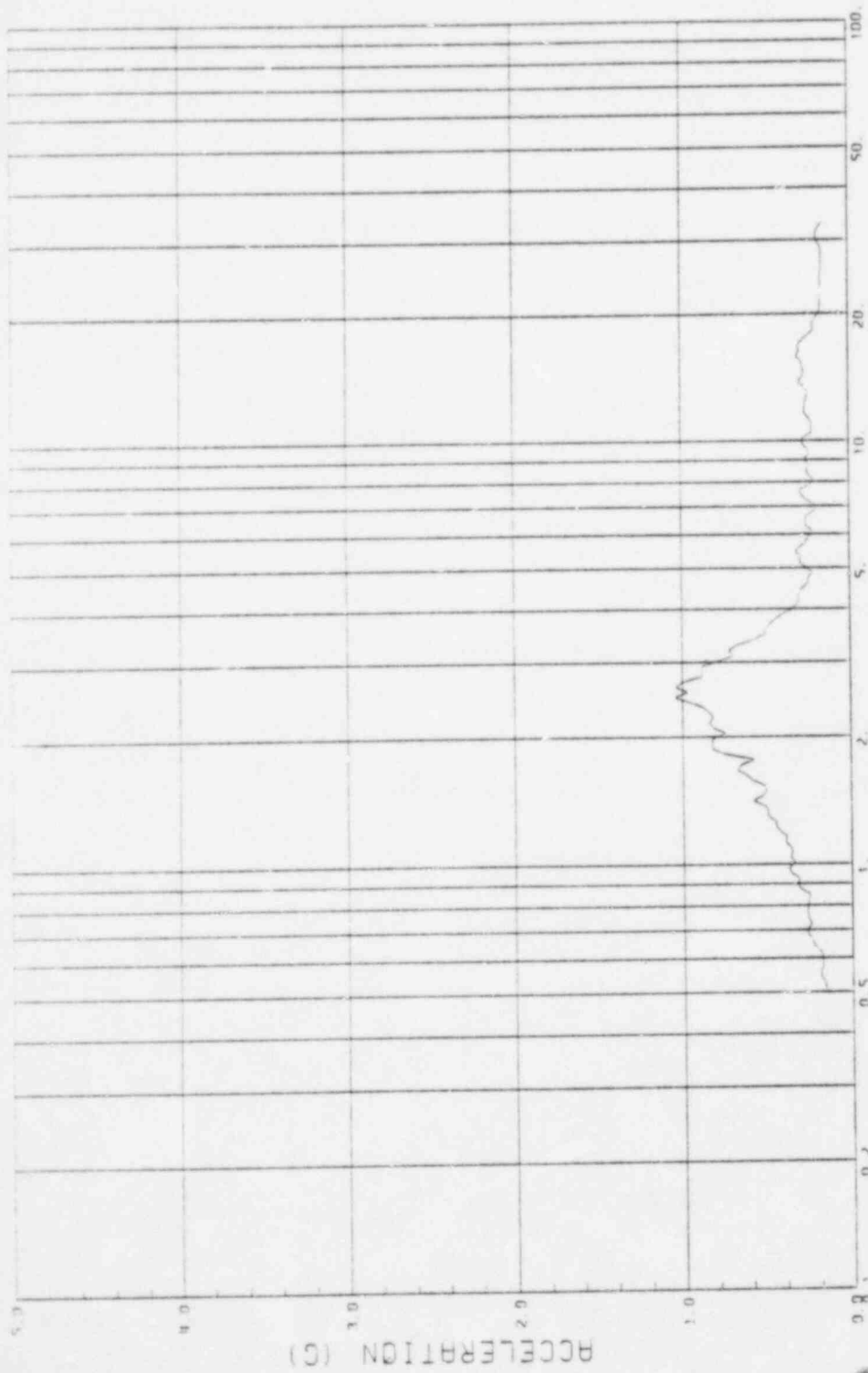
FREQUENCY (HZ)

GE CLASSI ANALYSES
CASE 3, GE-75-U-H2
NODE NO. 1



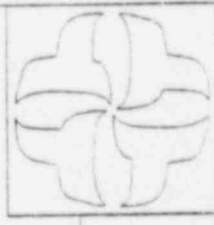
CESSAR II PLANT
SOIL - STRUCTURE INTERACTION

Figure A.25



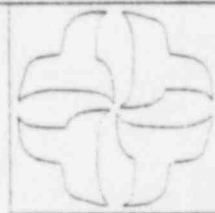
FREQUENCY (HZ)

GE CLASSI ANALYSES
 CASE 3. GE-75-U-H2
 NODE NO. 18



CESSAR II PLANT
 SOIL - STRUCTURE INTERACTION

Figure A.26



CESSAR 11 PLANT
SOIL - STRUCTURE INTERACTION

GE CLASS1 ANALYSES
CASE 3, GE-75-U-H2
NODE NO. 22

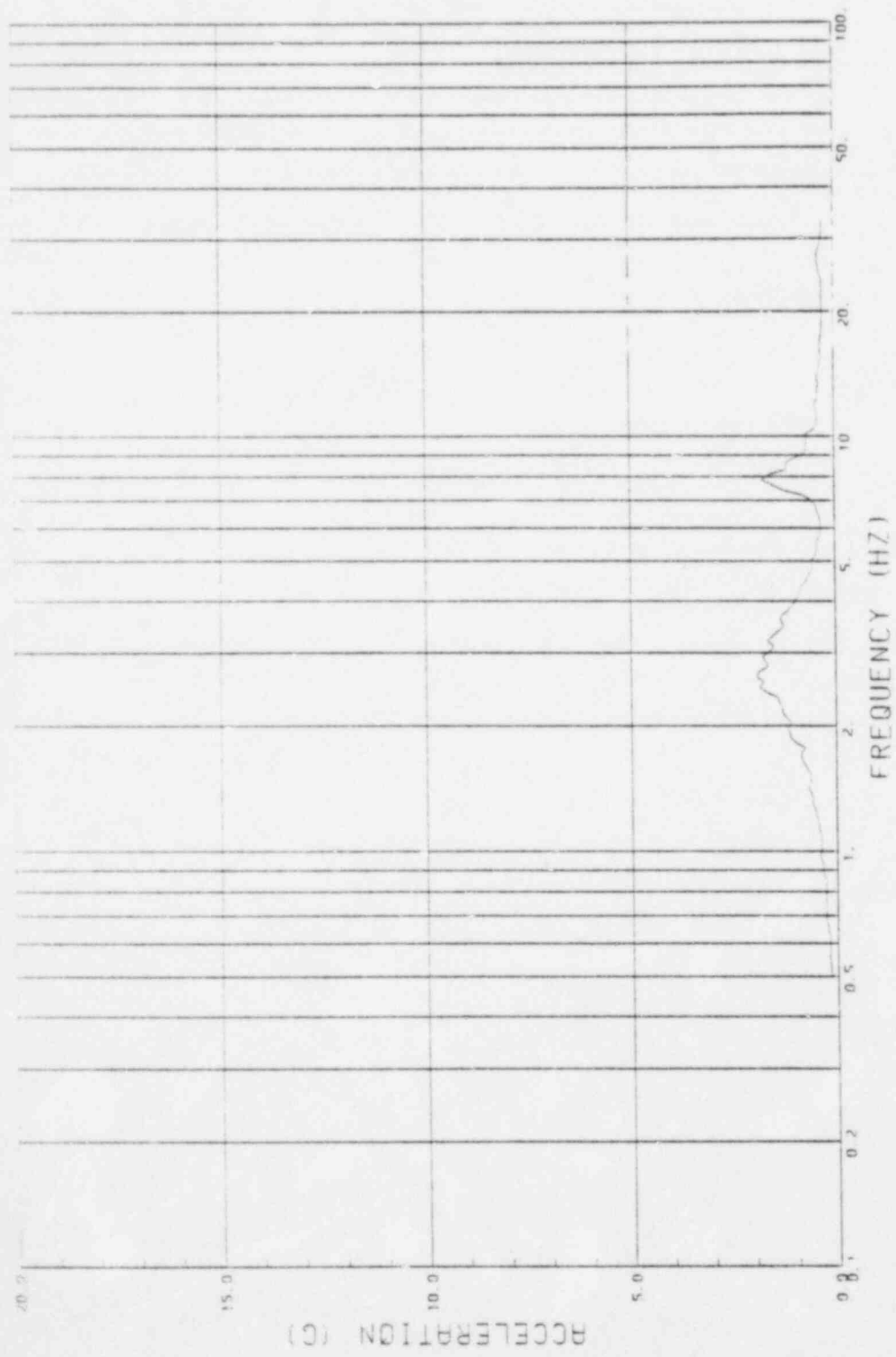
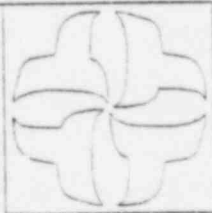


Figure A.27



CESSAR II PLANT
SOIL - STRUCTURE INTERACTION

CE CLASSI ANALYSES
CASE 3. CE-75-U-H2
NODE NO. 42

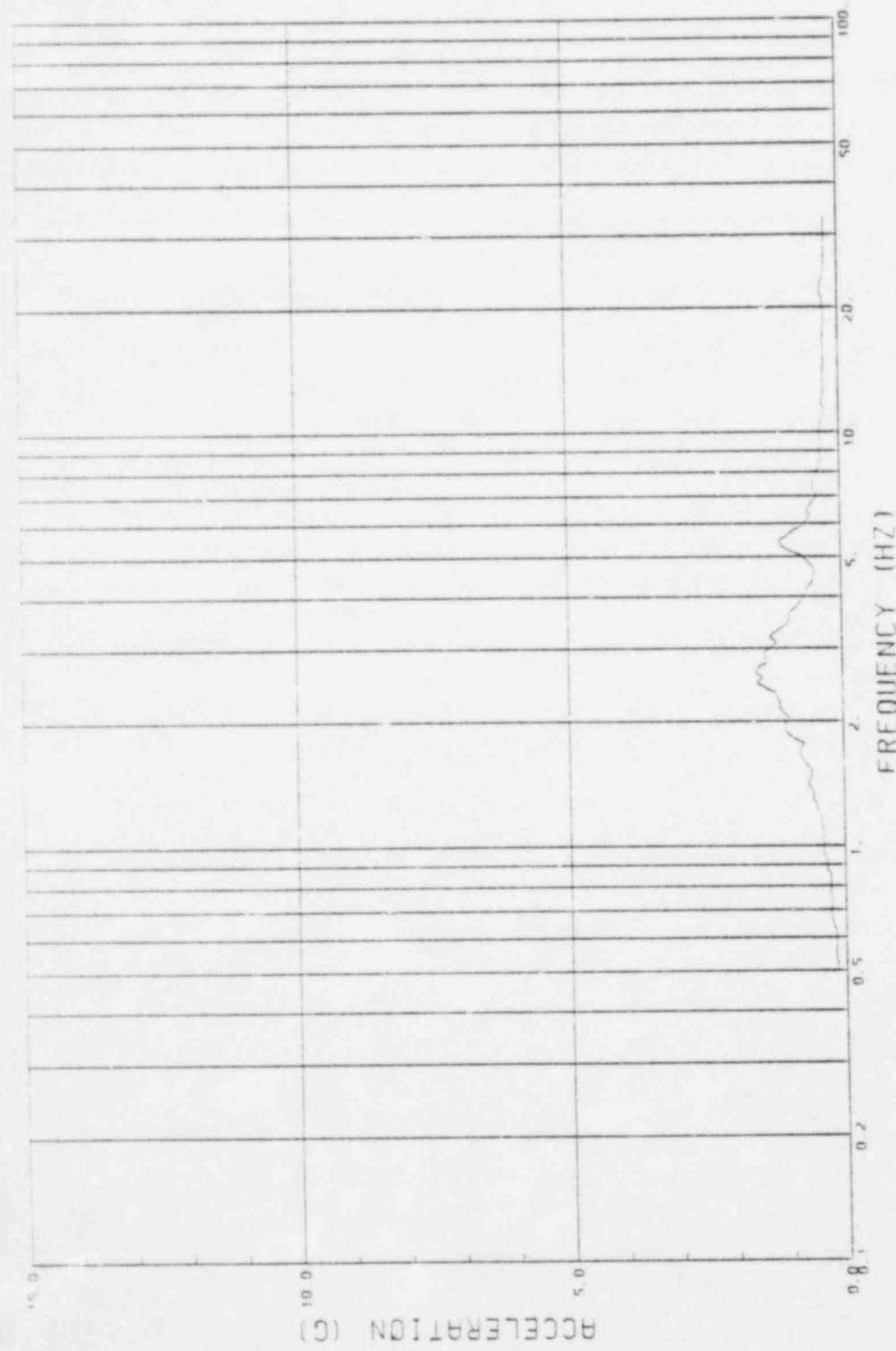
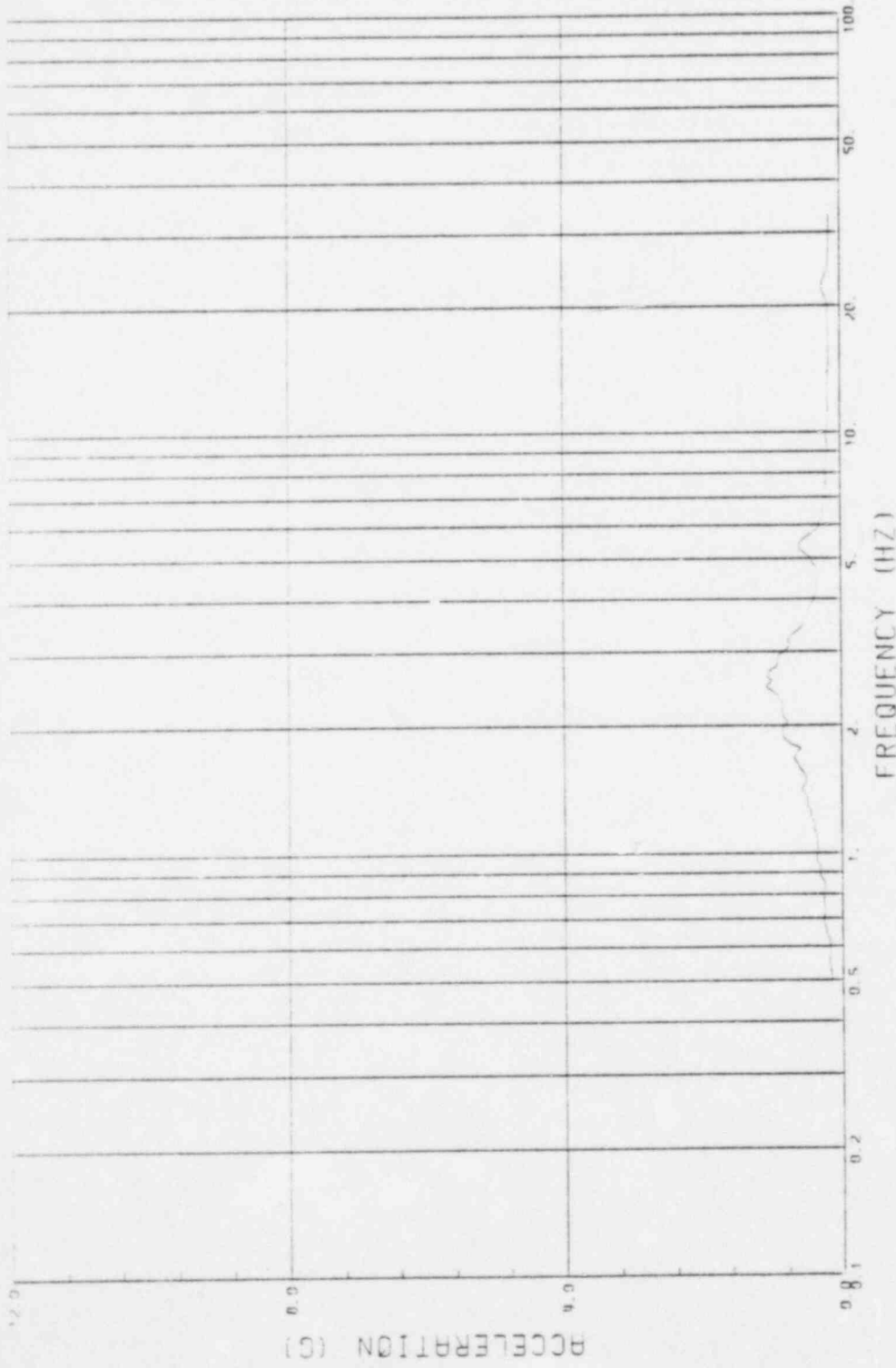
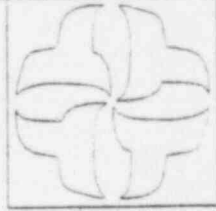


Figure A.28

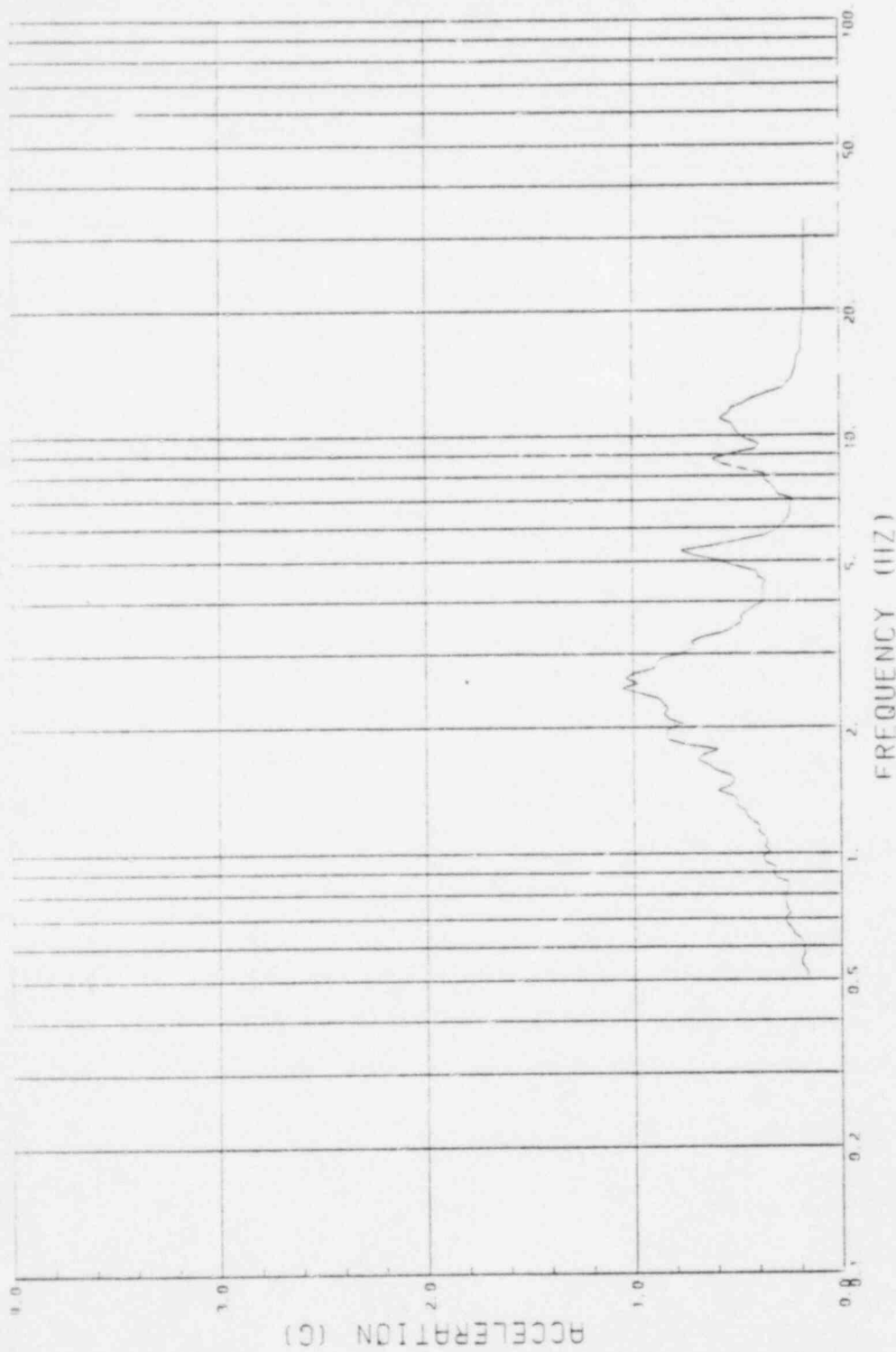


GE CLASSI ANALYSES
CASE 3, GE-75-U-H2
MODE NO. 46

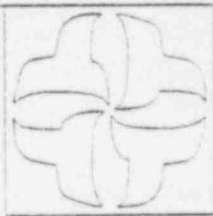


CESSAR II PLANT
SOIL - STRUCTURE INTERACTION

Figure A.29



GE CLASSI ANALYSES
CASE 3, GE-75-U-112
NODE NO. 60



CESSAR II PLANI
SOIL - STRUCTURE INTERACTION

Figure A.30

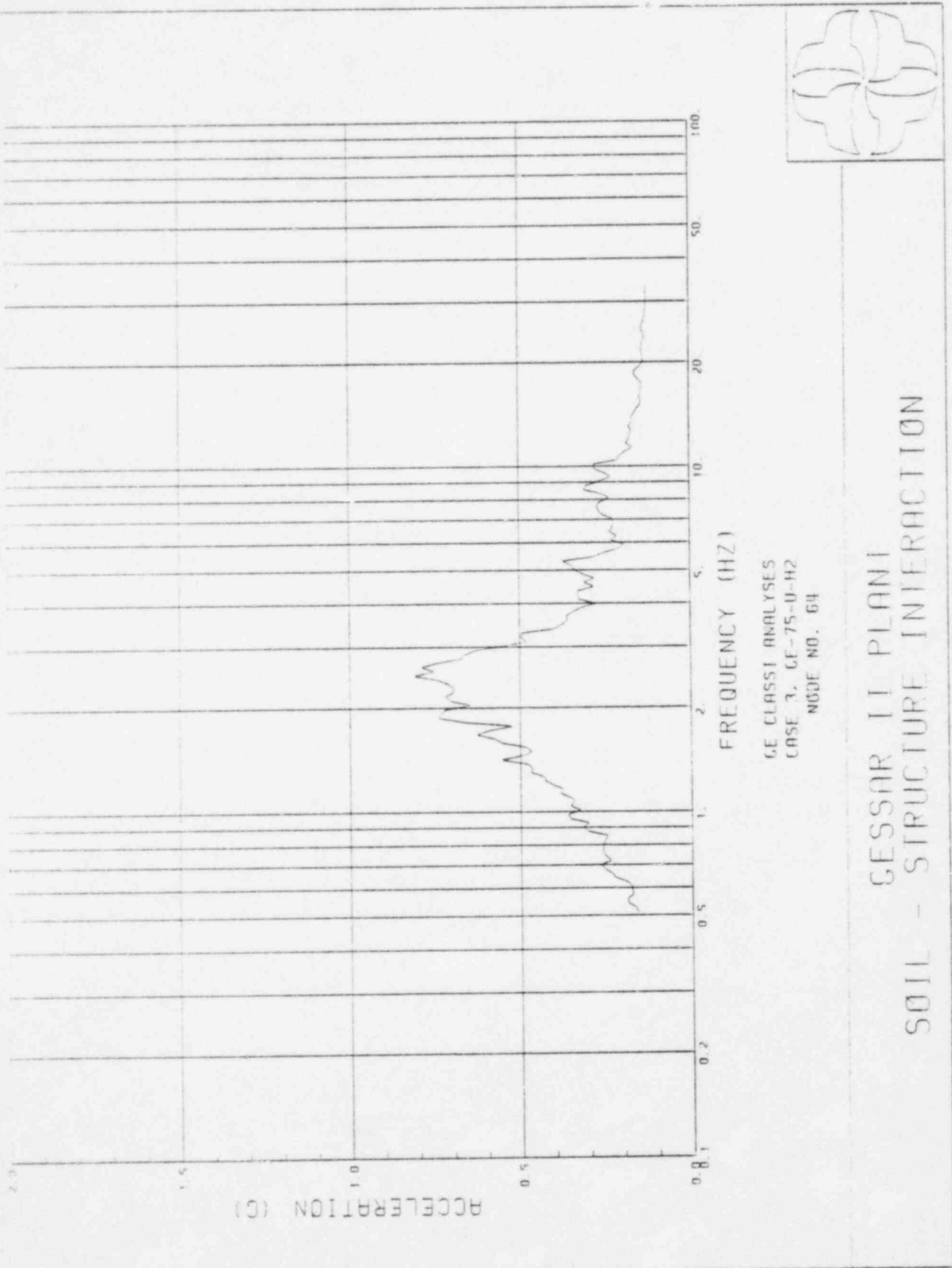
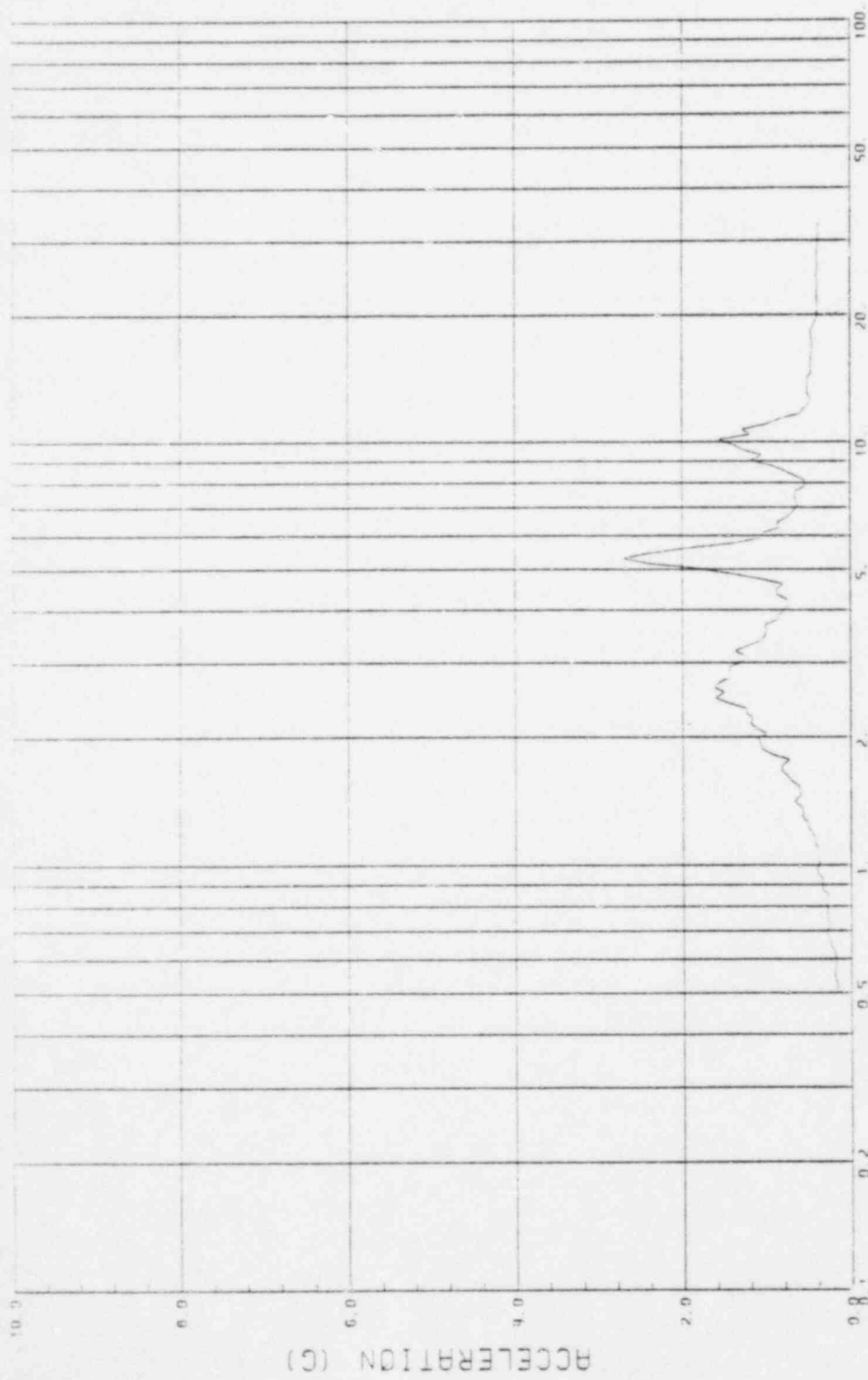


Figure A.31



GE CLASS1 ANALYSES
CASE 3, GE-75-U-H2
NODE NO. 101

CESSAR II PLANT
SOIL - STRUCTURE INTERACTION

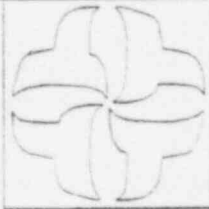
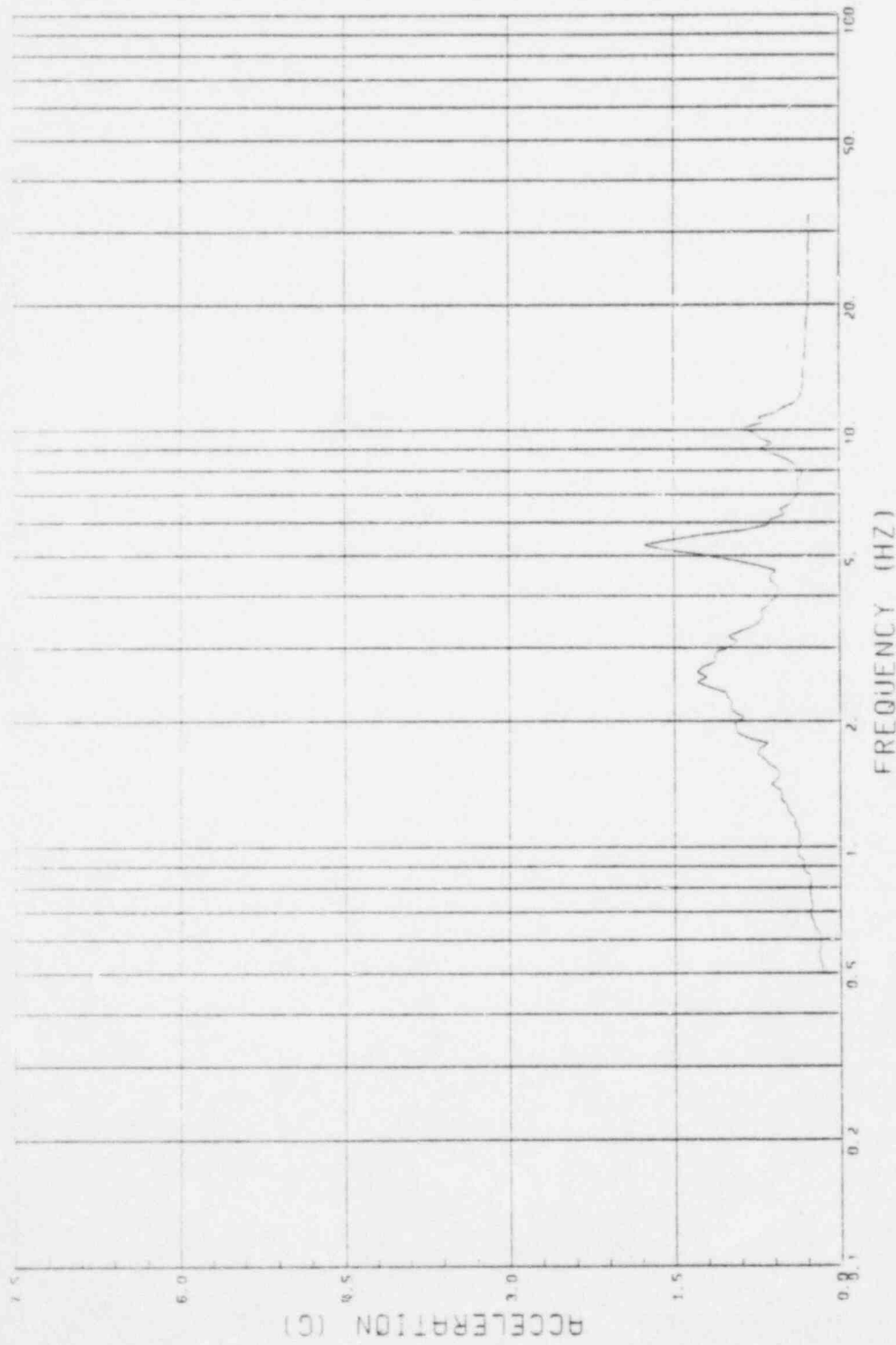


Figure A.32

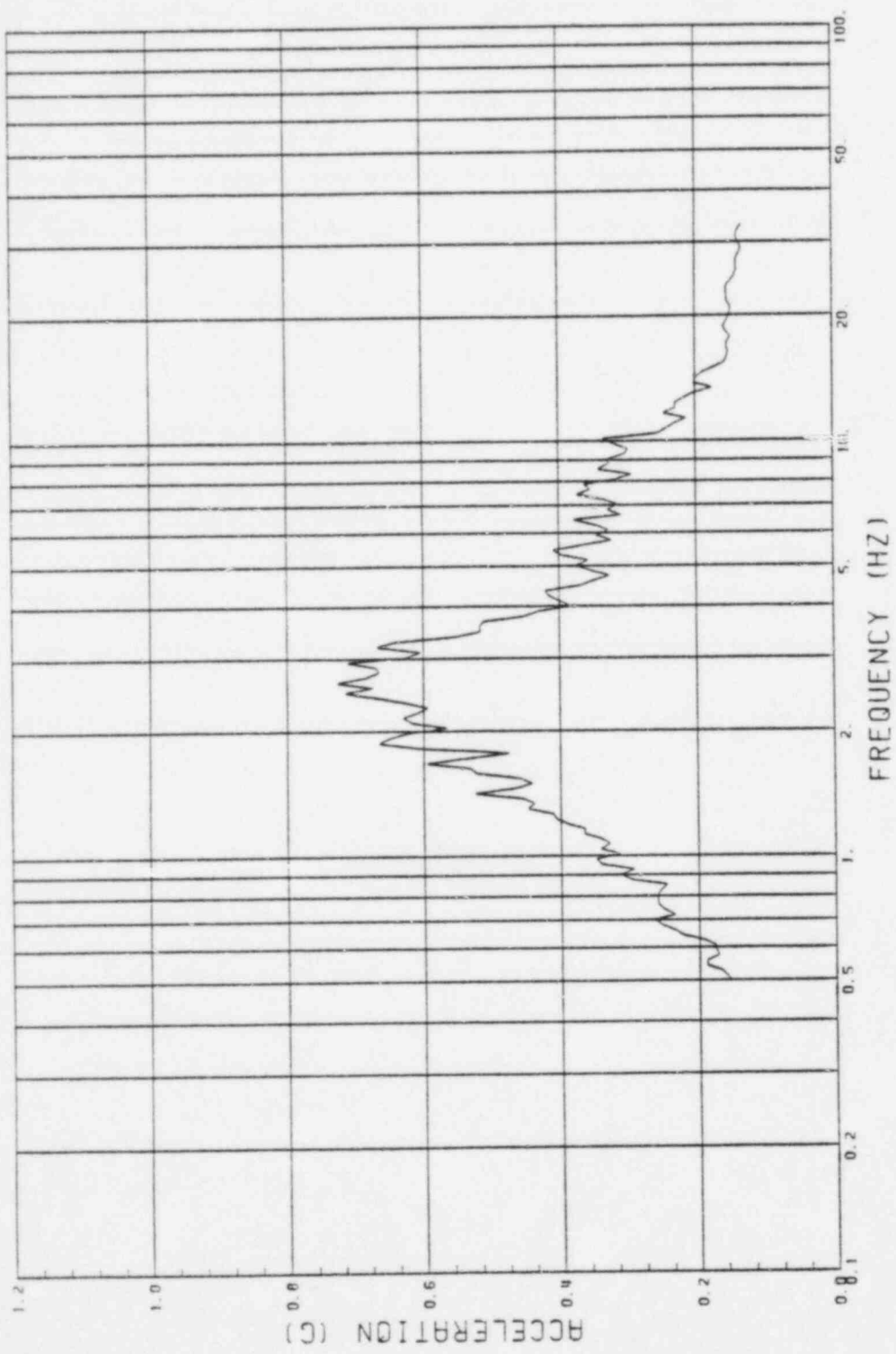


GE CLASS 1 ANALYSES
CASE 3, GE-75-U-H2
MODE NO. 109

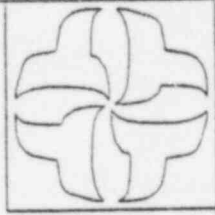


CESSAR II PLANT
SOIL - STRUCTURE INTERACTION

Figure A.33

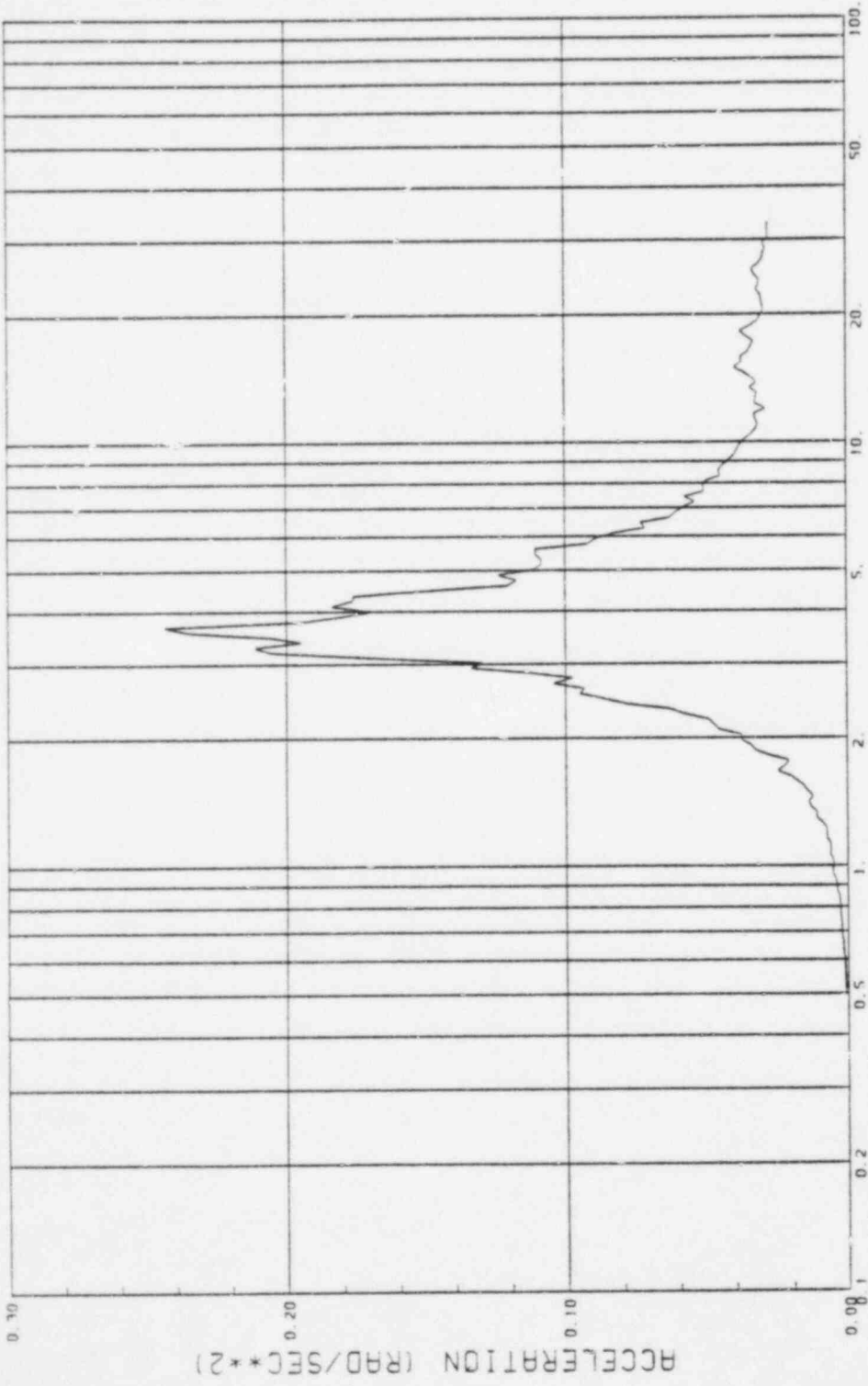


CE CLASSI ANALYSES
 CASE 4, CE-75-VP3-r2
 BASEMAT, NODE NO. 71 (TRANSLATION)

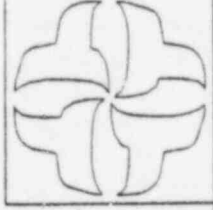


CESSAR II PLANT
 SOIL - STRUCTURE INTERACTION

Figure A.34

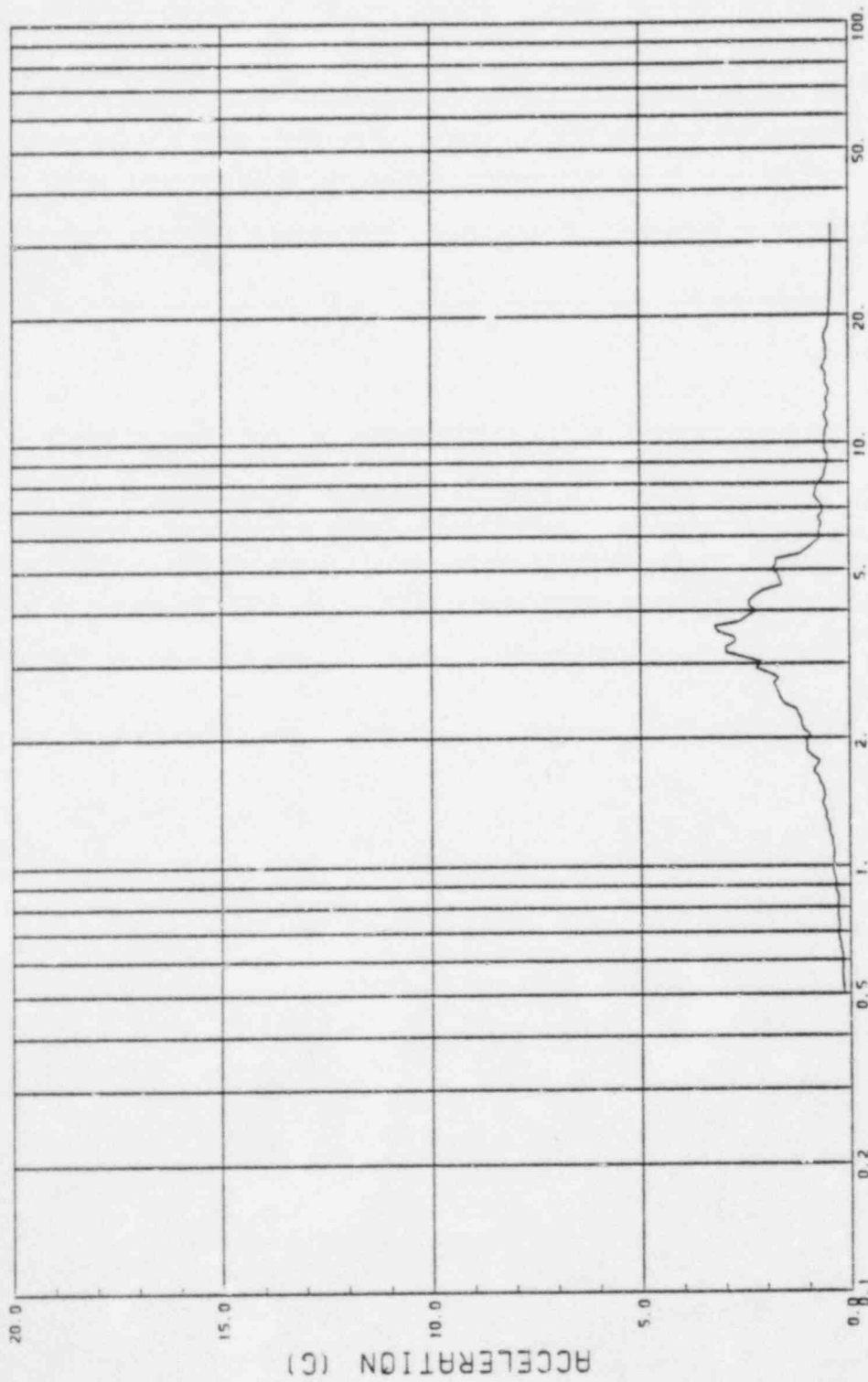


GE CLASS1 ANALYSES
CASE 4, CE-75-VP3-H2
BASEMAT, NODE NO. 71 (ROTATION)



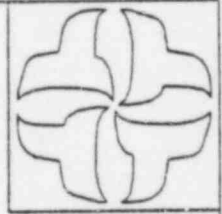
CESSAR II PLANT
SOIL - STRUCTURE INTERACTION

Figure A.35



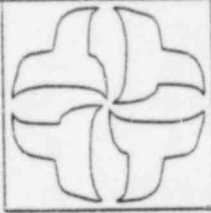
FREQUENCY (HZ)

GE CLASSI ANALYSES
CASE 4, GE-75-VP3-H2
NODE NO. 1



CESSAR II PLANT
SOIL - STRUCTURE INTERACTION

Figure A.36



CESSAR II PLANT
SOIL - STRUCTURE INTERACTION

CE CLASSI ANALYSES
CASE 4, CE-75-VP3-H2
NODE NO. 18

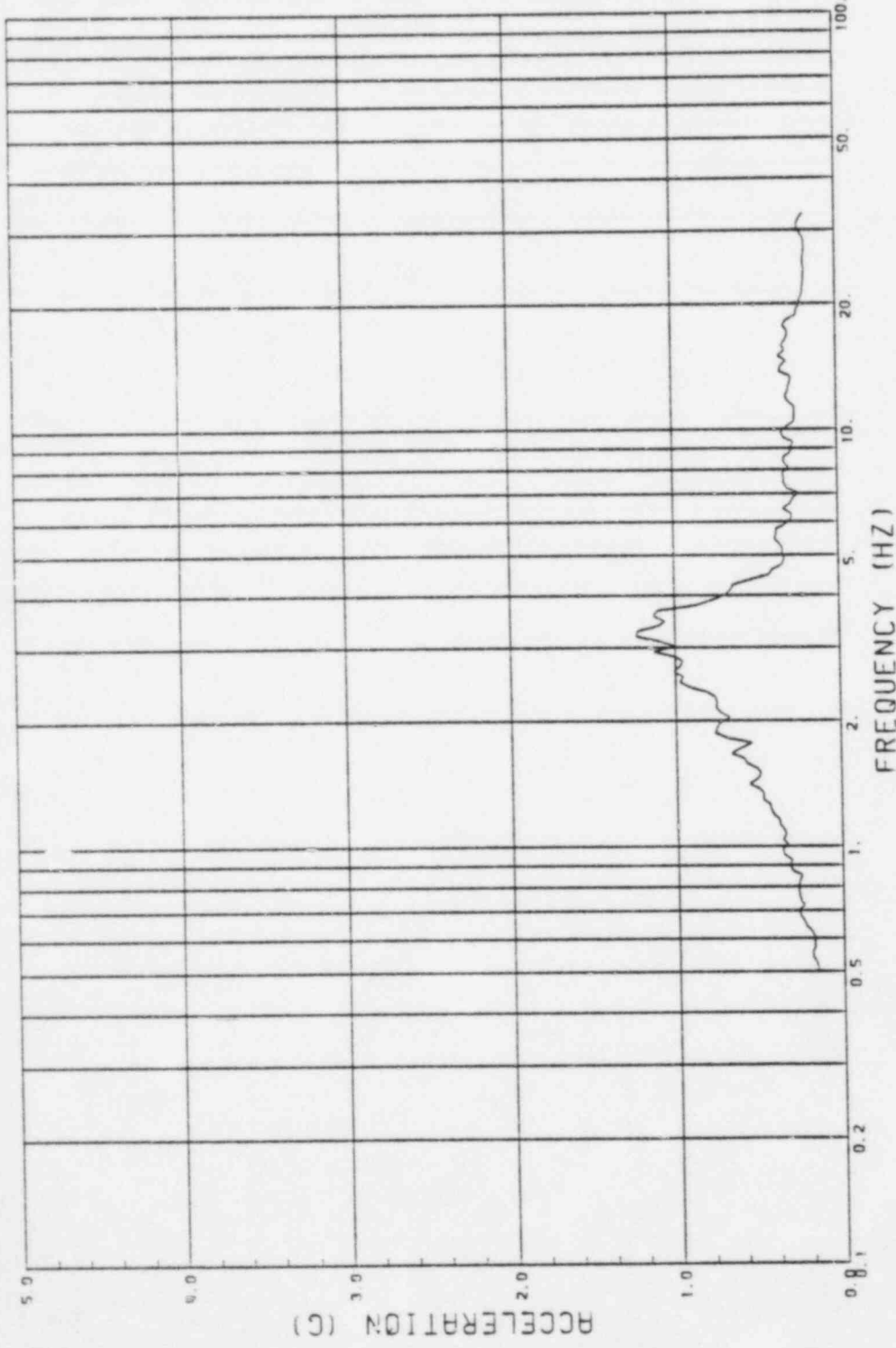
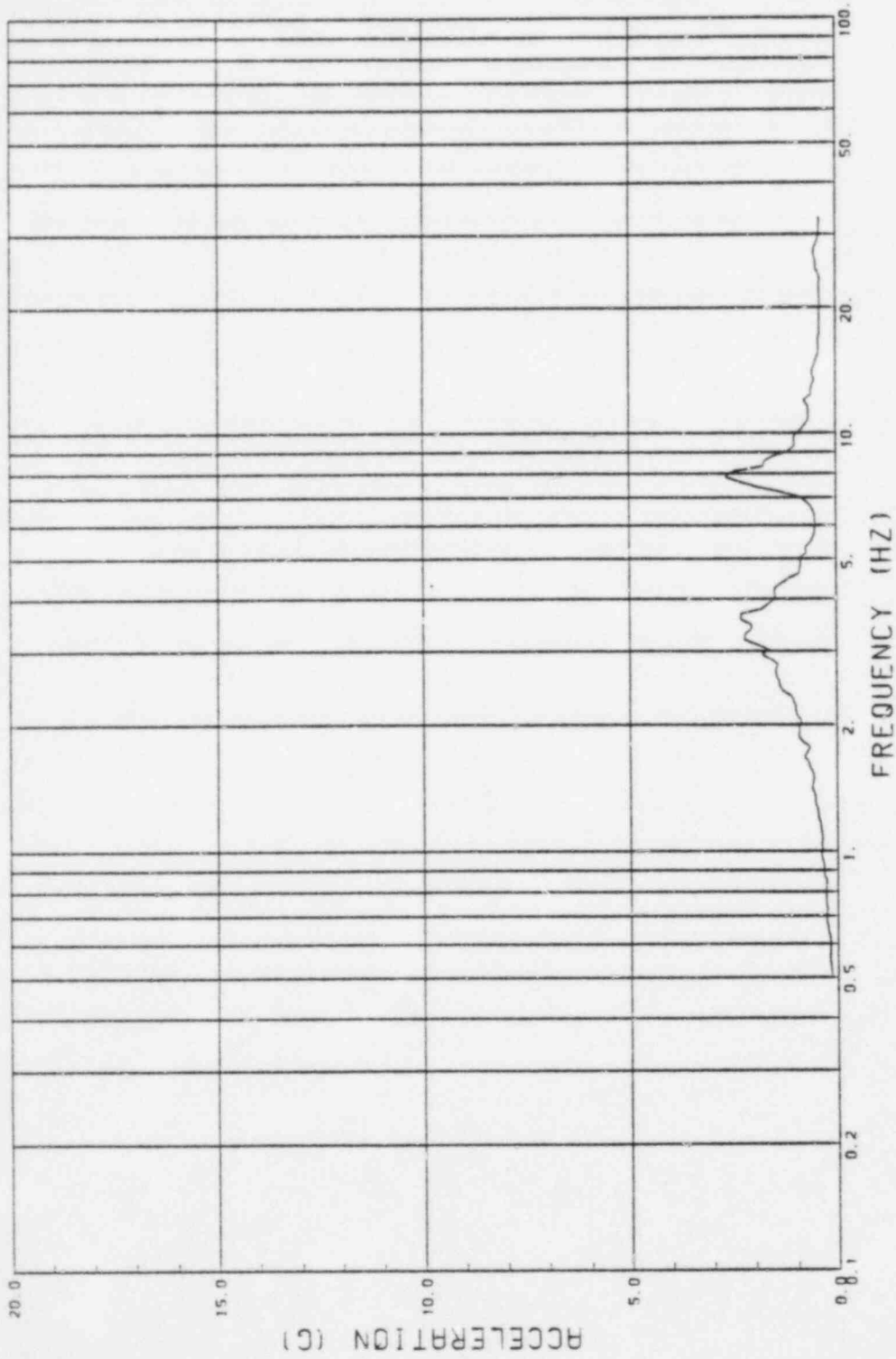
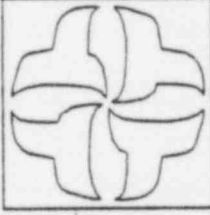


Figure A.37

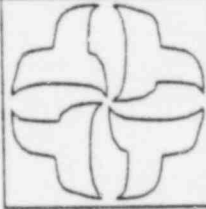


GE CLASS1 ANALYSES
CASE 4, GE-75-VP3-H2
NODE NO. 22



CESSAR II PLANT
SOIL - STRUCTURE INTERACTION

Figure A.38



CESSAR II PLANT
SOIL - STRUCTURE INTERACTION

GE CLASSI ANALYSES
CASE 4, GE-75-VP3-H2
NODE NO. 42

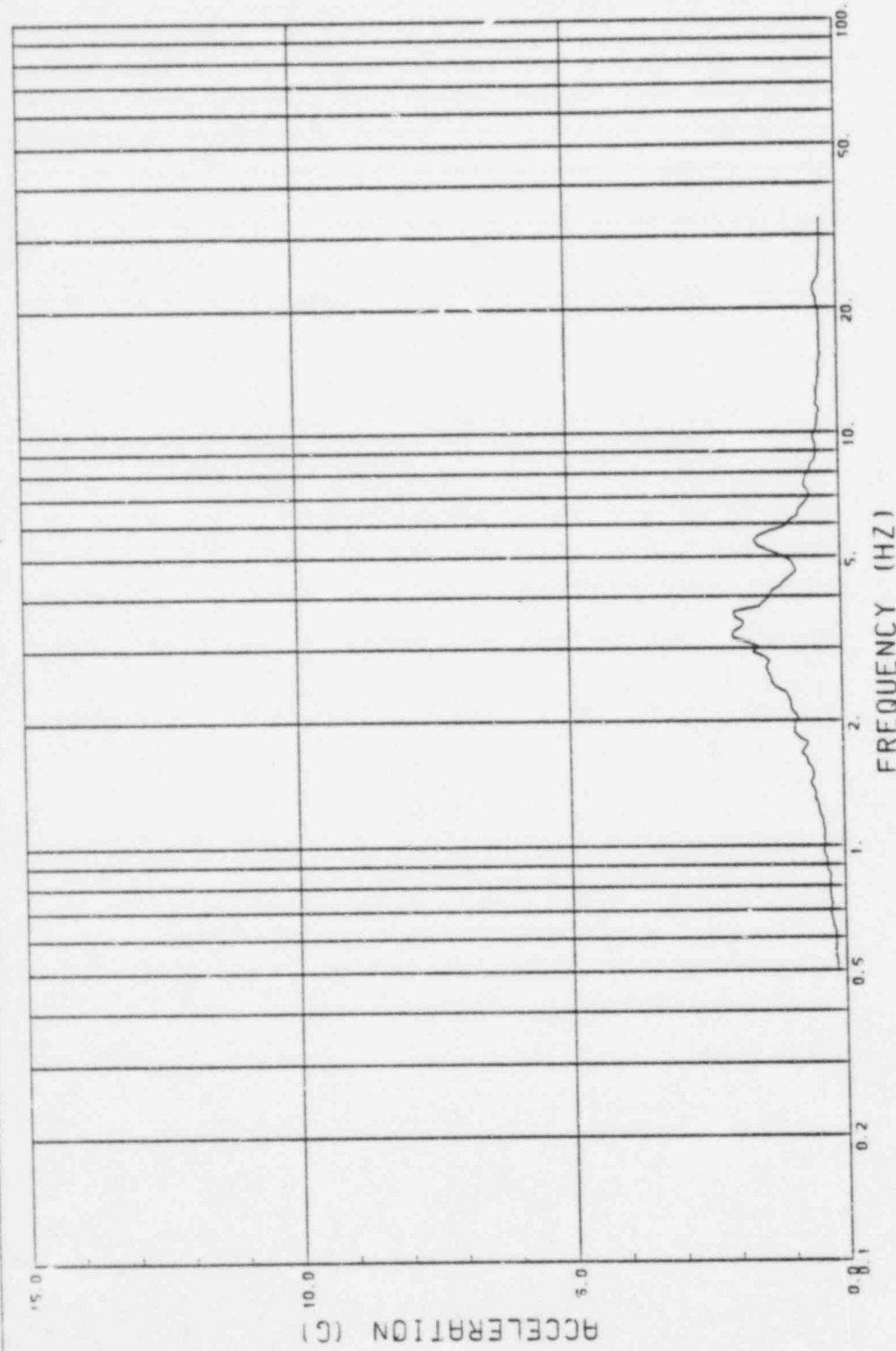
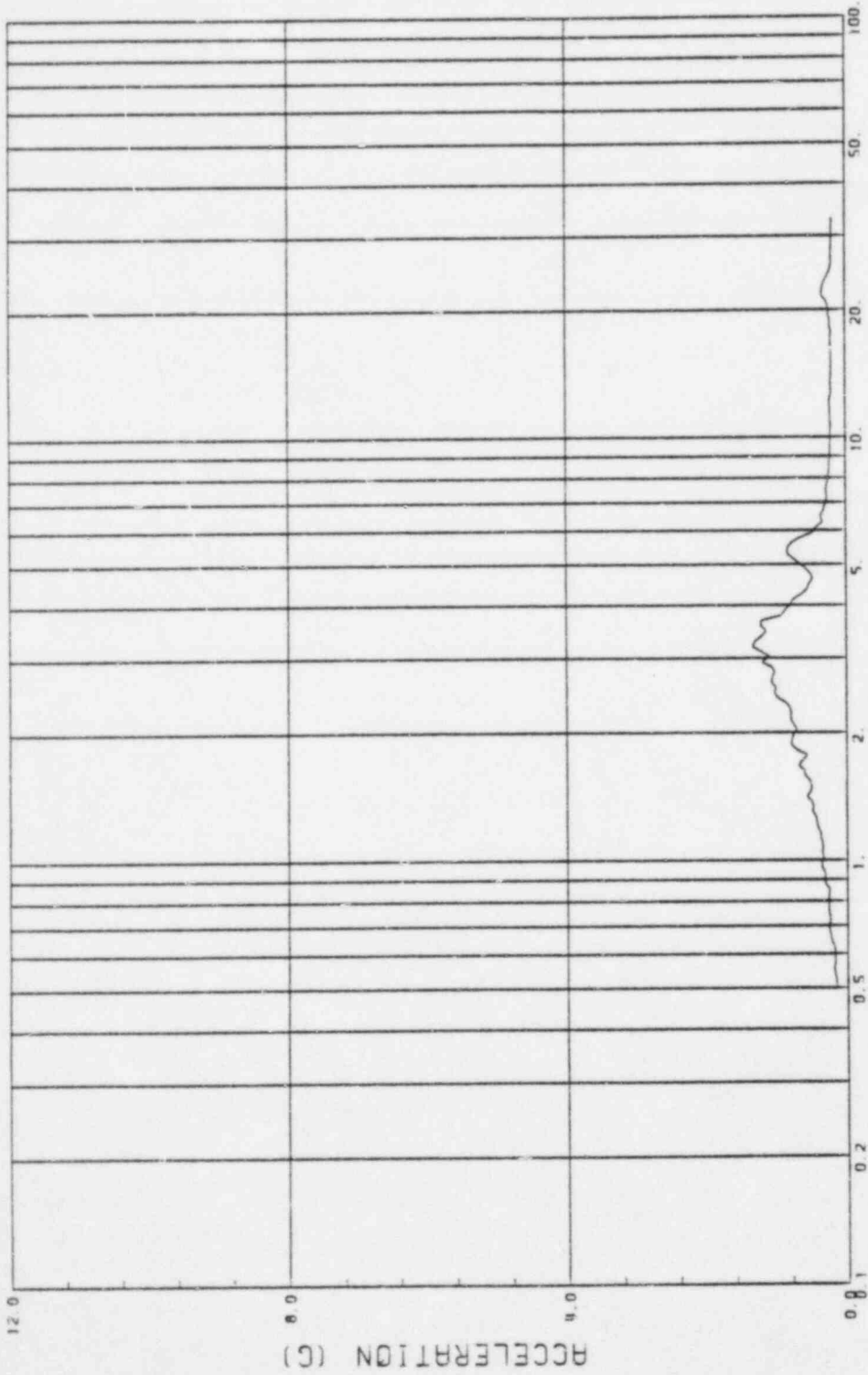
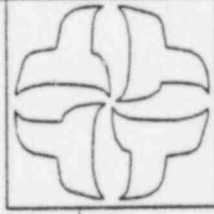


Figure A.39



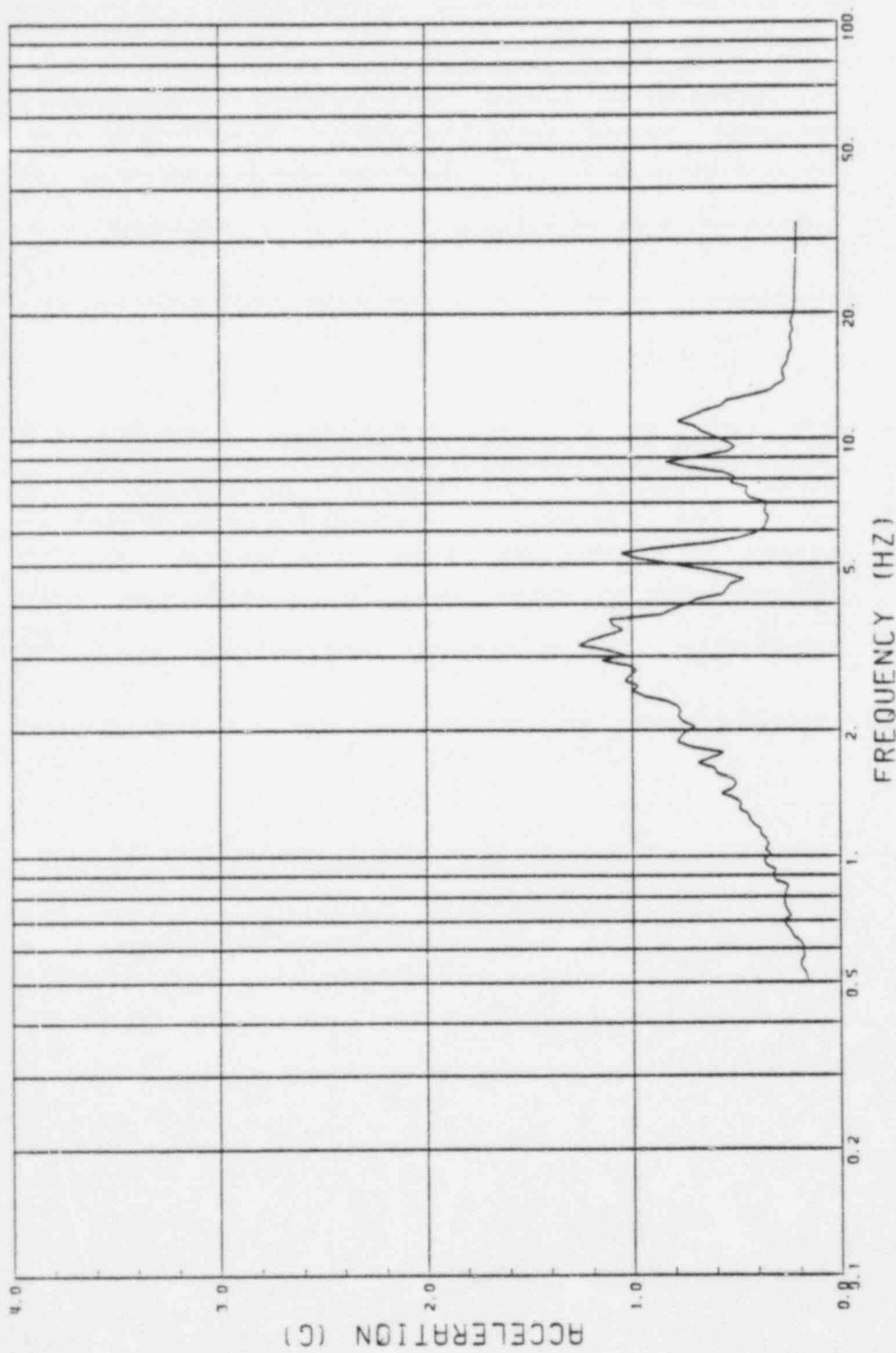
FREQUENCY (HZ)

GE CLASS1 ANALYSES
CASE 4, GE-75-VP3-H2
NODE NO. 46

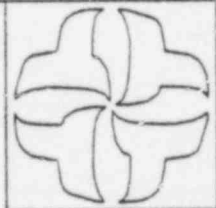


CESSAR II PLANT
SOIL - STRUCTURE INTERACTION

Figure A.40

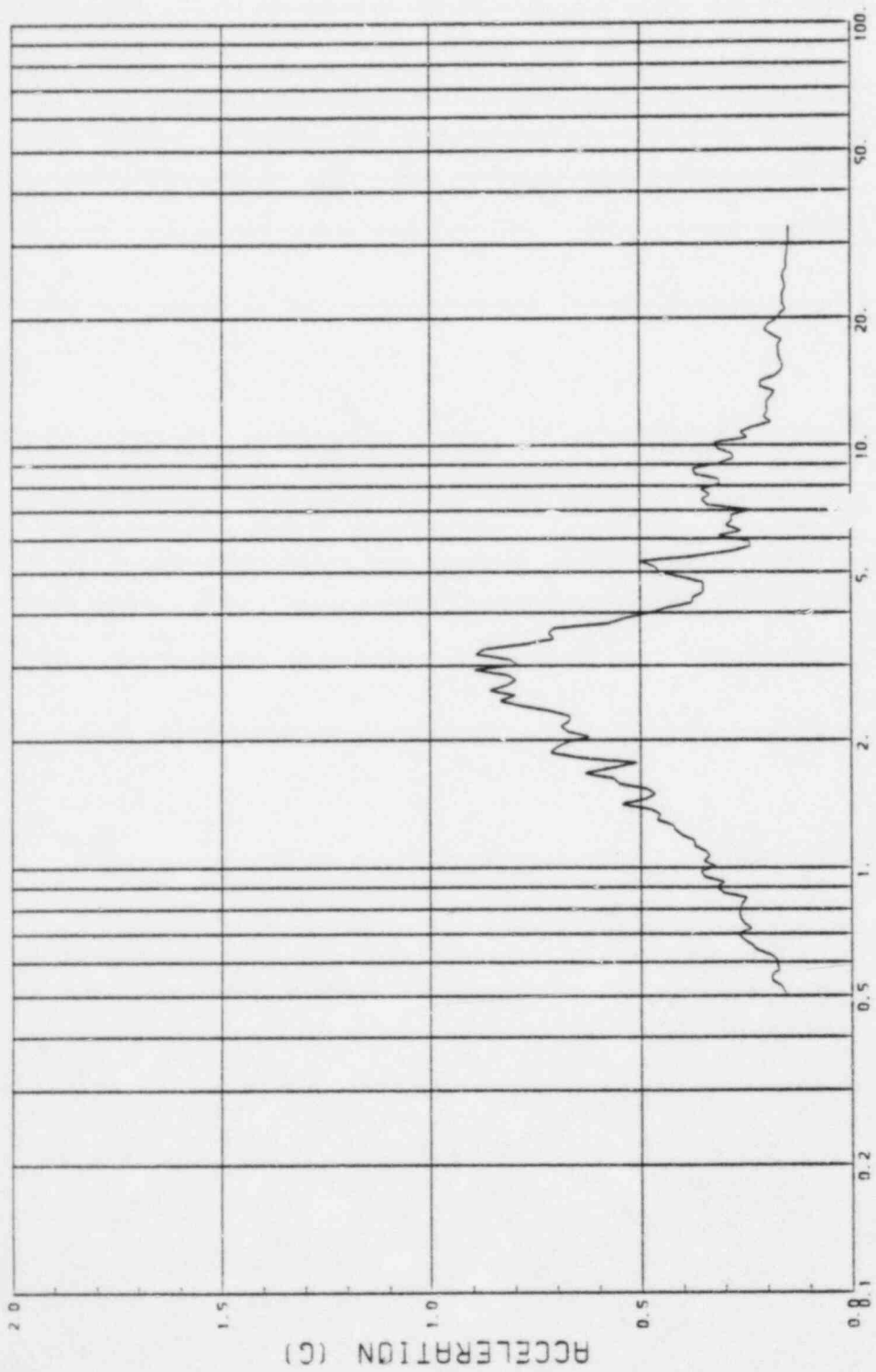


GE CLASSI ANALYSES
CASE 4, GE-75-VP3-H2
NODE NO. 60

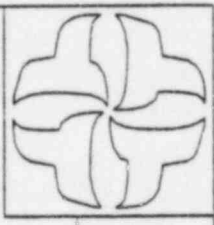


GESSAR II PLANT
SOIL - STRUCTURE INTERACTION

Figure A.41

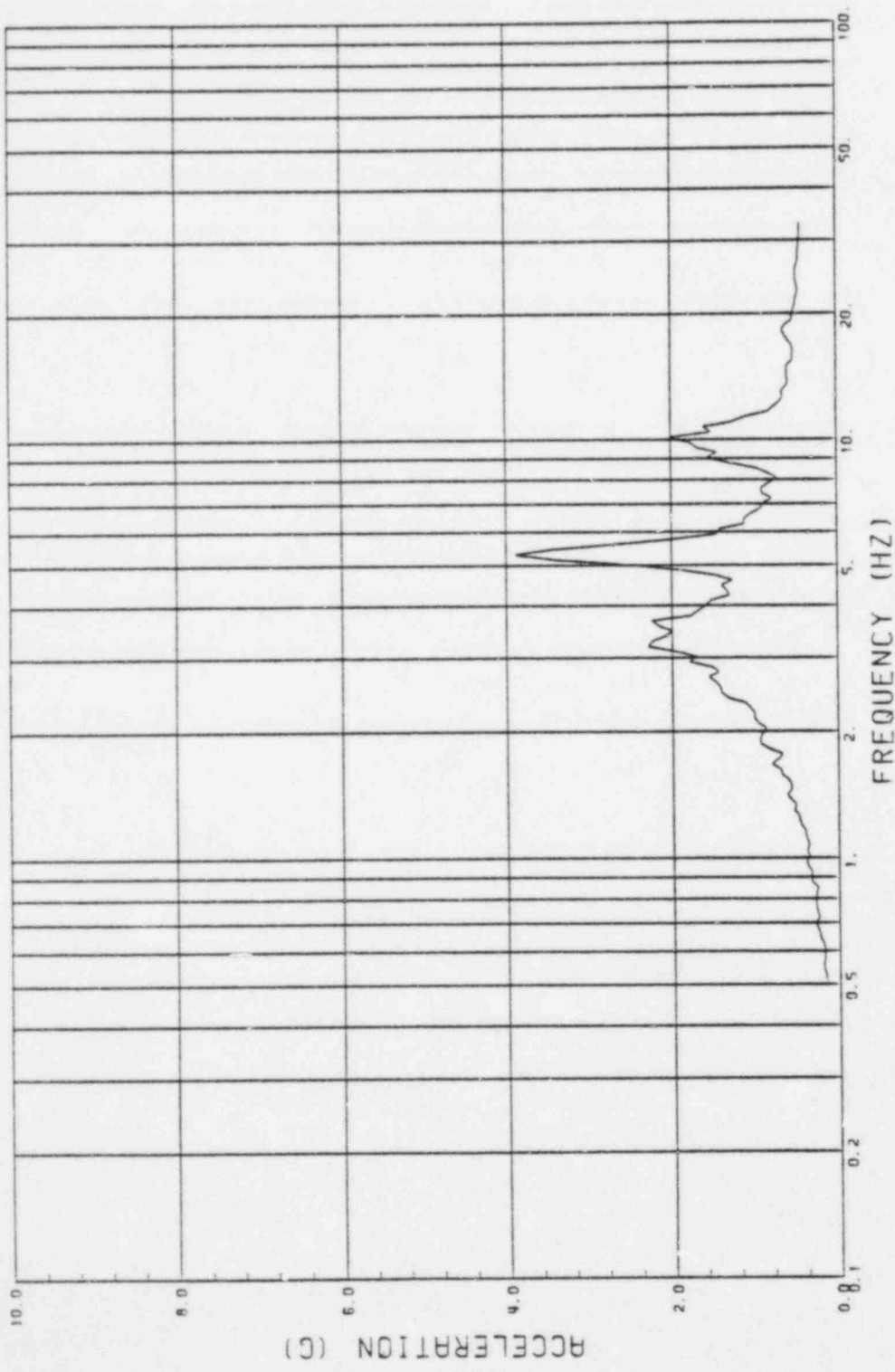


GE CLASSI ANALYSES
CASE 4, GE-75-VP3-H2
NODE NO. 64

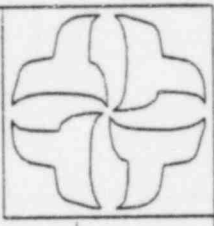


CESSAR II PLANT
SOIL - STRUCTURE INTERACTION

Figure A.42

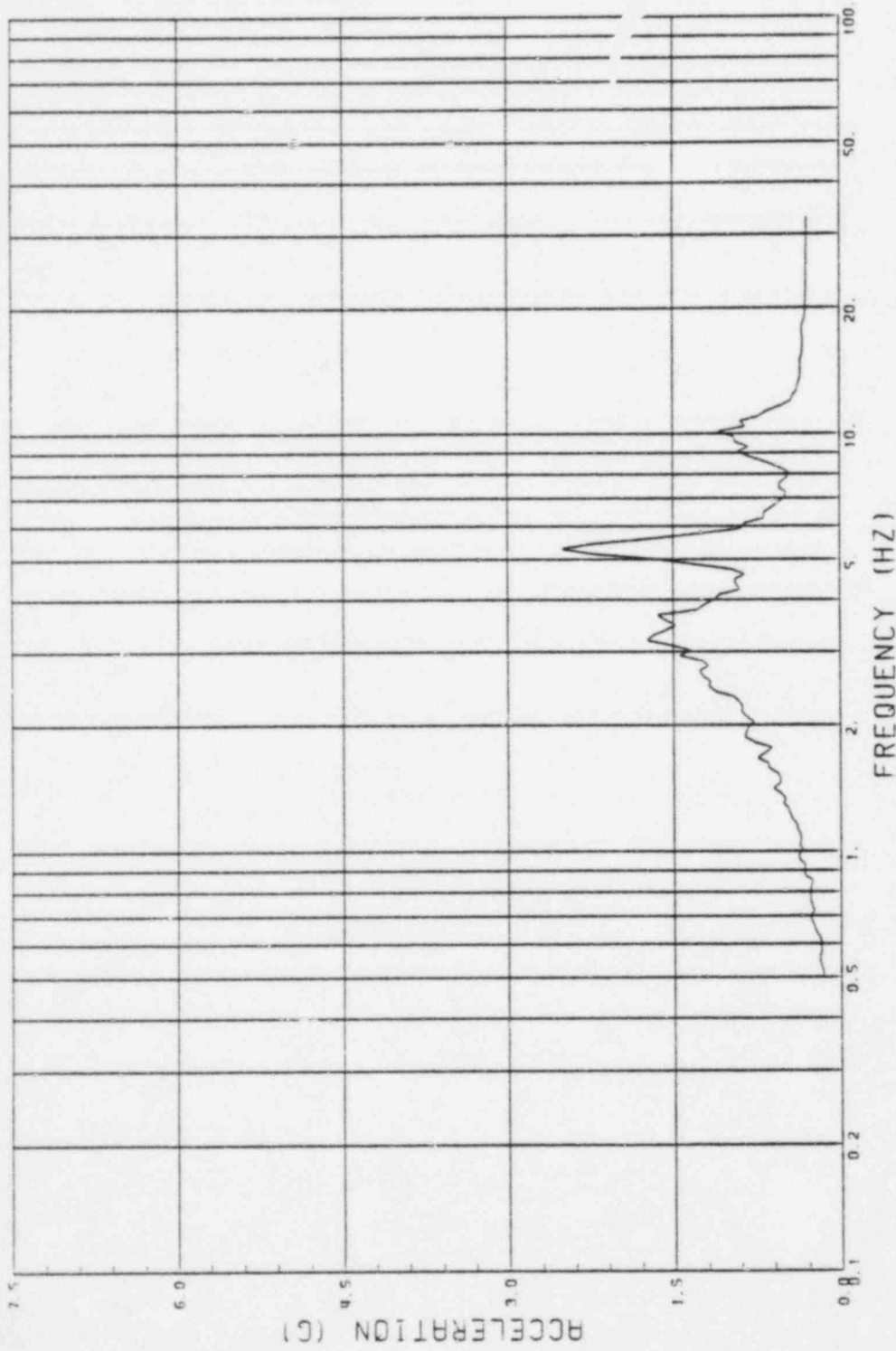
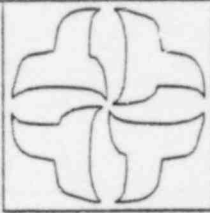


GE CLASS1 ANALYSES
CASE 4, GE-75-VP3-H2
NODE NO. 101



CESSAR II PLANT
SOIL - STRUCTURE INTERACTION

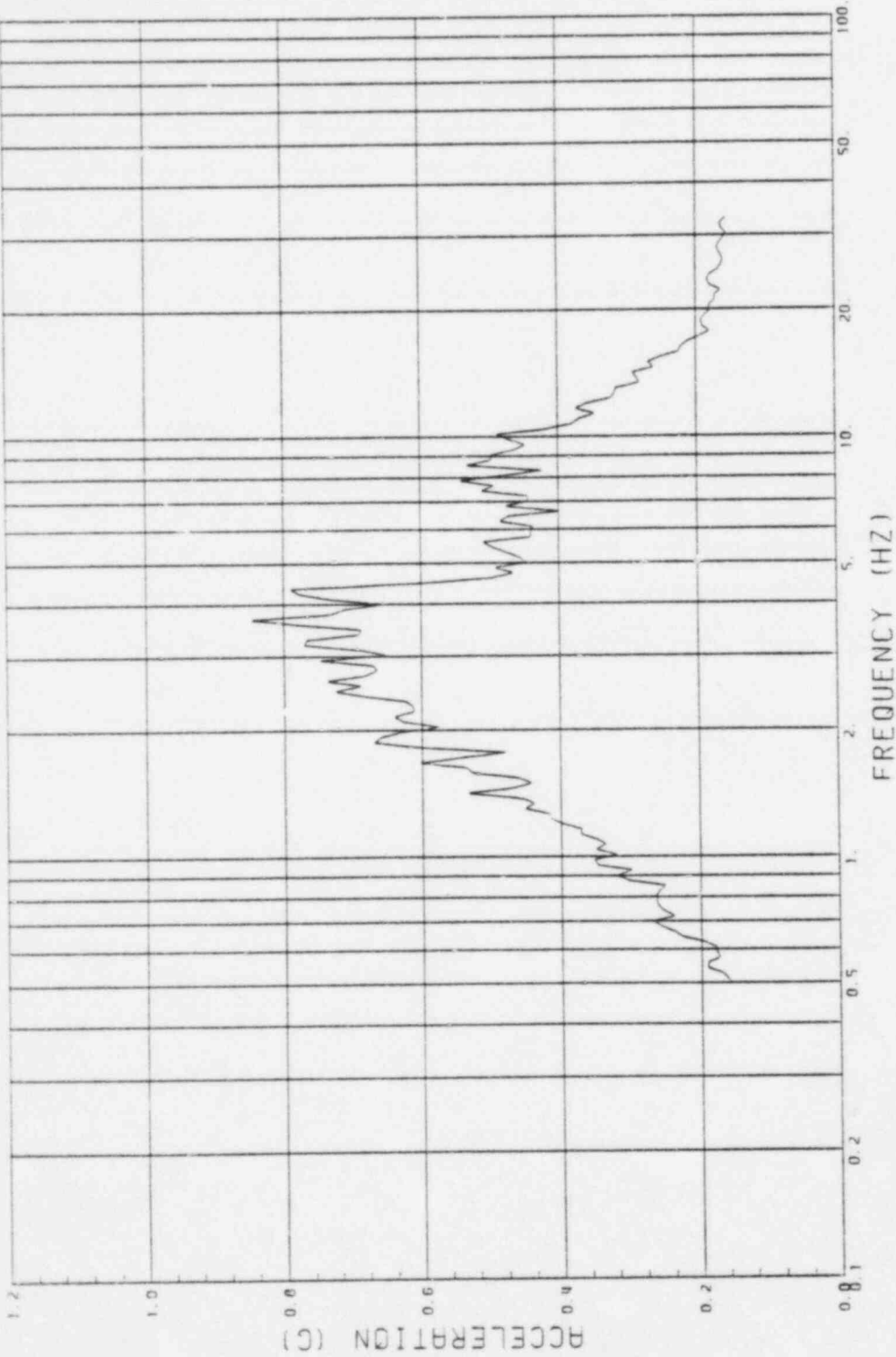
Figure A.43



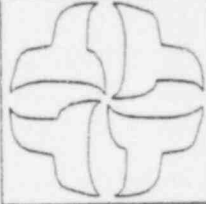
GE CLASS1 ANALYSES
CASE 4, GE-75-VP3-H2
NODE NO. 109

SOIL - STRUCTURE INTERACTION
GESSAR II PLANT

Figure A.44

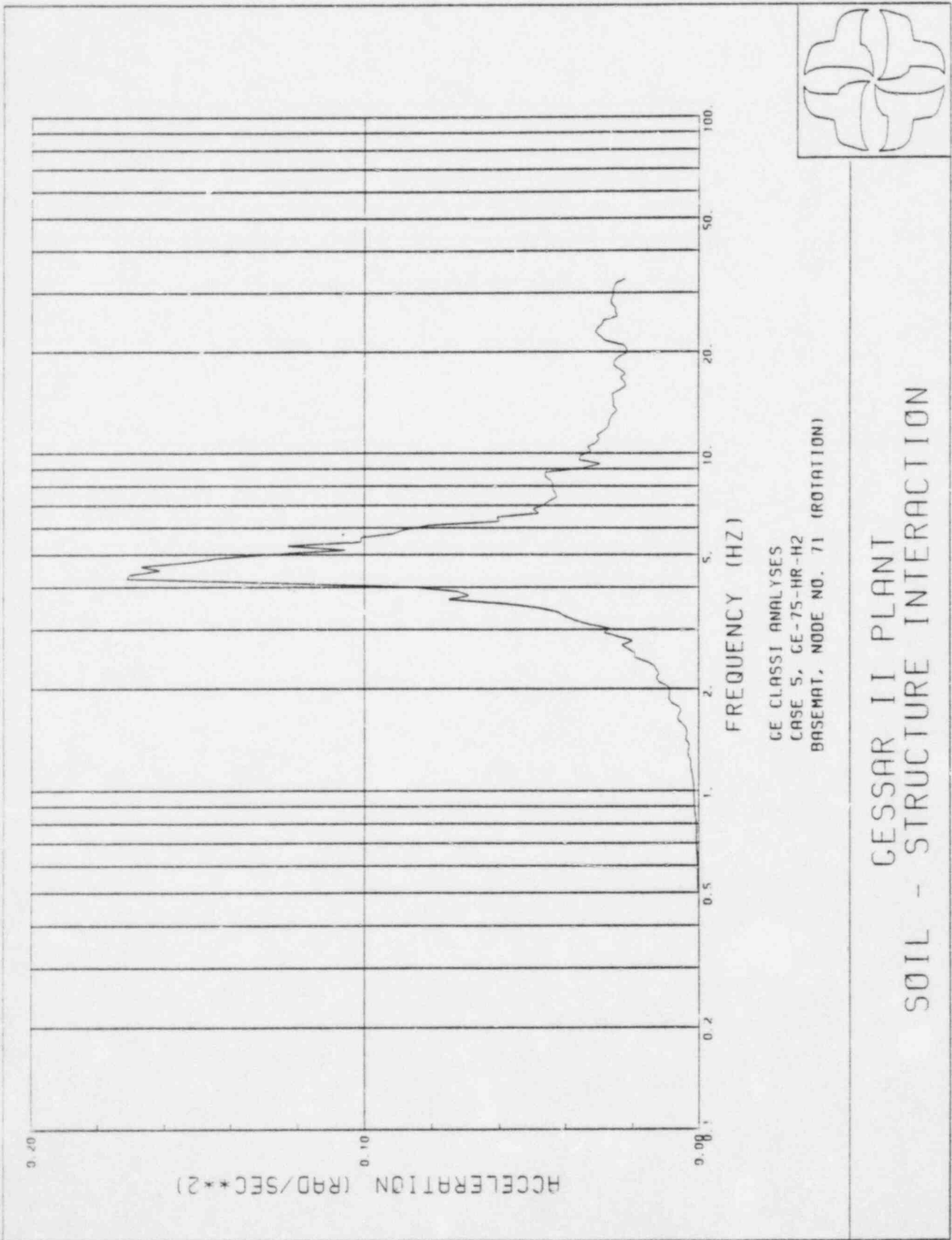


GE CLASSI ANALYSES
CASE 5, GE-75-HR-H2
BASEMAT, NODE NO. 7; (TRANSLATION)



SOIL - STRUCTURE INTERACTION
GESSAR II PLANT

Figure A.45



CESSAR II PLANT
SOIL - STRUCTURE INTERACTION

Figure A.46

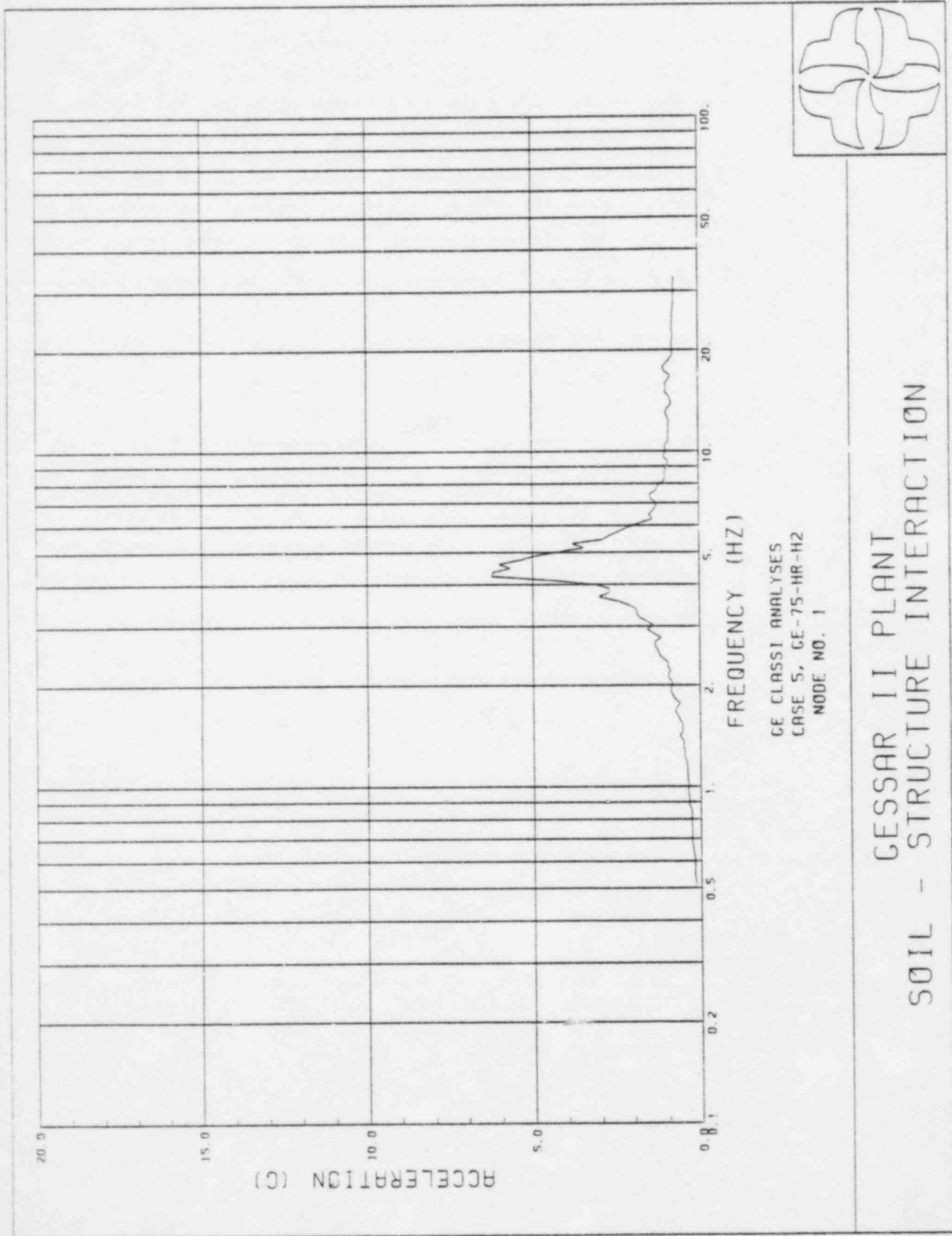
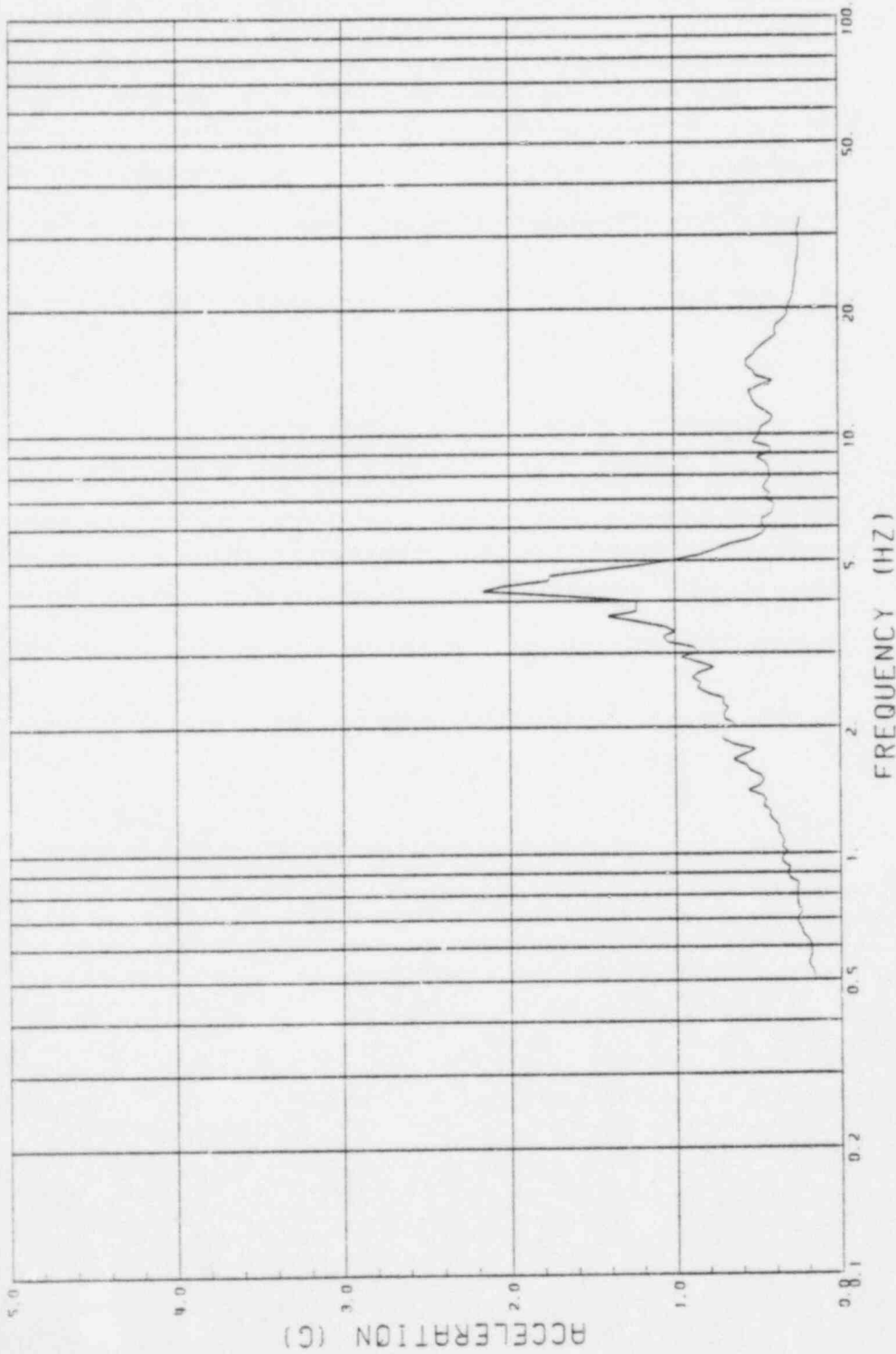
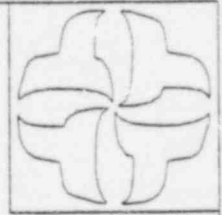


Figure A.47

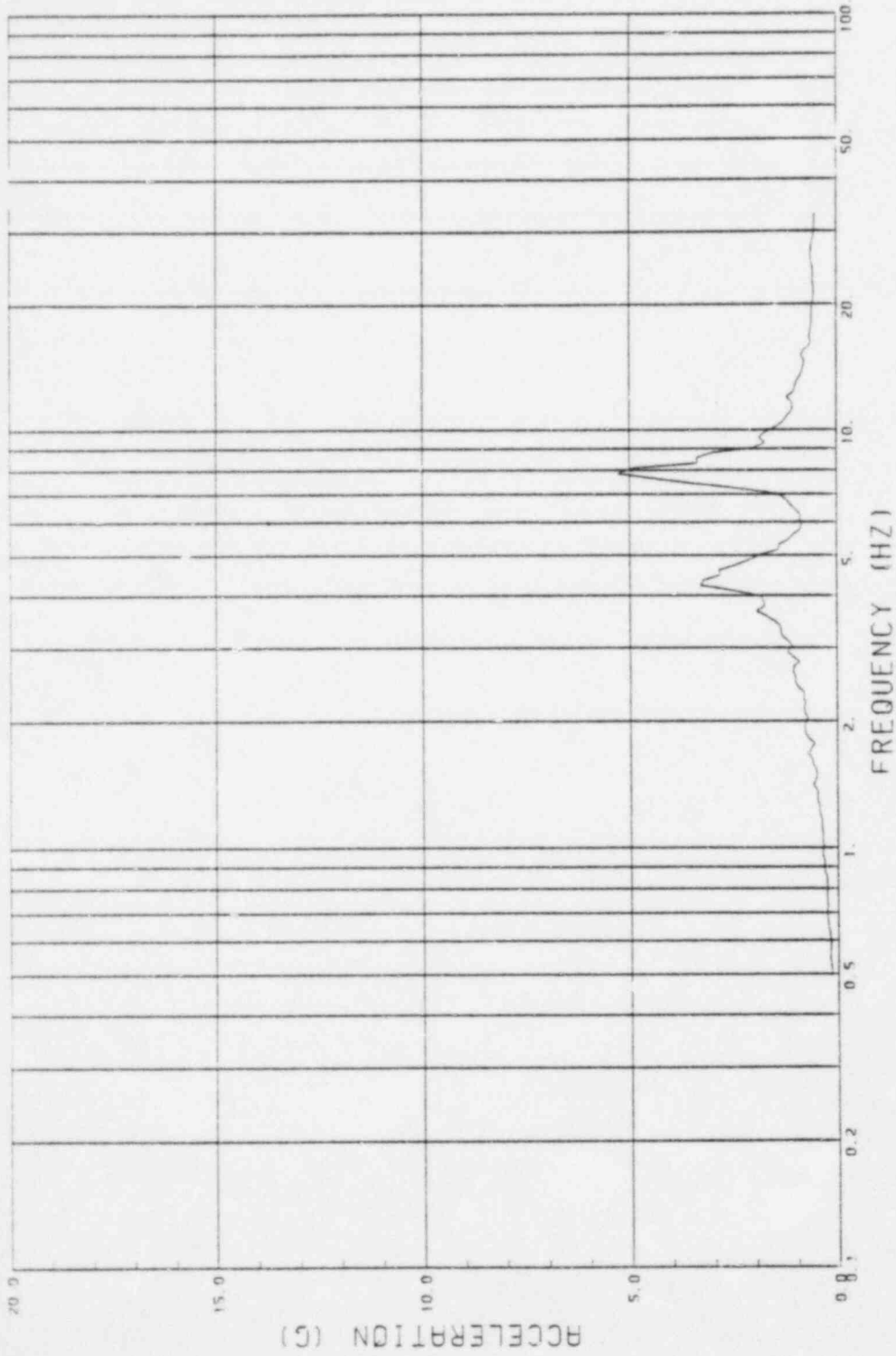


GE CLASSI ANALYSES
CASE 5, GE-75-HR-H2
NODE NO. 18

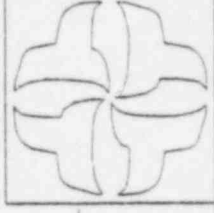


CESSAR II PLANT
SOIL - STRUCTURE INTERACTION

Figure A.48

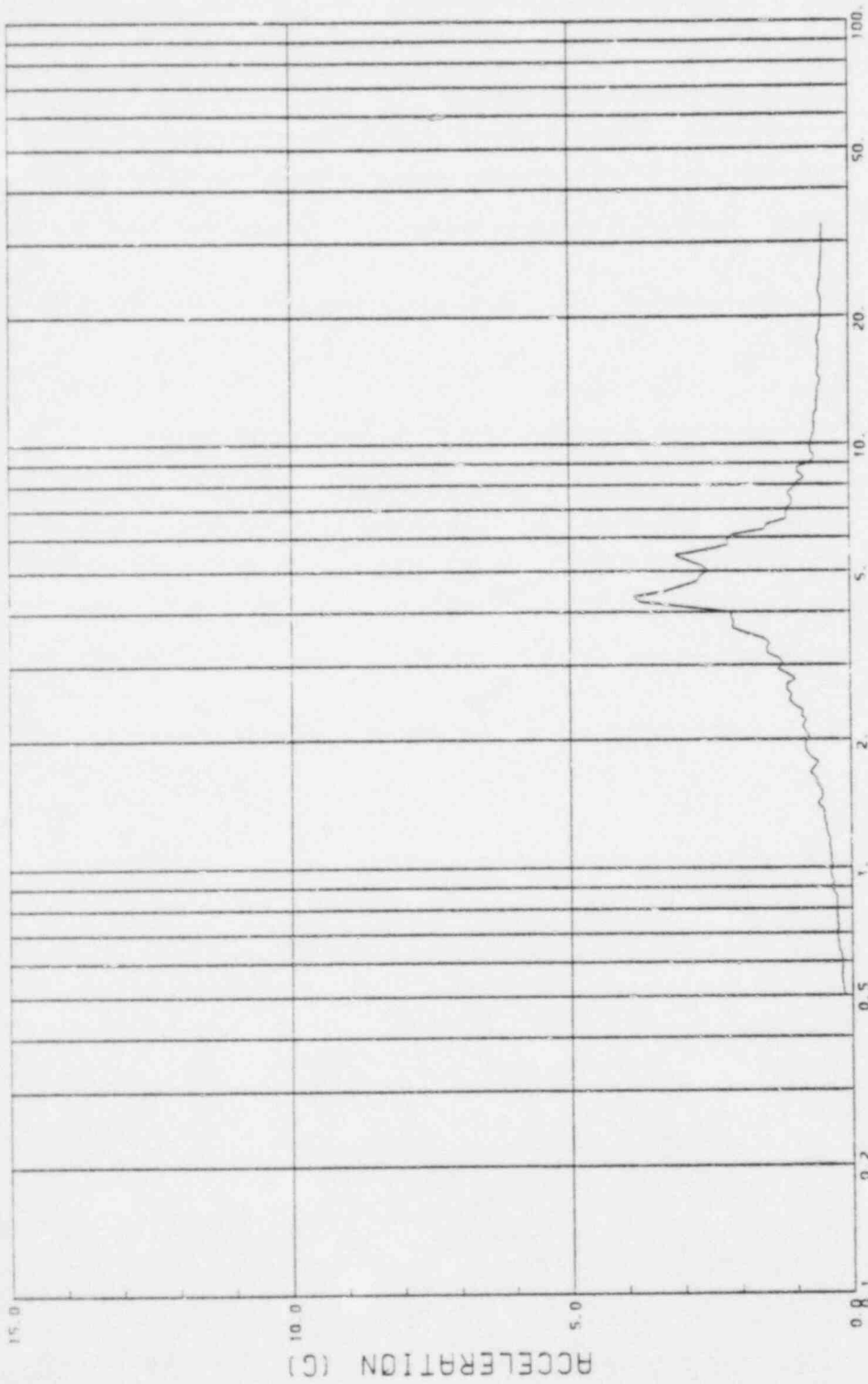


GE CLASS1 ANALYSES
CASE 5, GE-75-HR-H2
NODE NO. 22



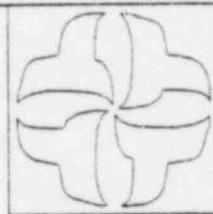
CESSAR II PLANT
SOIL - STRUCTURE INTERACTION

Figure A.49



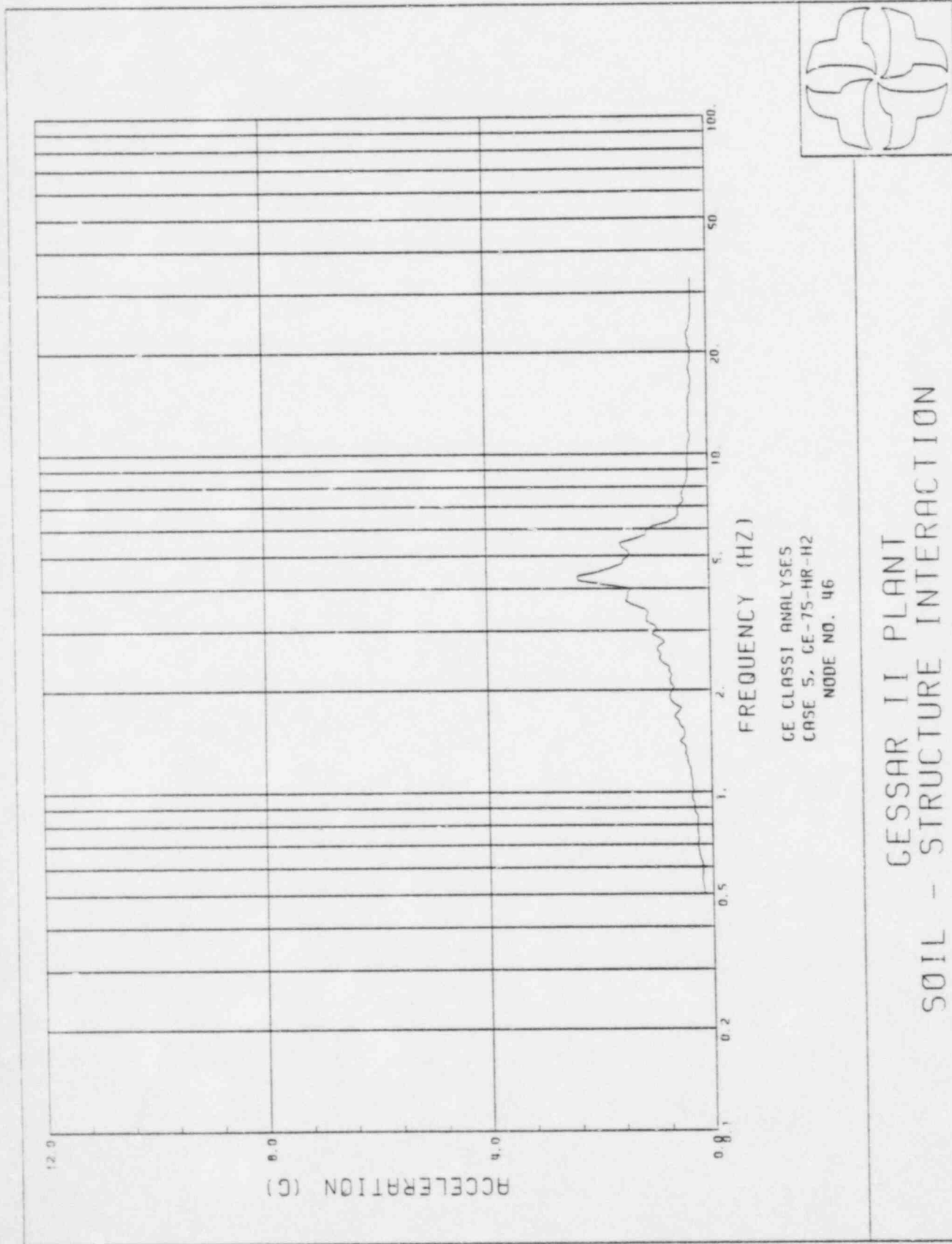
FREQUENCY (HZ)

GE CLASS1 ANALYSES
CASE 5, CE-75-HR-H2
NODE NO. 42



CESSAR II PLANT
SOIL - STRUCTURE INTERACTION

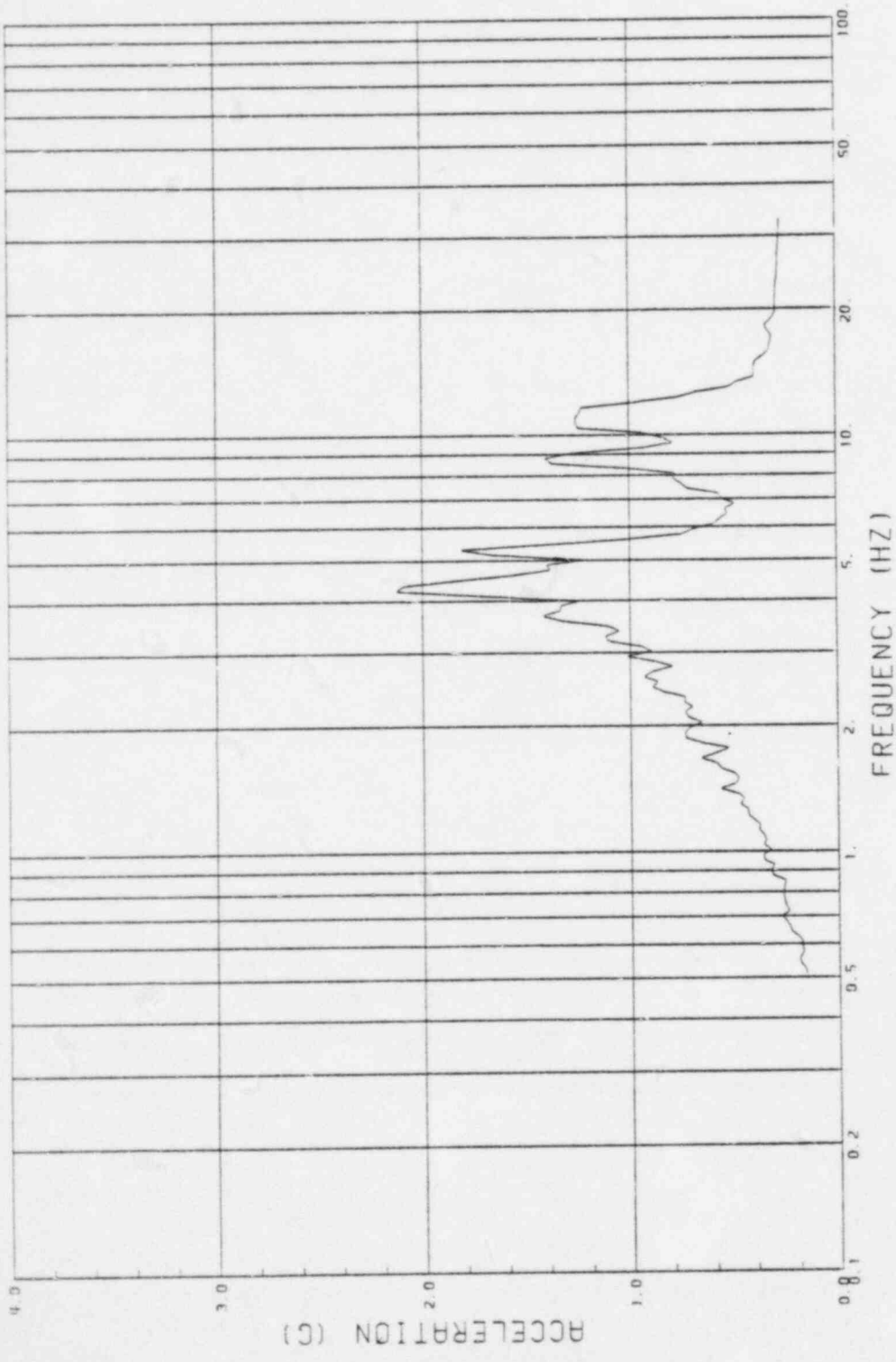
Figure A.50



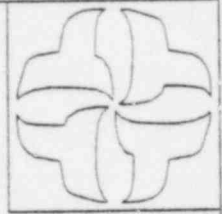
CE CLASSI ANALYSES
 CASE 5, CE-75-HR-H2
 NODE NO. 46

CESSAR II PLANT
 SOIL - STRUCTURE INTERACTION

Figure A.51

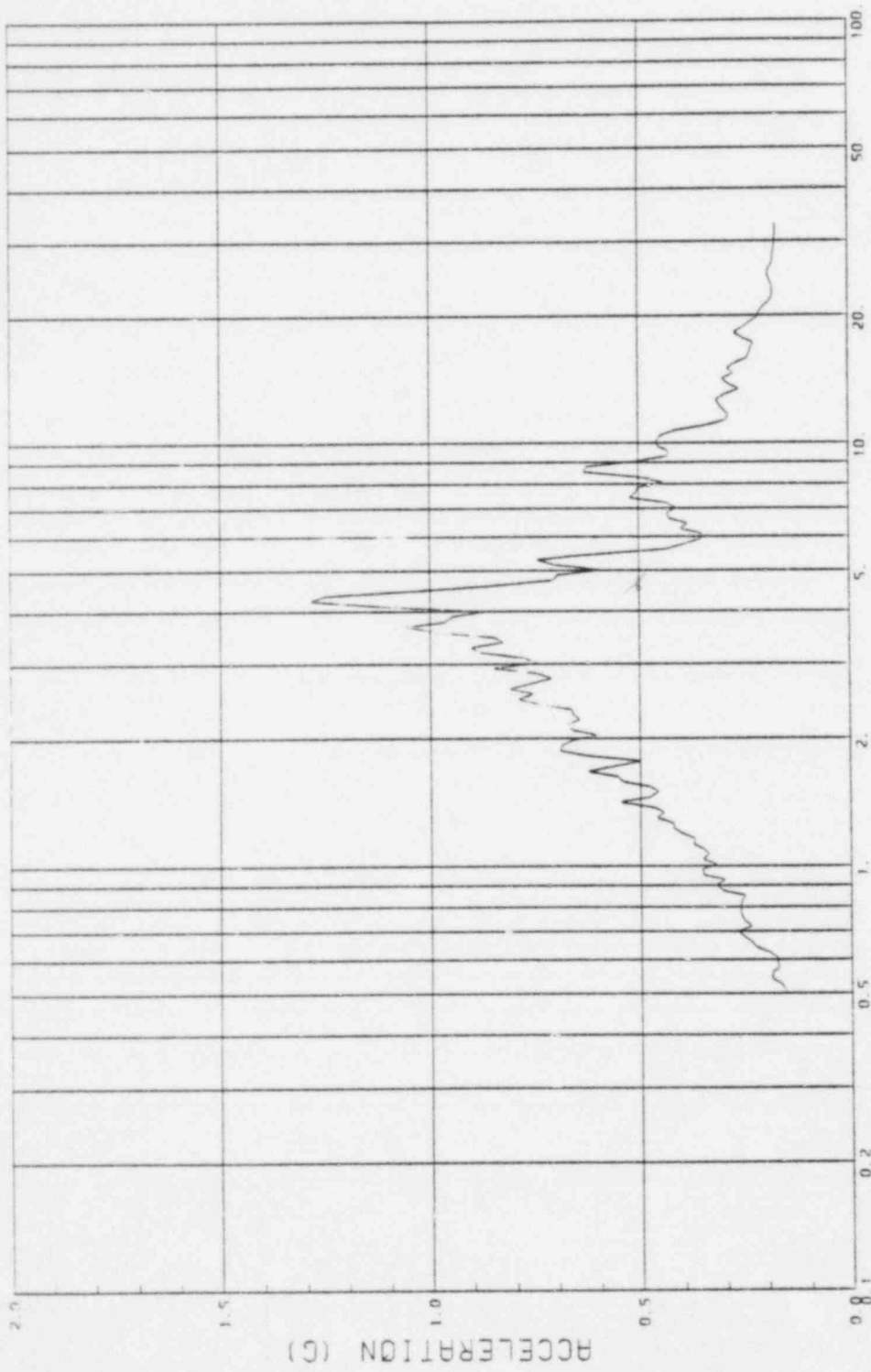


GE CLASSI ANALYSES
CASE 5, GE-75-HR-H2
NODE NO. 60



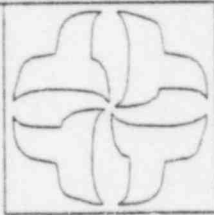
CESSAR II PLANT
SOIL - STRUCTURE INTERACTION

Figure A.52



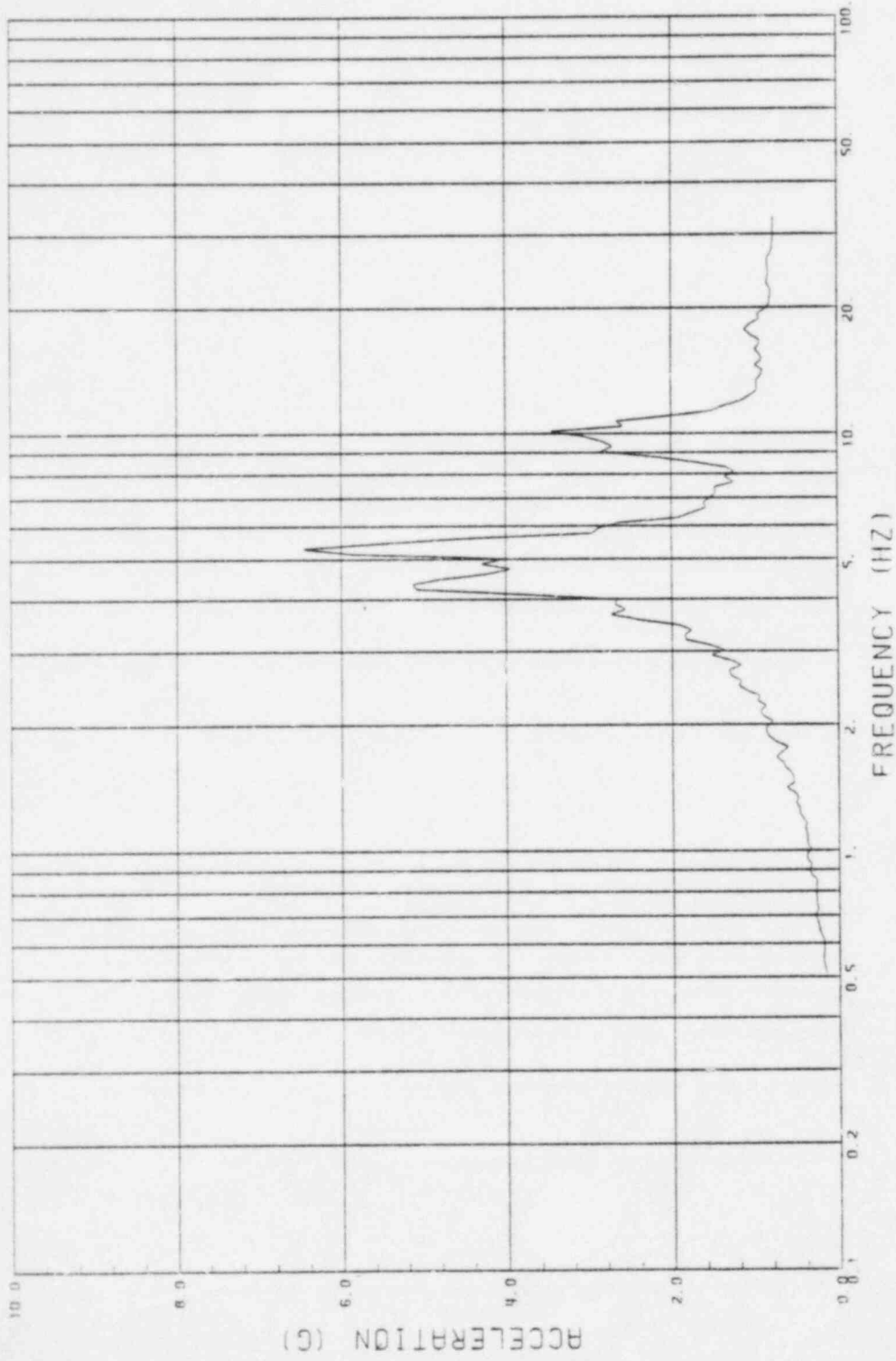
FREQUENCY (HZ)

GE CLASSI ANALYSES
CASE 5, GE-75-HR-H2
NODE NO. 64

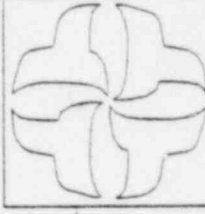


CESSAR II PLANT
SOIL - STRUCTURE INTERACTION

Figure A.53

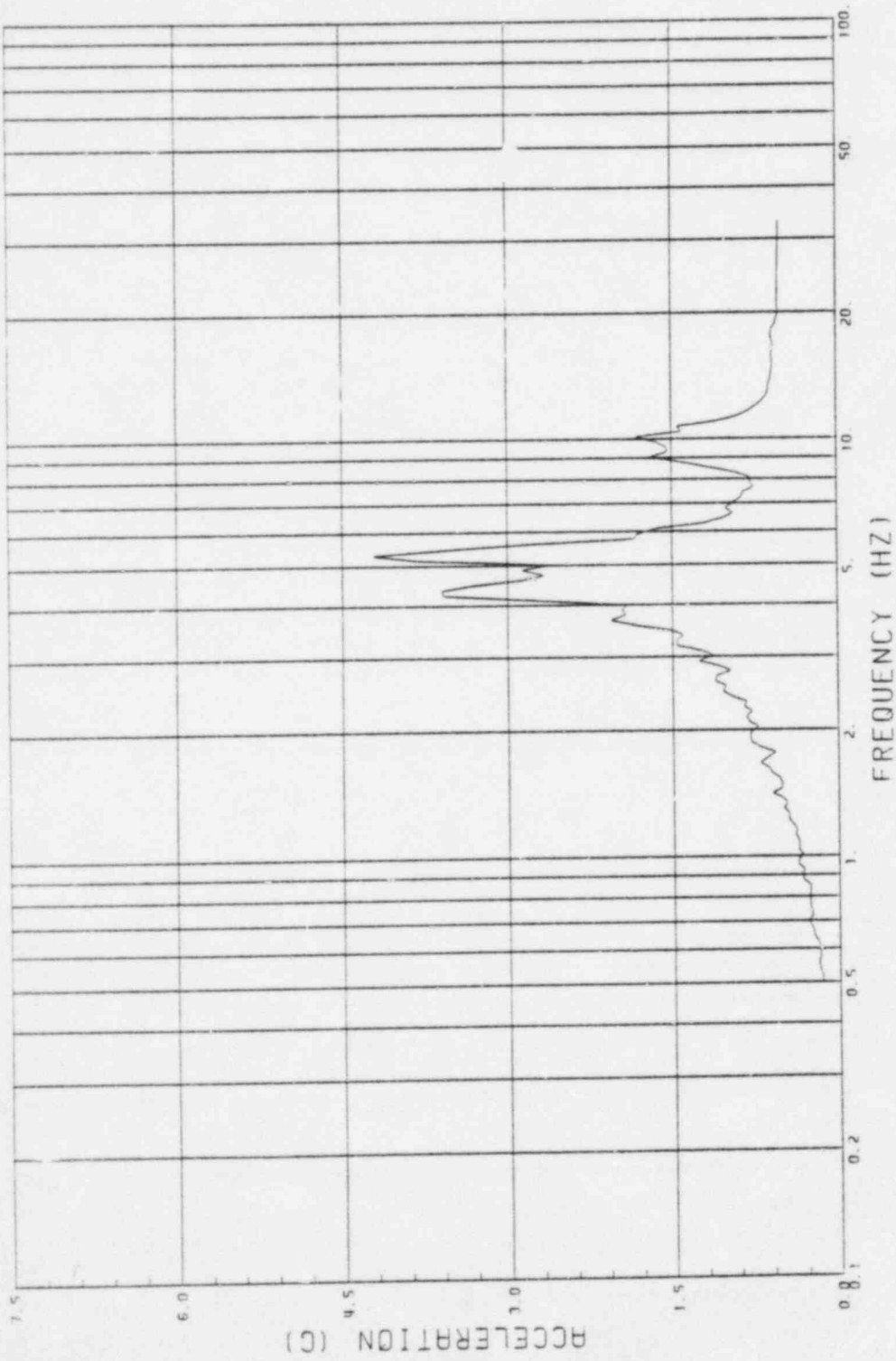


GE CLASSI ANALYSES
CASE 5, GE-75-HR-H2
NODE NO. 101

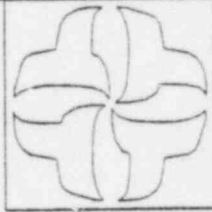


CESSAR II PLANT
SOIL - STRUCTURE INTERACTION

Figure A.54

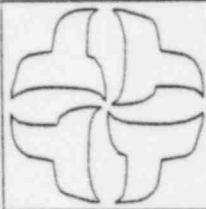


GE CLASSI ANALYSES
 CASE 5, GE-75-HR-H2
 NODE NO. 109

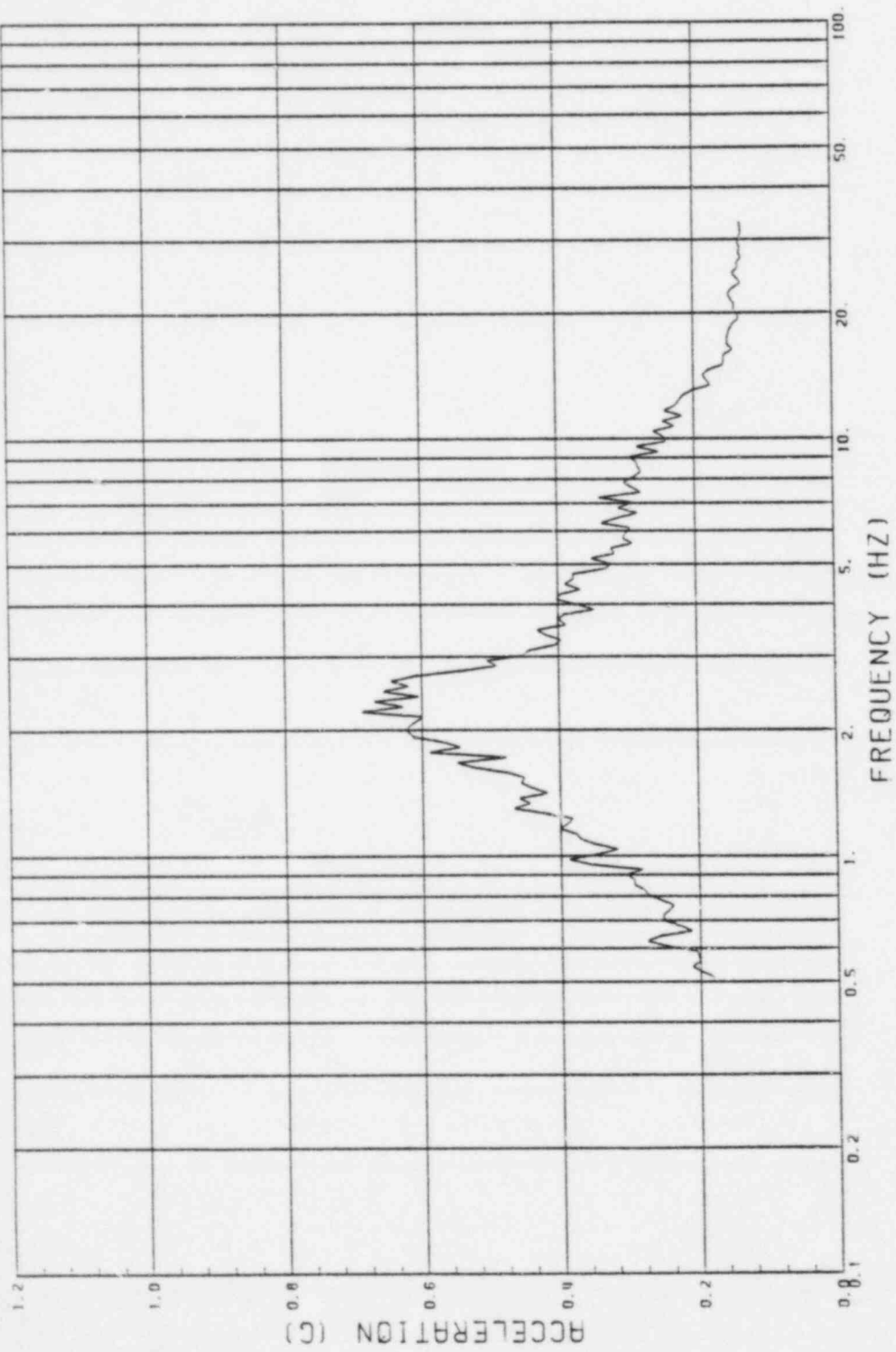


CESSAR II PLANT
 SOIL - STRUCTURE INTERACTION

Figure A.55

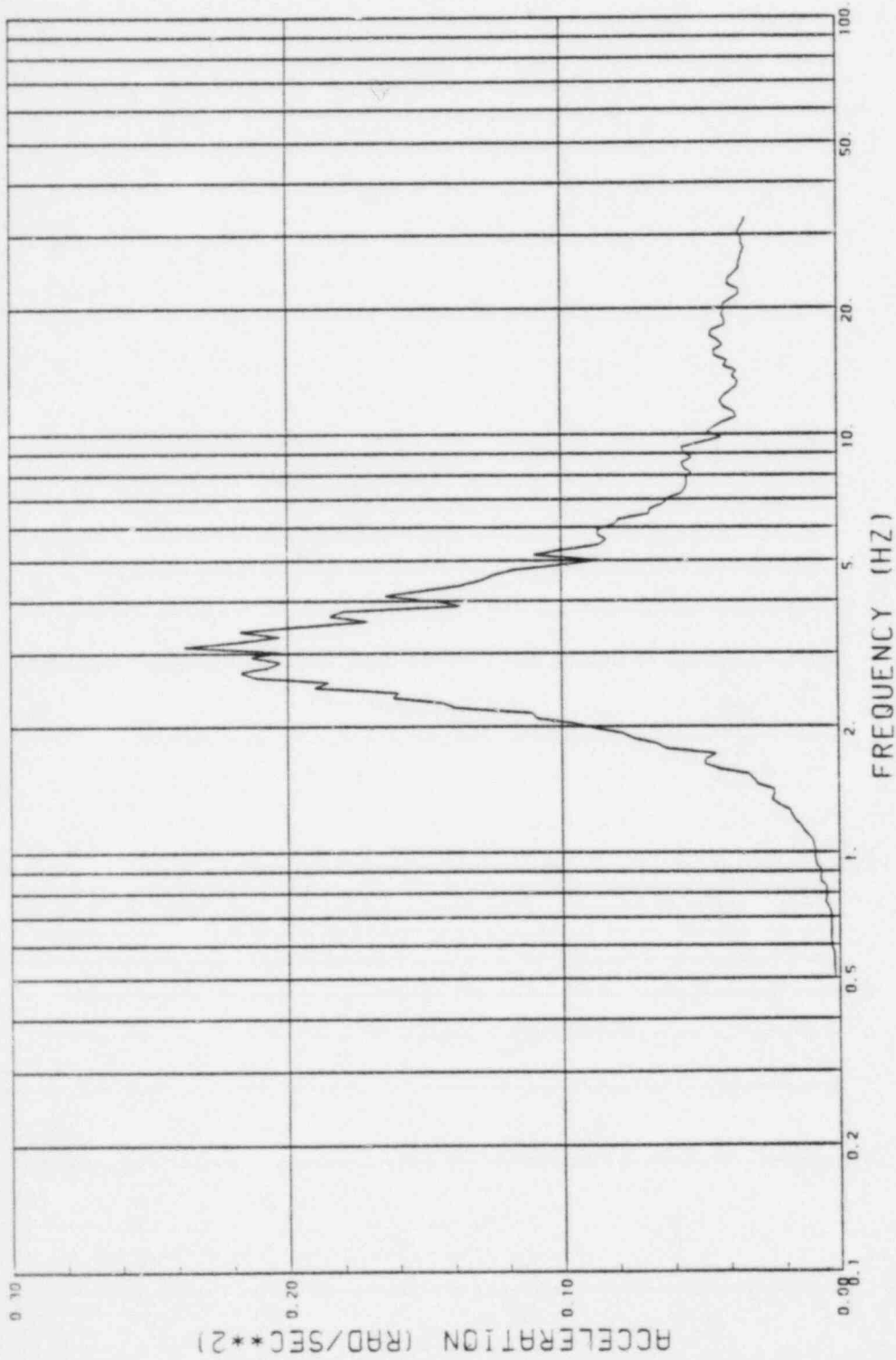


CESSAR II PLANT
SOIL - STRUCTURE INTERACTION

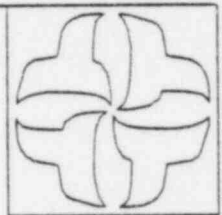


GE CLASS I ANALYSES
CASE 6, GE-75-U-HI
BASEMAT, NODE NO. 71 (TRANSLATION)

Figure A.56

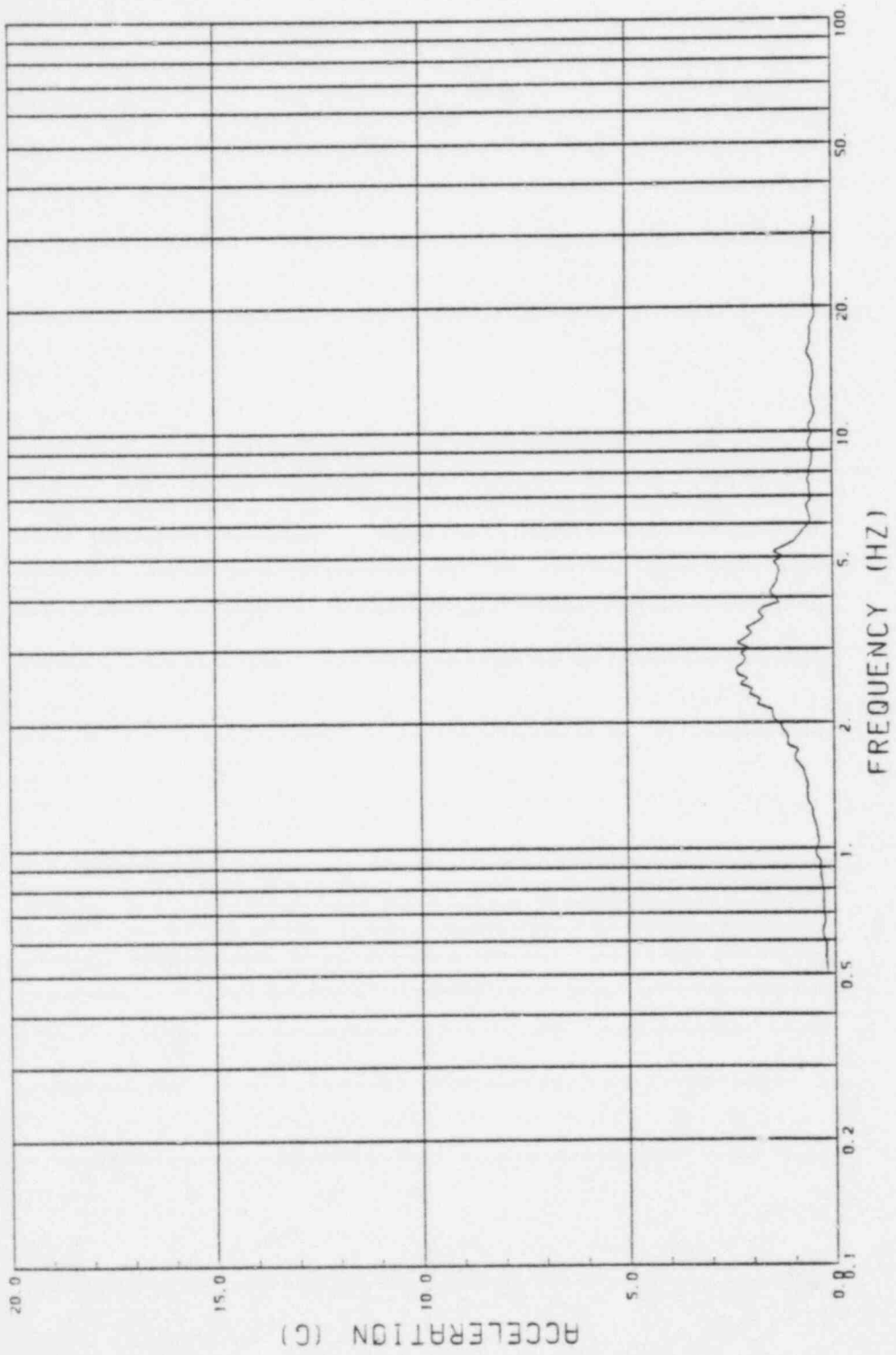


GE CLASS1 ANALYSES
CASE 6, GE-75-U-HI
BASEMAT, NODE NO. 71 (ROTATION)

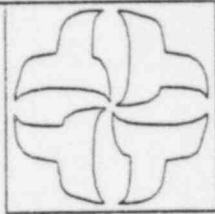


GESSAR II PLANT
SOIL - STRUCTURE INTERACTION

Figure A.57

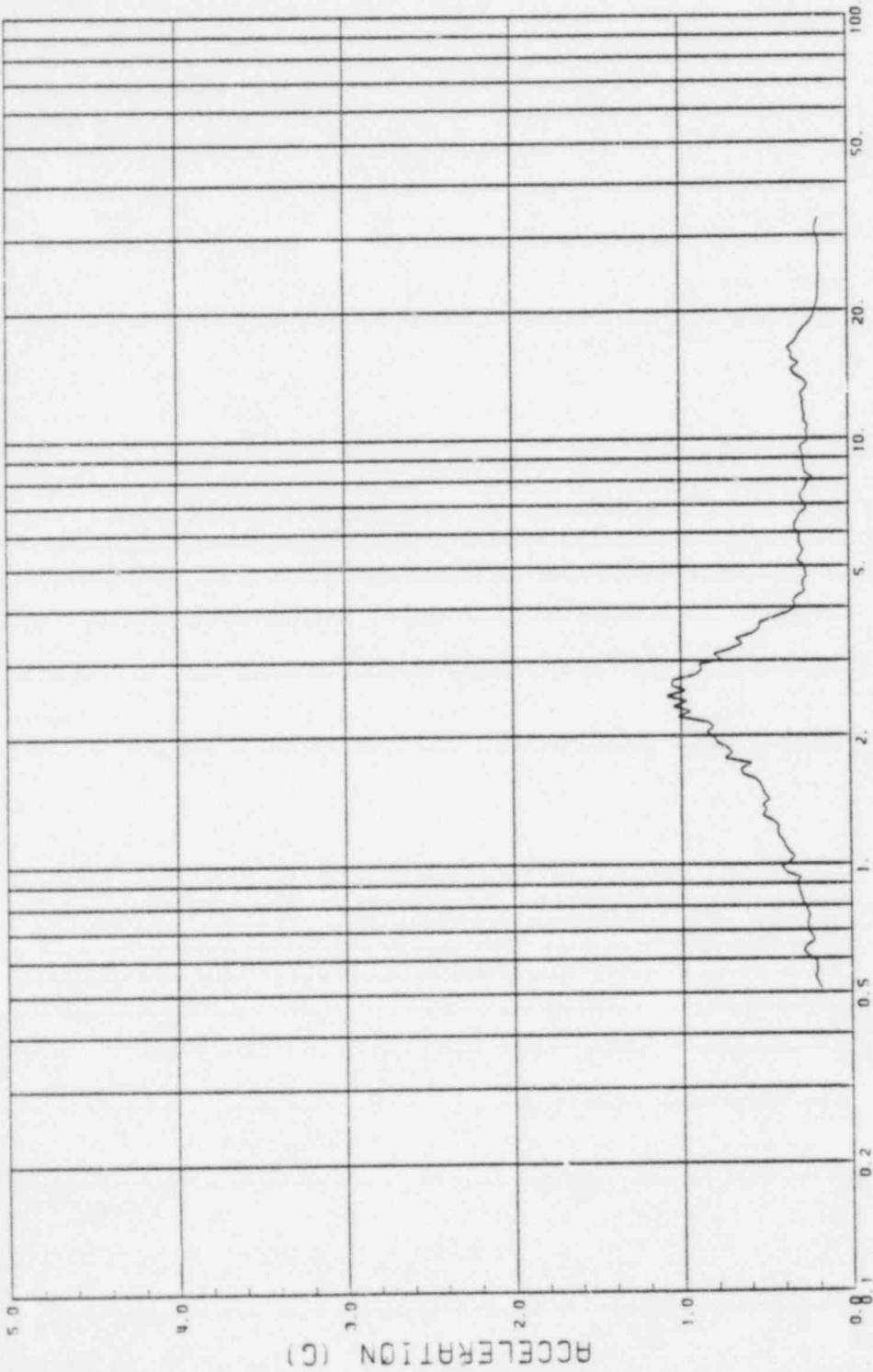


GE CLASS1 ANALYSES
CASE 6, GE-75-U-H1
NODE NO. 1

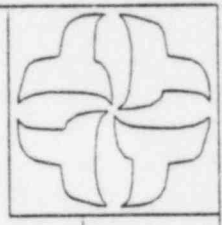


CESSAR II PLANT
SOIL - STRUCTURE INTERACTION

Figure A.58

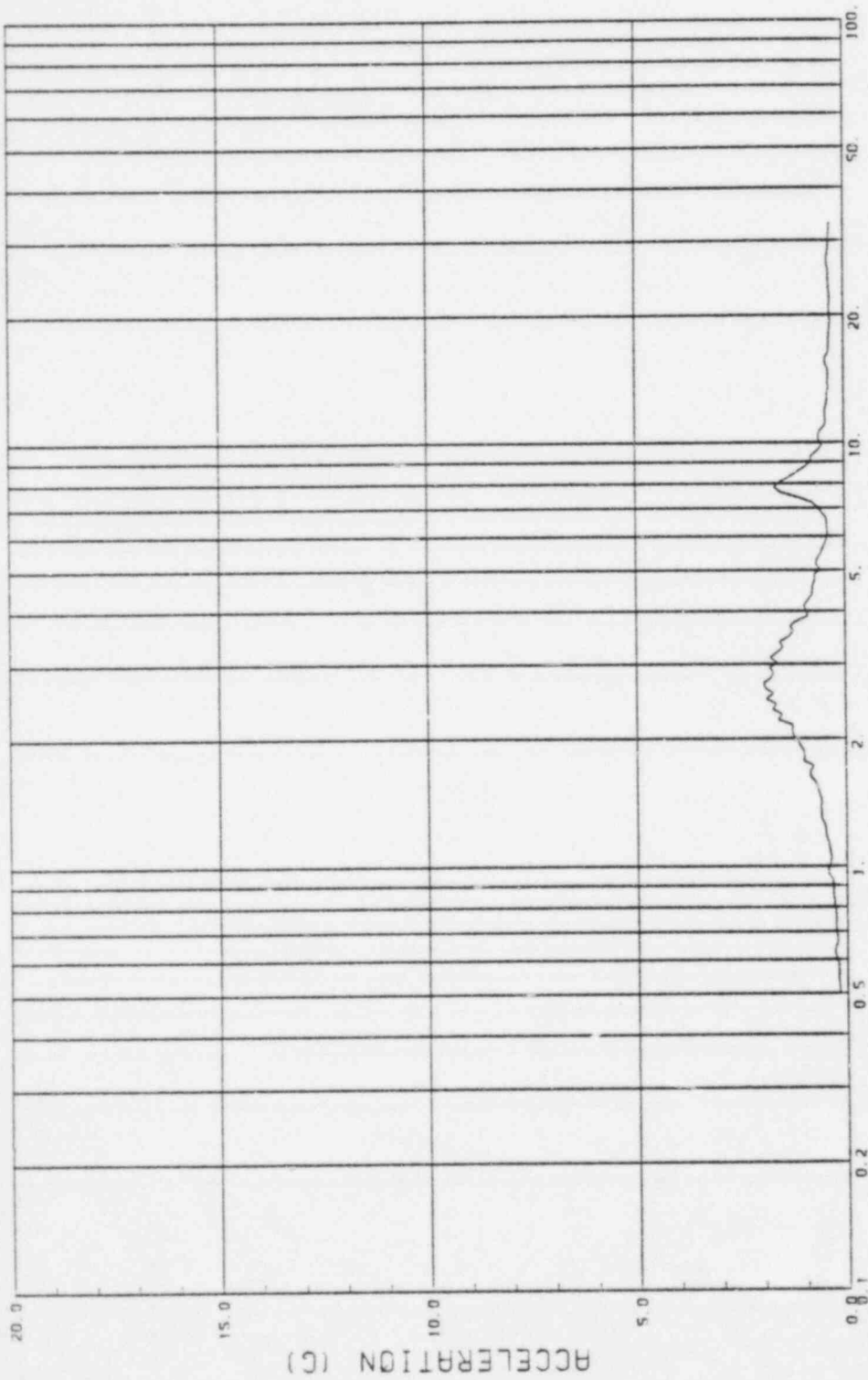


GE CLASS1 ANALYSES
CASE 6, GE-75-U-H1
NODE NO. 18



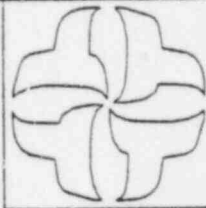
CESSAR II PLANT
SOIL - STRUCTURE INTERACTION

Figure A.59



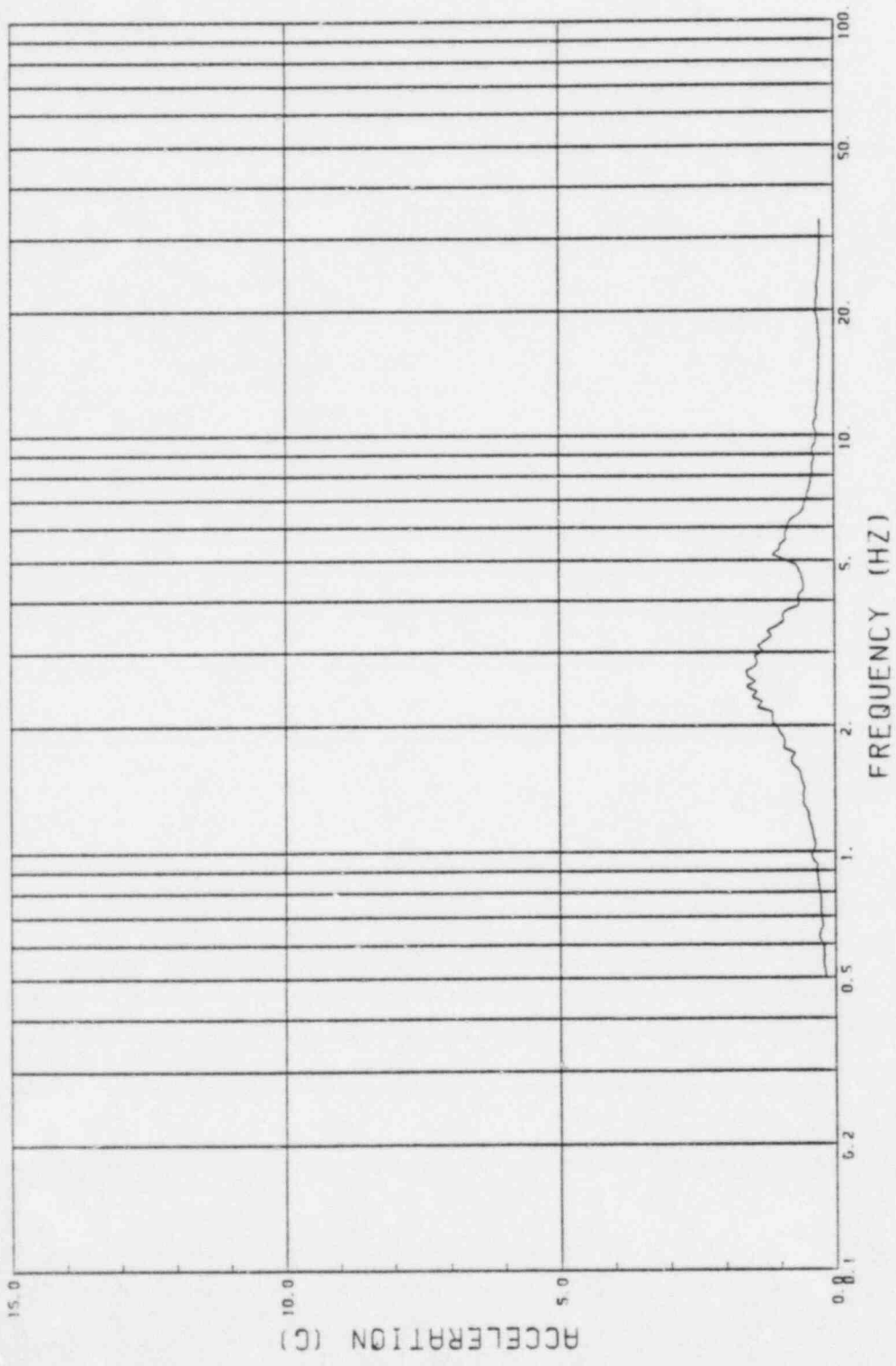
FREQUENCY (HZ)

GE CLASSI ANALYSES
CASE 6, GE-75-U-HI
NODE NO. 22

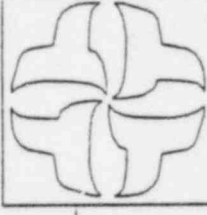


CESSAR II PLANT
SOIL - STRUCTURE INTERACTION

Figure A.60

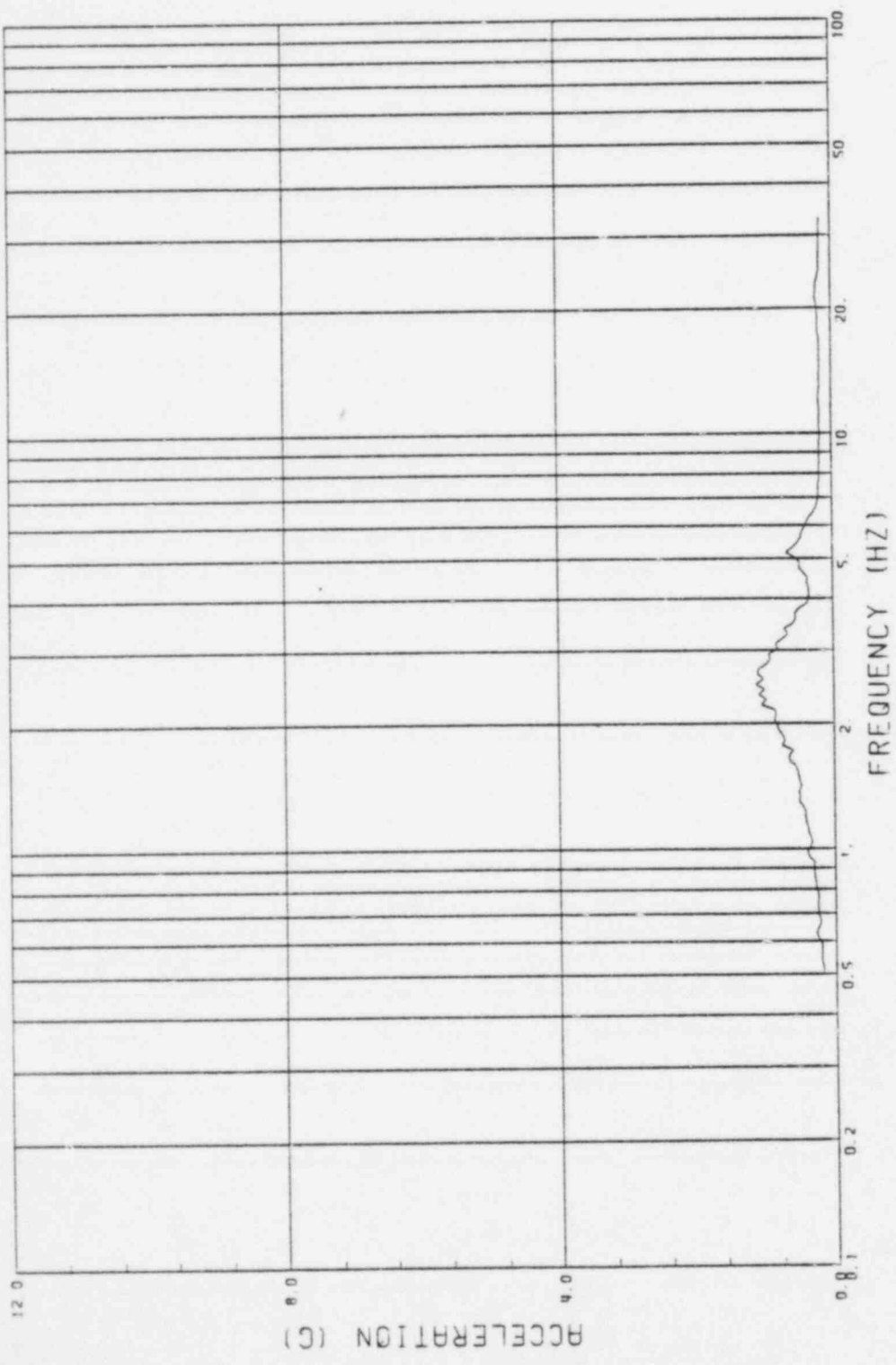


GE CLASS1 ANALYSES
CASE 6, GE-75-U-H1
NODE NO. 42

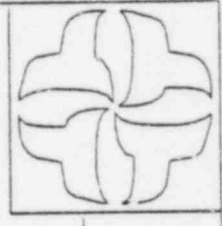


CESSAR II PLANT
SOIL - STRUCTURE INTERACTION

Figure A.61

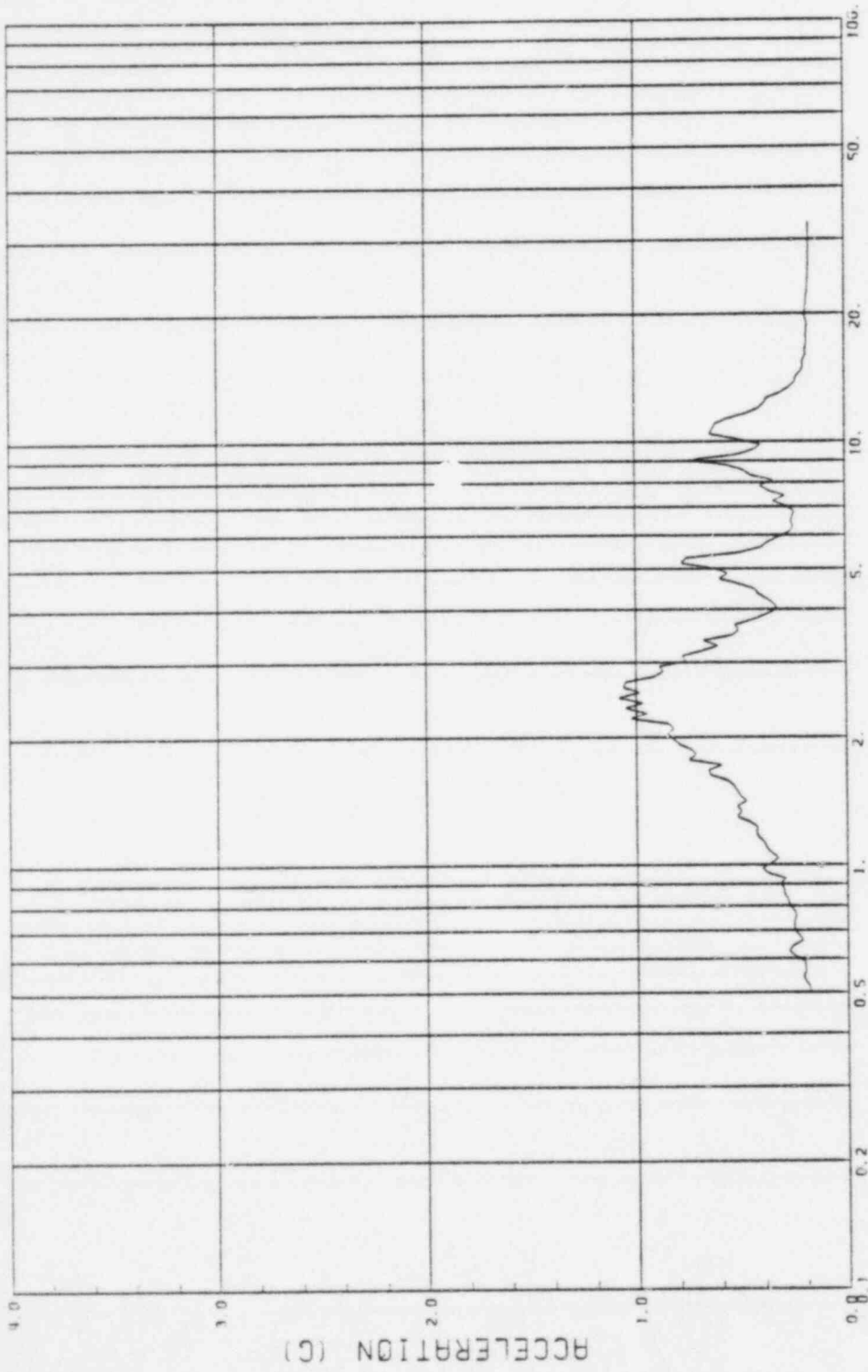


GE CLASSI ANALYSES
CASE 6, GE-75-U-HI
NODE NO. 46



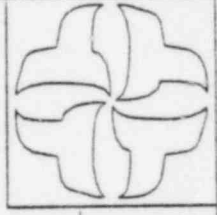
CESSAR II PLANT
SOIL - STRUCTURE INTERACTION

Figure A.62



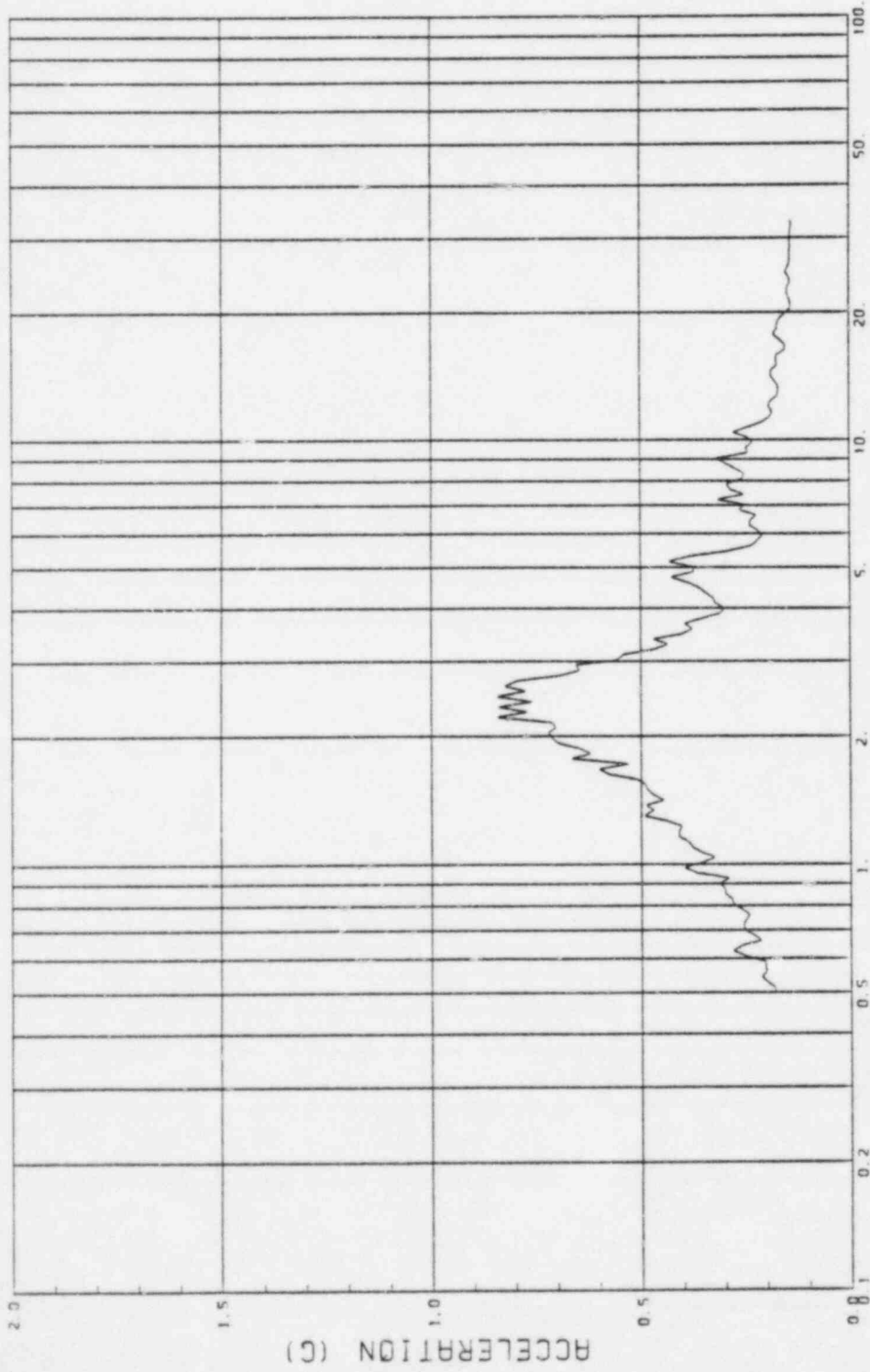
FREQUENCY (HZ)

GE CLASSI ANALYSES
CASE 6, GE-75-U-HI
NODE NO. 60



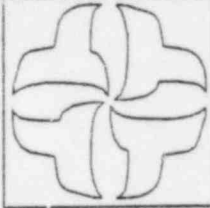
CESSAR II PLANT
SOIL - STRUCTURE INTERACTION

Figure A.63



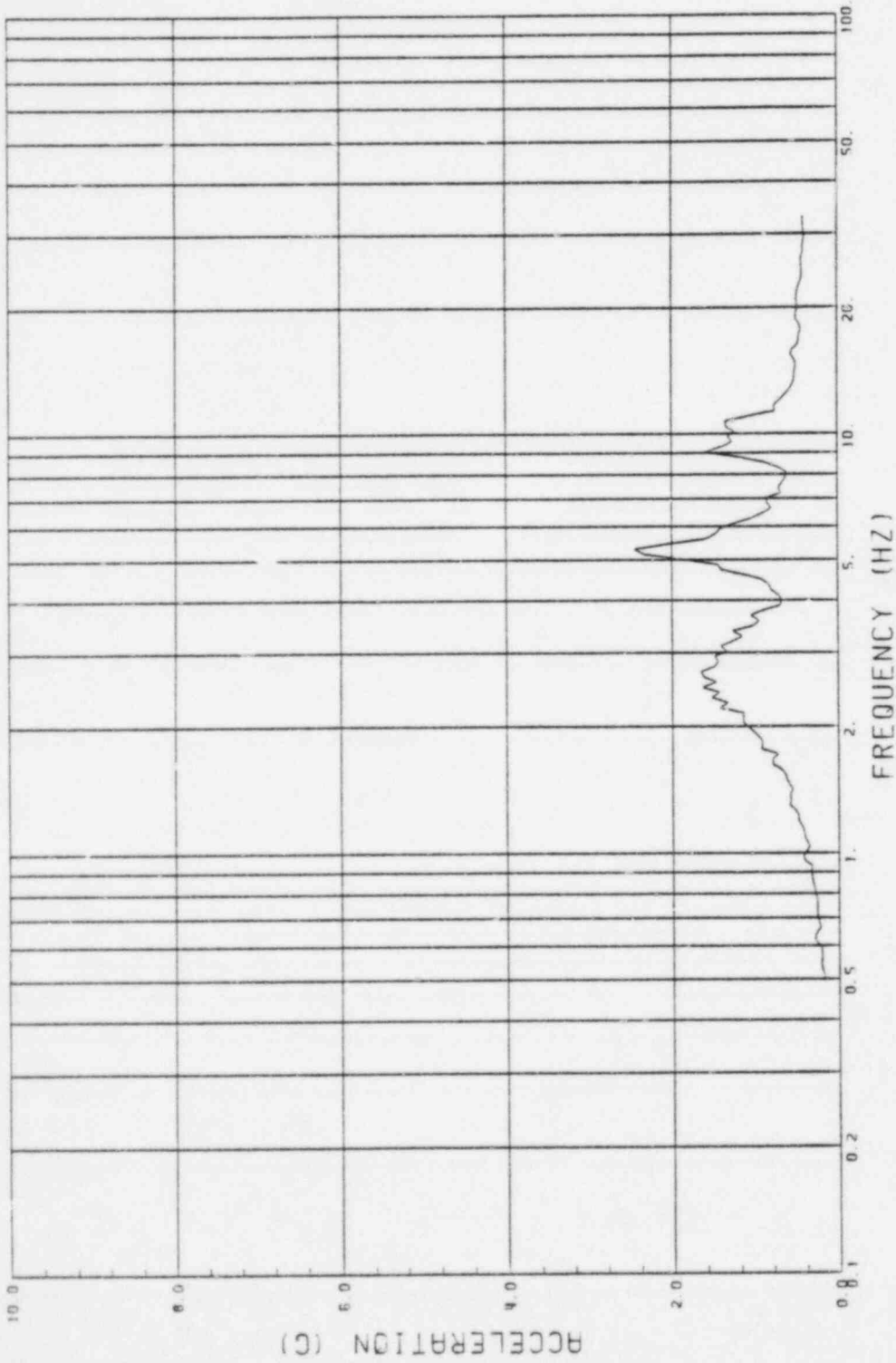
FREQUENCY (HZ)

CE CLASS1 ANALYSES
CASE 6, CE-75-U-HI
NODE NO. 64

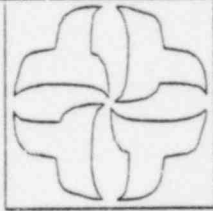


CESSAR II PLANT
SOIL - STRUCTURE INTERACTION

Figure A.64

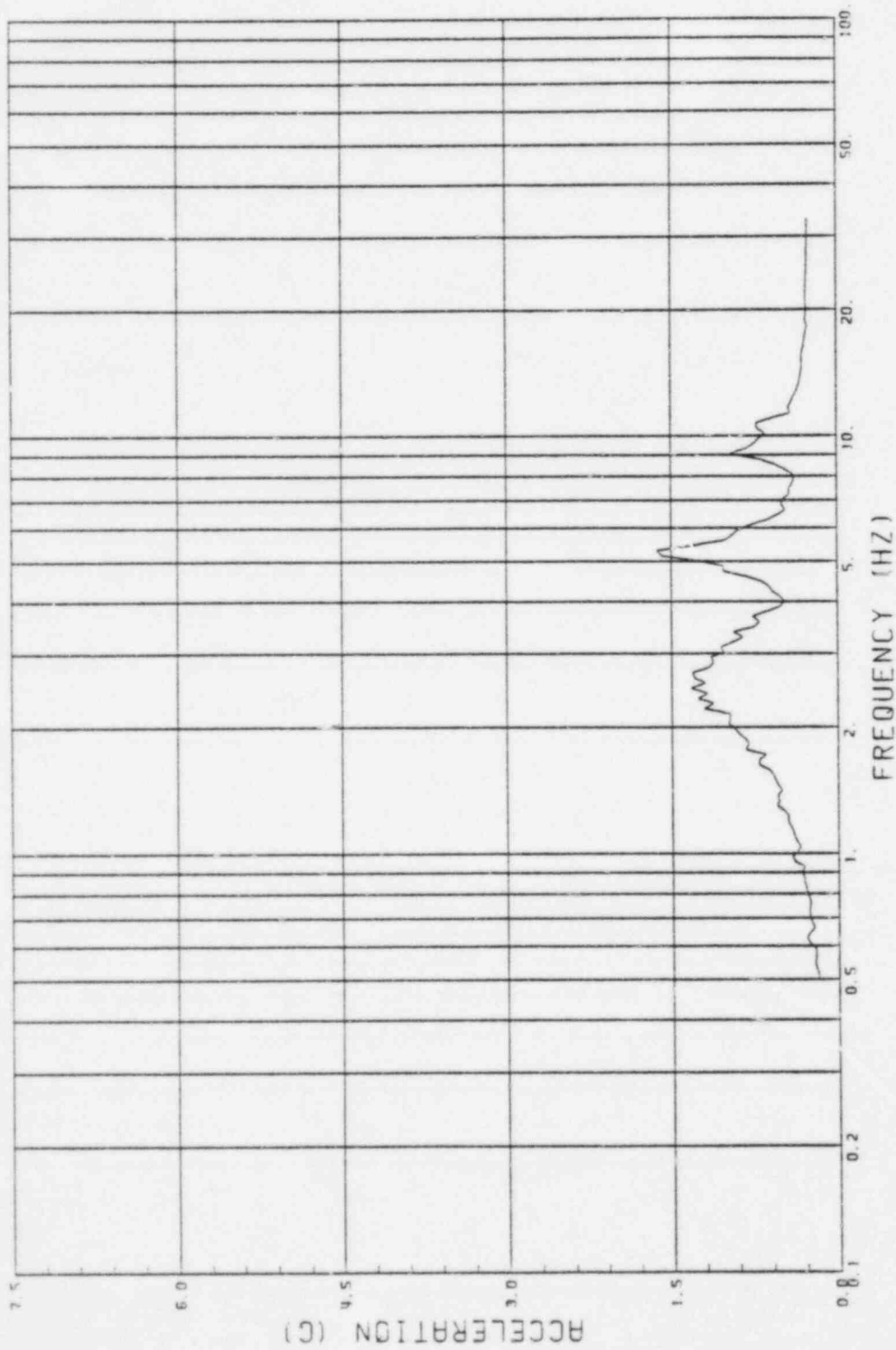


GE CLASS1 ANALYSES
CASE 6, GE-75-U-H1
NODE NO. 101

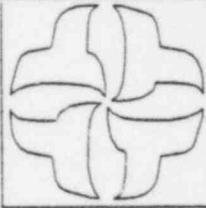


GESSAR II PLANT
SOIL - STRUCTURE INTERACTION

Figure A.65

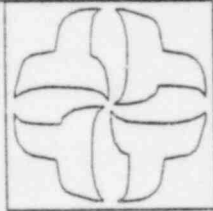


CE CLASS1 ANALYSES
CASE 6, CE-75-U-H1
NODE NO. 109



CESSAR II PLANT
SOIL - STRUCTURE INTERACTION

Figure A.66



CESSAR II PLANT
SOIL - STRUCTURE INTERACTION

GE LLASSI ANALYSES
CASE 7, CE-75-VP5-H2
BASEMAT, NODE NO. 71 (TRANSLATION)

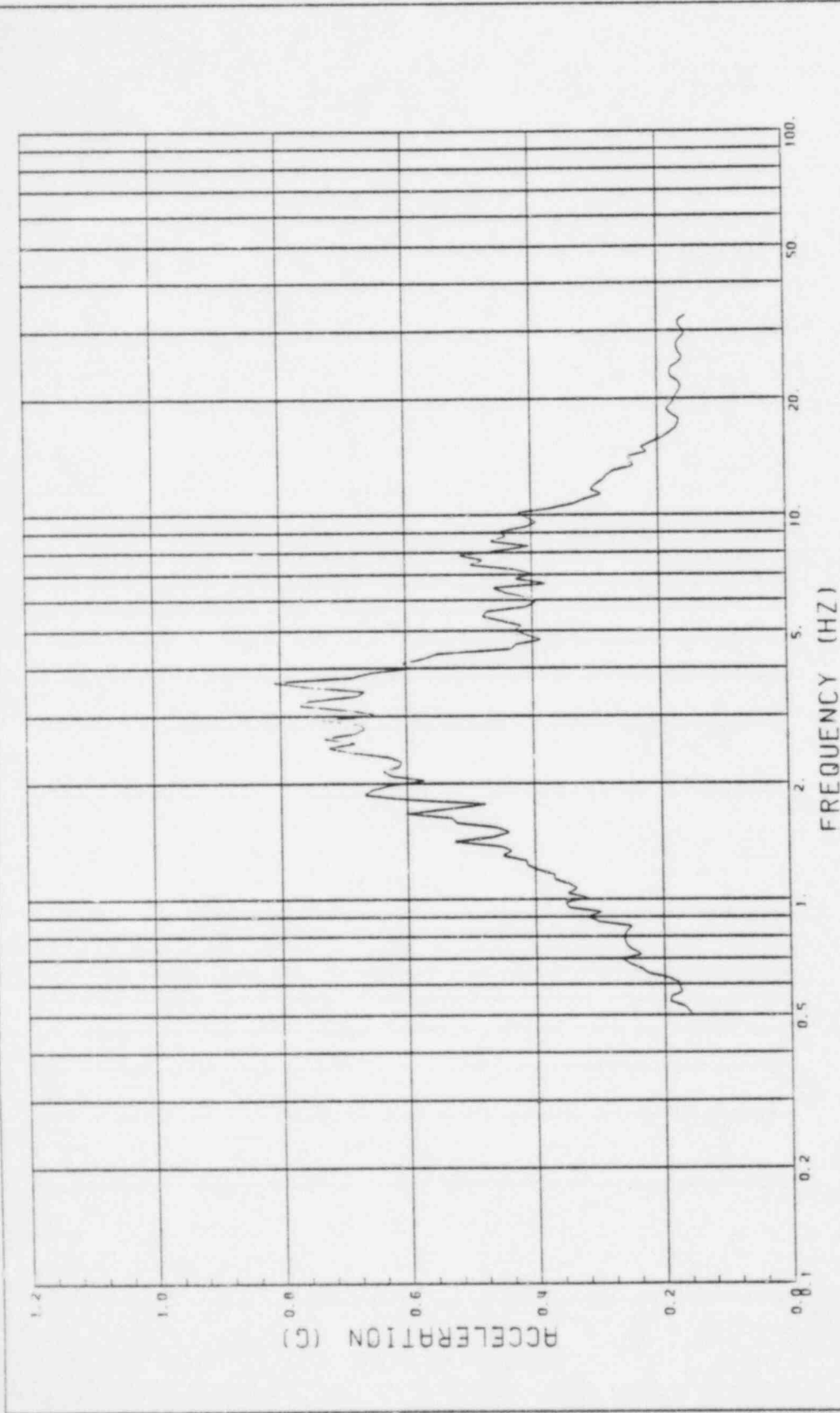
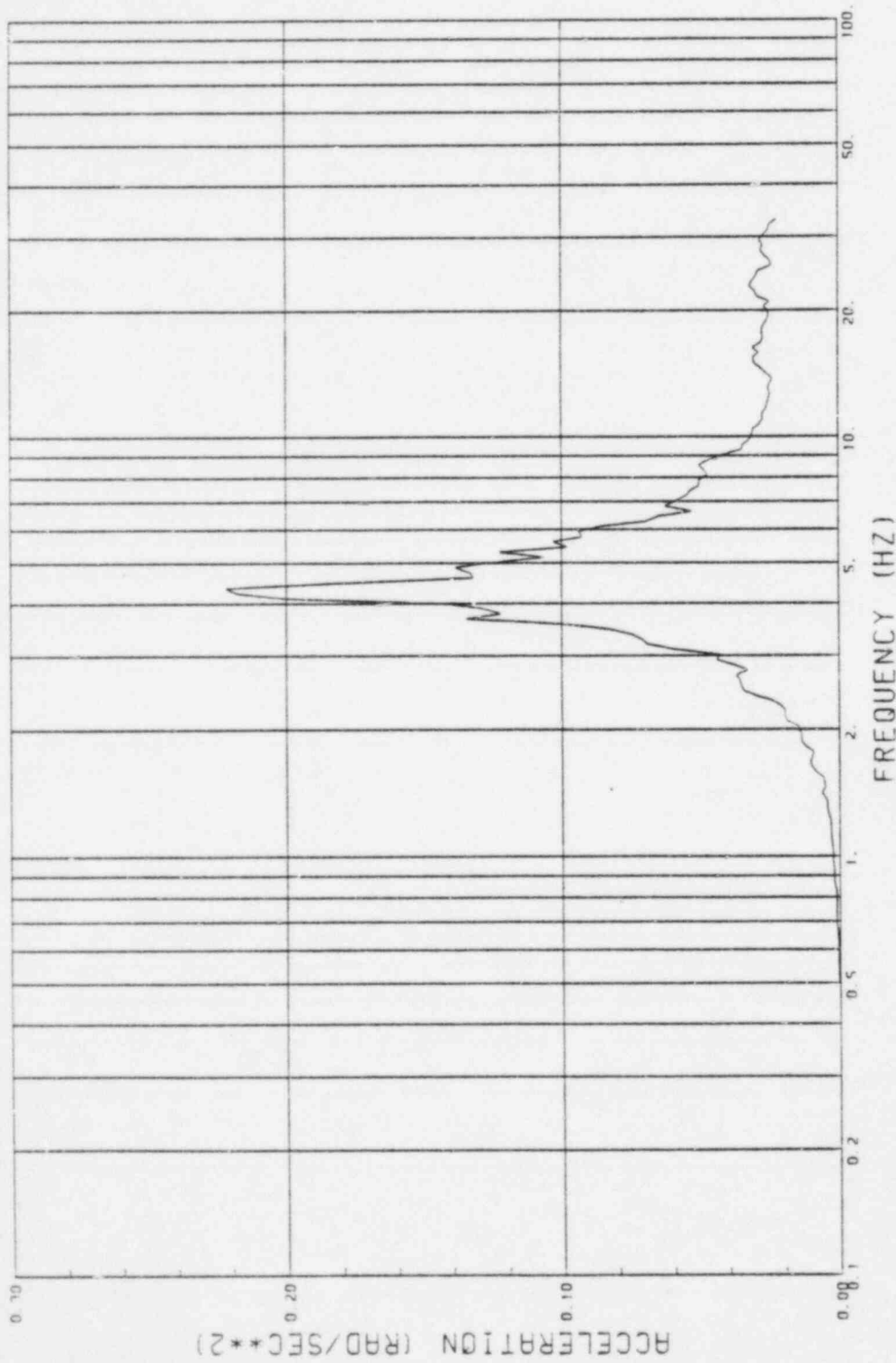
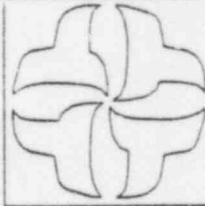


Figure A.67

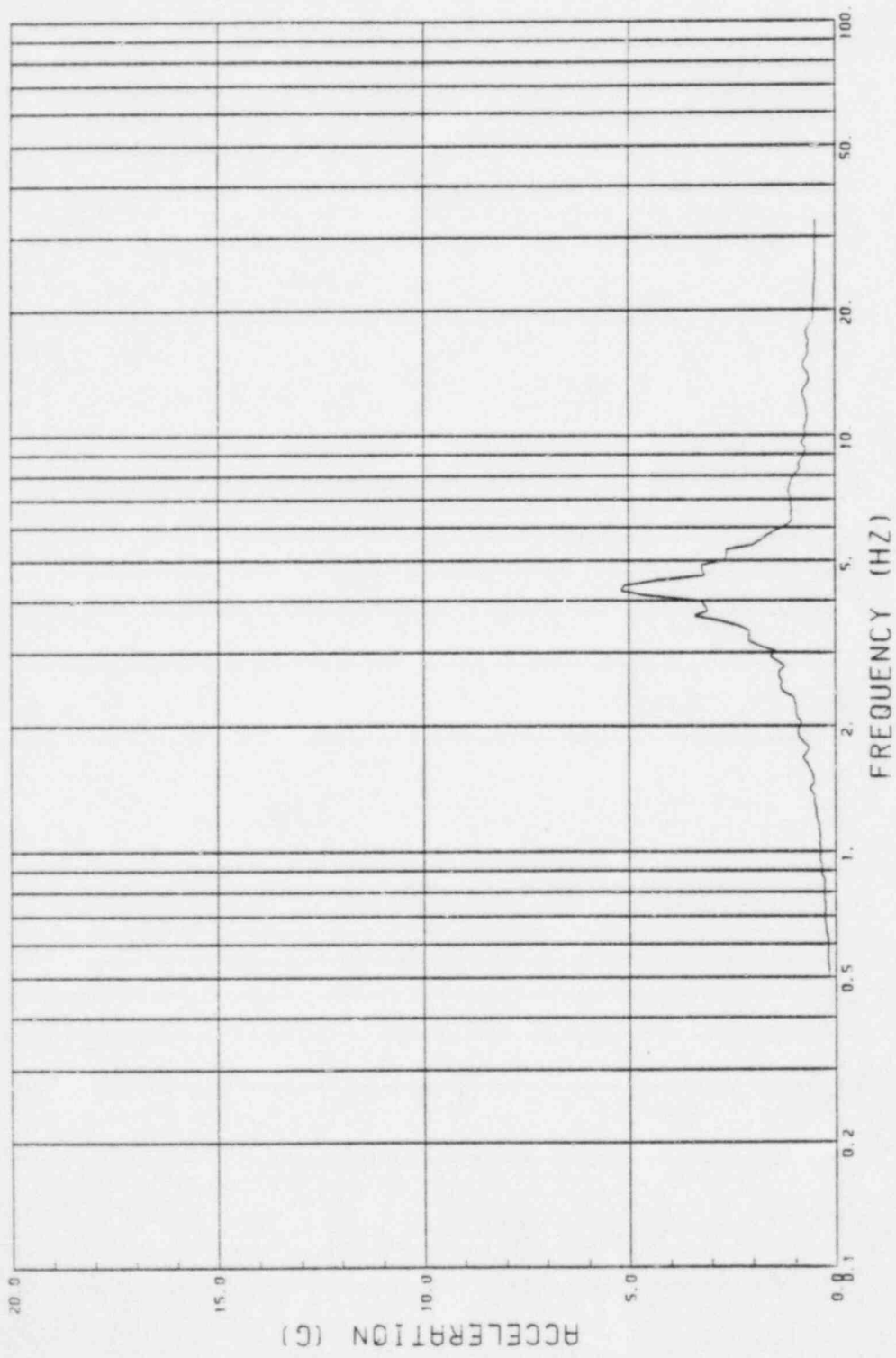


GE CLASS1 ANALYSES
 CASE 7, GE-75-VPS-H2
 BASEMAT, NODE NO. 71 (ROTATION)

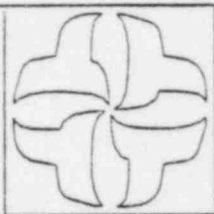


GESSAR II PLANT
 SOIL - STRUCTURE INTERACTION

Figure A.68

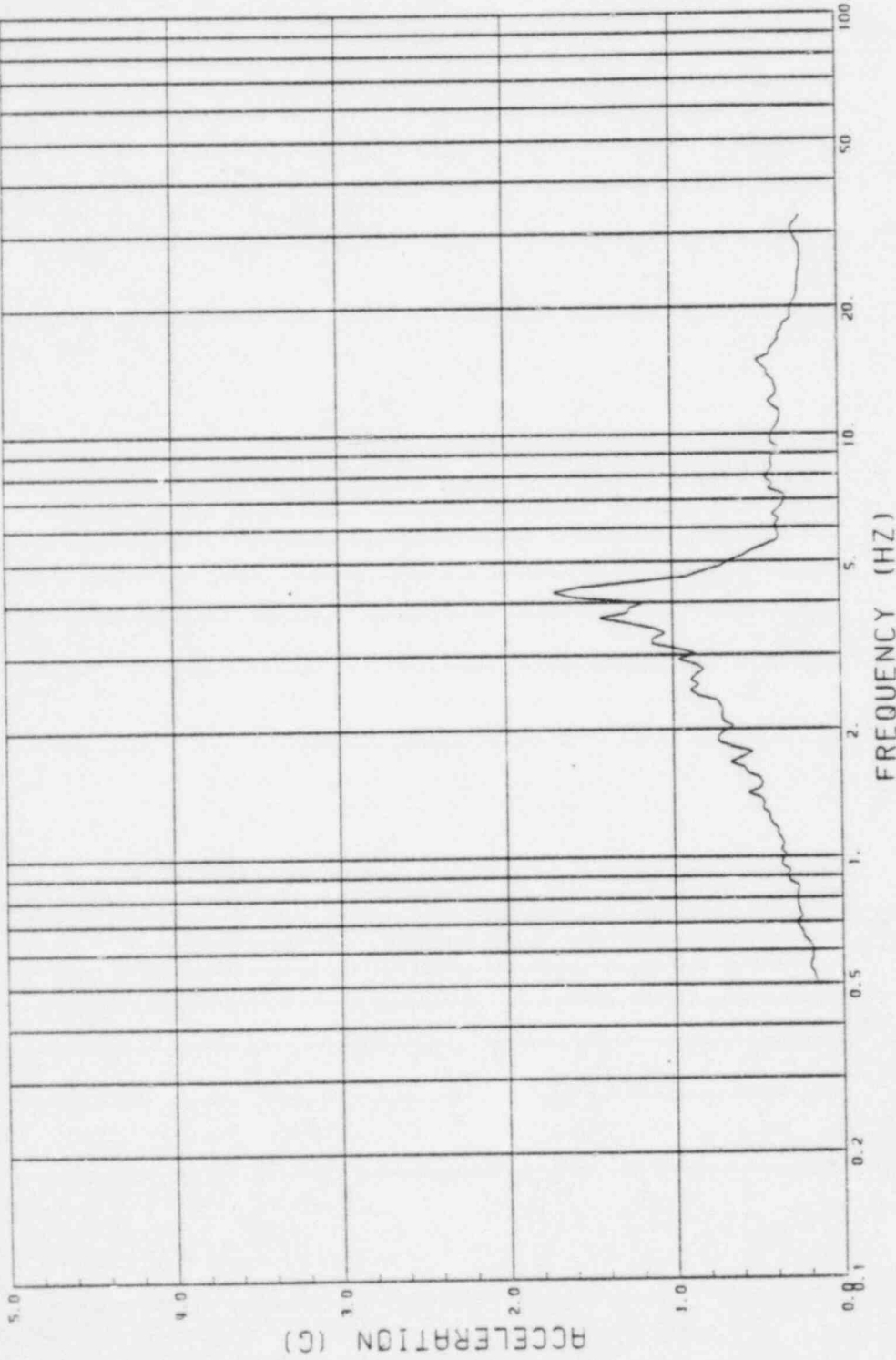


GE CLASSI ANALYSES
CASE 7, GE-75-VP5-H2
NODE NO. 1

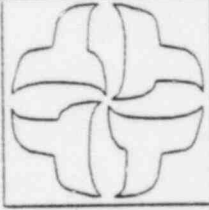


CESSAR II PLANT
SOIL - STRUCTURE INTERACTION

Figure A.69

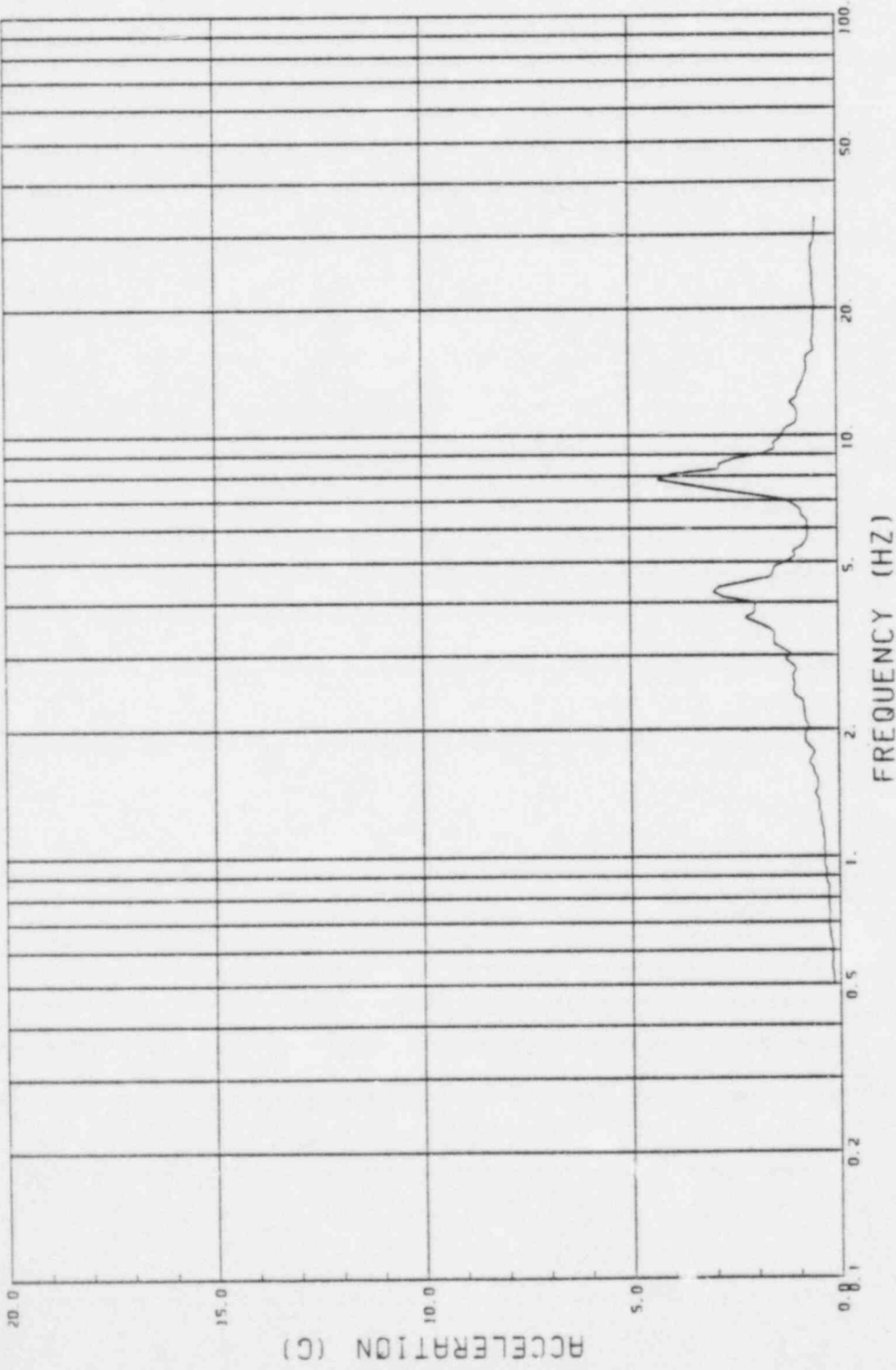


CE CLASSI ANALYSES
CASE 7, CE-75-VP5-H2
NODE NO. 18

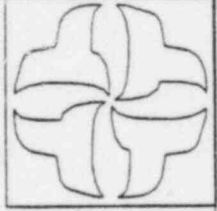


CESSAR II PLANT
SOIL - STRUCTURE INTERACTION

Figure A.70

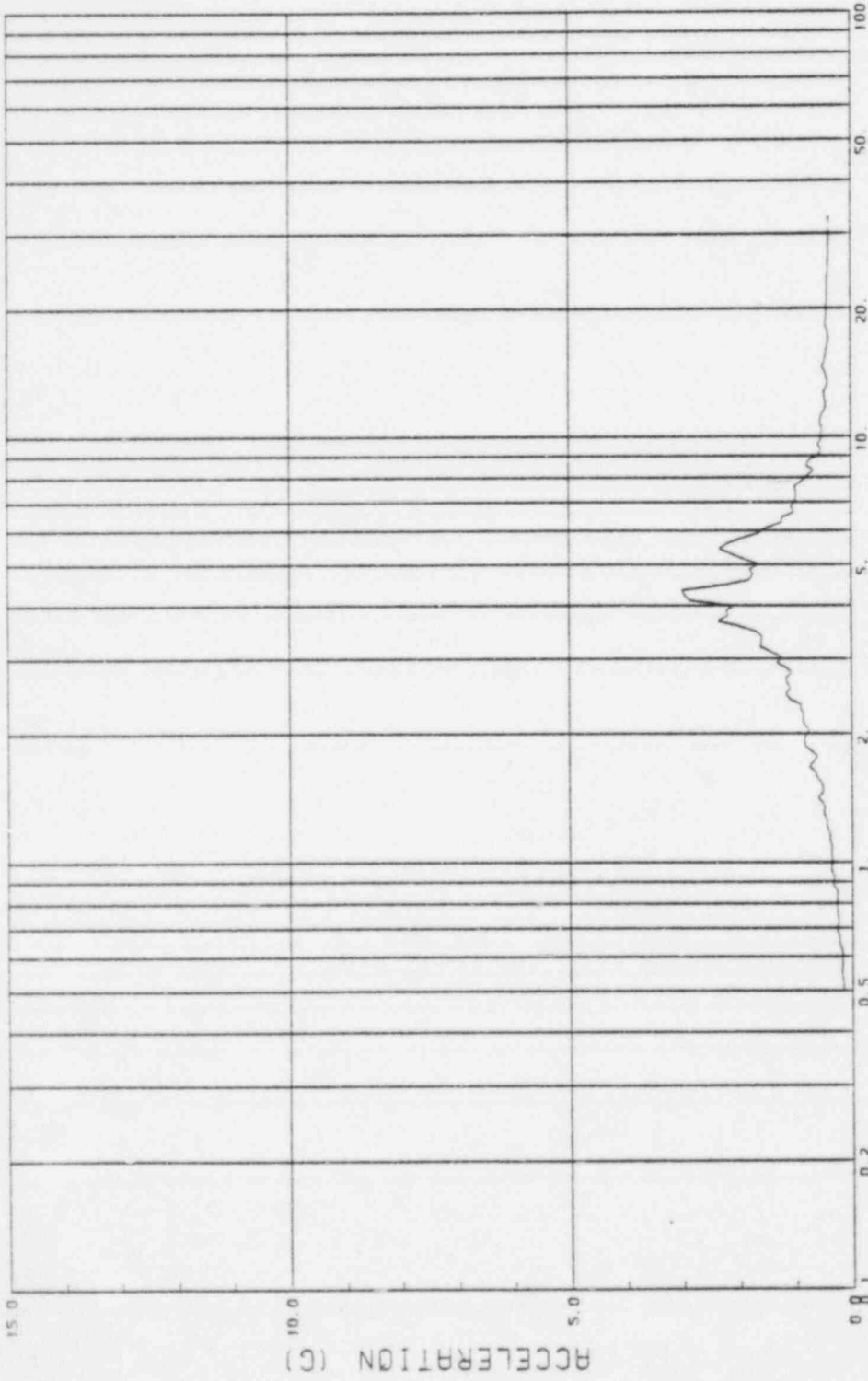


GE CLASS1 ANALYSES
CASE 7, GE-75-VP5-H2
NODE NO. 22



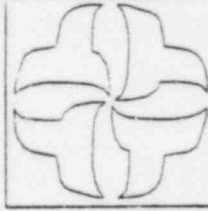
CESSAR II PLANT
SOIL - STRUCTURE INTERACTION

Figure A.71



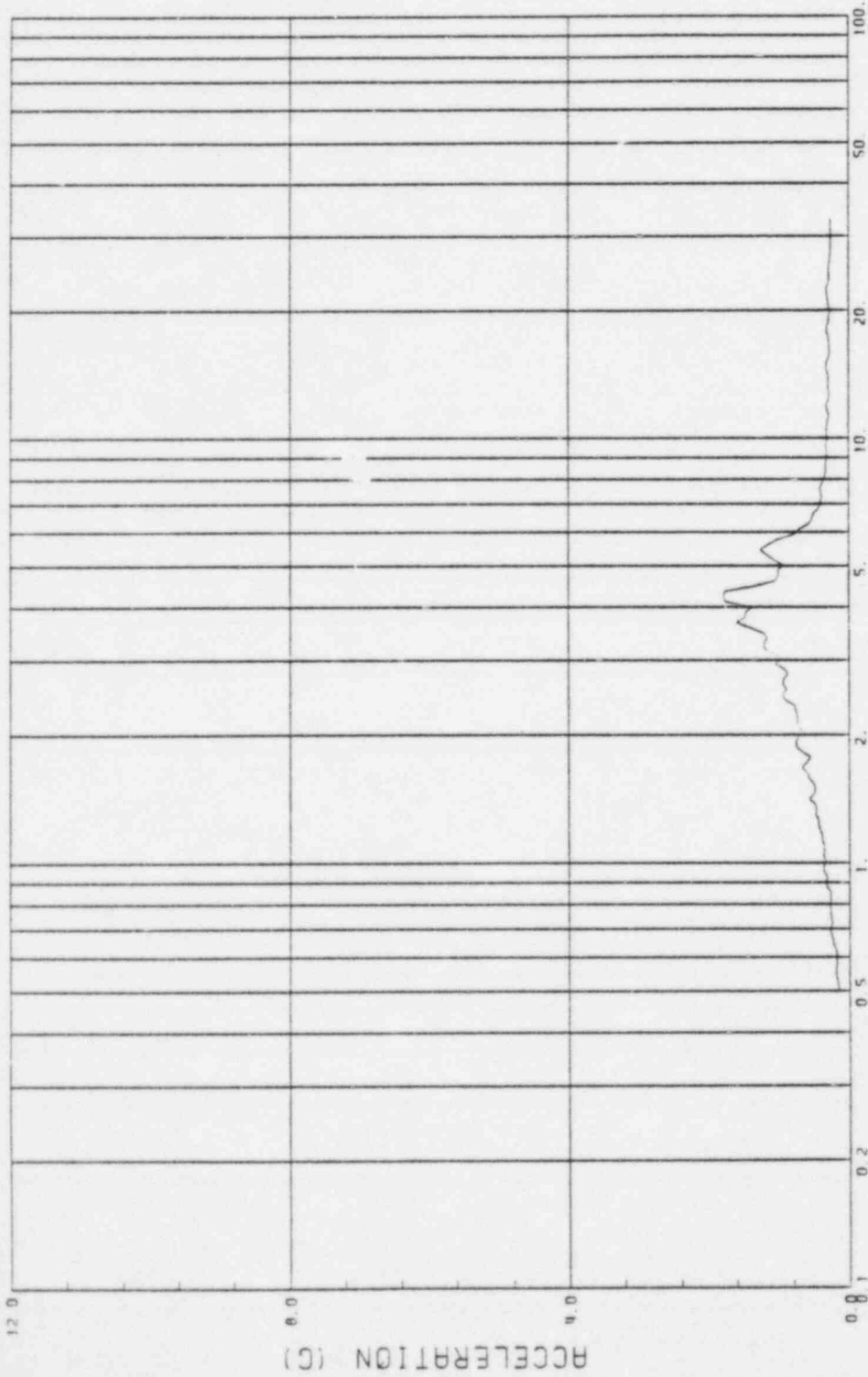
FREQUENCY (HZ)

GE CLASS1 ANALYSES
CASE 7, GE-75-VPS-H2
NODE NO. 42



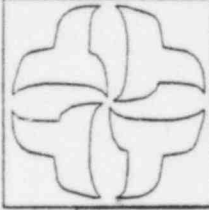
CESSAR II PLANT
SOIL - STRUCTURE INTERACTION

Figure A.72



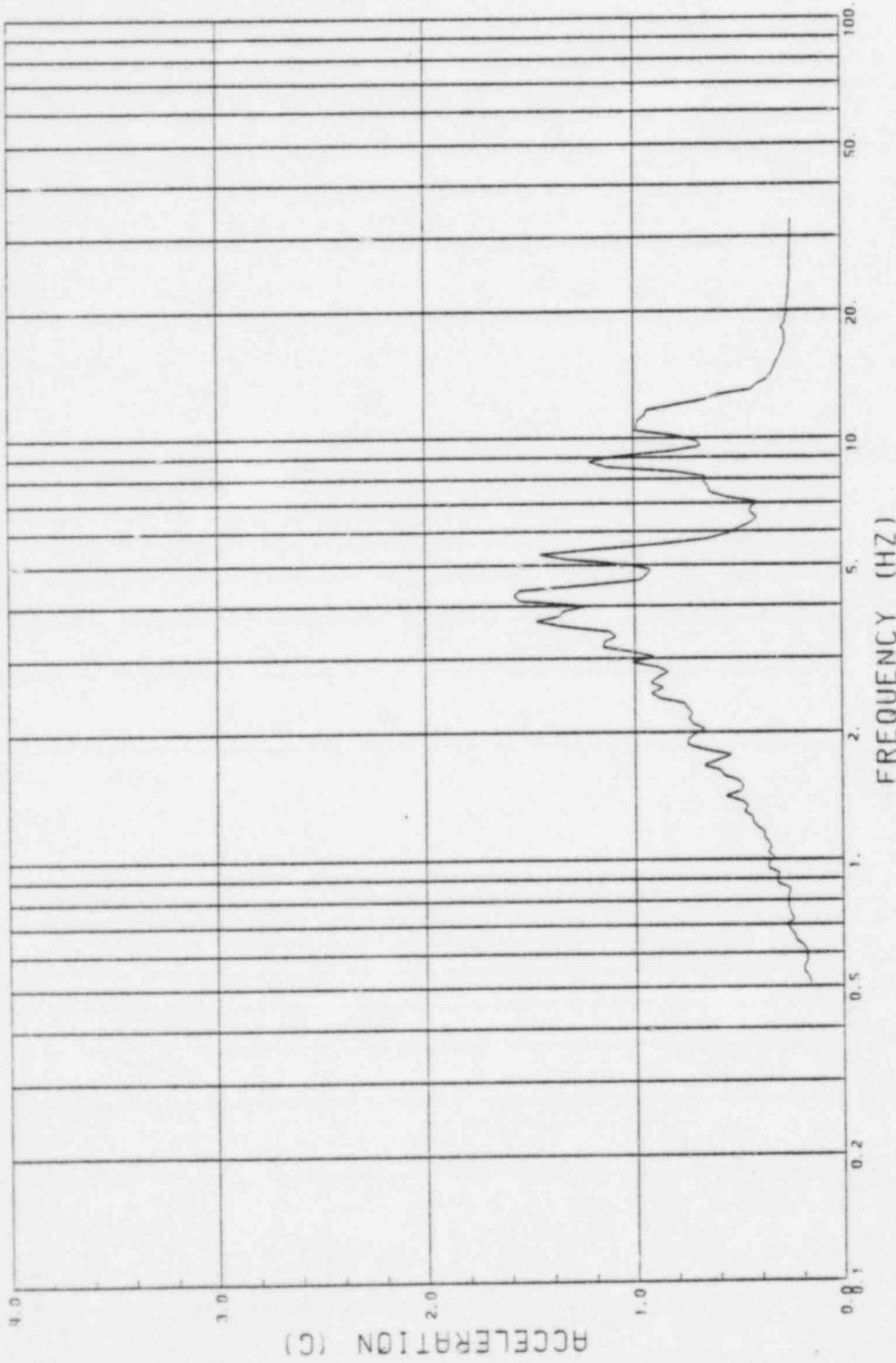
FREQUENCY (HZ)

GE CLASSI ANALYSES
CASE 7: GE-75-VP5-H2
NODE NO. 46

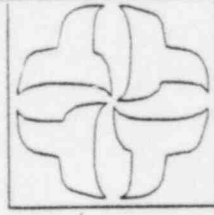


CESSAR II PLANT
SOIL - STRUCTURE INTERACTION

Figure A.73

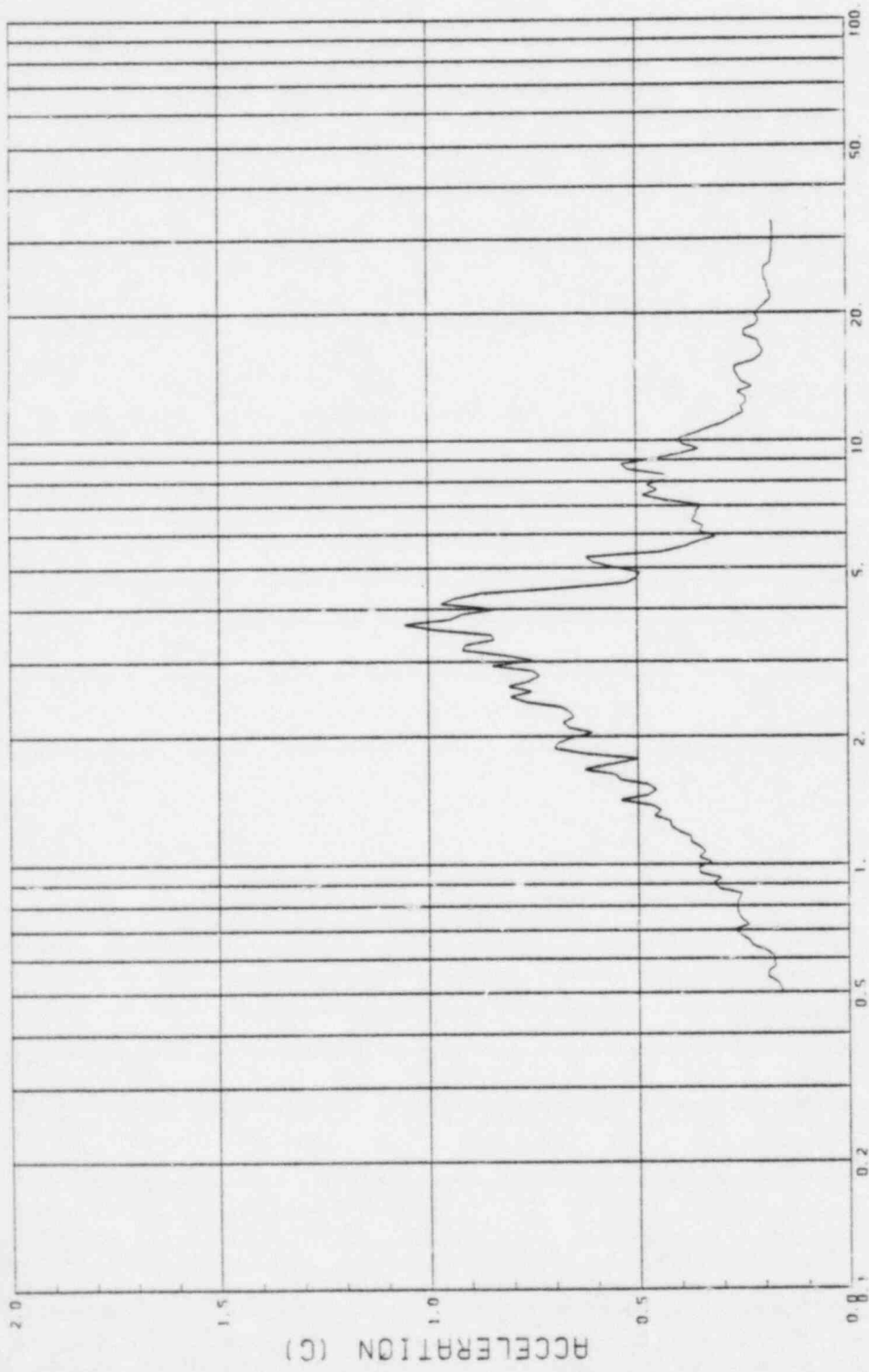


GE CLASSI ANALYSES
CASE 7, GE-75-VP5-H2
NODE NO. 60



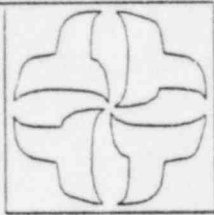
CESSAR II PLANT
SOIL - STRUCTURE INTERACTION

Figure A.74



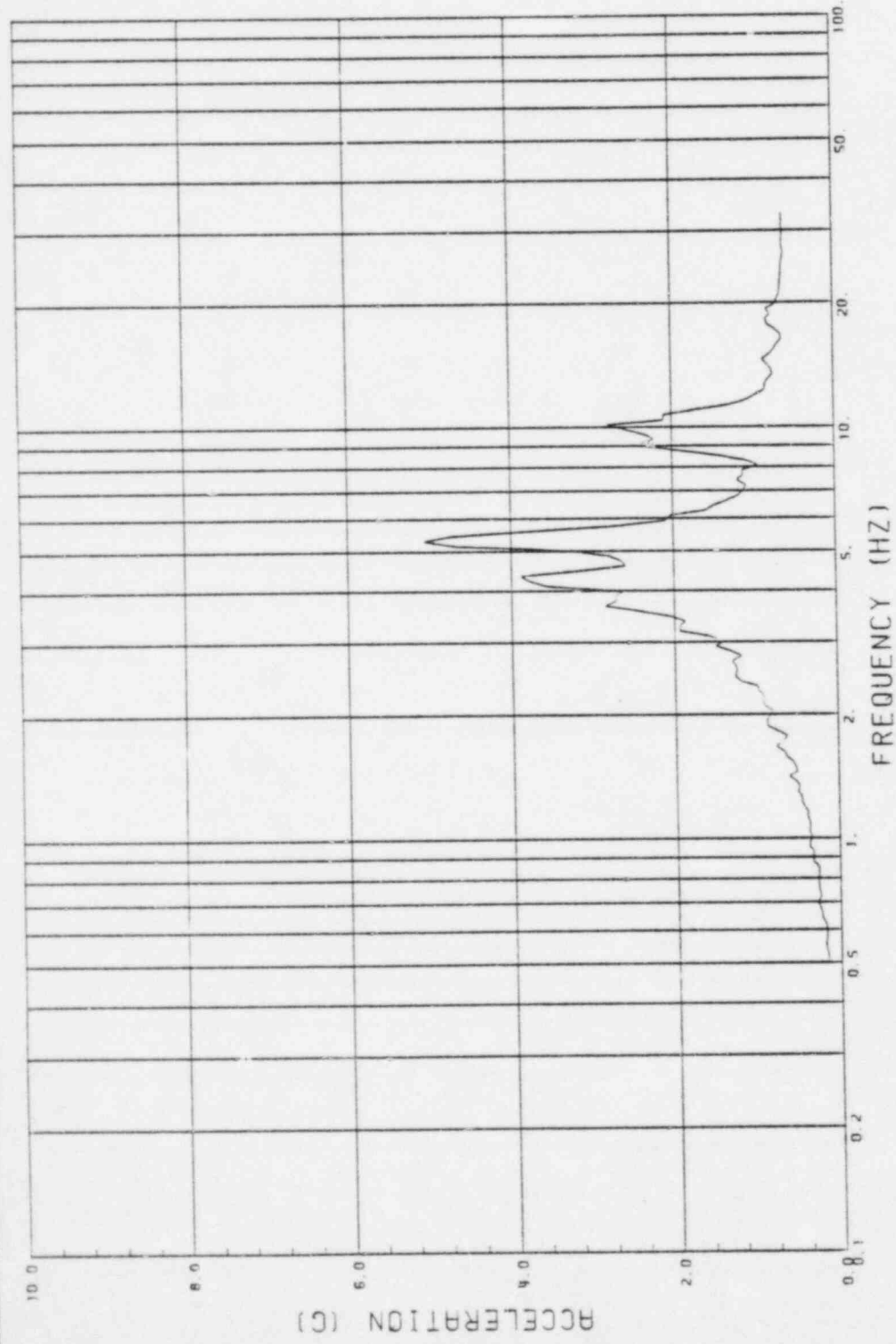
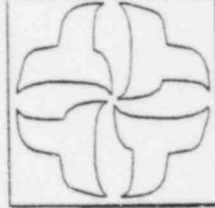
FREQUENCY (HZ)

GE CLASSI ANALYSES
CASE 7. GE-75-VPS-H2
NODE NO. 64



CESSAR II PLANT
SOIL - STRUCTURE INTERACTION

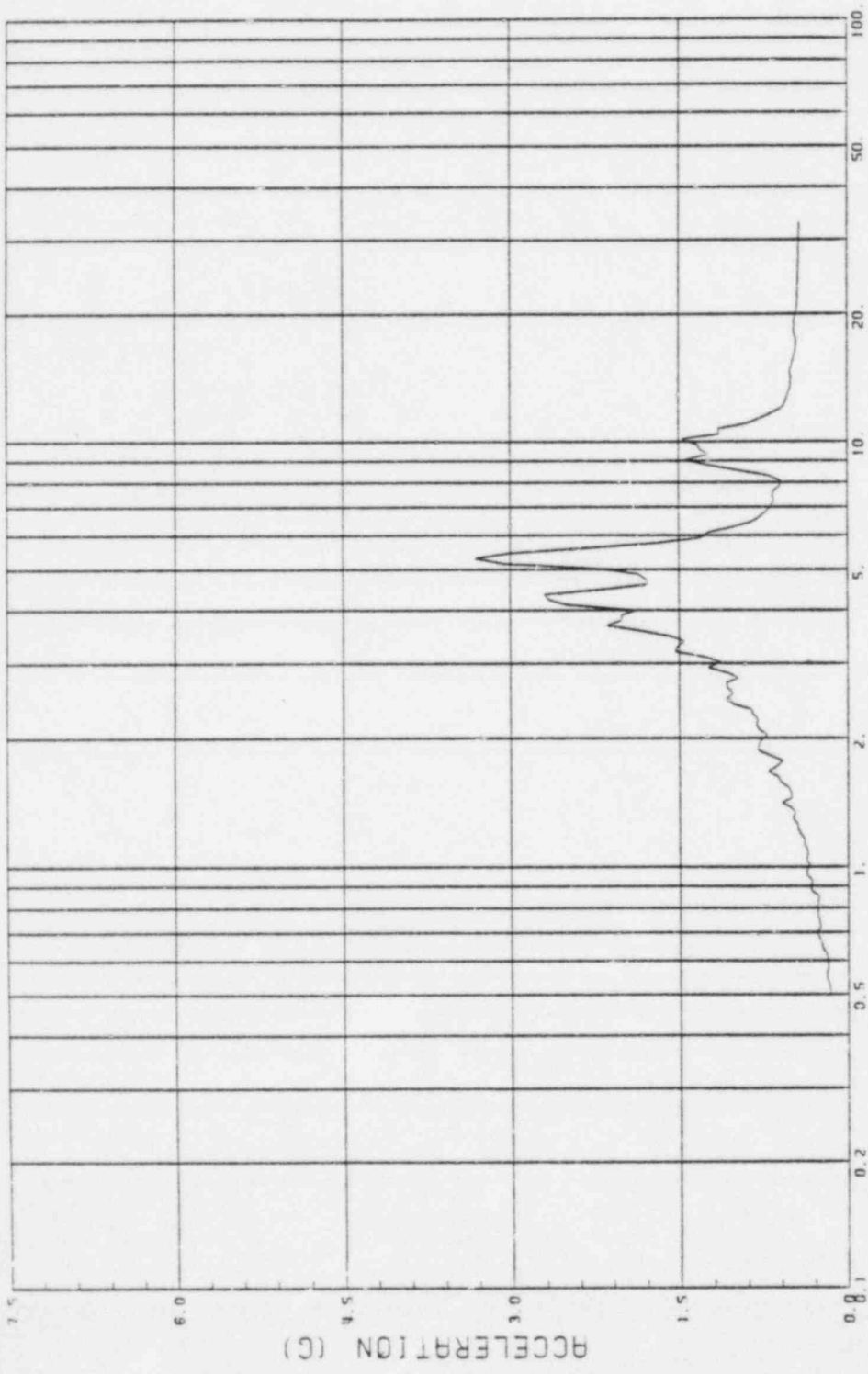
Figure A.75



GE CLASS1 ANALYSES
CASE 7, GE-75-VP5-H2
NODE NO. 101

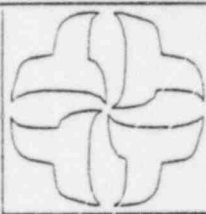
SOIL - STRUCTURE INTERACTION
GESSAR II PLANT

Figure A.76



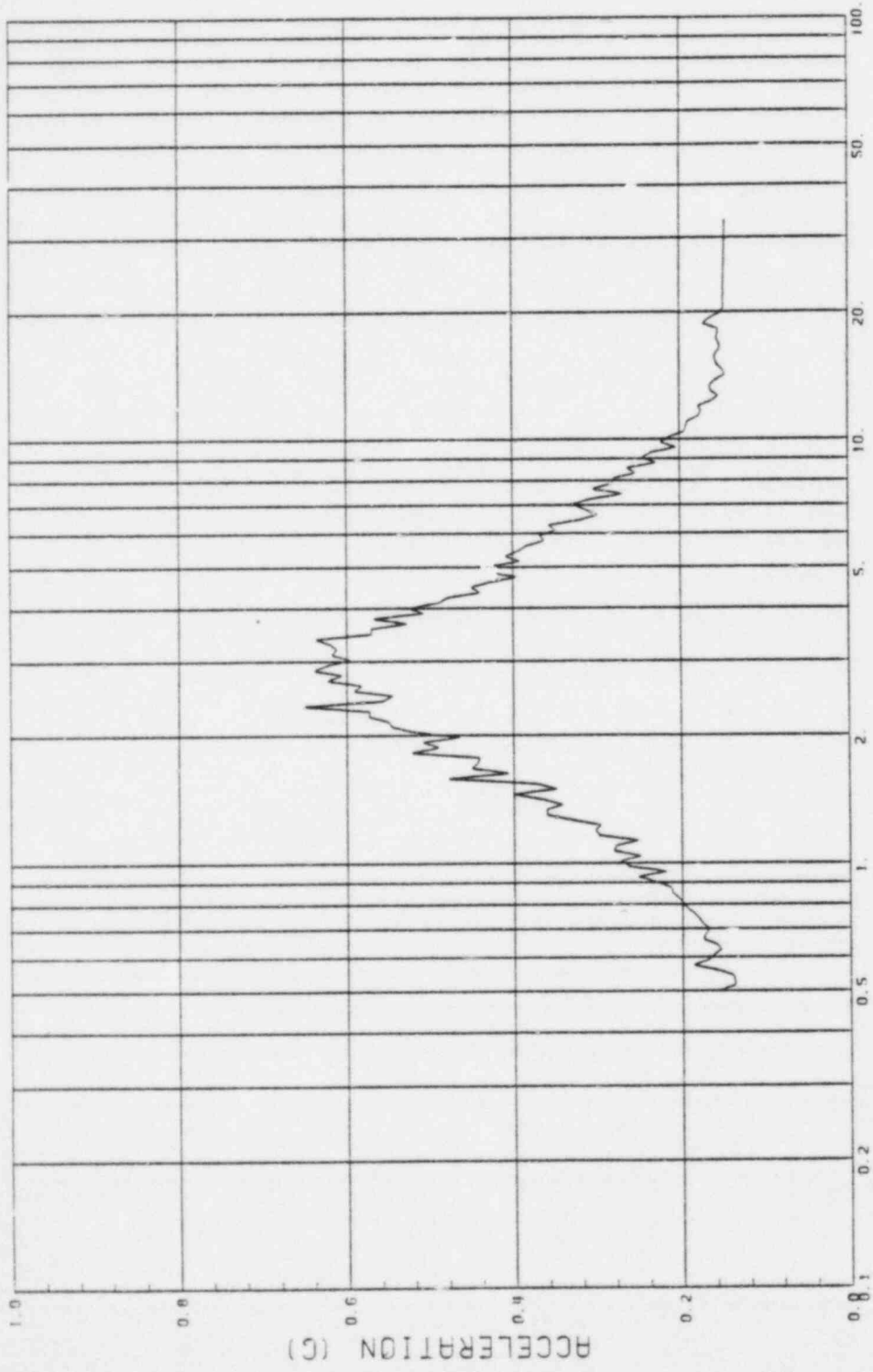
FREQUENCY (HZ)

GE CLASS1 ANALYSES
CASE 7, GE-75-VP5-H2
NODE NO. 109

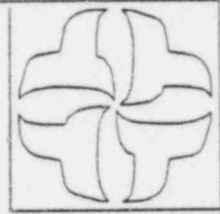


CESSAR II PLANT
SOIL - STRUCTURE INTERACTION

Figure A.77

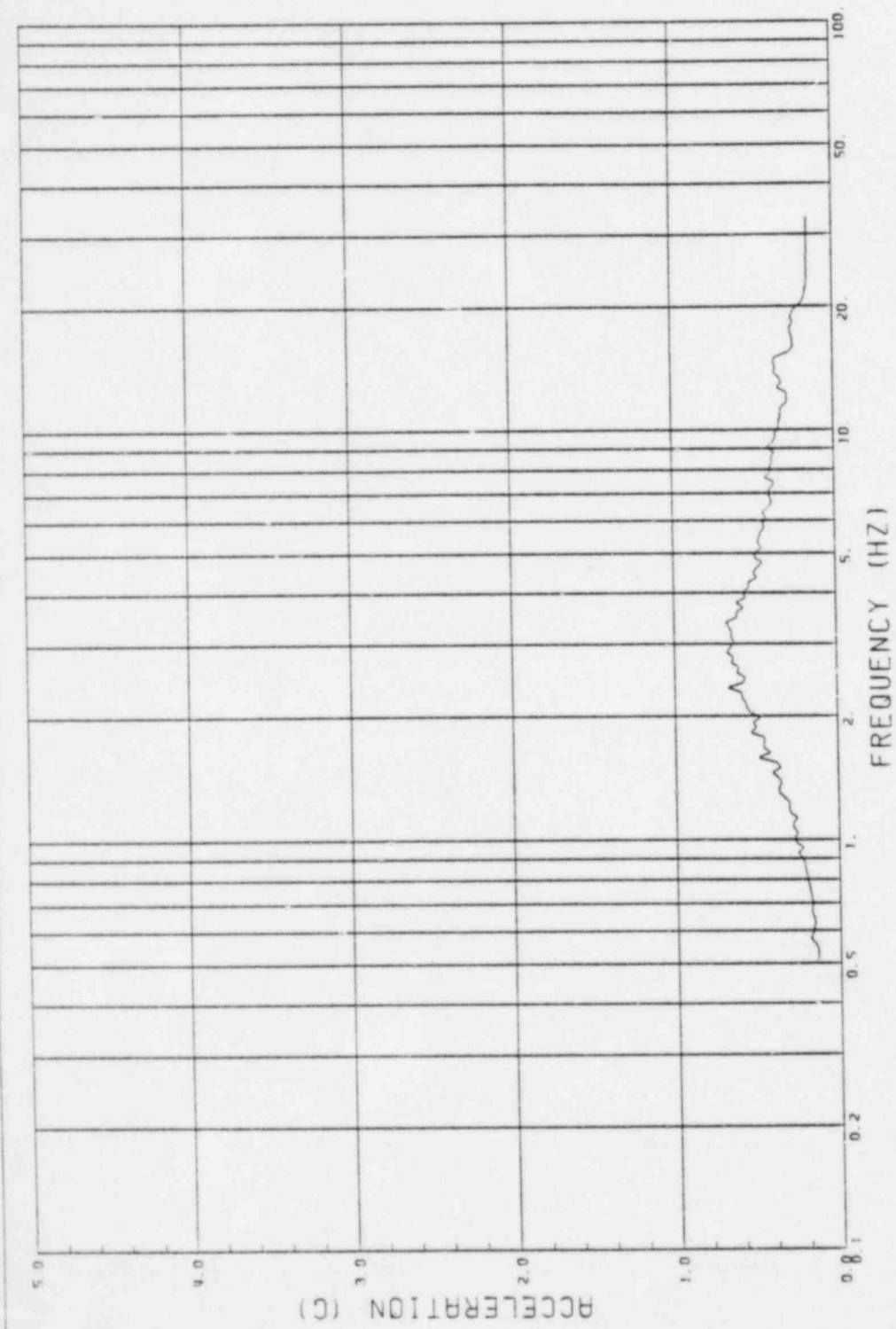
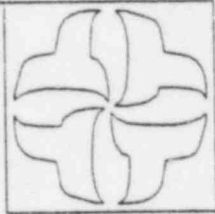


CE CLASS1 ANALYSES
 CASE 8, CE-75-A-V
 BASEMAT, NODE NO. 71 (TRANSLATION)



CESSAR II PLANT
 SOIL - STRUCTURE INTERACTION

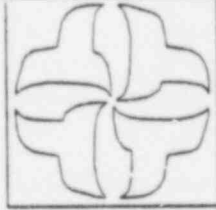
Figure A.78



GE CLASSI ANALYSES
CASE 8, GE-75-A-V
NODE NO. 1

CESSAR II PLANT
SOIL - STRUCTURE INTERACTION

Figure A.79



CESSAR II PLANT
SOIL - STRUCTURE INTERACTION

GE CLASS1 ANALYSES
CASE B. GE-75-A-V
NODE NO. 22

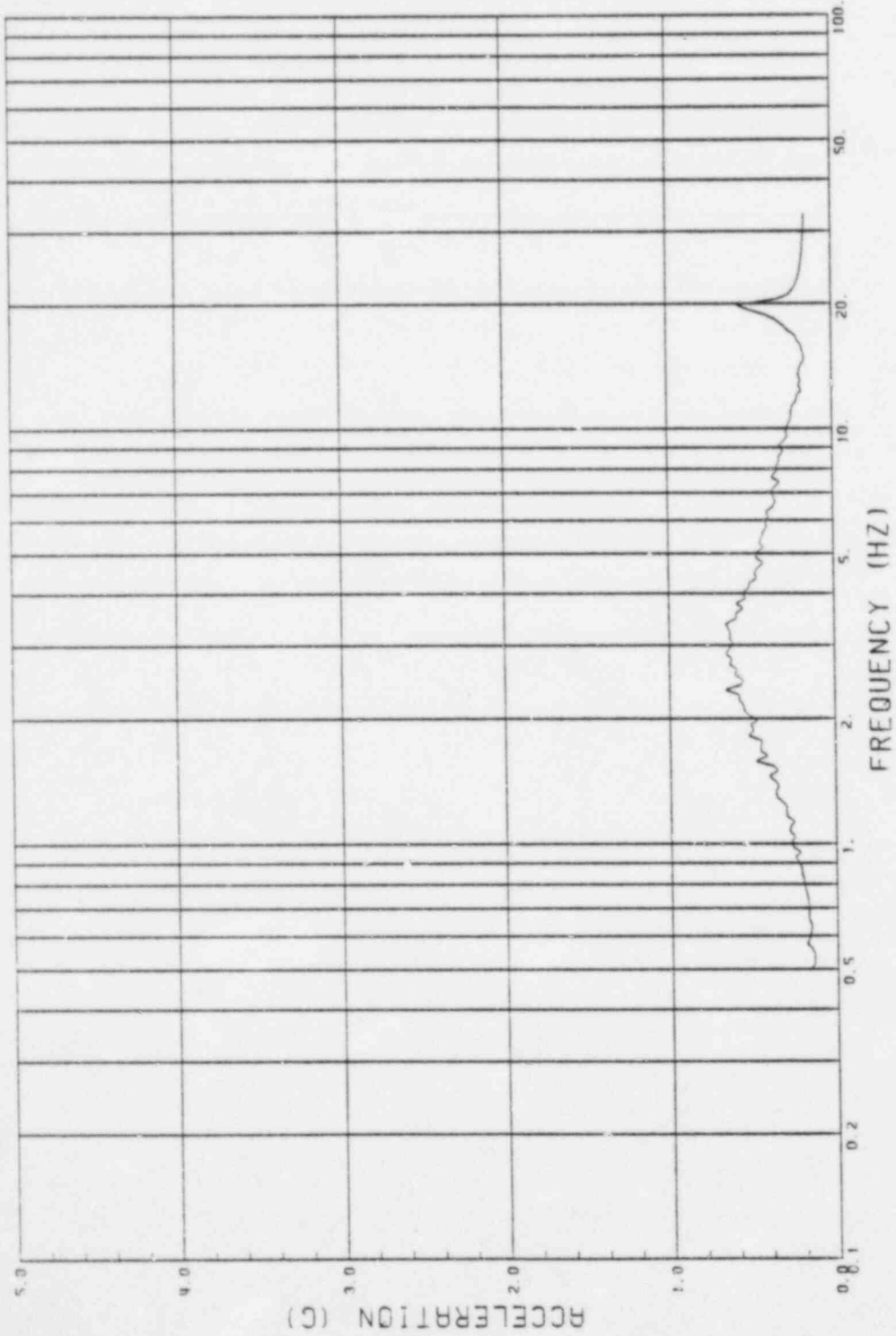
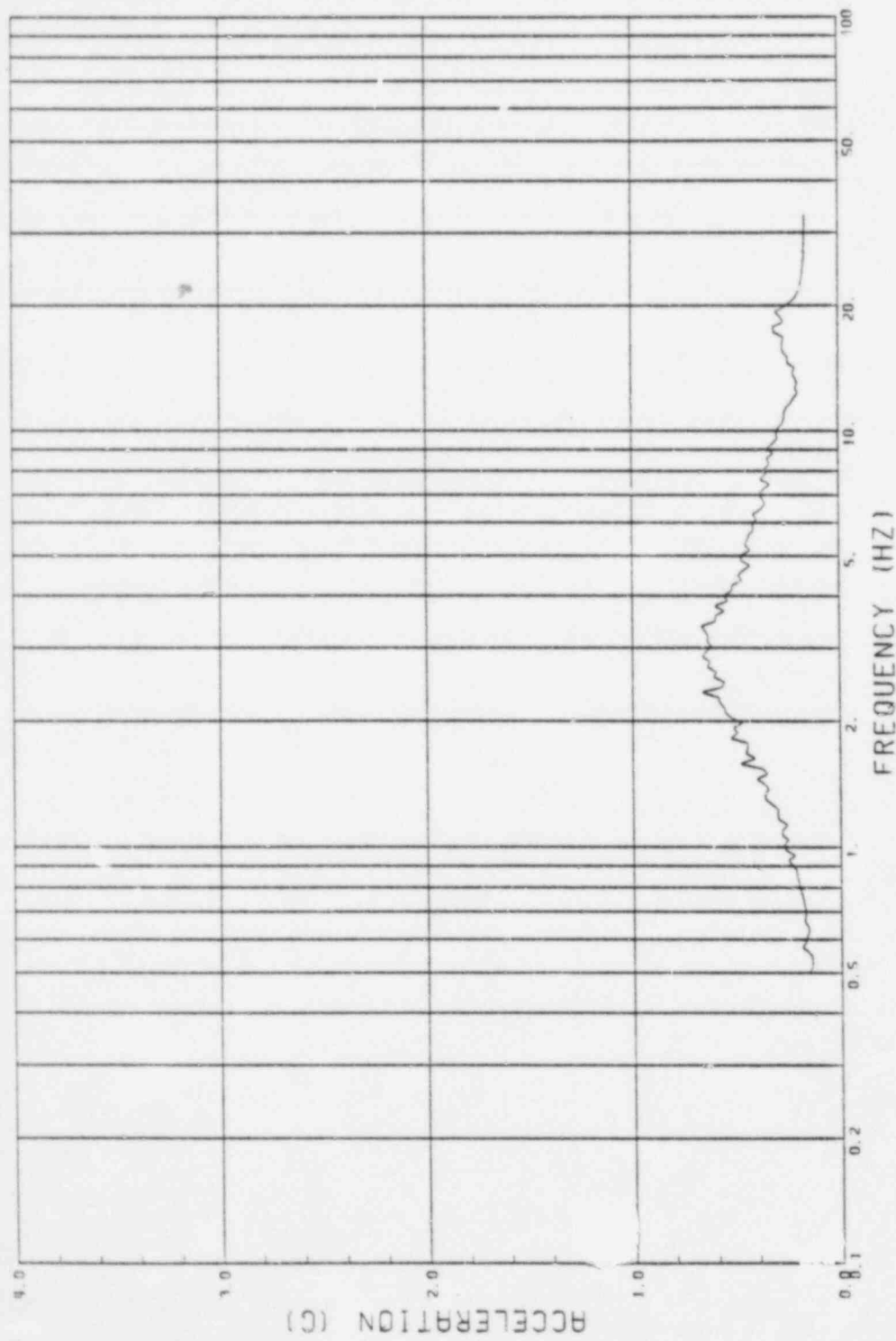
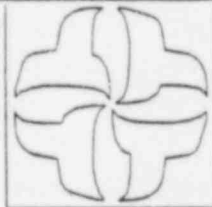


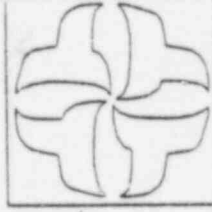
Figure A.80



GE CLASSI ANALYSES
CASE 8, GE-75-R-V
NODE NO. 42

CESSAR II PLANT
SOIL - STRUCTURE INTERACTION

Figure A.81



CESSAR II PLANT
SOIL - STRUCTURE INTERACTION

GE CLASSI ANALYSES
CASE 8, CE-75-A-V
NODE NO. 46

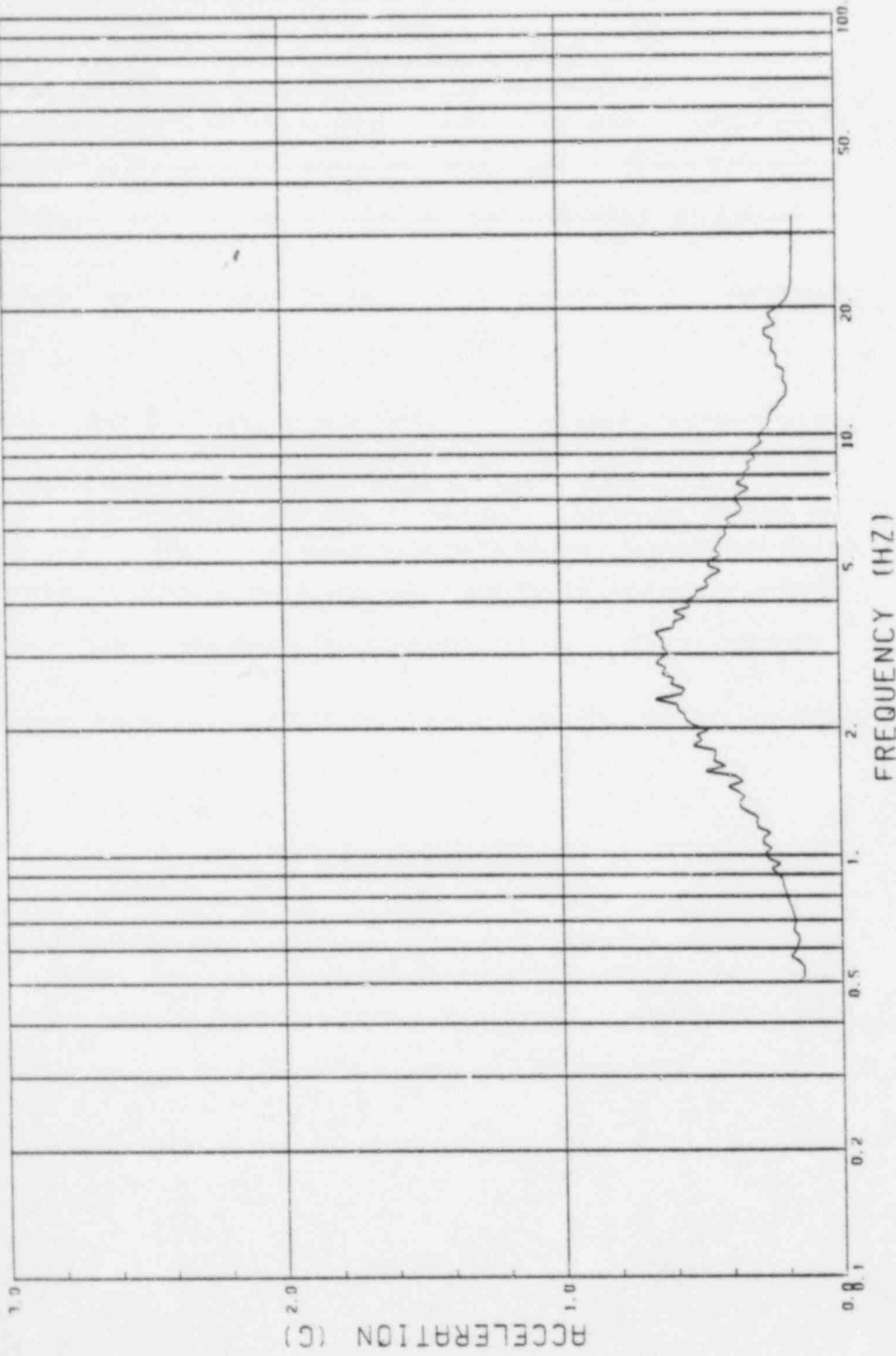
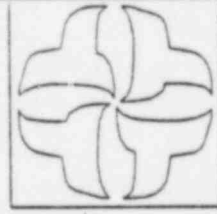


Figure A.82



CESSAR II PLANT
SOIL - STRUCTURE INTERACTION

GE CLASSI ANALYSES
CASE 8, GE-75-A-V
NODE NO. 60

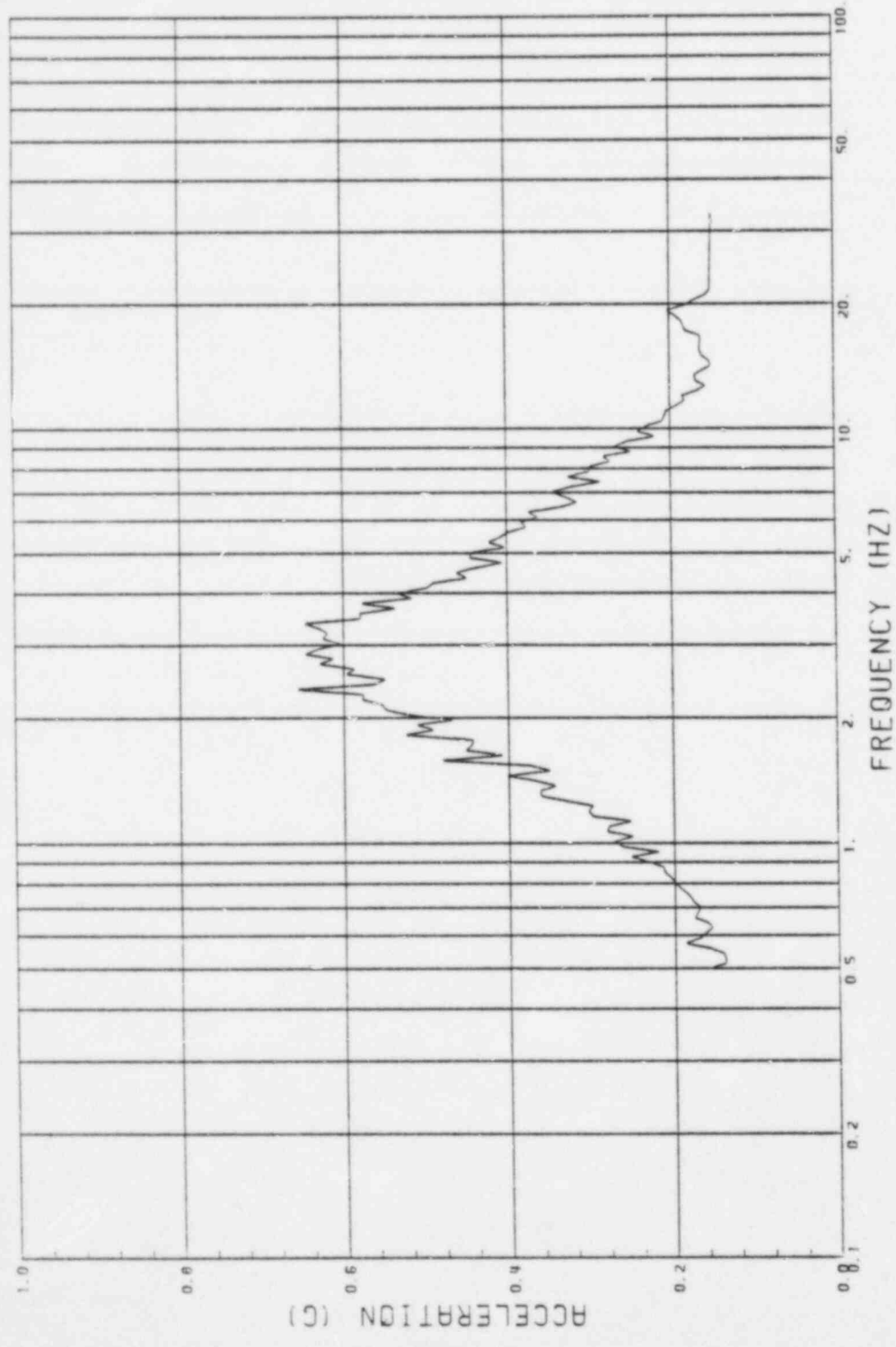
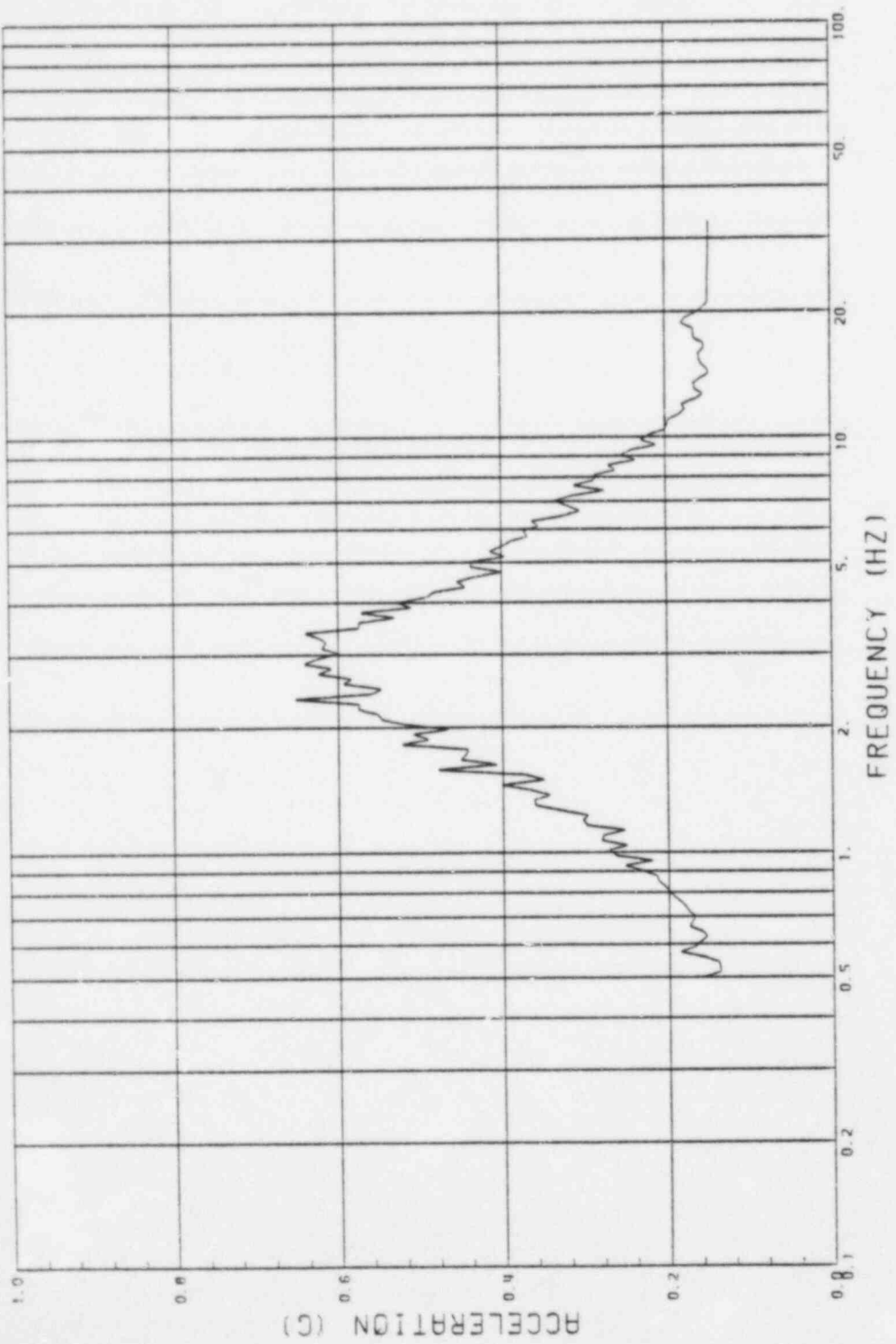
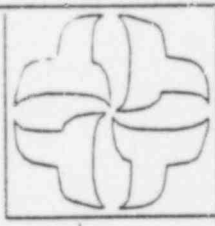


Figure A.83

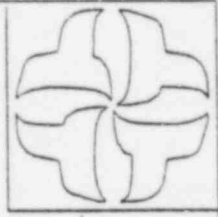


CE CLASSI ANALYSES
CASE 8, CE-75-A-V
NODE NO. 64



CESSAR II PLANT
SOIL - STRUCTURE INTERACTION

Figure A.84



CESSAR II PLANT
SOIL - STRUCTURE INTERACTION

GE CLASS1 ANALYSES
CASE 8, GE-75-A-V
NODE NO. 72

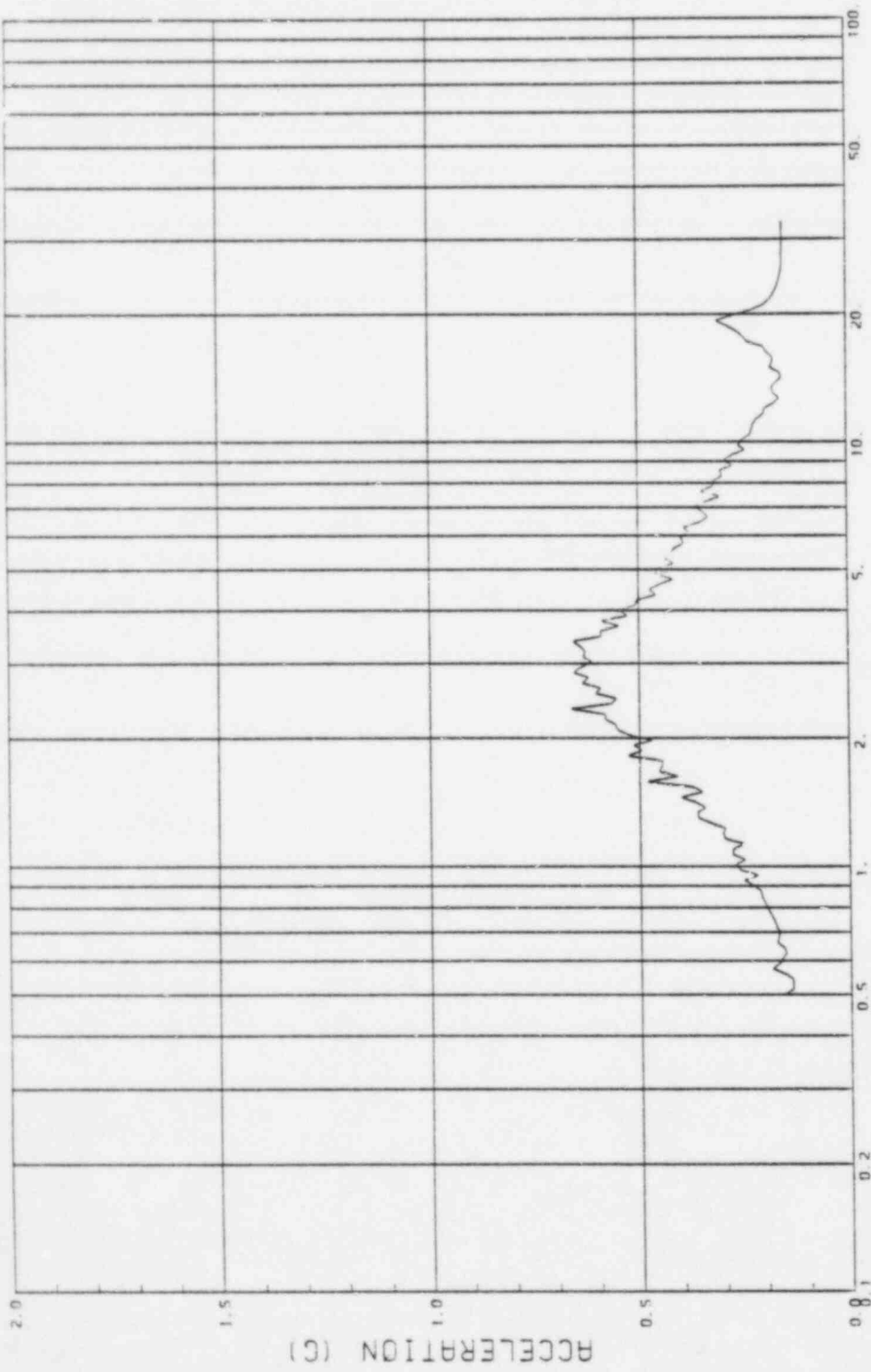
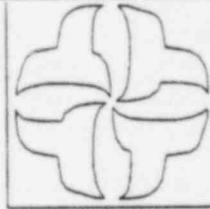


Figure A.85



CESSAR II PLANT
SOIL - STRUCTURE INTERACTION

GE CLASSI ANALYSES
CASE B, GE-75-A-V
NODE NO. 74

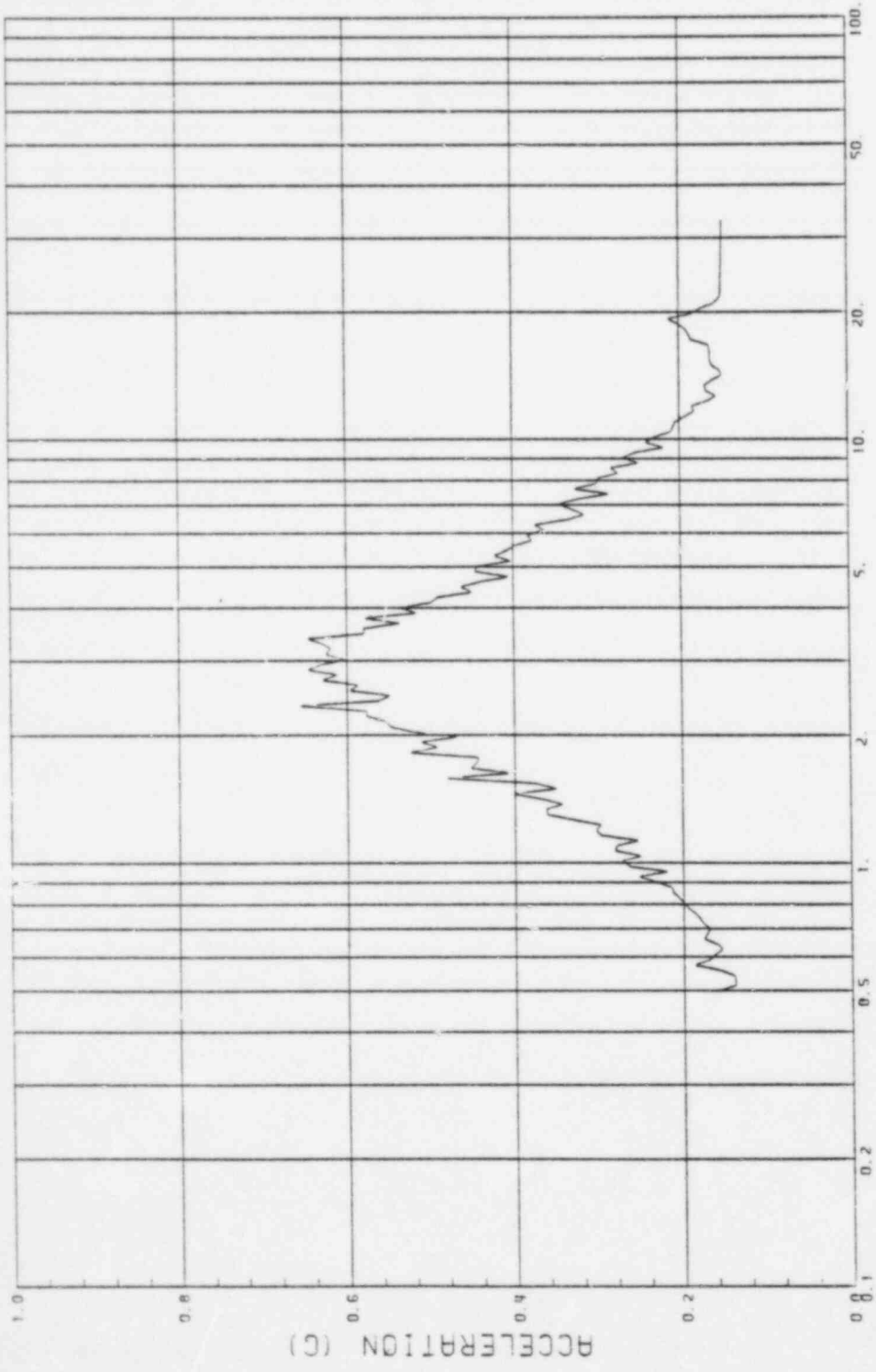
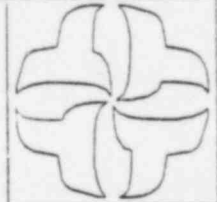


Figure A.86



SOIL - STRUCTURE INTERACTION
GESSAR II PLANT

GE CLASS1 ANALYSES
CASE 8, GE-75-A-V
NODE NO. 80

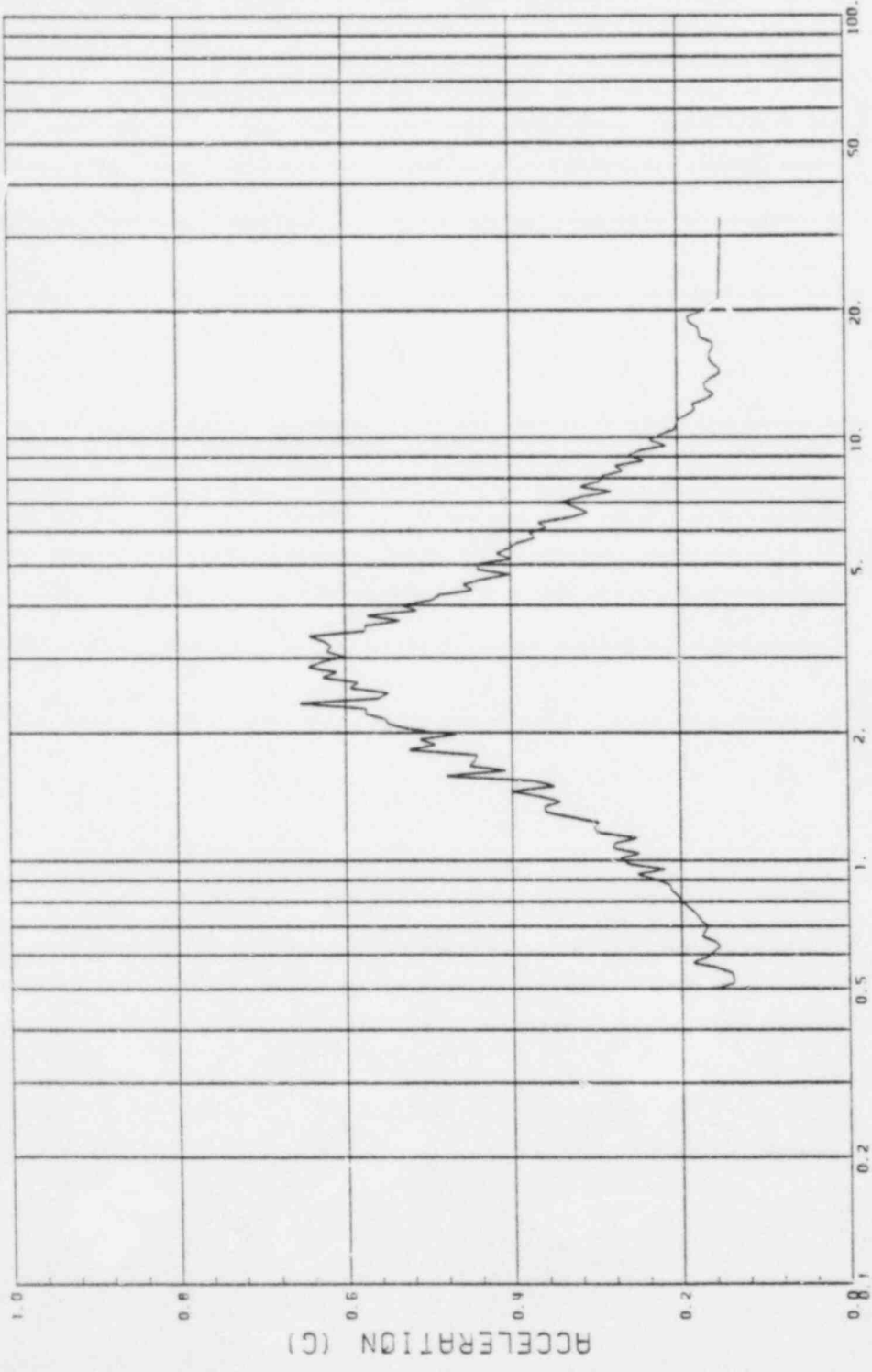


Figure A.87